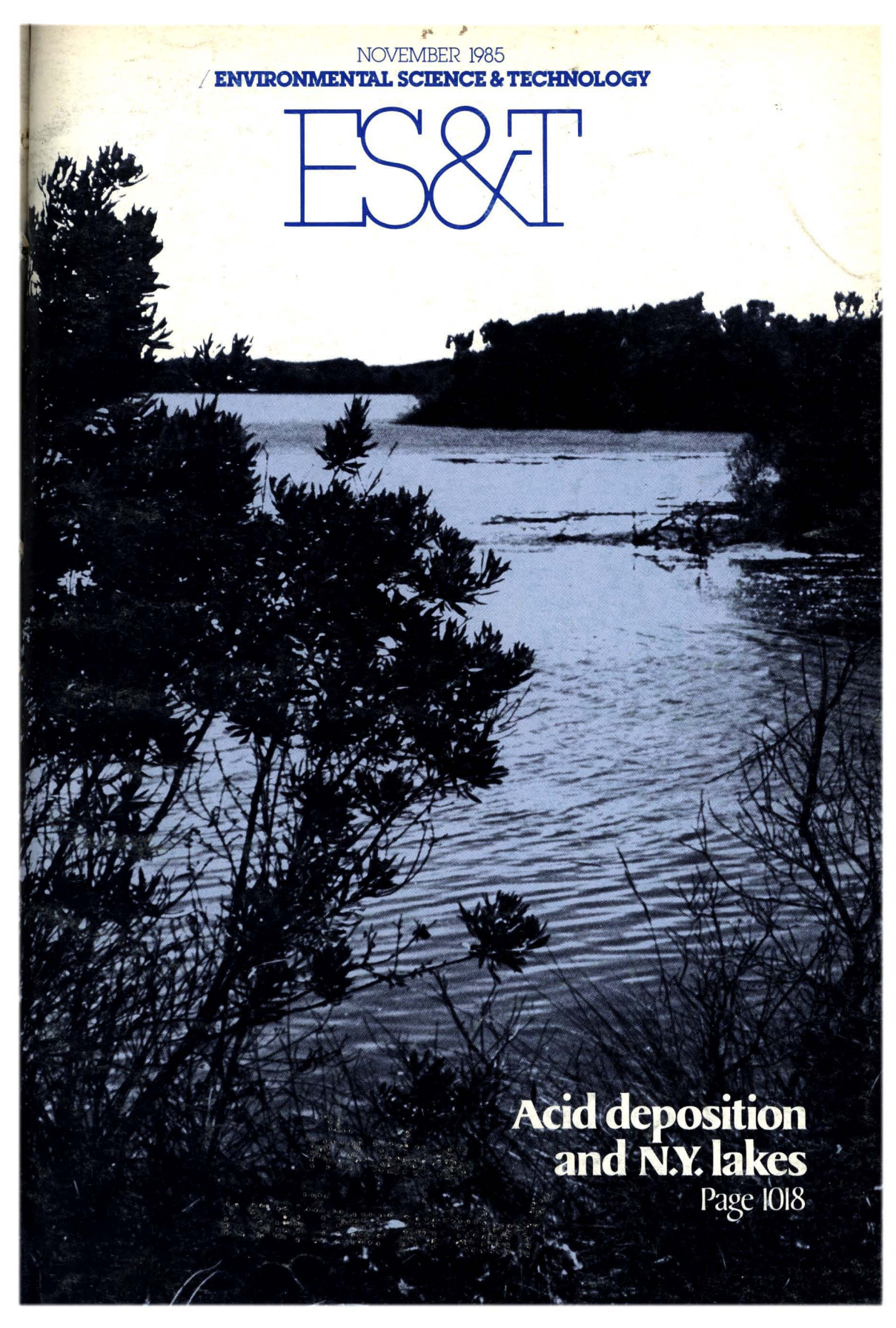


NOVEMBER 1985  
/ ENVIRONMENTAL SCIENCE & TECHNOLOGY

ES&T



**Acid deposition  
and N.Y. lakes**  
Page 1018

# WILEY BOOKS IN THE ENVIRONMENTAL SCIENCES...

Please Call for  
15-day  
Trial Copy

## ECOLOGY OF NATURAL RESOURCES

FRANÇOISE RAMADE, Université de Paris Sud (ORSAY)

1-90104-0 231 pages 1985 \$54.95

## POLLUTANTS AND THEIR ECOTOXICOLOGICAL SIGNIFICANCE

H.W. NÜRNBERG, Institute of Chemistry,  
Kernforschungsanlage Jülich, FRG

1-90509-7 515 pages 1985 \$74.95

## COASTLINE CHANGES

A Global Review

ERIC C.F. BIRD, University of Melbourne and United Nations University

1-90646-8 219 pages 1985 \$39.95

## POLLUTION CONTROL AND CONSERVATION

Edited by M. KOVACS, Hungarian Academy  
of Sciences

0-27509-X 492 pages December, 1985 \$112.00

## DRINKING WATER MATERIALS

Field Observations and Methods of Investigation

D. SCHOENEN and H.F. SCHOLER, Hygiene-Institute  
der Universität, FRG

0-20258-0 190 pages November, 1985 \$55.00

## CLOUD INVESTIGATION BY SATELLITE

R.S. SCORER, University of London

0-20253-X 320 pages December, 1985 \$68.95

## MUTAGENICITY TESTING IN ENVIRONMENTAL POLLUTION CONTROL

FK. ZIMMERMANN, Technical University of Darmstadt,  
FRG, and R.E. TAYLOR-MAYER, Slippery Rock  
University

0-20216-5 195 pages 1985 \$52.95



**JOHN WILEY & SONS, INC.**

605 Third Avenue, New York, N.Y. 10158  
In Canada 22 Worcester Road, Rexdale,  
Ontario M9W 1L1.

Prices subject to change and higher in Canada.



## SCOPE (Scientific Committee on Problems of the Environment)

Professor R.E. MUNN, Editor-in-Chief

SCOPE assembles, reviews and assesses information on man-made environmental changes and their effects on man. Presenting the best available scientific information, it has established itself as a corpus of informed advice for organizations and agencies studying the environment.

## PLANET EARTH IN JEOPARDY

Environmental Consequences of Nuclear War

LYDIA DOTTO

1-90908-4 180 pages January, 1986

\$9.95/paper

## ENVIRONMENTAL CONSEQUENCES OF NUCLEAR WAR SCOPE 28

Vol I: Physical and Atmospheric Effects

Edited by A. BARRIE PITTOCK *et al.*

1-90918-1 540 pages February, 1986 \$77.95

Vol II: Ecological and Agricultural Effects

Edited by MARK A. HARWELL *et al.*

1-90898-3 540 pages January, 1986 \$77.95

## CLIMATE IMPACT ASSESSMENT

Studies of the Interaction of Climate and Society  
SCOPE 27

Edited by ROBERT W. KATES *et al.*

1-90634-4 552 pages 1985 \$100.00

## METHODS FOR ESTIMATING RISK OF CHEMICAL INJURY

Human and Non-Human Biota and Ecosystems  
SCOPE 26

Edited by VELIMIR B. VOUK *et al.*

1-90546-1 680 pages 1985 \$89.95

## APPRAISAL OF TESTS TO PREDICT THE ENVIRONMENTAL BEHAVIOUR OF CHEMICALS SCOPE 25

Edited by PATRICK SHEEHAN *et al.*

1-90545-3 380 pages 1985 \$59.95

For additional information on these and other  
SCOPE titles, write: L. Culhane

To Order

**CALL TOLL-FREE: 1-800-526-5368**

In New Jersey, call collect (201) 342-6707.

Order Code #6-C558



Environmental Science & Technology  
© Copyright 1985 by the American Chemical Society

Editor: Russell F. Christman  
Associate Editor: John H. Seinfeld  
Associate Editor: Philip C. Singer

#### ADVISORY BOARD

Julian B. Andelman, Marcia C. Dodge, Steven Eisenreich, William H. Glaze, Michael R. Hoffmann, Lawrence H. Keith, Donald Mackay, Jarvis Moyers, Kathleen C. Taylor, Eugene B. Welch

#### WASHINGTON EDITORIAL STAFF

Managing Editor: Stanton S. Miller  
Associate Editor: Julian Josephson

#### MANUSCRIPT REVIEWING

Manager: Janice L. Fleming  
Associate Editor: Monica Creamer  
Associate Editor: Yvonne D. Curry  
Editorial Assistant: Diane Scott

#### MANUSCRIPT EDITING

Assistant Manager: Mary E. Scanlan  
Assistant Editor: Ruth A. Linville

#### GRAPHICS AND PRODUCTION

Production Manager: Leroy L. Corcoran  
Art Director: Alan Kahan  
Designer: Julie Katz  
Production Editor: Kate Kelly

#### BOOKS AND JOURNALS DIVISION

Director: D. H. Michael Bowen  
Head, Journals Department: Charles R. Bertisch  
Head, Production Department: Elmer M. Pusey  
Head, Research and Development Department: Lorrin R. Garson

#### ADVERTISING MANAGEMENT

Centcom, Ltd.  
For officers and advertisers, see page 1036.

Please send *research* manuscripts to Manuscript Reviewing, *feature* manuscripts to Managing Editor. For editorial policy and author's guide, see the January 1985 issue, page 22, or write Janice L. Fleming, Manuscript Reviewing Office, ES&T. A sample copyright transfer form, which may be copied, appears on the inside back cover of the January 1985 issue.

*Environmental Science & Technology*, ES&T (ISSN 0013-936X), is published monthly by the American Chemical Society at 1155 16th Street, N.W., Washington, D.C. 20036. Second-class postage paid at Washington, D.C., and at additional mailing offices. POSTMASTER: Send address changes to *Environmental Science & Technology*, Membership & Subscription Services, P.O. Box 3337, Columbus, Ohio 43210.

**SUBSCRIPTION PRICES 1985:** Members, \$26 per year; nonmembers (for personal use), \$35 per year; institutions, \$149 per year. Foreign postage, \$8 additional for Canada and Mexico, \$14 additional for Europe including air service, and \$23 additional for all other countries including air service. Single issues, \$3 for current year; \$13.75 for prior years. Back volumes, \$161 each. For foreign rates add \$1.50 for single issues and \$10.00 for back volumes. Rates above do not apply to nonmember subscribers in Japan, who must enter subscription orders with Maruzen Company Ltd., 3-10 Nihon bashi 2 chome, Chuo-ku, Tokyo 103, Japan. Tel: (03) 272-7211.

**COPYRIGHT PERMISSION:** An individual may make a single reprographic copy of an article in this publication for personal use. Reprographic copying beyond that permitted by Section 107 or 108 of the U.S. Copyright Law is allowed, provided that the appropriate per-copy fee is paid through the Copyright Clearance Center, Inc., 21 Congress St., Salem, Mass. 01970. For reprint permission, write Copyright Administrator, Books & Journals Division, ACS, 1155 16th St., N.W., Washington, D.C. 20036.

**REGISTERED NAMES AND TRADEMARKS,** etc., used in this publication, even without specific indication thereof, are not to be considered unprotected by law.

**SUBSCRIPTION SERVICE:** Orders for new subscriptions, single issues, back volumes, and microfiche and microform editions should be sent with payment to Office of the Treasurer, Financial Operations, ACS, 1155 16th St., N.W., Washington, D.C. 20036. Phone orders may be placed, using Visa, Master Card, or American Express, by calling toll free (800) 424-6747 from anywhere in the continental U.S. Changes of address, subscription renewals, claims for missing issues, and inquiries concerning records and accounts should be directed to Manager, Membership and Subscription Services, ACS, P.O. Box 3337, Columbus, Ohio 43210. Changes of address should allow six weeks and be accompanied by old and new addresses and a recent mailing label. Claims for missing issues will not be allowed if loss was due to insufficient notice of change of address, if claim is dated more than 90 days after the issue date for North American subscribers or more than one year for foreign subscribers, or if the reason given is "missing from files."

The American Chemical Society assumes no responsibility for statements and opinions advanced by contributors to the publication. Views expressed in editorials are those of the author and do not necessarily represent an official position of the society.

ES&T

# CONTENTS

Volume 19, Number 11, November 1985

## FEATURES



1018

**Chemical characteristics of Adiron-dack lakes.** Individual lakes respond differently to acid deposition. Charles T. Driscoll, Syracuse University, Syracuse, N.Y.; and Robert M. Newton, Smith College, Northampton, Mass.



1026

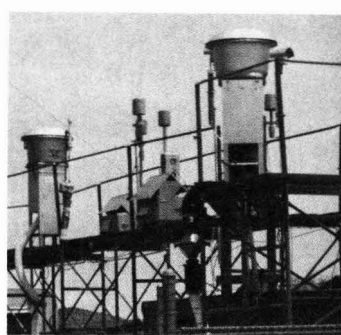
**Monitoring statistics.** The use of statistics is gaining increasing acceptance as a tool of environmental study. Glenn E. Schweitzer, National Research Council, Washington, D.C.; and Stuart C. Black, Environmental Protection Agency, Las Vegas, Nev.

## REGULATORY FOCUS

1031

**EPA's groundwater research.** Richard Dowd discusses the findings of a committee created by EPA's science advisory board to review the agency's groundwater research program.

## VIEWS



1032

**Jekyll Island meeting report.** George Hidy of the Desert Research Institute lectures on the need for atmospheric scientists to build monitoring programs that generate data of a defined quality.

## DEPARTMENTS

- 1011 Letters
- 1013 Editorial
- 1015 Currents
- 1034 Consulting services
- 1035 Classified

## UPCOMING

**Hazardous chemical waste management at colleges and universities**

**Models for freshwater acidification from atmospheric deposition of sulfuric acid**

ESTHAG 19(11) 1009-1136 (1985)  
ISSN 0013 936X

Cover: Julie Katz

Credits: p. 1015, Julian Josephson; p. 1026, Lois Embert, C&EN, p. 1026, courtesy Bethlehem Steel; p. 1026, New York State Department of Environmental Conservation; p. 1053, John Watson

## RESEARCH

1037

**Prediction of multicomponent adsorption equilibria using ideal adsorbed solution theory.** John C. Crittenden,\* Paul Luft, David W. Hand, Jacqueline L. Oravitz, Scott W. Loper, and Metin Ari

Ideal adsorbed solution theory is shown to predict multicomponent adsorption equilibrium data for up to six volatile organic compounds using single-solute isotherm data.

1044

**Scavenging of airborne polycyclic aromatic hydrocarbons by rain.** Paul C. M. van Noort\* and Erik Wondergem.

The presence in rain of gas-phase PAHs and aerosol-associated PAHs is proposed to result from below-cloud and in-cloud scavenging, respectively.

1048

**Effects of silicon on the crystallization and adsorption properties of ferric oxides.** Paul R. Anderson and Mark M. Benjamin\*

The bulk crystallinity and surface properties of solids that form when ferrihydrite is aged in the presence of silicate at elevated temperature and pH are characterized.

1053

**Trace organic compounds in rain. 4. Identities, concentrations, and scavenging mechanisms for phenols in urban air and rain.** Christian Leuenberger, Mary P. Ligoeki, and James F. Pankow\*

Air and rain analyses find phenols almost exclusively in the gaseous and dissolved forms. Gas scavenging is more important than particle scavenging for phenols.

1059

**Wall loss of gaseous pollutants in outdoor Teflon chambers.** Daniel Grosjean

Loss rates in FEP Teflon chambers are measured for approximately 20 gaseous pollutants in darkness and in sunlight.

1065

**Activation and reactivity of calcareous sorbents toward sulfur dioxide.** Jerald A. Cole,\* John C. Kramlich, W. Randall Seeker, Michael P. Heap, and Gary S. Samuelsen

Rate of calcination, surface area development, regeneration of gas-phase sulfur species, and SO<sub>2</sub> capture ability are examined as a function of gas-phase environment and sorbent type.

1072

**Interactions between polycyclic aromatic hydrocarbons and dissolved humic material: Binding and dissociation.** John F. McCarthy\* and Braulio D. Jimenez

Binding of PAHs to dissolved humic material is examined by equilibrium dialysis and fluorescence techniques.

1076

**Seasonal variations in weathering and toxicity of crude oil on seawater under arctic conditions.** Leiv K. Sydes,\* Tor H. Hemmingsen, Sølvi Skare, Sissel H. Hansen, Inger-Britt Falk-Petersen, Sunniva Lønning, and Kjetill Østgaard.

The oxidation of oil and the dissolution of toxic oil-derived compounds in the Arctic marine environment parallel the influx of solar energy.

1082

**Determination of organic acids (C<sub>1</sub>–C<sub>10</sub>) in the atmosphere, motor exhausts, and engine oils.** Kimitaka Kawamura, Lai-Ling Ng, and Isaac R. Kaplan\*

Formic, acetic, and benzoic acids are detected as major species of used engine oil, but in new oil their content is negligible.

1086

**Microbial degradation of chlorolignins.** Karl-Erik Eriksson\* and Marie-Claude Kolar

High molecular mass <sup>14</sup>C-labeled chlorolignins are degraded slowly by bacteria but quickly by the white-rot fungus, *Sporotrichum pulverulentum*.

1089

**Fluorescence spectroscopic study of kinetics of gas-surface reactions between nitrogen dioxide and adsorbed pyrene.** Ching-Hsong Wu\* and Hiromi Niki

The kinetics of gas-surface reactions between nitrogen dioxide and pyrene adsorbed on silica plates are studied by using a fluorescence spectroscopic method.

1094

**The mutagenic activity of the products of ozone reaction with propylene in the presence and absence of nitrogen dioxide.** Paul B. Shepson,\* Tadeusz E. Kleindienst, Edward O. Edney, Larry T. Cupitt, and Larry D. Claxton

The mutagenic activity of propylene ozonolysis products is relatively low and cannot account for the large mutagenic activity observed in the irradiated propylene-NO<sub>x</sub> system.

1099

**Emissions of vapor-phase fluorine and ammonia from the Columbia coal-fired power plant.** Christopher F. Bauer\* and Anders W. Andren

Emission measurements of two pulverized-coal furnaces show that 4–86% of the fluorine available in coal is emitted in the vapor phase, whereas ammonia emissions are negligible.

1104

**Behavior of methyltin compounds under simulated estuarine conditions.** Olivier F. X. Donard and James H. Weber\*

A 2<sup>3</sup>-factorial design is used to study the behavior of MeSnCl<sub>3</sub>, Me<sub>2</sub>SnCl<sub>2</sub>, and Me<sub>3</sub>SnCl under laboratory-simulated estuarine conditions.

1110

**Microcomputer-controlled two size fractionating aerosol sampler for outdoor environments.** Hans-Christen Hansson\* and Stefan Nyman

The results of tests carried out on a microcomputer-controlled aerosol sampler to investigate internal losses, impactor characteristics, and filter efficiency are presented.

1115

**Formation of nitroarenes from the reaction of polycyclic aromatic hydrocarbons with dinitrogen pentaoxide.** James N. Pitts, Jr.,\* Janet A. Sweetman, Barbara Zielinska, Roger Atkinson, Arthur M. Winer, and William P. Harger

Reactions of six polycyclic aromatic hydrocarbons deposited on glass fiber filters with gaseous N<sub>2</sub>O<sub>5</sub> are reported.

## NOTES

1122

**Evaluation of sorptive partitioning of nonionic pollutants in closed systems by headspace analysis.** Doug R. Garbarini and Leonard W. Lion\*

Experiments examining the sorption of toluene and TCE demonstrate the applicability of the headspace technique to sorption studies.

1128

**Concentrations of krypton-85 near the Nevada Test Site.** R. Frank Grossman\* and Robert W. Holloway

Data collected from a network of noble gas samplers over a 12-y period are reviewed to identify long-term trends and to present descriptive statistics.

1132

**Decontamination of soil through enhanced formation of bound residues.** Duane F. Berry and Stephen A. Boyd\*

This research reports the development of an in situ method for detoxifying contaminated soil.

1134

**A theory for critical flow through hypodermic needles.** Thomas J. Overcamp

The classical theory of isothermal, compressible flow through a long tube is used to predict critical flow through hypodermic needles, which are frequently used in air sampling.

\* To whom correspondence should be addressed.

This issue contains no papers for which there is supplementary material in microform.



# ES&T LETTERS

## Acid deposition: benefit vs. cost

Dear Sir: "Acid deposition control" (*ES&T*, February 1985, pp. 112-16) by Thomas Crocker and James Regens attempts to support two primary conclusions: that cost-benefit analysis "may be impossible without reliance on limited scientific data and allowance for large margins of error" and that the lack of scientific certainty in the area of acid deposition implies that "methods are better viewed as a set of tools that illustrate the natural system consequences of market responses and people's adaptations to variations in acid deposition levels." The first conclusion is accepted as true by most observers; the second is an artifact of the authors' own analysis.

Their first conclusion points out a truth that lies at the heart of evaluating policy options for acid deposition: There is considerable uncertainty regarding the extent and time scale of effects on lakes, forests, and other areas. Any analysis, whether or not it is called "cost-benefit," that fails to deal with the implications of this uncertainty (i.e., "limited scientific data") will certainly be seriously flawed. In their second conclusion, the authors cast around for something that cost-benefit analysis *can* do; they assume that it *cannot* do what is most important.

The central issue of acid deposition policy analysis is finding constructive methods of discussing scientific uncertainty and formulating strategies appropriate to that uncertainty. The range of uncertainty is best illustrated by pointing to the authors' claim that "benefits appear to be highly subtle and intangible." In other articles, however, proponents of controls have argued that acid deposition kills fish, can poison reservoirs, poses a menace to crops and forests, and disfigures buildings (1). These effects are neither subtle nor intangible. The plain fact is that there is no agreement that these effects are widespread, will be widespread, or would be avoided by the proposed controls if they were widespread.

Due to their own inability to include uncertainties, the authors present single-number estimates for several categories of potential effects (materials, forests, agriculture, and aquatic systems). These estimates have not been published previously in a peer-reviewed

journal and have been strongly criticized in the only written review of them of which I am aware (2).

The article does not provide ranges or probability distributions over the potential benefits of acid deposition control measures or discuss why one might want to construct such ranges or distributions. This omission is particularly ironic in view of the editorial in the same issue ("Uncertainty and environmental risk assessment," p. 99) calling for scientists to present uncertainty in the form of such distributions.

It is a lack of scientific knowledge that lies at the heart of acid deposition policy analysis. We need not relegate cost-benefit analysis to insignificance, as Crocker and Regens seem to do. There are practical, tested methods for presenting scientific uncertainty as probability distributions (3). Posing acid deposition policy in terms of making decisions with the knowledge of our uncertainty allows cost-benefit analysis to expand its traditional horizons (4). This would allow us to evaluate control options that are contingent on the resolution of scientific uncertainty, to determine whether we can afford to await the outcome of scientific research, to rank research programs according to their value in making better policy decisions, and to understand the role of risk aversion and value trade-offs.

I urge your readers to compare the benefits of expanding cost-benefit analysis—to consider these important issues—with the benefits of the methods proposed by Crocker and Regens.

**Stephen C. Peck**

Technical Director, Environmental and  
Economic Integration Staff  
Electric Power Research Institute  
Palo Alto, Calif. 94303

## References

- (1) Boyle, R. H.; Boyle, R. A. *Amicus J.*, 1983 (Winter), pp. 22-37.
- (2) "A Review and Critique of the Crocker, Tschirhart, and Adams Assessment of the Benefits of Controlling Acid Precipitation," submitted to the Utility Air Regulatory Group by ICF Inc., Aug. 2, 1983.
- (3) Spetzler, C. S.; Stael von Holstein, C.A.S. *Manag. Sci.* **1975**, 22, 340-58.
- (4) Balson, W. E.; Boyd, D. W.; North, E. W. "Acid Deposition: Decision Framework," EA-2540; Electric Power Research Institute: Palo Alto, Calif., 1982.

## The authors reply:

Stephen Peck disagrees with two features of our discussion. He first com-

plains about the absence of a treatment of the uncertainties surrounding the estimate of a maximum of \$5 billion in 1978 control benefits if all acid deposition effects had been eliminated. Although we said that the estimate was highly tentative, it is true that a thorough treatment of the inherent, statistical, and model uncertainties surrounding the acid deposition issue was not supplied. As for our inability to deal either analytically or empirically with uncertainties in benefit-cost analysis we refer the reader to References 1-5.

We regard Peck's second disagreement as more worthy of comment. It illustrates a fundamental philosophical difference about what the primary purpose of benefit-cost analysis *should* be. Because of the dynamic and stochastic elements that dominate the acid deposition issue, we advised caution in using the numbers (total benefits less total costs of a change) that such an analysis provides as the basis for policy choices. Our opinion would have been even more precisely conveyed if we had said that the numbers rarely, if ever, should be used as the sole basis for policy choice, whether or not dynamic and stochastic elements are taken into account because "policy decisions must reflect societal values" (6).

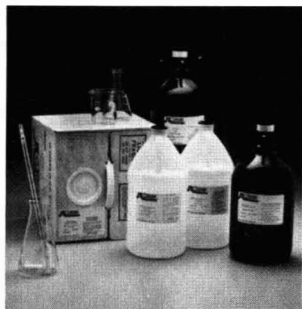
A statement this strong undoubtedly would have caused Peck to use harsher phrases than "an artifact of the authors' own analysis." He apparently believes that the primary purpose of benefit-cost analysis is to generate bottom-line numbers, especially numbers stated in probabilistic terms.

We, however, believe that its primary purpose is to provide information about marginal shifts in opportunity costs that can be used by contestants in the political arena to become informed about what a given change is likely to hold for them. Occasionally, bottom-line numbers will be informative. More often, information about market response and agent adaptations (allowing the beholder to draw inferences about the particulars of a change as it affects him) will be much more useful. He can then use this information to construct a political strategy; knowledge about aggregate benefits and costs is, at best, of only abstract interest to him.

We point out in the article that net benefits and economic efficiency are

# Selection

Another good reason  
for choosing Anderson  
BANCO® products.



With over 2,000 specific BANCO® solutions, reagents and chemicals, Anderson Laboratories can fill virtually all of your laboratory needs. We have the broadest listing of prepared and standardized chemical reagents in the United States including:

Standardized Laboratory  
Solutions

Reagent Grade Laboratory  
Solvents

Karl Fischer Reagent

A.P.H.A., E.P.A., A.S.T.M.,  
U.S.G.S., A.O.A.C. Test  
solutions and Reagents for  
Water Pollution and other  
Determinations

Atomic Absorptions Standards  
Buffers (Standard and Color  
Coded)

Indicating Solutions

Biological Staining Solutions

In-Vitro Diagnostic Reagents

For more information call or  
write your BANCO® dealer;  
we have over 200 throughout  
the United States. Our dealers  
are listed in the yellow pages  
under Laboratory Equipment  
and Supplies.



Anderson Laboratories, Inc.  
5901 Fitzhugh Avenue  
Fort Worth, Texas 76119  
Telephone: (817) 457-4474

identical only if effective markets exist in which the good in question can be traded. In effective markets, all potential gains from voluntary exchanges are realized. With benefit-cost analysis, those theoretically possible exchanges are realized, but they also need never occur in reality.

Those who gain from a change never have to compensate losers. Government is viewed as a rational planner that denies the relevance of individual circumstances to implement its conception of the collective will. Losers are to be coerced into a change if the collective will is served. Any defense of such a posture clearly must take one well beyond the bounds of technical economics into the realm of political philosophy and ethics.

Moreover, it represents a position that is incompatible with the day-to-day practices of Western democracies. These practices use the give-and-take of government to create and transfer wealth, particularly in circumstances where markets are ineffective or otherwise rejected. As a result, we question the implication that government has or should have the values of a private firm in which the *important* thing to do is tote up the personal advantages and disadvantages of an option and act only if the net advantages are positive. The bottom-line numbers of benefit-cost analysis are useful only to those who will gain if government does efficient accounting.

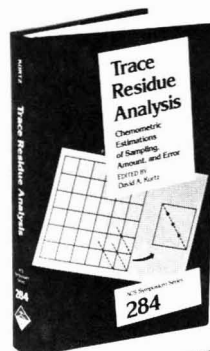
Economic efficiency, in our view, is more likely to be served if the analytical framework that supports the *process* of benefit-cost analysis is used to inform participants in collective-choice exercises of the particular economic consequences to them of a proposed change. Musing about nonexistent rational central planners who must keep the accounts serves neither the process of benefit-cost analysis nor the process of collective choice. When applied under that assumption, benefit-cost analysis is reduced to practical insignificance because it informs very few collective-choice participants of what a change holds for them.

## References

- (1) Crocker, T. D. In "Cost-Benefit Analysis and Water Pollution Policy"; Peskin, H. M.; Seskin, E. P. Eds; Urban Institute: Washington, D.C., 1975; pp. 341-59.
- (2) Regens, J. L. In "Economic Perspectives on Acid Deposition Control"; Crocker, T. D., Ed.; Butterworth: Boston, Mass., 1984; pp. 5-20.
- (3) Adams, R. N.; Crocker, T. D.; Katz, R. W. *Rev. Econ. Stat.* **1984**, *66*, 568-75.
- (4) Regens, J. L.; Crocker, T. D. *Manage. Sci. Pol. Anal.* **1984**, *1*, 12-17.
- (5) Atkinson, S. E.; Crocker, T. D.; Murdock, R. G. *J. Urban Econ.* **1985**, *17*, 319-34.
- (6) Malès, R. H. *Environ. Sci. Technol.* **1985**, *19*, 13.

## Trace Residue Analysis

### Chemometric Estimations of Sampling, Amount, and Error



**NEW!**

David A. Kurtz, Editor  
The Pennsylvania State University

Explains the use of chemometrics to analyze trace residue of pesticides and environmental contaminants. Discusses the use of statistical methods to determine calibration graphs and their error bounds. Also looks at the limits of detection and at the selection and number of samples. Defines the computer methods used to sort, classify, display, and interpret data. Makes these methods easily understandable so that bench chemists will be able to obtain more meaningful results and to interpret results quickly.

## CONTENTS

Statistics: A Child of Our Time? • Sampling for Chemical Analysis of the Environment • Sampling and Variance in Measurements of Trifluralin Disappearance from a Field Soil • Processing Outliers in Statistical Data • Dimensions of Detection in Chemical Analysis with Emphasis on One-Dimensional Calibration Curve • Introduction to the Theory of Correlation Chromatography • Developments in Correlation Chromatography: Application in Trace Analysis • Calibration-Curve-Based Analysis: Use of Multiple-Curve and Weighted Least-Squares Procedures with Confidence Band Statistics • Linear Calibration Graph and Its Confidence Bands from Regression on Transformed Data • Use of Cubic Spline Functions in Solving Calibration Problems • Comparison of Calibration Graph Amount and Estimated Amount Intervals • Application of Soft Independent Method of Class Analysis in Isomer Specific Analysis of Polychlorinated Biphenyls • From Data to Information to Knowledge: Problems of Metamorphosis

Developed from a symposium cosponsored by the Divisions of Pesticide and Analytical Chemistry of the American Chemical Society

ACS Symposium Series No. 284  
284 pages (1985) Clothbound  
LC 85-11226 ISBN 0-8412-0925-1  
US & Canada \$59.95 Export \$71.95

Order from:  
American Chemical Society  
Distribution Office Dept. 81  
1155 Sixteenth St., N.W.  
Washington, DC 20036  
or CALL TOLL FREE 800-424-6747  
and use your credit card.



---

ES&T

# GUEST EDITORIAL

## Clean shirts *and* clean water

Soap and detergents belong to the category of mass-produced chemical substances. Worldwide, the 30 million tons produced each year poses a substantial potential for harm to the aquatic environment. In North America and Western Europe each person uses an average of 23 kg of household detergents each year. These products contain "wash active" substances, builders, and other additives such as bleach and optical brighteners; a few hundred grams of these substances is dispersed into every cubic meter of wastewater.

The imposition of stringent requirements on the ecological compatibility of soap and detergents is justified to protect the processing operations at wastewater treatment plants and to safeguard aquatic ecosystems. First, all organic detergent components should be fully biodegradable and should contain no decomposition intermediates; second, detergents should not contain algal nutrients that contribute to the man-made eutrophication of lakes. These two requirements are not met by many of the detergent formulations in common use today. But manufacturers deserve credit for mitigating the foam problem that plagued sewage treatment plants and receiving waters in the early 1960s.

The June *ES&T* editorial ("Phosphate here, phosphate there . . ." p. 467) stated that "natural variations in the complex interrelations among nutrient levels, light availability, and plant growth are so substantial that single control measures . . . are likely to have extremely variable results, if applied over large areas." Here I disagree; for every pollutant the cause-effect relationship is complicated, but our power to predict the effect of phosphate loadings on lakes (of different morphology and hydraulic residence time) is remarkably quantitative and suited to generalization.

The entire limnological research community is united in the opinion that reduction of the supply of phosphate to receiving waters is the only cure against man-made eutrophication. Even in turbid waters, such as those found in the southeastern U.S., 100 g of algae (dry weight), derived from about 1 g of soluble phosphorus, will upon decomposition cause an oxygen de-

mand of 100–140 g. Phosphate removal in treatment plants is necessary but insufficient because some wastes unavoidably escape treatment; not all households are connected to treatment plants and storm water overflows.

It is important to decide whether we should prevent pollutants at the source or rely on some "end of pipe" therapy in a treatment plant. Some states in the U.S. ban the use of phosphates in home laundry detergents. Canada has a federal limit of 2.2% phosphorus. Most European countries have set other limits.

In Switzerland, a land of many lakes, the history of Lake Zurich became the first well-documented case of man-made eutrophication; it is a history that has since been repeated in tens of thousands of lakes throughout the world. The Swiss government recently banned phosphates from home laundry detergents. This legislation complements that already in existence requiring chemical phosphate removal in sewage treatment plants.

In Japan, detergent makers decided on total reformulations. As a result, within only two years more than 90% of the detergents produced and sold in Japan are phosphate-free; they contain zeolites instead. It is technologically feasible to manufacture phosphate-free detergents that contain fully biodegradable surfactants.

We can have clean shirts and clean water.

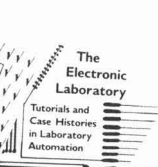
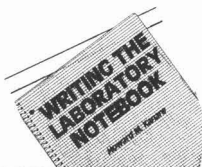
*Werner Stumm*



**Werner Stumm** is a professor at the Swiss Federal Institute of Technology in Zurich and head of its Laboratory of Water Resources and Water Pollution Control (Institute for Aquatic Sciences and Water Pollution Control, EAWAG, CH-8600 Dübendorf, Switzerland).

# NEW BOOKS FROM ACS

*You won't  
want to be  
without*



## Comet Halley: Once in a Lifetime

by Mark Littmann and Donald K. Yeomans

The astronomical event of our age is coming soon! Take your first look at Halley's Comet through this unique new book. Read about the myths and misconceptions surrounding past comet appearances. Examine the theories that comets may have contributed to both the evolution and destruction of life on earth. Journey back in time to past comet appearances. Look forward to this visit with a complete guide to 1985-86 sightings, including month-by-month descriptions, sky charts, and explanations of how to recognize what you see. This volume is lavishly illustrated—an excellent guide and a valuable keepsake.

190 pages (1985)

Cloth: US & Canada \$19.95 Export \$23.95

Paper: US & Canada \$12.95 Export \$15.95

## Writing the Laboratory Notebook

by Howard M. Kanare

Finally—all the information you need on how to keep a proper and permanent laboratory notebook! This new book will show you how to create proper records, write with greater clarity, and increase your awareness of what is being done in the lab. Essential for lab students and scientists beginning their industrial careers. Good for professors and lab supervisors who need to instruct and evaluate their employees and students. Includes examples of notebook entries and features a chapter on the electronic notebook. The definitive source on this important aspect of professional life.

150 pages (1985)

Cloth: US & Canada \$19.95 Export \$23.95

Paper: US & Canada \$12.95 Export \$15.95

## The Electronic Laboratory

by Raymond E. Dessy

Explore the future of laboratory automation today! This important new book will help you discover the possibilities of the electronic laboratory, including local area networks; lab information management systems; robots, graphics and voice input/output; operating systems and languages; and management of the electronic lab, including important information on security and archiving. Includes case histories of successful industrial labs, offering the valuable insight of industrial chemists into electronic laboratory problems, solutions, and practices.

148 pages (1985)

Cloth: US & Canada \$29.95 Export \$35.95

Paper: US & Canada \$17.95 Export \$21.95

## The ACS Style Guide

Janet S. Dodd, Editor

The essential desk reference for authors, editors, publishers and presenters of scientific research is here! The ACS Style Guide is a complete stylistic handbook for the scientist, covering all phases of publishing and presenting the scientific paper. Includes in-depth information on grammar, style and usage; illustrations, chemical structures, tables, and lists; copyright and permissions; how to submit papers electronically; and how to give effective oral presentations. From start to finish, this handbook will help you make the most effective written and oral presentations possible. Greatly expands and updates the ACS "Handbook for Authors."

200 pages (1985)

Cloth: US & Canada \$24.95 Export \$29.95

Paper: US & Canada \$14.95 Export \$17.95

## ORDER FORM

Title	Qty.	US & Can.	Export	Total
Comet Halley: Once In A Lifetime				
Hardbound:		\$19.95	\$23.95	
Paperbound:		\$12.95	\$15.95	
Writing The Laboratory Notebook				
Hardbound:		\$19.95	\$23.95	
Paperbound:		\$12.95	\$15.95	
The Electronic Laboratory				
Hardbound:		\$29.95	\$35.95	
Paperbound:		\$17.95	\$21.95	
The ACS Style Guide				
Hardbound:		\$24.95	\$29.95	
Paperbound:		\$14.95	\$17.95	
		Total:		

ORDERS FROM INDIVIDUALS MUST BE PREPAID. Prepaid and credit card orders receive free postage and handling. Prices subject to change without notice. Please allow 4-6 weeks for delivery. Foreign payment must be made in US currency by international money order, UNESCO coupons, or US bank draft. Order through your local bookseller or directly from ACS. To charge your books by phone, CALL TOLL FREE (800) 424-6747.

Mail this order form with your payment or purchase order to:  
American Chemical Society, Distribution Office Dept. 130,  
1155 Sixteenth St., N.W., Washington, DC 20036

☐ Payment enclosed (make checks payable to American Chemical Society).

☐ Purchase order enclosed. P.O. # \_\_\_\_\_

Charge my ☐ MasterCard ☐ VISA ☐ Access ☐ Barclaycard ☐ American Express  
☐ Diners Club/Carte Blanche.

Account # \_\_\_\_\_

Expires \_\_\_\_\_ Interbank # \_\_\_\_\_  
(MC and Access)

Name of cardholder \_\_\_\_\_ Phone # \_\_\_\_\_

Signature \_\_\_\_\_

Ship books to: Name \_\_\_\_\_

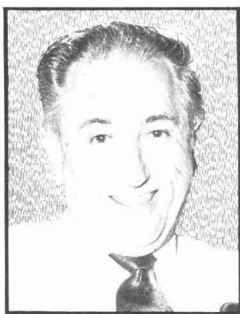
Address \_\_\_\_\_

City, State, Zip \_\_\_\_\_



# ES&T CURRENTS

## INTERNATIONAL



*Lee: More environmental loans*

The World Bank addressed environmental concerns in its annual report for the first time in its 40-year history. Issued in September, the report warned that environmental destruction is assuming massive proportions, especially in Africa where deforestation has caused a fuel wood shortage for 100 million persons. The report also notes that the World Bank made a record \$800 million available in loans last year for reforestation and other environmental programs in the Third World. This sum represents about 5% of the bank's total lending. James Lee, environmental adviser to the World Bank, says that he expects more resources to be allocated to mitigating environmental problems in Third World countries.

## FEDERAL

The Risk Assessment Research and Development Act of 1985, introduced by Rep. Don Ritter (D-Pa.) as H.R. 2479, has been endorsed by American Chemical Society President Ellis Fields. Fields says that the act would provide a means for public understanding and acceptance of the use of risk assessment in regulatory decision making because it would enable the public to make informed decisions about what constitutes acceptable risk. He says he is pleased that the bill calls for the designation of an "appropriate federal scientific advisory agency to assist federal

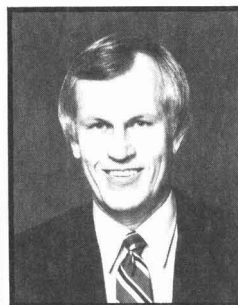
agencies in improving their use of risk assessment."

In September, EPA issued a final rule to control the discharge of wastewater pollutants from pesticide chemical plants. The rule affects manufacturers of organic and metallo-organic pesticides and pesticide chemical formulators and packagers. It sets direct discharge and pretreatment standards for existing and future pesticide chemical manufacturing plants. The principal groups of chemicals involved are phenols, nitrosamines, cyanide, copper, zinc, ammonia, and finished pesticides. EPA estimates that the new rule will result in the removal of nearly 2 million lb/y of pollutants, including almost 1.14 million lb/y of toxic substances.

EPA has established the Environmental Methods Testing Site in Chattanooga, Tenn., to conduct field evaluations of environmental monitoring equipment and research techniques and to assess methods of measuring or predicting exposure to chemical compounds. Chattanooga was chosen because of its mix of topographical features, industries, climate, and pollution. Studies carried out at the site should provide a comprehensive data base that will allow future field tests to be carried out at lower costs. The site was established in accordance with the requirements of the Toxic Substances Control Act of 1976, which directs EPA to develop and refine methods for assessing human exposure to toxic substances.

EPA revoked existing secondary or welfare-based standards for carbon monoxide in September on the grounds that there is no damage to vegetation or materials caused by CO concentrations normally found in ambient air. The agency had planned to make certain minor revisions to the primary or health-based standards, but these will be deferred until new scientific data indicate the need for a change. The primary standard, as monitored over an eight-hour

period, will stay at 9 ppm. For CO monitored over a one-hour period, the standard will remain at 35 ppm. The standards may be exceeded only once each year.



*Stenholm: Toxic cleanup legislation*

A bill requiring EPA to create an office to promote and oversee demonstration projects for Superfund technology was introduced by Rep. Charles Stenholm (D-Tex.). Stenholm remarked that H.R. 3211, which was introduced Aug. 1, "would relieve a regulatory paralysis that is holding back technological innovation." He explained that most private developers of new cleanup technologies "are small businesses or individuals who cannot demonstrate their techniques at hazardous waste sites on the National Priority List because of the regulatory structure of Superfund." Stenholm expresses hope that new techniques "will lead to the detoxification, destruction, or reuse of waste, rather than its removal and redistribution."

EPA intends to cancel the registration of daminozide, a pesticide used primarily on apples but also applied to other fruits and vegetables. The agency has submitted the proposed cancellation to its scientific advisory panel, as required by the Federal Insecticide, Fungicide, and Rodenticide Act. Research conducted by EPA has determined that unreasonable health risks result from long-term exposure to the pesticide; the chemical has shown carcinogenic effects on rats and mice. A metabolic by-product also is suspected of causing can-

cer. Daminozide, the trade name for which is Alar, was registered in 1963 by Uniroyal, its only registrant.

## STATES

**New York State's Department of Environmental Conservation proposed regulations in late August** that will require reduced sulfur content of oil and coal fuels. The new rules, slated to go into effect Jan. 1, 1988, would reduce the limit on sulfur in fuel oil from 2% to 1%. The limit on sulfur in coal would be lowered from 2.5 lb/million Btu to 1.7 lb/million Btu. The department expects the new rules to result in an annual reduction of SO<sub>2</sub> emissions in the state to 146,000 t below the 1980 level of 857,000 t.



*Tschinkel: National groundwater law*

**Florida's Secretary of Environmental Regulation has called for a national groundwater protection act.** Victoria Tschinkel suggests that the level of protection given to a drinking-water aquifer may vary from state to state but that it should not fall below an EPA-established minimum. Tschinkel told a U.S. Senate committee in June that most states support EPA's current policy, which leaves the implementation of groundwater protection to the states. She added, however, that many of the states will find groundwater protection hard to carry out without financial assistance from the federal government. Tschinkel notes that Florida is the only state that requires testing of drinking water; it tests for almost 120 potential contaminants.

**The Virginia State Water Control Board has received a grant of \$148,700 from EPA to develop a comprehensive groundwater protection strategy for the state.** The strategy will include an assessment of existing state activities in this field and a plan for improvements. A spokesman said that one important facet of the program will be the development of a data base on ground-

water availability, use, and contamination. He added that the data base will help Virginia authorities combat several problems with groundwater protection, including those associated with leaking surface impoundments, septic tanks, and underground storage tanks.

**Three of Idaho's water quality standards may be overruled by EPA.** Agency representatives announced in August that EPA will require the state to tighten standards for dissolved oxygen (DO) and ammonia and that the state must rescind an exemption from meeting water quality standards accorded to operators of dams (*Fed. Regist.* 1985, 50, 33672). Current state standards allow DO concentrations of no less than 5 mg/L; EPA wants a cold-water DO standard of 9.5 mg/L, based on a seven-day mean, and a warm-water standard of 5.5 mg/L, based on a 30-day mean. The revised standards' principal objective is the protection of fish. The ammonia standards would vary according to the temperature and acidity of the receiving water.

**Cities that have not yet complied with the Clean Water Act were to explain to EPA how they will provide secondary sewage treatment before July 1, 1988, or be subject to enforcement actions by the agency.** The explanations were due Sept. 30. As many as 230 cities could be affected, and spokesmen for some of the cities say that sewage treatment deadlines could not be met because of huge capital costs and limited funds now available under federal grant programs. EPA maintains that cities must comply with the Clean Water Act regardless of whether they receive federal aid.

## SCIENCE

**To find out why forests are declining,** the Electric Power Research Institute (EPRI, Palo Alto, Calif.) and other organizations are sponsoring research in the U.S., Scandinavia, West Germany, and other parts of Europe. The research concerns climatic stress, management practices, acid deposition, and pollutants such as ozone and heavy metals. An article in the September 1985 issue of *EPRI Journal* explains that although scientists agree that forest decline is a problem, they disagree about its causes and about what strategies should be used to combat it. Some experts call for remedial action "now, before it's too late"; others

argue that it is futile to take any action until the causes and mechanisms of forest decline are determined through scientific study.

**Guidelines for the selection and use of mathematical models in evaluating the effectiveness of remedial action at uncontrolled hazardous waste sites** were published by EPA's Environmental Research Laboratory (Athens, Ga.) in August. They are intended to assist regulatory officials in incorporating models into the planning process for remedial action at federal and state Superfund sites. For example, a model would be of help in selecting techniques for evaluating contamination problems in soil, groundwater, and surface water. The report presents practical methods for evaluating remedial action and gives examples of their use.

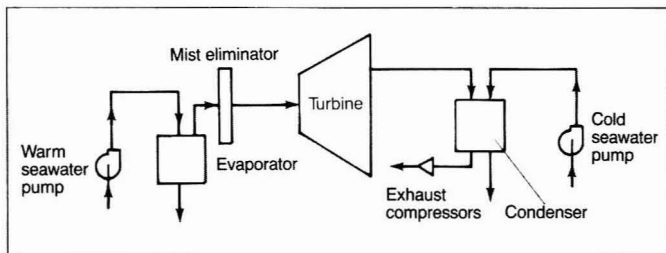
**Individuals deficient in the blood enzyme glucose 6-phosphate dehydrogenase (G6PD)** are probably not at risk from ambient levels of ozone or NO<sub>2</sub>, much of which comes from motor vehicle exhaust. In the U.S., about 2 million persons, primarily black males, have this condition. It had been believed that exposure to ozone and NO<sub>2</sub> placed these persons at risk of breakdown of their red blood cells. Marie Amuroso of Rutgers Medical School (Newark, N.J.) recently prepared a report on the subject for the Health Effects Institute (Cambridge, Mass.), the nation's center for the study of health effects of motor vehicle emissions. Amuroso's findings do not fully disprove the original hypothesis, but they do suggest that it is much less likely to be correct.

## TECHNOLOGY

**The nation's largest scale demonstration plant for atmospheric fluidized-bed combustion (AFBC)** is now under construction. It produces electricity while it burns coal cleanly (*ES&T*, October 1985, p. 894). The 160-MW facility will be located at the Shawnee Steam Plant (Paducah, Ky.), which is operated by the Tennessee Valley Authority (TVA). The process will allow utility companies to burn high-sulfur, high-ash coal without using expensive flue gas desulfurization systems, according to TVA. An AFBC power plant is expected to have capital and operating costs 10-15% lower than its conventional coal-burning counterpart. Completion is expected in mid-1988, and the demonstration project will continue until 1992.



## Experimental open-cycle OTEC system



Source: SERI In Review, July 1985

**An open-cycle ocean thermal energy conversion (OTEC) system** is being developed by the Solar Energy Research Institute (SERI, Golden, Colo.). The system works by condensing a fluid in a vessel located in deep, cold ocean water and then pumping the fluid up to a portion of the system in shallower, warmer water where the fluid boils and powers an electricity-generating turbine. SERI's 165-kW OTEC system is designed for installation at the Natural Energy Laboratory in Hawaii. At that site, the difference in temperature between cold ocean bottom water and near-surface water approaches 20 °C, which is suitable for a trial.

**A demonstration project for the disposal of sewage sludge on land** was carried out by EPA's Water Engineering Research Laboratory (Cincinnati, Ohio). Sewage sludge from three Ohio cities and one county was applied to agricultural land in Ohio over a period of several years. The aim was to detect any sludge-related health risks to rural residents and their livestock. The study showed that health risks are insignificant when sludge is applied at low rates. It also showed that municipalities—in this case, Columbus, Springfield, and Defiance—can work cooperatively with large numbers of farmers in the implementation of this kind of project.

**Microbes will manufacture the pesticides of the future**, Alan Putnam of Michigan State University (East Lansing) told the Chicago meeting of the American Chemical Society. He predicts the formation of insecticides and other pesticides by bacteria, fungi, and actinomycetes and foresees that such compounds will pose less environmental danger than many chemical compounds in use now. Putnam is investigating

allelochemicals, compounds plants manufacture to fight off insects, diseases, and weeds. Allelochemicals also are being studied for pesticidal performance by the U.S. Agricultural Research Service (Beltsville, Md.). One promising source may be the neem tree, native to parts of tropical Asia and Africa, which produces a compound that deters more than 80 pest species.

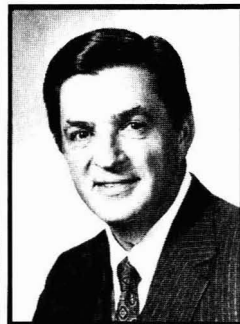
## BUSINESS

**Representatives of the chemical industry and environmental advocates have announced** that they have reached an agreement about how to reauthorize the Federal Insecticide, Fungicide, and Rodenticide Act (FIFRA). The agreement breaks a 13-year deadlock. Among the proposed changes to FIFRA are a pesticide reregistration fee industry would pay to help defray costs for additional health and safety studies EPA would have to complete within two years of reauthorization. Other changes are a speed-up in the cancellation process for pesticides deemed to endanger health or the environment, a requirement for registration of inert components of pesticides—if those compounds are found to threaten health—and public notification on possible health and safety effects of pesticides before they are registered (current law requires such notification only after registration).

**Engineering-Science (Arcadia, Calif.) has begun the last phase of a project to evaluate the safety of using reclaimed municipal wastewater to irrigate crops of vegetables that are eaten raw.** This portion of the 10-year, \$9-million contract, awarded by the Monterey Regional Water Pollution Control Agency, involves exhaustive analysis of data collected from nearly 75,000 samples of water, soils, and crops grown in 96 test

plots. The crops being tested include two varieties of lettuce and cauliflower, broccoli, and celery. Extensive tests of survival and transmission of viruses from the wastewater have so far shown that the viruses pose no threat. A final report is due next fall.

**The first contract under Superfund to clean up contaminated groundwater** was awarded to Metcalf & Eddy (Boston, Mass.). The New Hampshire Water Supply and Pollution Control Commission awarded the contract, which calls for treating 130 million gal of contaminated groundwater at a Superfund site in Nashua, N.H. Removed pollutants will be burned in a closely monitored fume incinerator, and treated residuals will be placed in a secure on-site landfill. When groundwater treatment is complete, the site will be closed and the landfill will be covered with vegetation. Operations are scheduled to start this month and last for two years.

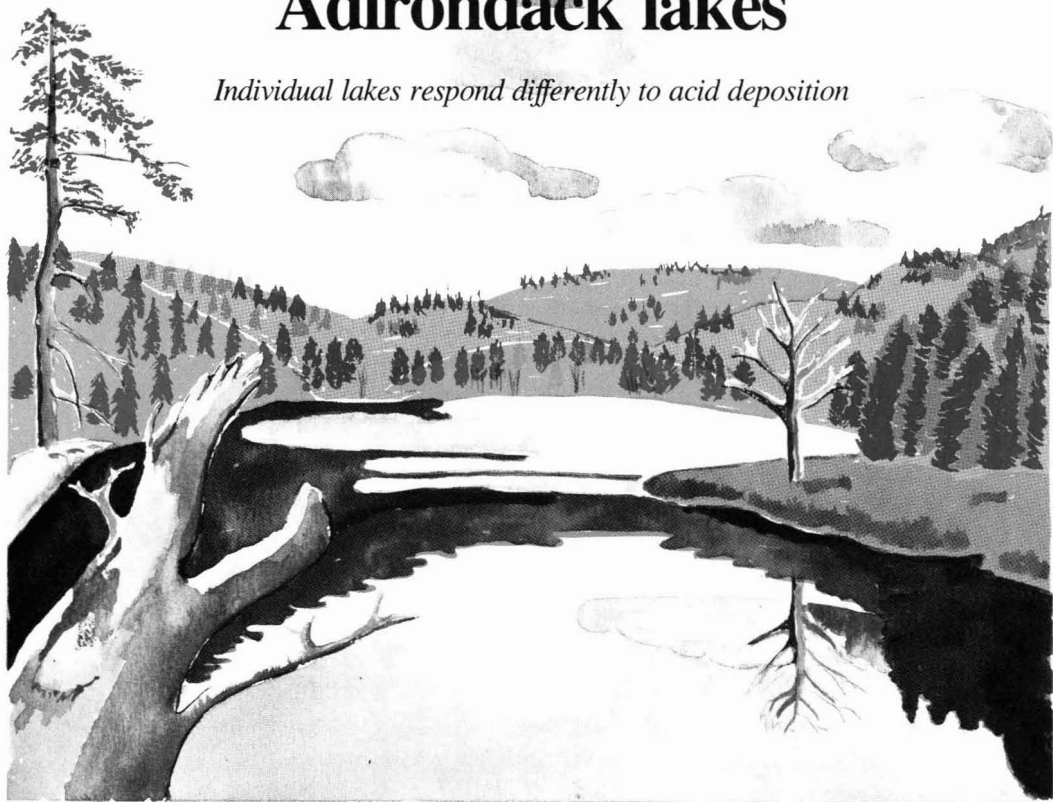


Corbett: Strengthen protection

**A Monsanto executive says that existing programs to curb pollution of groundwater** can be strengthened by local, state, and federal governments "provided we continue moving at a deliberate pace." Harold Corbett, senior vice-president of Monsanto, told a conference of the National Association of Towns and Townships that groundwater does not pose "the sort of emergency situation that prevailed with air and water pollution in the late 1960s." Corbett added, "We cannot write off polluted groundwater that may be needed for drinking or other high-purity uses, but on the other hand, we cannot afford to clean up rigorously every polluted groundwater source, regardless of its use." He suggested that state and local governments should be responsible for groundwater management, with aid from the federal government.

# Chemical characteristics of Adirondack lakes

*Individual lakes respond differently to acid deposition*



**Charles T. Driscoll**  
Syracuse University  
Syracuse, N.Y. 13210

**Robert M. Newton**  
Smith College  
Northampton, Mass. 01063

There is much concern over the role of atmospheric deposition of mineral acids in the acidification of low-ionic-strength (dilute) surface waters in remote regions. Surface water acidification has been attributed to atmospheric deposition of  $\text{H}_2\text{SO}_4$  (or  $\text{SO}_2$ ) (1) and  $\text{HNO}_3$  (2), the oxidation of organic nitrogen from soil, the production of soluble organic acids through the decay of

dead plant and animal material in soil (3), the oxidation of naturally occurring sulfide minerals (4), and changes in land use (5, 6).

In the northeastern U.S., many areas are sensitive to mineral acidity. Acid-sensitive watersheds are generally underlain by granitic bedrock and have small pools of readily available (exchangeable or easily weatherable) basic cations ( $\text{C}_B$ ;  $\text{Ca}^{2+}$ ,  $\text{Mg}^{2+}$ ,  $\text{Na}^+$ ,  $\text{K}^+$ ).

These watersheds are also characterized by an inability to retain inputs of acidic anions ( $\text{SO}_4^{2-}$ ,  $\text{NO}_3^-$ ,  $\text{Cl}^-$ ). That is, atmospheric inputs are transported through the watershed, rather than being retained. Therefore, high loadings of acidic anions will not be attenuated

in the soil but will be removed from the watershed with drainage water. Anionic solutes must be accompanied by an equivalent charge of cations to maintain electroneutrality (charge balance). Complete neutralization of acidity can be accomplished by the dissolution or exchange of basic cations within the soil.

In the absence of readily available pools of basic cations, however, neutralization will be incomplete, and acidic cations— $\text{H}^+$ , labile monomeric Al ( $\text{Al}^{\text{m}+}$ )—will be transported from the soil to the surface water (7). The effects of this process cause concern because high concentrations of acidic cations appear to be harmful to aquatic biota

and surface water quality (8-11).

The research reported here was conducted as part of the Regionalized Integrated Lake-Watershed Acidification Study (RILWAS), the objectives of which are discussed in detail elsewhere (12). Our intent was to evaluate the general chemical characteristics of lakes in the Adirondack region of New York and to assess the mechanisms that regulate the acid-base chemistry of these waters.

### Study sites and methods

Twenty lakes and watersheds in the Adirondacks were sampled for a period of 26 months at approximately monthly intervals (Figure 1; Table 1). More intensive sampling was done during spring snowmelt. Samples were collected from drainage lake outlets and seepage lake surfaces. In an effort to evaluate mechanisms that control the sensitivity of Adirondack lakes to acidification, the study lakes were selected to include a range of geologic and hydrologic characteristics (Table 1).

The analytical methods used in this study are summarized in Table 2. Samples were measured for temperature and pH and extracted for monomeric Al in the field to minimize transformations (e.g., changes in temperature and degassing of  $\text{CO}_2$ ) that might alter the measurements of pH and Al. Samples were refrigerated after collection and transported to a laboratory at Syracuse University. There they were analyzed for dissolved inorganic carbon (DIC) and nitrogen forms, placed in ampules for the determination of dissolved organic carbon (DOC), and processed for the determination of nonlabile monomeric Al. These samples were analyzed as soon after collection as possible, generally within 72 h. Samples were stored at 4 °C until all analytical determinations had been made.

The distribution of DIC and labile monomeric (inorganic) Al was calculated using a chemical equilibrium model. The equilibrium constants and enthalpy values used for this analysis are summarized elsewhere (23). Calculations were corrected for the effects of ionic strength, using the Debye-Huckel approximation for individual ion activity coefficients (24), and temperature.

Charge balance calculations were made on all samples. Cationic equivalence (charge) was assumed to be distributed among basic cations ( $\text{Ca}^{2+}$ ,  $\text{Mg}^{2+}$ ,  $\text{Na}^+$ ,  $\text{K}^+$ ),  $\text{NH}_4^+$ ,  $\text{H}^+$ , and  $\text{Al}^{3+}$ . The charge equivalence of  $\text{Al}^{3+}$  was calculated by determining  $\text{OH}^-$ ,  $\text{F}^-$ , and  $\text{SO}_4^{2-}$  complexes, using a chemical equilibrium model. Anionic equivalence was distributed among acidic anions ( $\text{SO}_4^{2-}$ ,  $\text{NO}_3^-$ ,  $\text{Cl}^-$ ), free  $\text{F}^-$ ,  $\text{HCO}_3^-$ , and free organic anions

( $\text{RCOO}^-$ ). The amount of bicarbonate was calculated from DIC, pH, and temperature measurements, using the equilibrium model. The concentration of free organic anions was calculated as the difference between the charge of inorganic cations and the charge of inorganic anions. To allow a comparison between labile (inorganic) and nonlabile (organic) forms of monomeric Al, nonlabile monomeric Al was assumed to be trivalent and bound by an equivalent organic ligand.

### Chemical characteristics

The Adirondack region of New York State receives substantial atmospheric deposition of mineral acids ( $0.5\text{--}0.75$  kiloequivalents [ $\text{keq}$ ]/ha-y  $\text{SO}_4^{2-}$ ;  $0.25\text{--}0.4$   $\text{keq}/\text{ha-y}$   $\text{NO}_3^-$ ) (25). Soils within the region are generally Spodosols, which adsorb minimal quantities of  $\text{SO}_4^{2-}$  (26). Sulfate in surface waters apparently originates largely from atmospheric deposition (27, 28).

Although much of the region is underlain by acid-sensitive bedrock, the chemistry of surface waters varies widely from about neutral to acidic (29, 30). These variations are the result of the geologic and hydrologic characteristics of the different watersheds (31,

32). In some of the watersheds, natural sources of acidity significantly influence the acid-base chemistry of surface waters.

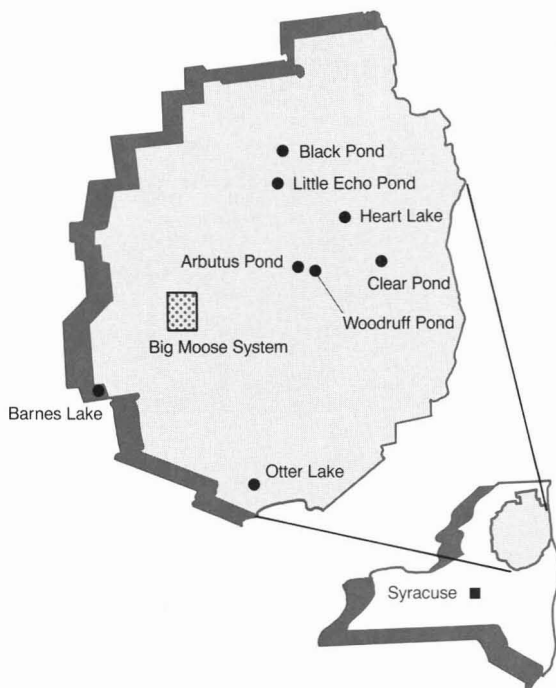
Average values of relevant chemical characteristics for the 20 lakes in this study are summarized in Table 3. There is a wide range of pH, acid-neutralizing capacity (ANC),  $\text{NO}_3^-$ ,  $\text{Ca}^{2+}$ , Al, and DOC in the lakes. Sulfate is the dominant anion in all lakes, except for the relatively insensitive Black and Woodruff ponds, in which  $\text{HCO}_3^-$  is the major anion. There is a relatively narrow range of  $\text{SO}_4^{2-}$  concentrations among Adirondack drainage lakes ( $106\text{--}154$   $\mu\text{eq/L}$ ; this range does not include Barnes Lake and Little Echo Pond, which are seepage lakes).

We have selected a subset of five lakes to illustrate the range in chemical compositions of Adirondack waters (Figure 2). A study of the chemistry of these lakes, together with the geology and hydrology of their watersheds, allows us to make an evaluation of the significant processes controlling sensitivity to acid deposition.

### Seepage lakes

Seepage lakes are those that have no surface inlets or outlets. They are gen-

FIGURE 1  
Adirondack lakes in the study<sup>a</sup>



<sup>a</sup>Sites not specifically indicated are located within the Big Moose system



TABLE 1

## Location and physical characteristics of Adirondack study lakes and their watersheds

Lake	Location	Elevation (m)	Lake type	Surficial geology	Maximum depth (m)	Surface area (ha)	Volume (10 <sup>6</sup> m <sup>3</sup> )
Arbutus Pond	43°58'N, 74°14'W	513	Drainage	Thin/thick till	8.4	50	146
Barnes Lake	43°34'N, 75°14'W	397	Seepage	Glacial sand	9.0	5.1	7.7
Big Moose Lake	43°49'N, 74°53'W	557	Chain drainage	Thin till	22.0	520	3600
Black Pond	44°26'N, 74°18'W	494	Drainage	Thick till/stratified drift	14.0	32	199
Bubb Lake	43°57'N, 74°51'W	554	Chain drainage	Thin till	3.0	20	42
Cascade Lake	43°48'N, 74°53'W	554	Drainage	Thin/thick till	5.0	40	172
Clear Pond	43°59'N, 74°50'W	582	Drainage	Thin/thick till	24.0	73	660
Constable Pond	43°49'N, 74°50'W	584	Chain drainage	Thin till	4.0	23	45
Darts Lake	43°48'N, 74°53'W	536	Chain drainage	Thin till	16.0	144	415
Heart Lake	44°26'N, 74°18'W	662	Drainage	Thin/thick till	13.0	11	54
Little Echo Pond	44°18'N, 74°22'W	481	Seepage	Sphagnum bog	5.0	0.8	2.8
Merriam Lake	43°51'N, 74°51'W	651	Drainage	Thin till	4.9	7.8	11.5
Moss Lake	43°46'N, 74°51'W	536	Chain drainage	Thin/thick till	15.0	45	272
Otter Lake	43°11'N, 74°30'W	488	Chain drainage	Thin till	4.5	10	22
Lake Rondaxe	43°11'N, 74°55'W	525	Chain drainage	Thin/thick till	10.0	92	220
Squash Pond	43°48'N, 74°51'W	650	Drainage	Thin till	7.0	3.9	7.2
Townsend Pond	43°48'N, 74°51'W	561	Drainage	Thin till	—	—	—
West Pond	43°48'N, 74°52'W	579	Drainage	Peat/thin till	4.0	12	—
Windfall Pond	43°48'N, 74°51'W	595	Drainage	Thin till	5.5	1.5	4.9
Woodruff Pond	43°48'N, 74°10'W	470	Drainage	Carbonate; thin/thick till	3.4	18.1	34

TABLE 2

## Chemical characteristics analyzed in the study

Characteristics	Methods	Reference
SO <sub>4</sub> <sup>2-</sup> , NO <sub>3</sub> <sup>-</sup> , Cl <sup>-</sup>	Ion chromatography	13
NH <sub>4</sub> <sup>+</sup>	Phenate colorimetry; autoanalysis	14
Ca <sup>2+</sup> , Mg <sup>2+</sup> , Na <sup>2+</sup> , K <sup>+</sup>	Atomic absorption spectroscopy (AAS)	15
pH	Potentiometric with glass electrode; field measurement	16
Acid neutralizing capacity (ANC)	Strong acid titration with Gran plot analysis	17
Dissolved inorganic carbon (DIC)	Syringe stripping of CO <sub>2</sub> ; gas chromatography	18
Dissolved organic carbon (DOC)	Filtration; persulfate oxidation; syringe stripping of CO <sub>2</sub> ; gas chromatography	19
Dissolved silica	Heteropoly blue complex colorimetry; autoanalysis	16
Total F	Potentiometric with ion-selective electrode after addition of total ionic strength adjustment buffer	20
Monomeric Al	Field extraction by 8-hydroxy quinoline into methylisobutyl ketone; analysis by AAS; graphite furnace atomic absorption	21, 22
Nonlabile monomeric Al	Fractionation by ion exchange column; analysis for monomeric Al	22
Specific conductance	Conductivity bridge	16
Temperature	Thermometer	

erally found in areas covered by highly permeable glaciofluvial sand and gravel. The two seepage lakes in this study are isolated from the surrounding groundwater systems. Barnes Lake is a perched clearwater seepage lake isolated above the regional water table by organic-rich bottom sediments (Figure 3a). Little Echo Pond is a brownwater seepage lake surrounded by thick (~8 m) peat deposits (Figure 3b). The low permeability of the peat prevents significant movement of groundwater into this lake.

The concentrations of C<sub>B</sub>, Al, and dissolved Si are low in both lakes (Figure 2). These low concentrations and the hydrology of the two lakes are indications that water enters primarily from precipitation. The lack of surface runoff or groundwater in the lakes is the reason the waters are deficient in dissolved Si and contain low concentrations of Al, despite their low pH. Lakes that receive most of their water directly from precipitation are extremely sensitive to atmospheric deposition.

Although both lakes are acidic, there

are significant differences in their chemical characteristics. The dominant anion in Barnes Lake is SO<sub>4</sub><sup>2-</sup>; in Little Echo Pond there appear to be comparable concentrations of SO<sub>4</sub><sup>2-</sup> and organic anions (on an equivalence basis), demonstrated by the large discrepancy in charge balance. This relatively large concentration of organic anions is consistent with the high concentrations of DOC in Little Echo Pond. Although much of the acidity of the pond can be attributed to atmospheric deposition of H<sub>2</sub>SO<sub>4</sub>, it appears that the peat deposits and the sphagnum mat surrounding the pond release substantial quantities of naturally occurring organic acids. These substances then dissociate and contribute to overall acidity.

### Drainage lakes

The chemistry of drainage lakes, for example, Merriam Lake, West Pond, and Cascade Lake (Figure 2), is considerably different from that of seepage lakes. Drainage lakes have outlet streams and receive water by stream discharge and seepage, as well as by direct atmospheric deposition. The higher ionic strength and higher concentrations of C<sub>B</sub> and dissolved Si are the result of contact between the drainage water and the soil (Figure 4).

Merriam Lake contains highly acidic drainage water. It is a headwater lake into which water drains from very shallow (<1-m deep) acidic soil. Because of a lack of readily available C<sub>B</sub>, the neutralization of mineral acid deposited in this catchment is accomplished in part by the dissolution of Al in the soil. Consequently, SO<sub>4</sub><sup>2-</sup> is the dominant anion and H<sup>+</sup> and Aln<sup>+</sup> are found in significant concentrations.

TABLE 3  
Chemical characteristics of Adirondack study lakes<sup>a</sup>

Lake	pH	ANC (μeq/L)	NO <sub>3</sub> <sup>-</sup> (μeq/L)	SO <sub>4</sub> <sup>2-</sup> (μeq/L)	Ca <sup>2+</sup> (μeq/L)	Monomeric Al (μmol/L)	DOC (μmol/L)
Arbutus Pond	6.2 ± 0.3	58 ± 21	10 ± 6	141 ± 10	152 ± 11	1.0 ± 0.6	420 ± 65
Barnes Lake <sup>b</sup>	4.7 ± 0.1	-14 ± 10	2 ± 3	65 ± 12	30 ± 4	1.1 ± 0.6	450 ± 136
Big Moose Lake	5.1 ± 0.1	1 ± 10	24 ± 5	140 ± 11	93 ± 10	8.9 ± 2.7	340 ± 78
Black Pond	6.8 ± 0.2	200 ± 21	4 ± 5	130 ± 3	191 ± 11	0.3 ± 0.6	350 ± 65
Bubb Lake	6.1 ± 0.2	41 ± 28	16 ± 7	131 ± 14	108 ± 13	1.8 ± 1.3	280 ± 82
Cascade Lake	6.5 ± 0.3	95 ± 52	29 ± 9	139 ± 10	159 ± 24	2.8 ± 1.9	310 ± 92
Clear Pond	7.0 ± 0.2	100 ± 19	1 ± 2	139 ± 11	157 ± 21	0.8 ± 0.7	320 ± 64
Constable Pond	5.2 ± 0.6	8 ± 22	17 ± 12	149 ± 19	98 ± 10	10.5 ± 4.3	420 ± 80
Darts Lake	5.2 ± 0.2	6 ± 12	24 ± 5	139 ± 7	97 ± 9	7.6 ± 2.7	320 ± 86
Heart Lake	6.4 ± 0.3	43 ± 12	5 ± 6	106 ± 11	119 ± 12	0.6 ± 0.6	310 ± 51
Little Echo Pond <sup>b</sup>	4.3 ± 0.1	-51 ± 17	0 ± 0	78 ± 17	36 ± 6	1.2 ± 0.5	1100 ± 153
Merriam Lake	4.5 ± 0.2	-25 ± 15	21 ± 13	137 ± 11	58 ± 7	19.0 ± 0.6	480 ± 110
Moss Lake	6.4 ± 0.2	66 ± 25	26 ± 6	141 ± 8	146 ± 15	2.2 ± 1.6	310 ± 61
Otter Lake	5.5 ± 0.5	13 ± 16	9 ± 9	138 ± 21	88 ± 11	5.0 ± 3.6	200 ± 54
Lake Rondaxe	5.9 ± 0.5	33 ± 25	23 ± 6	134 ± 7	112 ± 10	4.4 ± 3.0	300 ± 60
Squash Pond	4.6 ± 0.6	-22 ± 39	24 ± 17	131 ± 18	65 ± 28	19.2 ± 7.6	580 ± 127
Townsend Pond	5.2 ± 0.6	18 ± 21	27 ± 15	154 ± 30	95 ± 16	9.9 ± 7.9	260 ± 81
West Pond	5.2 ± 0.5	29 ± 50	10 ± 6	111 ± 13	94 ± 24	6.6 ± 2.1	670 ± 204
Windfall Pond	5.9 ± 0.4	44 ± 30	26 ± 14	141 ± 17	143 ± 19	5.6 ± 2.4	390 ± 92
Woodruff Pond	6.9 ± 0.2	410 ± 140	2 ± 3	147 ± 17	430 ± 120	1.0 ± 1.1	710 ± 161

<sup>a</sup> Arithmetic mean and standard deviations shown for the samples collected  
<sup>b</sup> Barnes and Little Echo are seepage lakes; the others are drainage lakes

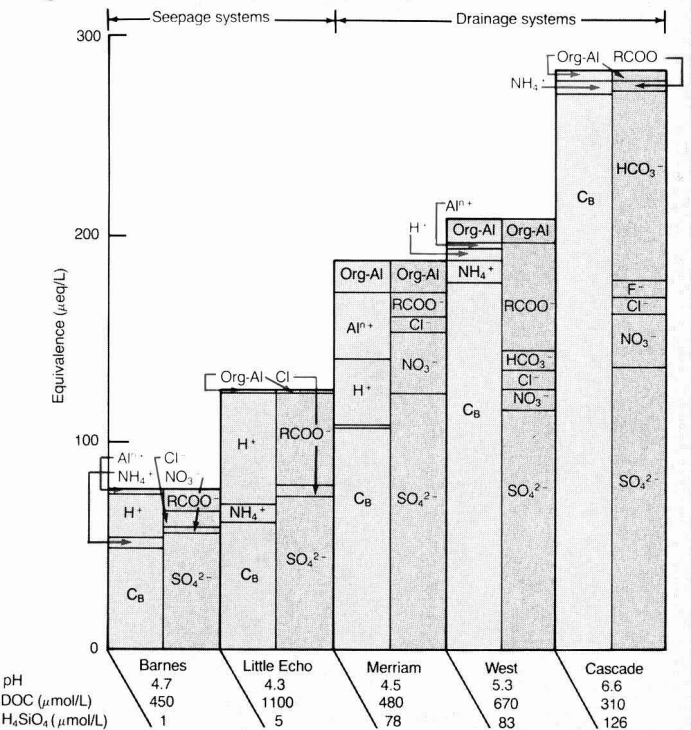
Although SO<sub>4</sub><sup>2-</sup> is the predominant anion in Merriam Lake waters, elevated concentrations of NO<sub>3</sub><sup>-</sup> and, to a lesser extent, organic anions also may contribute to the acidity. The modest concentrations of DOC, organic anions, and nonlabile monomeric Al probably are indicators of the importance of forest floor mineralization processes in the shallow acidic soils within the watershed.

Nitrate represents a significant source of acidity in many Adirondack drainage lakes (33). Moreover, short-term increases in H<sup>+</sup> and Al<sup>3+</sup> that occur in chronically acidic lakes during hydrologic events are associated with NO<sub>3</sub><sup>-</sup> inputs (33). The source of the NO<sub>3</sub><sup>-</sup> is unclear, but it may be the result of snow or seasonal variations in the mineralization and assimilation of nitrogen by terrestrial biota and microorganisms.

The chemistry of Merriam Lake is characteristic of chronically acidic lakes. In these lakes, the equivalence of SO<sub>4</sub><sup>2-</sup> exceeds that of C<sub>B</sub> and NH<sub>4</sub><sup>+</sup>. This difference suggests that H<sup>+</sup> and Al<sup>3+</sup> acidity is largely the result of sulfuric acid deposition. Aluminum in clearwater acidic lakes such as Merriam occurs primarily in an inorganic (labile) form (aquo Al and Al in OH<sup>-</sup>, F<sup>-</sup>, and SO<sub>4</sub><sup>2-</sup> complexes), which is thought to be toxic to fish (10, 34, 35) and other aquatic life (36).

West Pond is a bog drainage system with thick deposits of peat that cover a large area immediately adjacent to the pond. Although the pond is characteris-

FIGURE 2  
Charge distribution in Adirondack lake waters<sup>a</sup>



<sup>a</sup> Values represent 26-month averages  
Barnes and Little Echo are clearwater and brownwater seepage ponds, respectively; Merriam, West, and Cascade are acidic, bog, and neutral pH drainage lakes, respectively  
C<sub>B</sub> is the sum of basic cation (Ca<sup>2+</sup>, Mg<sup>2+</sup>, Na<sup>+</sup>, K<sup>+</sup>) equivalence  
The equivalence of labile monomeric Al (Al<sup>3+</sup>) is calculated by considering the various inorganic complexes  
Nonlabile monomeric Al (Org-Al) is assumed to be trivalent and balanced by an equivalent organic ligand  
Free organic anions are calculated as the difference between inorganic cations and inorganic anions

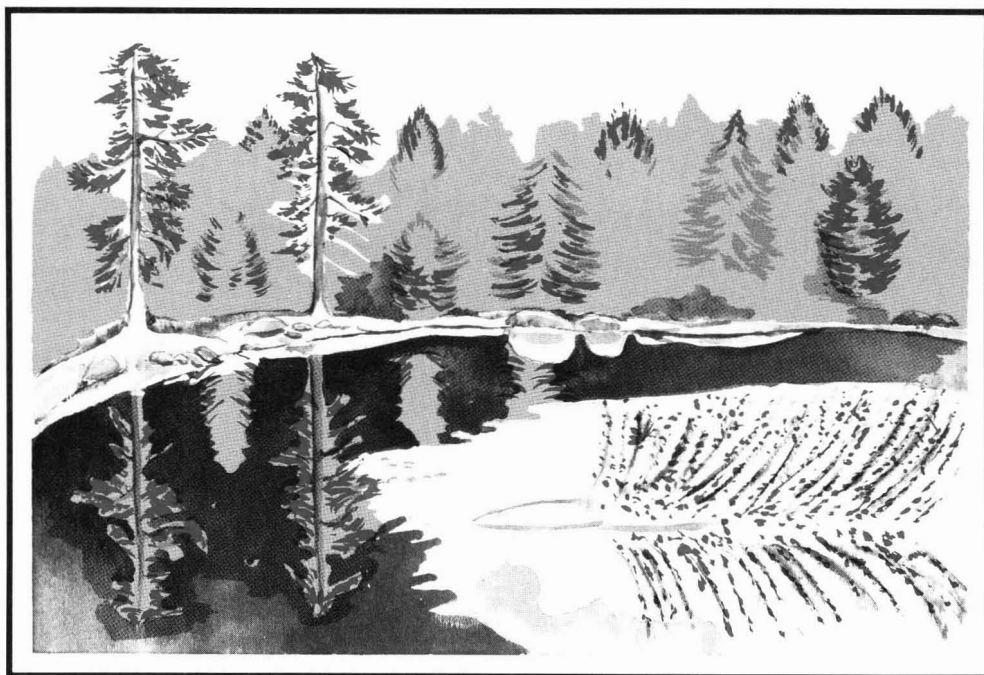
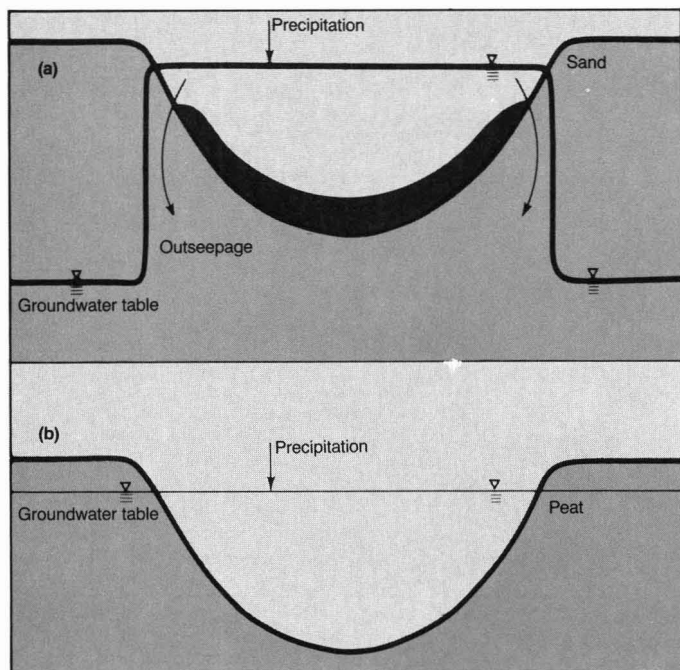


FIGURE 3  
Acid-sensitive seepage lakes<sup>a</sup>



<sup>a</sup>Surface water in these lakes is isolated from the surrounding groundwater. In perched seepage lakes (a) the water is above the regional groundwater table because of the low permeability of organic rich bottom sediments. Bog seepage lakes (b) are surrounded by thick peat deposits that restrict significant movement of groundwater into the lake. Solute concentrations in isolated seepage lakes are strongly influenced by atmospheric deposition.

tically acidic, unlike clearwater acidic lakes its acidity is attributed to sulfuric and organic acids alike. Because West Pond is surrounded by thick organic peat deposits, most of the Al appears to be associated with organic matter (in the nonlabile monomeric form) and therefore is probably less toxic to aquatic organisms than the labile inorganic form of Al (10, 35).

Cascade Lake is generally illustrative of Adirondack waters that are relatively insensitive to atmospheric deposition of mineral acids. Although there are significant concentrations of  $\text{SO}_4^{2-}$  in the drainage waters, deposition of acids appears to be entirely compensated for by the dissolution of  $\text{C}_B$  from the soil. The high concentrations of  $\text{HCO}_3^-$  and dissolved Si indicate that the extent of weathering reactions is greater there than in more acidic lake systems. In part, these trends are the result of thick till deposits (that is, soil and gravel deposited by prehistoric glaciation) within the catchment area that allow the waters that move through the watershed to have greater contact with the mineral soil (Table 1).

The approximately neutral pH values and low DOC concentrations in Cascade Lake are consistent with the low concentrations of monomeric Al. The low concentrations of Al appear to be associated largely with organic solutes (in a nonlabile monomeric form).

#### Differences in lake chemistry

It is evident that there are profound lake-to-lake variations in sensitivity to

acidification and acidification processes. The southern and western Adirondacks receive the highest loading of  $\text{SO}_4^{2-}$ , whereas the northeastern section receives less (25). Although there are differences in the atmospheric loading of  $\text{SO}_4^{2-}$  in the Adirondacks, these intraregional variations appear minor, as evidenced by the uniform  $\text{SO}_4^{2-}$  concentrations found in drainage waters (Table 3).

Differences in lake sensitivity and water chemistry are largely the result of variations in water flow paths and in the contact of water with the surrounding surficial geology (Figures 3 and 4) (31, 32). For example, the presence of thick peat deposits can have a profound effect on water chemistry. Waters that come into contact with such deposits are rich in organic acids, which contribute to acidity and bind potentially toxic forms of Al. The brownwater lakes are probably naturally acidic, although deposition of  $\text{SO}_4^{2-}$  undoubtedly has enhanced their acidity (e.g., Little Echo and West ponds; Figure 2).

Clearwater lakes show a distinct range in sensitivity to acid deposition. This sensitivity is a function of flow paths of water through catchments or of the presence of weatherable minerals (e.g., calcite) or both. Seepage lakes isolated from the local water table (e.g., Barnes Lake) are extremely sensitive to strong acids because of the minimal contact of water with the mineral soil and therefore the minimal neutralization of acidity from the release of  $\text{C}_B$  (Figure 3).

Waters that drain from shallow acidic soils also are sensitive to mineral acids. Pools of exchangeable or easily weatherable  $\text{C}_B$  in the soil are small, and the retention time of water in the mineral soil is short (32). Therefore,  $\text{H}^+$  neutralization is incomplete and results in the dissolution of  $\text{Al}^{3+}$  and the transport of  $\text{H}^+$  and  $\text{Al}^{3+}$  to surface waters (Figure 4).

If there is adequate contact of drainage waters with deeper mineral soil—thick till, for example—or an abundance of easily weatherable minerals, such as carbonate,  $\text{C}_B$  will be released to compensate for mineral acids and will neutralize  $\text{CO}_2$  acidity in the soil. These processes result in completely neutralized mineral acids and produce  $\text{HCO}_3^-$  in solution (Figure 4).

The sensitivity of surface water to acidification largely depends on the extent to which  $\text{C}_B$  is released relative to the deposition and retention of acidic anions. In the Adirondacks, as the equivalents of  $\text{SO}_4^{2-}$  and  $\text{NO}_3^-$  in solution approach and exceed the equivalents of  $\text{C}_B$ , neutralization of mineral acids is incomplete, and elevated concentrations of potentially harmful

acidic cations ( $\text{H}^+$ ,  $\text{Al}^{3+}$ ) are evident in surface waters (Figure 5). Although organic acids are the main cause of brownwater lake acidity,  $\text{H}_2\text{SO}_4$  and, to a lesser extent,  $\text{HNO}_3$  are predominantly responsible for the acidification of clearwater Adirondack lakes.

#### Acknowledgment

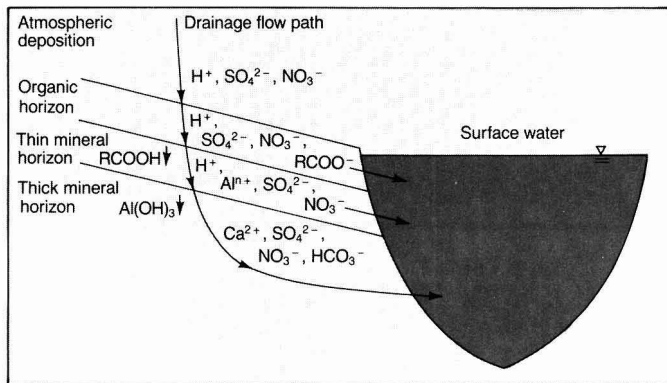
This article is Contribution No. 49 of the Upstate Freshwater Institute.

We would like to thank C. V. Bowes, F. J. Unangst, and C. Yatsko for their assistance; R. D. Fuller for his critical review of the manuscript; and R. A. Goldstein, S. A. Gherini, and C. W. Chen for their support and encouragement during the study. This research was conducted as part of the Regionalized Integrated Lake-Watershed Acidification Study, funded by the Electric Power Research Institute, Palo Alto, Calif., and Empire State Electric Energy Research Corporation, Schenectady, N.Y.

Before publication, this article was re-

FIGURE 4

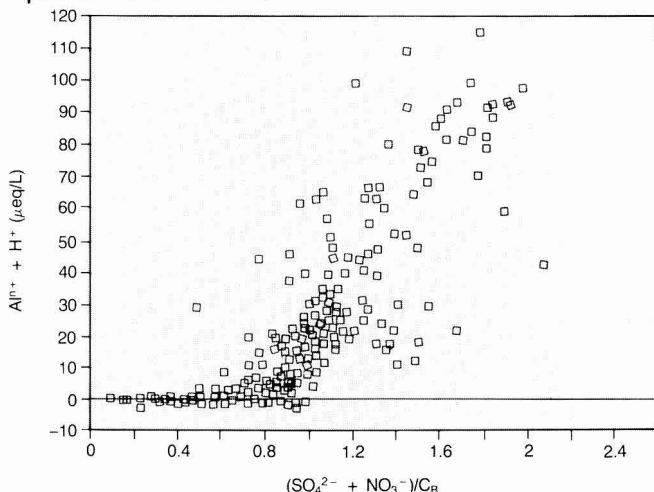
#### Chemical transformations associated with water flow paths to a drainage lake



As water containing acidic deposition migrates through organic soil and peat, the resulting solution will contain mineral and organic acids. Water moving through shallow acidic soil will deposit organic solutes and mineral acids will solubilize Al, causing a solution with concentration levels of  $\text{H}^+$  and Al. If acidic solutions are transported through thick mineral soil,  $\text{H}^+$  and Al will be neutralized by the release of basic cations

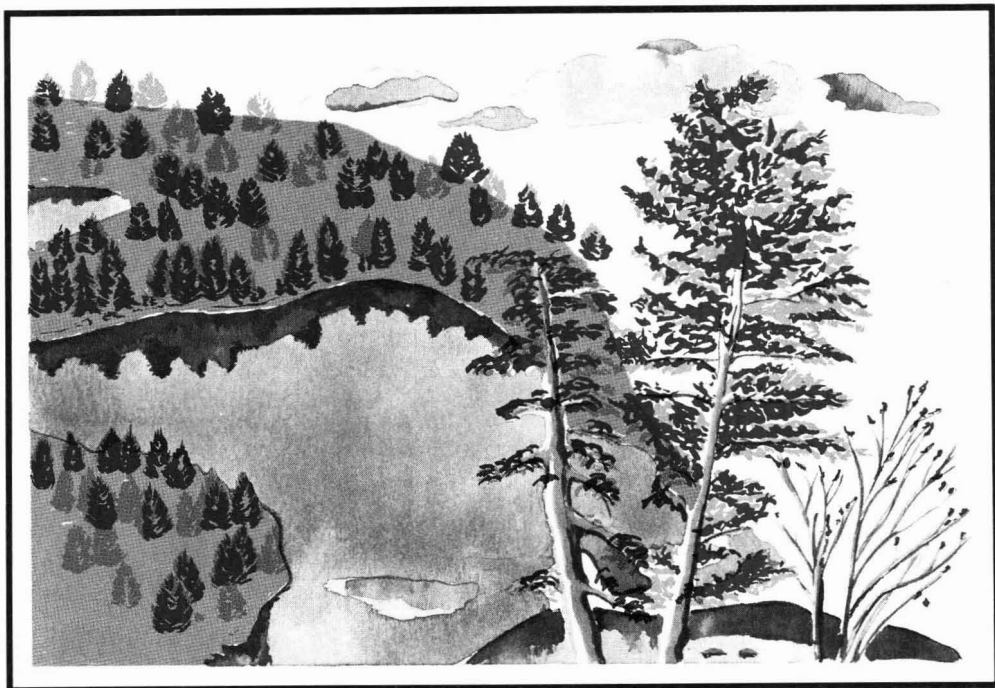
FIGURE 5

#### Equivalence of acidic cations<sup>a</sup>



<sup>a</sup>( $\text{Al}^{3+}$ ) as a function of the ratio of  $\text{SO}_4^{2-}$  and  $\text{NO}_3^-$  equivalence to basic cation ( $\text{C}_B$ ) equivalence for the 20 lakes in the study

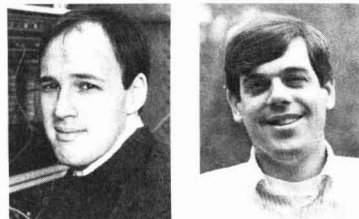




viewed for suitability as an *ES&T* feature by Magda Havas, University of Toronto, Toronto, Ont. M5S 1A4, Canada, and Steven Eisenreich, University of Minnesota, Minneapolis, Minn. 55455.

## References

- (1) Henriksen, A. *Nature* **1979**, 278, 542-45.
- (2) Galloway, J. N. et al. In "Ecological Impact of Acid Precipitation"; Drablos, D.; Tollan, A., Eds.; SNSF Project; Sur Nederskogs Pål Skog og Fisk: Oslo, Norway, 1980; pp. 264-65.
- (3) Glover, G. M.; Webb, A. H. *Water Res.* **1979**, 13, 661-67.
- (4) Everett, A. G. et al. In "Proceedings of the 2nd National Symposium on Acid Rain"; Kostik, M. D., Ed.; Greater Pittsburgh Chamber of Commerce: Pittsburgh, Pa., 1982.
- (5) Rosenqvist, I. T. "Acid Soil-Acid Water"; Ingeniørforlaget: Oslo, Norway, 1977.
- (6) Krug, E. C.; Frink, C. R. *Science*, **1983**, 221, 520-25.
- (7) van Breemen, N.; Driscoll, C. T.; Mulder, J. *Nature* **1984** 307, 599-604.
- (8) Leivestad, H. et al. In "Impact of Acid Precipitation on Forest and Freshwater Ecosystems in Norway"; Braeke, F. H., Ed.; SNSF Project FR 6/76; Sur Nederskogs Pål Skog og Fisk: Oslo, Norway, 1976; pp. 81-111.
- (9) Cronan, C. S.; Schofield, C. L. *Science* **1979**, 204, 304-6.
- (10) Baker, J. P.; Schofield, C. L. *Water Air Soil Pollut.* **1982**, 18, 289-309.
- (11) Effler, S. W.; Schafran, G. C.; Driscoll, C. T. *Can. J. Fish. Aquat. Sci.*, in press.
- (12) Goldstein, R. A. et al. *Phil. Trans. R. Soc. Lond.* **1984**, 305, 409-25.
- (13) Small, H.; Stevens, T. S.; Bauman, W. C. *Anal. Chem.* **1975**, 47, 1801-9.
- (14) "Methods for Chemical Analysis of Water and Wastes," EPA-600/4-79-020; Environmental Monitoring and Support Laboratory, EPA: Cincinnati, Ohio, 1983; pp. 350.1-1 to 350.1-6.
- (15) Slavine, W. "Atomic Absorption Spectroscopy"; Wiley-Interscience: New York, N.Y., 1968.
- (16) "Standard Methods for Analysis of Water and Wastewater," 14th ed.; American Public Health Association: Washington, D.C., 1975.
- (17) Gran, G. *Int. Cong. Anal. Chem.* **1952**, 77, 661-71.
- (18) Stainton, M. P. *J. Fish. Res. Board Can.* **1973**, 30, 1441-45.
- (19) Menzel, D. W.; Vaccaro, R. F. *Limnol. Oceanogr.* **1964**, 9, 138-42.
- (20) "Fluoride Electrodes," instruction manual; Orion Research: Cambridge, Mass., 1976.
- (21) Barnes, R. B. *Chem. Geol.* **1976**, 15, 177-91.
- (22) Driscoll, C. T. *Int. J. Environ. Anal. Chem.* **1984**, 16, 267-84.
- (23) Ball, J. W.; Nordstrom, D. K.; Jenne, E. A. "Additional and Revised Thermochemical Data for WATEQ2-A Computerized Model for Trace and Major Element Speciation in Mineral Equilibria of Natural Waters," Report No. 78-116; U.S. Geological Survey Water Resources Investigations; USGS: Menlo Park, Calif., 1980.
- (24) Stumm, W.; Morgan, J. J. "Aquatic Chemistry"; Wiley: New York, N.Y., 1981.
- (25) Stensland, G. L. In "The Acidic Deposition Phenomenon and Its Effects: Critical Assessment Review Papers"; Altschuler, A. P., Ed.; EPA: Washington, D.C., 1984; Vol. 1, pp. 8/28-8/70.
- (26) Fuller, R. D.; David, M. B.; Driscoll, C. T. *Soil Sci. Soc. Am. J.* **1985**, 49, 1034-40.
- (27) Likens, G. E. et al. "Biogeochemistry of a Forested Ecosystem"; Springer-Verlag: New York, N.Y., 1981.
- (28) Galloway, J. N. et al. In "Ecological Impact of Acid Precipitation"; Drablos, D.; Tollan, A., Eds.; SNSF Project; Sur Nederskogs Pål Skog og Fisk: Oslo, Norway, 1980; pp. 254-55.
- (29) Schofield, C. L. "Acidification of Adirondack Lakes by Atmospheric Precipitation: Extent and Magnitude of the Problem," Final Report, Project F-28-R; New York State; U.S. Fish and Wildlife Service, 1977.
- (30) Pfeiffer, M. H.; Festa, P. J. "Acidity Status of Lakes in the Adirondack Region of New York in Relation to Fish Resources," FGW-P168; New York State Department of Environmental Conservation: Albany, N.Y., 1980.
- (31) Newton, R. M.; April, R. H. *NE Environ. Sci.* **1982**, 1, 143-50.
- (32) Chen, C. W. et al. *Water Resour. Res.* **1984**, 20, 1875-82.
- (33) Driscoll, C. T.; Schafran, G. C. *Nature* **1984**, 310, 308-10.
- (34) Henriksen, A.; Skogheim, O. K.; Roseland, B. O. *Vatten* **1984**, 40, 255-60.
- (35) Driscoll, C. T. et al. *Nature* **1980**, 284, 161-64.
- (36) Hall, R. J. et al. *Limnol. Oceanogr.* **1985**, 30, 212-20.



**Charles T. Driscoll** (l.) is a professor of civil engineering at Syracuse University. He holds a B.S. from the University of Maine and an M.S. and a Ph.D. from Cornell University. His research interests include the chemistry and transport of elements in lakes and forested ecosystems.

**Robert M. Newton** (r.) is an associate professor of geology at Smith College. He received a B.A. from the University of New Hampshire, an M.S. from the State University of New York, at Binghamton, and a Ph.D. from the University of Massachusetts. His research interests include surficial geology and hydrogeochemistry.



All forward thinking environmental scientists depend on ES&T. They get the most authoritative technical and scientific information on environmental issues—and so can you! Have *your own*

subscription delivered directly to you each month!

☐ **YES!** Enter my own subscription to *ENVIRONMENTAL SCIENCE & TECHNOLOGY* at the rate I've checked below: 1985

One Year	U.S.	Mexico & Canada	Europe	All Other Countries
ACS Members *	<input type="checkbox"/> \$ 26	<input type="checkbox"/> \$ 34	<input type="checkbox"/> \$ 40	<input type="checkbox"/> \$ 49
Nonmembers—Personal *	<input type="checkbox"/> \$ 35	<input type="checkbox"/> \$ 43	<input type="checkbox"/> \$ 49	<input type="checkbox"/> \$ 58
Nonmembers—Institutional	<input type="checkbox"/> \$149	<input type="checkbox"/> \$157	<input type="checkbox"/> \$163	<input type="checkbox"/> \$172

☐ Payment Enclosed (Payable to American Chemical Society)

☐ Bill Me ☐ Bill Company Charge my: ☐ VISA ☐ MasterCard

Card No. \_\_\_\_\_

Exp. Date \_\_\_\_\_ Interbank # \_\_\_\_\_ (Mastercard Only)

Signature \_\_\_\_\_

Name \_\_\_\_\_

Title \_\_\_\_\_ Employer \_\_\_\_\_

Address \_\_\_\_\_

City, State, Zip \_\_\_\_\_

Employer's Business: ☐ Manufacturing, type \_\_\_\_\_

☐ Academic ☐ Government ☐ Other \_\_\_\_\_

\*Subscriptions at these rates are for personal use only.

All foreign subscriptions are now fulfilled by air delivery. Foreign payment must be made in U.S. currency by international money order, UNESCO coupons, U.S. bank draft, or order through your subscription agency. For nonmember subscription rates in Japan, contact Maruzen Co., Ltd.

Please allow 45 days for your first copy to be mailed. Redeem until December 31, 1985.

MAIL THIS POSTAGE-PAID CARD TODAY!

3144P



All forward thinking environmental scientists depend on ES&T. They get the most authoritative technical and scientific information on environmental issues—and so can you! Have *your own*

subscription delivered directly to you each month!

☐ **YES!** Enter my own subscription to *ENVIRONMENTAL SCIENCE & TECHNOLOGY* at the rate I've checked below: 1985

One Year	U.S.	Mexico & Canada	Europe	All Other Countries
ACS Members *	<input type="checkbox"/> \$ 26	<input type="checkbox"/> \$ 34	<input type="checkbox"/> \$ 40	<input type="checkbox"/> \$ 49
Nonmembers—Personal *	<input type="checkbox"/> \$ 35	<input type="checkbox"/> \$ 43	<input type="checkbox"/> \$ 49	<input type="checkbox"/> \$ 58
Nonmembers—Institutional	<input type="checkbox"/> \$149	<input type="checkbox"/> \$157	<input type="checkbox"/> \$163	<input type="checkbox"/> \$172

☐ Payment Enclosed (Payable to American Chemical Society)

☐ Bill Me ☐ Bill Company Charge my: ☐ VISA ☐ MasterCard

Card No. \_\_\_\_\_

Exp. Date \_\_\_\_\_ Interbank # \_\_\_\_\_ (Mastercard Only)

Signature \_\_\_\_\_

Name \_\_\_\_\_

Title \_\_\_\_\_ Employer \_\_\_\_\_

Address \_\_\_\_\_

City, State, Zip \_\_\_\_\_

Employer's Business: ☐ Manufacturing, type \_\_\_\_\_

☐ Academic ☐ Government ☐ Other \_\_\_\_\_

\*Subscriptions at these rates are for personal use only.

All foreign subscriptions are now fulfilled by air delivery. Foreign payment must be made in U.S. currency by international money order, UNESCO coupons, U.S. bank draft, or order through your subscription agency. For nonmember subscription rates in Japan, contact Maruzen Co., Ltd.

Please allow 45 days for your first copy to be mailed. Redeem until December 31, 1985.

MAIL THIS POSTAGE-PAID CARD TODAY!

680

3144P



(800) 424-6747 (U.S. only)



NO POSTAGE  
NECESSARY  
IF MAILED  
IN THE  
UNITED STATES

## BUSINESS REPLY CARD

FIRST CLASS PERMIT NO. 10094 WASHINGTON D.C.

POSTAGE WILL BE PAID BY ADDRESSEE

### American Chemical Society

Periodicals Marketing Dept.

1155 Sixteenth Street, N.W.

Washington, D.C. 20036



(800) 424-6747 (U.S. only)



NO POSTAGE  
NECESSARY  
IF MAILED  
IN THE  
UNITED STATES

## BUSINESS REPLY CARD

FIRST CLASS PERMIT NO. 10094 WASHINGTON D.C.

POSTAGE WILL BE PAID BY ADDRESSEE

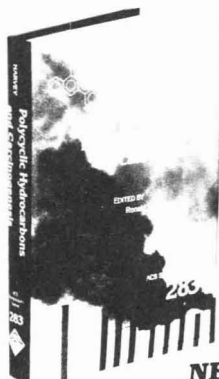
### American Chemical Society

Periodicals Marketing Dept.

1155 Sixteenth Street, N.W.

Washington, D.C. 20036

## Polycyclic Hydrocarbons and Carcinogenesis



**NEW!**

Ronald G. Harvey, Editor  
University of Chicago

Reviews and reports the latest research on polycyclic aromatic hydrocarbons, the cancer-causing agents found in polluted air, car exhaust, tobacco smoke, and many foods. Brings together leading experts to provide an in-depth look at why only certain PAH exhibit tumorigenic activity. Focuses on the mechanics of PAH carcinogenesis from a chemical-molecular aspect, rather than from a biological one. Provides a thorough treatment of PAH-DNA interaction, the critical event in the mechanisms of tumor induction. Offers a rational basis for the design of approaches for the prevention and cure of cancer.

### CONTENTS

Polycyclic Aromatic Hydrocarbon Carcinogenesis: An Introduction • Stereoselective Metabolism and Activation of PAH • Synthesis of Dihydrodiol and Diol Epoxide Metabolites of Carcinogenic Polycyclic Hydrocarbons • The Bay Region Theory of PAH Carcinogenesis • Effects of Methyl and Fluorine Substitution on the Metabolic Activation and Tumorigenicity of PAH • Mechanisms of Interaction of Polycyclic Aromatic Diol Epoxides with DNA and Structures of the Adducts • X-ray Analyses of Polycyclic Hydrocarbon Metabolite Structures • PAH-DNA Adducts: Formation, Detection, and Characterization • Intercalation of Metabolite Model Compounds into DNA • Binding of Benzo[a]pyrene Diol Epoxides to DNA • One-Electron Oxidation in Aromatic Hydrocarbon Carcinogenesis • Hydroperoxide-Dependent Oxygenation of PAH and Their Metabolites • Mutational Consequences of DNA Damage Induced by Benzo[a]pyrene • Chemical Properties of Ultimate Carcinogenic Metabolites of Arylamines and Arylamides • The In Vitro Metabolic Activation of Nitro PAH

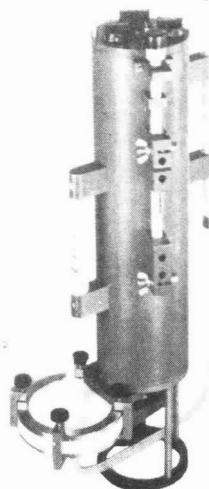
Developed from a symposium sponsored by the Division of Organic Chemistry of the American Chemical Society

ACS Symposium Series No. 283  
406 pages (1985) Clothbound  
LC 85-13384 ISBN 0-8412-0924-3  
US & Canada \$74.95 Export \$89.95

Order from: American Chemical Society  
Distribution Office Dept. 80  
1155 Sixteenth St., N.W.  
Washington, DC 20036  
or CALL TOLL FREE 800-424-6747  
and use your credit card.

## The SEASTAR IN SITU WATER SAMPLER

- ultra trace extraction of organics, PAH's, PCB's, hydrocarbons and trace metals.
- you select: flow rate, volume, sampling mode
- microprocessor controlled
- large volume extraction
- self powered
- optional filter assembly
- re-useable columns



**SEASTAR  
INSTRUMENTS LTD**

2045 MILLS RD., SIDNEY, B.C., CANADA V8L 3S1  
TELEPHONE: (604) 656-0891 TELEX 049-7526

## The Chain Straighteners

### Fruitful Innovation: The Discovery of Linear and Stereoregular Synthetic Polymers

by Frank M. McMillan

Presents the story of a key event in polymer science—the discovery of linear and stereoregular synthetic polymers. Karl Ziegler and Giulio Natta are the star players in this scientific drama, which has as its supporting cast the most renowned names in polymer science. Details the dynamic interplay of people and events that led to this fruitful innovation.

### CONTENTS

The Stage is Set • The Shadows Before ("Prediscoveries") • Karl Ziegler and the Max Planck Institute • Giulio Natta and the Milan Polytechnic Institute • Fruitful Innovation—1. The Polyethylene Discovery • Harvesting the Fruits of Innovation—Polyethylene • Fruitful Innovation—2. Polypropylene • The Falling Out • Harvesting the Fruits of Innovation—Polypropylene • Fruitful Innovation—3. Synthetic Rubber • The Crest of the Wave—and the

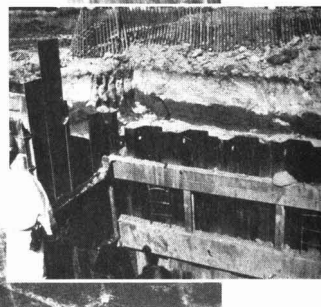
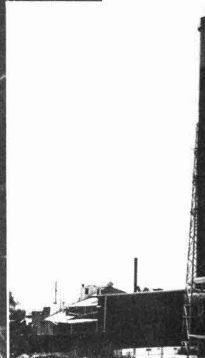
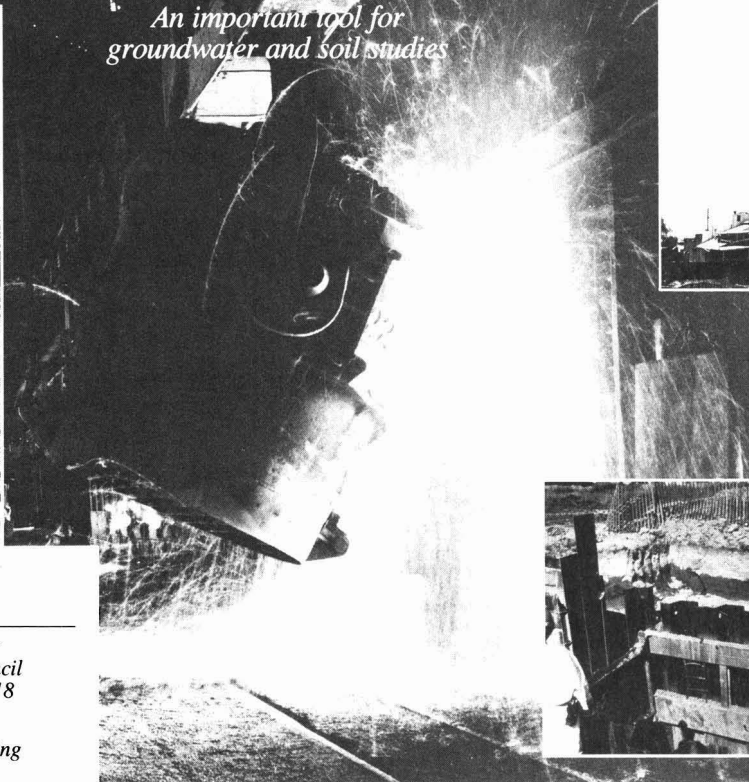
Trough • Shadows of the Future • Interpretations  
Published by The Macmillan Press Ltd.  
206 pages (1979) Clothbound  
ISBN 0-333-25929-7  
US & Canada only \$31.95

Order from:  
American Chemical Society  
Distribution Office Dept. 17  
1155 Sixteenth St., N.W.  
Washington, DC 20036  
or CALL TOLL FREE 800-424-6747  
and use your VISA, MasterCard  
or American Express credit card.



# Monitoring statistics

*An important tool for  
groundwater and soil studies*



**Glenn E. Schweitzer**  
*National Research Council  
Washington, D.C. 20418*

**Stuart C. Black**  
*Environmental Monitoring  
Systems Laboratory  
Environmental Protection Agency  
Las Vegas, Nev. 89114*

Statistics increasingly is recognized as an important component of soil and groundwater monitoring programs. In the design of these programs, reliance on subjective professional judgments unaccompanied by statistically based objective information has become less acceptable to enforcement agencies and the scientific community. The use of statistics is now considered necessary to determining the location of sampling sites, the frequency of sampling, and the representativeness of individual samples. Statistical analysis is also used in quality assurance procedures for sampling in the field and for analysis in the laboratory, as well as for interpreting monitoring data.

Standardized approaches for determining minimum detection levels, precision, and bias are evolving rapidly. EPA recently prepared detailed guidance on the analytical and statistical methods to be used in its programs for calculating these parameters (1).

Useful statistical procedures have

long been available for examining anomalies, differences, and trends in data. The development of these procedures intensified during the 1950s with the increase in interest in monitoring programs designed to measure radioactivity in environmental samples. The need to distinguish between changes in radioactivity caused by human activities and those ascribable to natural background variations, as well as recognition of the value of statistics in predicting radioactive decay, led to equations for combining errors of analysis and for determining the confidence level of the result.

Additional procedures were developed by the early 1960s that led to the issuance of guidelines to cover many aspects of quality control for analytical techniques. The use of control charts and methods for determining precision, accuracy, and minimum detection levels also were included. These guidelines have been updated and expanded recently (2-5).

Also during the 1960s, similar approaches for use in chemical monitor-

ing were published in a handbook by the National Bureau of Standards (6). This handbook includes many of the radiation concepts (such as detection limits and control charts) and methods of testing hypotheses of distributions and concentrations of chemical contaminants.

Statistical procedures often were based on the premise that the data contained negligible measurement errors—a questionable assumption in many environmental monitoring programs. Newer techniques do not rely as heavily on such an assumption. Recently, the field of chemometrics has attracted considerable attention. This field includes computer programs that analyze large sets of data through pattern recognition and related methods (7).

Until recently, only limited effort has been directed toward the statistical aspects of designing procedures for sampling under field conditions. Too often, unwarranted quantitative extrapolations have been made from small sets of data, or excessive numbers of samples have been taken to ensure the adequacy

of monitoring coverage. Now, the costs of cleaning up contaminated areas and of laboratory analysis have become so large that neither of these sampling approaches is acceptable. What is necessary, rather, is an optimum number of samples that furnishes a sufficient but not excessive amount of data points to characterize a contamination problem and to provide the degree of confidence in the quality of the data necessary to support their intended use.

The American Chemical Society guidelines in "Principles of Environmental Analysis" touch on this topic (8). The guidelines provide general sampling rules and simple equations for determining sample size if the required precision and allowable error are specified in advance or can be estimated. The principles pertain mainly to laboratory analyses; a companion set of ACS guidelines for environmental sampling is in preparation.

Recently, a government contractor prepared a series of bulletins discussing various statistical designs for monitoring programs, such as random, stratified, and grid designs and designs based on professional judgment (9). These bulletins are essentially a condensed presentation of techniques found in many textbooks on statistics, and they can be used readily by field personnel.

A major area of concern is the assurance that an individual sample is representative of the environmental condition it is intended to define. The representativeness of the analytical data developed is directly affected by the exact location and timing of sampling, the methods of preparing composite samples, and the techniques of preparing samples for chemical analysis.

Soil and groundwater contamination are three-dimensional problems; the size of the individual sample and the number and location of the samples are critical in any attempt to portray environmental conditions. Sampling for trend analysis adds temporal variation as another dimension of the problem.

The use of statistics now plays a greater role in the design of sampling programs because of groundwater regulations promulgated by EPA under the Resource Conservation and Recovery Act (RCRA) (10). As applied to interim status sites (disposal sites operating under general regulations pending individual permitting), RCRA regulations call for a minimum of one upgradient and three downgradient monitoring wells. Total organic carbon (TOC), total organic halogen (TOX), pH, and specific conductance—the *indicator parameters*—must be measured on a site-by-site basis. A statistical technique, known as the Student's t test, is used to

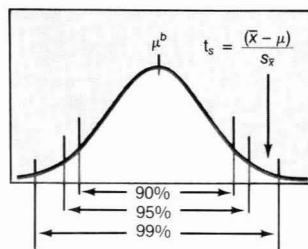
compare upgradient and downgradient measurements (Figure 1).

One problem with such sampling arises because samples often are taken from a small number of wells; therefore, they may not be representative of actual upgradient or downgradient conditions. Also, the direction of movement of groundwater contaminants may not be in total conformity with gradient conditions, and the direction of contaminant flow may vary over time. Another problem is that it is difficult to determine the extent to which the indicator parameters represent contaminant patterns involving a large number of chemicals. Researchers within and outside of EPA are working toward improving statistical procedures for characterizing contamination problems without incurring unacceptable costs for monitoring at waste disposal sites.

The report of an ACS-EPA workshop on environmental sampling for hazardous wastes provides an overview of current designs of field sampling programs (11). Case studies underscore the continuing importance of professional judgments in addressing field problems when work must be done quickly. The report highlights the importance of the statistician working with other scientists in designing field programs and selecting models for data interpretation. It presents recently developed mathematical techniques for addressing spatial correlations among data points and for comparing data from contaminated areas with data from background or control areas.

Two of the major questions that arise when risk assessments are conducted at hazardous waste sites relate to the level and extent of contamination and to the way in which contamination compares with background levels. Two recent EPA monitoring programs illustrate how statistics have been used to assess monitoring data in addressing these

FIGURE 1  
Student's t test<sup>a</sup>



<sup>a</sup>Determines whether downgradient contamination is statistically greater than upgradient contamination

<sup>b</sup>If  $\mu$  = upgradient mean value,  $\bar{x}$  = downgradient mean value, and  $s_x$  = standard error of  $\bar{x}$ , then  $t_s$  is the value to be tested. Using  $t_{0.95}$ , which is dependent on the number of samples used to determine  $\bar{x}$ , test whether  $t_s > t_{0.95}$ . If so, then  $\bar{x}$  is statistically greater than  $\mu$  with a probability  $P < 0.05$  (the probability is less than 0.05 that the means were derived from the same sample). The downgradient mean level would be represented by the same curve as that shown above, but displaced leftward; it was omitted for the sake of clarity. The term  $t_{0.95}$  represents  $t$  from a table at the 95% confidence level

questions. They provide some guidance as to how statistics might be used more effectively in the future. These programs—the 1980 Love Canal Study and the 1982 Dallas Lead Study—have attracted considerable attention from the scientific community and the public. In a sense, they were bellwether cases for subsequent monitoring efforts.

### Contamination at Love Canal

In 1980, EPA began a program to obtain environmental data that would assist researchers in determining the habitability of homes near Love Canal, N.Y. The project was allotted limited time and money, and access to some of the desired sampling sites also was limited. Thus, from the outset of the program, it was recognized that efforts to conduct rigorous statistical analyses of the monitoring data would not be possible, either as a basis for quantitative risk assessment or as a means of comparing contamination near the canal with background contamination.

The primary interpretation of the data for characterizing contamination was based on descriptive and graphic presentations that would be helpful in determining health risks to the population. Despite known shortcomings in the data base, particularly in the limited number of samples from the control areas, limited statistical analyses also were carried out to identify questionable aspects of the descriptive presentations (12).

For each medium—soil, groundwater, sumps, indoor and outdoor air, drinking water, food, and biota—monitoring data were aggregated for three

### Sample size estimates

Number of samples =  $(Z\sigma_p/e)^2$

Number of replicates =  $(Z\sigma_m/E)^2$

Z = Standard normal variate (from tables) ( $t$  from Student's t test may be used instead of Z if number of samples or replicates is less than seven)

$\sigma_p$  = Assumed standard deviation of population

$\sigma_m$  = Standard deviation of the measurement

$e$  = Acceptable error of the mean of the samples

$E$  = Acceptable confidence interval

Source: Reference 8

## Fisher's exact test

	Number of samples with values above detection limit	Number of samples with values below detection limit	Totals
Test area	A	B	A + B
Control area	C	D	C + D
	A + C	B + D	N

$$P_0 = \frac{(A+C)!(B+D)!(C+D)!(A+B)!}{A!B!C!D!N!}$$

This *difference of percentages* test determines whether contamination in a test area is more extensive than contamination in a control area. Here is how the test is applied:

If A or C is not 0, decrease the smaller value by 1 and change the other three values so that the margin totals remain constant, that is, so that the *numerator* of the equation remains constant. Calculate a new probability,  $P_1$ , using the new values of A, B, C, and D in the *denominator* (N will not change). Continue to *decrease* the smaller value by 1 until A or C is 0. Add the results,  $P_0 + P_1 + \dots$ , to calculate the exact probability of null hypothesis, namely, that contamination in the test area is no more extensive than that in the control area.

geographical areas: the canal area, an unoccupied residential area immediately adjacent to the canal; the declaration area, an area within 1–2 mi of the canal that included occupied residences; and control areas several miles from the canal. The statistical tabulations and analyses consisted of substance-by-substance comparisons of frequencies of detection and median concentration levels for up to 150 analytes in each area.

The *extent* of contamination in an area was defined as the percentage of samples that included a chemical contaminant at a trace or greater concentration level. A difference of percentages test, using Fisher's exact test to compute probability values, was used to determine whether statistically significant differences in the extent of chemical contamination existed among the canal, declaration, and control areas. An example of the results of applying this test is shown in Table 1.

TABLE 1

### Shallow groundwater contamination at Love Canal<sup>a</sup>

Compound or element	Percentage detected <sup>b</sup> (Number of samples)			Comparison <sup>c</sup>	
	Declaration	Control	Canal	Canal with declaration	Declaration with control
2,4-Dichlorophenol	2.1 (47)	9.1 (11)	18.8 (16)	Yes <sup>d</sup>	No <sup>d</sup>
2,4,6-Trichlorophenol	0.0 (47)	0.0 (11)	13.3 (15)	Yes	No
1,4-Dichlorobenzene	0.0 (47)	0.0 (11)	12.5 (16)	Yes	No
1,2-Dichlorobenzene	0.0 (47)	0.0 (11)	12.5 (16)	Yes	No
1,2,4-Trichlorobenzene	0.0 (47)	0.0 (11)	12.5 (16)	Yes	No
1,2,3,4-Tetrachlorobenzene	0.0 (47)	0.0 (11)	12.5 (16)	Yes	No
Acenaphthalene	4.3 (47)	0.0 (11)	18.8 (16)	Yes	No
Fluorene	4.3 (47)	0.0 (11)	18.8 (16)	Yes	No
1,1-Dichloroethylene	2.3 (47)	0.0 (11)	14.3 (21)	Yes	No
Tetrachloroethylene	2.3 (43)	27.3 (11)	19.0 (21)	Yes	No
2-Chlorotoluene	0.0 (43)	0.0 (11)	19.0 (21)	Yes	No
3-Chlorotoluene	0.0 (43)	9.1 (11)	10.0 (20)	Yes	No
4-Chlorotoluene	0.0 (43)	0.0 (11)	9.5 (21)	No <sup>e</sup>	No
Chlorobenzene	2.3 (43)	0.0 (11)	23.8 (21)	Yes	No
Chromium	66.0 (43)	70.0 (10)	92.9 (14)	Yes	No
Lead	72.3 (47)	77.8 (9)	100.0 (13)	Yes	No

<sup>a</sup>Significant differences observed in *extent* of contamination

<sup>b</sup>Percentage detected is the number of analyses showing trace or quantifiable amounts of a contaminant divided by the total number of analyses

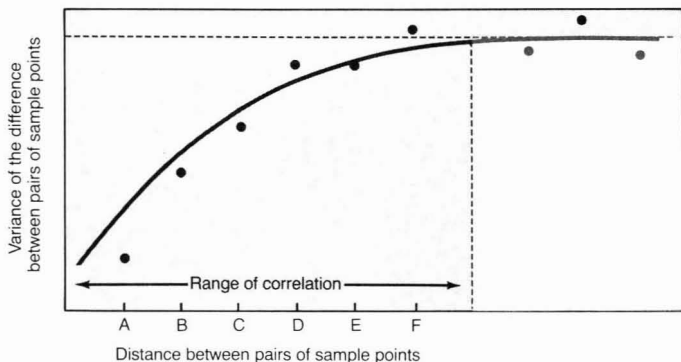
<sup>c</sup>The canal area is compared with the declaration area, and the declaration area is compared with the control area based on the one-tailed, difference-of-proportions test, used to determine statistically whether values of a parameter in one domain will be greater than the values of the same parameter in another domain. This test is based on Fisher's exact test

<sup>d</sup>"Yes" means that the level of contaminants in one area is *significantly* greater than the level in another area; "no" means that there is no significant difference

<sup>e</sup> $\alpha = 0.104$ , where  $\alpha$  is the probability of being wrong. When  $\alpha = 0.104$  there is a 10.4% probability of a false positive or negative. For the one-tailed, difference-of-proportions test described above,  $\alpha = 0.10$

FIGURE 2

## Relationships between sample observations



The *degree* of contamination was defined as the median concentration of all sample measurements for a chemical contaminant in the area of interest. A difference of medians test, again using Fisher's exact test to compute probability values, was used to determine whether statistically significant differences in the degree of chemical contamination levels existed among the three areas.

Other statistical procedures used to summarize the data consisted of grouping the data into frequency distributions in which intervals were defined according to concentration levels, computing various percentiles of interest, reporting finite (quantified) minimum and maximum observed concentrations, and computing the mean (arithmetic average) value of the observed finite concentrations.

The statistical analyses were consistent with the descriptive and graphical interpretations of the data. They indicated substantial contamination in the canal area; there was no evidence of such contamination in the declaration area. There was concern about the adequacy of the power of the statistical analyses to detect contamination differences of possible interest between the declaration and the control areas, given the limited number of samples from the control area (13). For this reason, the statistical analyses were not a pivotal factor in the determination of the habitability of the area, but they were helpful in confirming at least an upper limit to possible differences in contamination levels.

The approach of comparing contaminant levels in contaminated and control areas, as attempted in the Love Canal study, is now used frequently. Even with small amounts of data, statistical interpretations can help to point out possible problem areas, although such

interpretations are seldom completely reliable. Moreover, practical considerations often limit the number of samples.

### Contamination in Dallas

In 1982, EPA conducted a soil monitoring program around two lead smelter sites in Dallas, Tex. The study made extensive use of geostatistics—the application of statistics to geological problems—to determine the location of sampling sites and to interpret the monitoring data (14). Geostatistics recog-

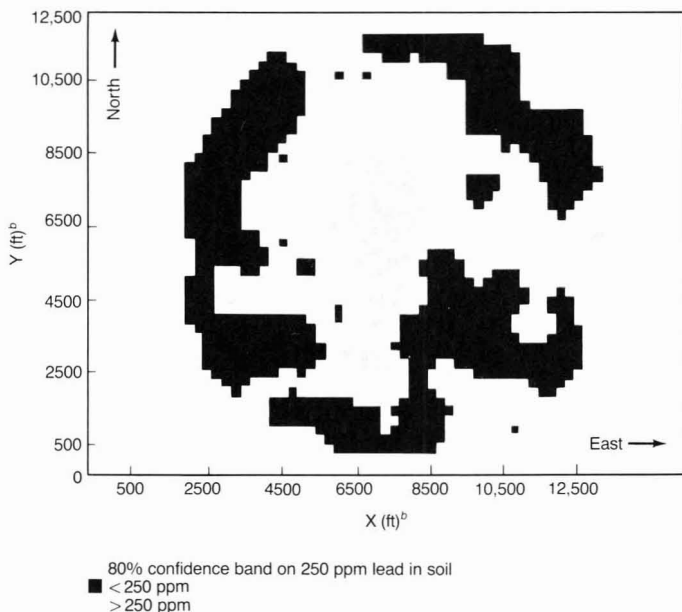
nizes the spatial dependence within sampling patterns, as in the case of the deposition of materials in an air contaminant plume from a lead smelter (Figure 2).

Figure 2 shows that as the distance between two samples increases and their correlation weakens, the difference in their values also increases, as represented by a rising curve. When this difference becomes great enough, the sample values become independent of one another, and the curve becomes a horizontal line.

The distance along the X-axis, through which the semivariogram curve rises, represents the *range of correlation*, or the distance within which samples may be correlated. This range is used to determine the grid design for sampling. A grid spacing of two thirds of the range of correlation usually ensures that the sampling points are close enough to one another to have correlated values. To sample at closer distances would provide little new information; sampling at greater distances could miss a change in pollutant levels.

A technique called *kriging* interpolates pollutant levels at points between the sampling sites so that the isopleths of pollutant levels can be mapped. The kriging estimate of the pollutant level at any particular point is the weighted average of the values of the nearest neighboring samples. The size of the neigh-

FIGURE 3

Lead contamination in Dallas<sup>a</sup>

<sup>a</sup>Data obtained by geostatistical analysis from vicinity of one smelter site  
<sup>b</sup>Origin is arbitrary



borhood is determined by the range of correlation. By kriging, one can compute the standard errors of estimation for sample values when the range of correlation is used. Error estimates also can be mapped.

On the basis of data from preliminary sampling, which indicate the degree of spatial correlation, geostatistics can be used to determine the appropriate spacing between sampling sites. The use of geostatistics also permits easy and objective interpolations of values between data points and makes it possible to estimate errors that could be associated with the interpolations and with the data points themselves.

Figure 3 shows one technique for displaying the results from the Dallas study. The interpolated concentration levels and the associated error estimates were used to develop maps that showed which areas could be identified with a specified degree of confidence as being contaminated at levels above or below an action level, that is, the level of contamination that triggers remedial action.

The soil-monitoring program in Dallas, which measured only one pollutant, was much less complicated than most monitoring programs. Still, the principles used can be applied to other situations—particularly to the study of contaminant plumes from waste sites—because spatial dependence among samples is probably the rule rather than the exception.

### Improving data interpretation

Research is under way to improve the statistical techniques for guiding the design of monitoring programs and for improving the interpretation of monitoring data. Methods are being developed for combining the use of statistics—especially geostatistics—with the application of hydrogeological and other models. Although such research efforts are helpful, the most immediate need is in the application of elementary statistical techniques to operational monitoring programs.

A clear understanding of the purposes of the monitoring effort and of the quality of the data required to achieve these purposes is essential to the selection of statistical techniques. Many monitoring programs, however, are undertaken with neither a proper understanding of their purposes nor an appreciation of the need for data quality assurance.

Experience has underscored the importance of many characteristics of successful sampling programs. These include the need for preliminary sampling, for adequate numbers of samples from control areas, and for using quality assurance procedures in providing

### Improving statistical procedures

Experience with the application of statistical techniques to monitoring programs has highlighted several areas that need more attention.

The first problem area involves combining monitoring data with factors that are based on professional judgment about the likely subsurface behavior of contaminants. When monitoring data are inadequate in one aspect or another, such factors often help regulators to reach decisions. Guidelines and appropriate models should be developed that will permit assessment of the advantages and limitations of combining such factors with data.

Another problem area involves statistics for small sample sets. In many cases, the number of samples available is limited, and the variance of the results is so large that regulatory decisions cannot be reached, even when professional judgments are made. It would be helpful if methods could be developed to use such limited information with greater confidence. For example, the "bootstrap" technique, which is used to manipulate small sample sets in large numbers of different combinations, might be useful (15).

Statistical analyses of long-term monitoring under varying background conditions also should be examined. Trends in long-term monitoring results can be detected readily when the background data remain constant over time, but problems increase when the background changes because of variability attributable to natural causes.

data that will meet specific criteria of acceptability.

### Acknowledgment

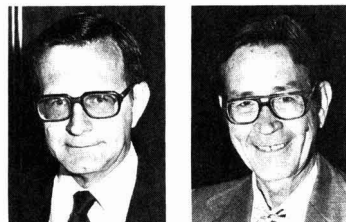
George Flatman, Kenneth Brown, Robert Snelling, and Leslie McMillion of EPA's Environmental Monitoring Systems Laboratory in Las Vegas, Nev., contributed to the development and review of this article.

Before publication, this article was reviewed for suitability as an *ES&T* feature by John M. Hosenfeld, Midwest Research Institute, Kansas City, Mo. 64110; and Hubert A. Scoble, Massachusetts Institute of Technology, Cambridge, Mass. 02139.

### References

- (1) "Calculation of Precision, Bias and Method Detection Limit for Chemical and Physical Measurements," Quality Assurance Management Staff Guidance Document; Office of Research and Development; EPA: Washington, D.C., 1984.
- (2) Loevinger, R.; Berman, M. *Nucleonics* 1951, 9, 26.
- (3) Altshuler, B.; Pasternack, B. *Health Phys.* 1963, 9, 293-98.

- (4) Rosenstein, M.; Goldin, A. S. *Health Lab. Sci.* 1965, 2, 93-102.
- (5) "Upgrading Environmental Radiation Data," EPA 520/1-80-012; Watson, J. E., Ed.; Office of Radiation Programs; EPA: Washington, D.C., 1980.
- (6) Natrella, M. G. "Experimental Statistics," NBS Handbook 91; National Bureau of Standards: Washington, D.C., 1966.
- (7) "Environmental Applications of Chemometrics"; Breen, J.; Robinson, P., Eds.; ACS Symposium Series No. 292; American Chemical Society: Washington, D.C., in press.
- (8) "Principles of Chemical Analysis," *Anal. Chem.* 1983, 55, 2210-18.
- (9) "TRANS-STAT (Statistics for Environmental Studies)," Reports PNL-SA-11551, PNL-SA-12180; Gilbert, R. O., Ed.; Battelle Pacific Northwest Laboratory: Richland, Wash., 1984.
- (10) Code of Federal Regulations, 40 CFR 165, Subpart F, 1983; pp. 506-10.
- (11) "Environmental Sampling for Hazardous Wastes"; Schweitzer, G. E.; Santolucito, J. A., Eds.; ACS Symposium Series No. 267; American Chemical Society: Washington, D.C., 1984.
- (12) "Environmental Monitoring at Love Canal," EPA 600/4-82-030a; Office of Research and Development; EPA: Washington, D.C., 1982; Vol. 1.
- (13) "Habitability of the Love Canal Area," Technical Memorandum; Office of Technology Assessment: Washington, D.C., 1983.
- (14) Brown, K. W. et al. "Documentation of EMSL-LV Contribution to the Dallas Lead Study," Report 600/x-83-007; Environmental Monitoring Systems Laboratory; EPA: Las Vegas, Nev., 1983.
- (15) Diaconis, P.; Efron, E. *Sci. Am.* 1983, 248, 116-30.



**Glenn E. Schweitzer** (l.) recently was appointed director of Soviet and East European Affairs for the National Research Council. Until April 1985, he was director of EPA's Environmental Monitoring Systems Laboratory in Las Vegas, Nev., where he directed a variety of research and development activities, including innovative field sampling programs at a number of locations throughout the country. He also served as director of EPA's Office of Toxic Substances. Schweitzer has an M.S. in mechanical engineering from the California Institute of Technology.

**Stuart C. Black** (r.) is chief of the Dose Assessment Branch, Nuclear Radiation Assessment Division at EPA's Environmental Monitoring Systems Laboratory. He has worked in the fields of radiation biology, radiation monitoring, and analytical quality assurance for EPA and the U.S. Public Health Service. Most recently, Black has been responsible for the statistical aspects of field monitoring programs, including EPA's monitoring efforts at Love Canal and in Dallas. He has a Ph.D. in biophysics from the University of Rochester, N.Y.

# EPA's groundwater research



Richard M. Dowd

A special subcommittee of EPA's Science Advisory Board, created to review EPA's groundwater research program, has reported its findings. The review covers the transport, fate, and effects of contaminants; abatement and control technologies; modeling; monitoring and analytical methods; and quality assurance. The report makes useful reading for anyone interested in groundwater protection and in the regulatory pattern that is emerging.

The increasing concern over groundwater quality and the need to protect groundwater and to identify sources of contamination (industrial and nonpoint) can be taken to mean that we know a great deal about how, when, and where to protect groundwater. But the report points out that in fact there are large gaps in our knowledge of the sources of groundwater contamination. Nor are we completely sure of how groundwater and contaminants move, of what the appropriate methods are for measuring, monitoring, and controlling contaminants, or of how groundwater resources should be protected for future use.

The committee concludes in the report that although EPA's research program is basically sound, it is in need of improvement. The members emphasize a need for centralized direction and management of the groundwater research program, for increased technology transfer and training, and for increased resources.

The committee also recommends that

Superfund appropriations (perhaps 1-2% of the Fund) be authorized for such research. Even this small percentage would effectively double EPA's groundwater research funding over the existing level of \$18.2 million. Recommended funding improvements in the areas of monitoring, predictive modeling, and aquifer cleanup would more than double existing levels.

## Control of contaminant sources

The committee's discussion of source controls indicates that substantial gaps exist in the research on the consequences of land disposal of hazardous wastes. The committee observes that even under the current prohibitions against land disposal there are ultimately only three kinds of disposal sites possible: the atmosphere, surface waters, and land. Because land will continue to be used for the treatment and disposal of many wastes, including some regulated hazardous wastes, research on land treatment techniques should be accelerated.

Another recommendation points to the need to identify "the magnitude and importance of groundwater contamination from nonhazardous waste disposal operations, and to specify the technical and economic feasibility" of controls for those sources.

The committee also focuses attention on monitoring groundwater quality. Groundwater monitoring provides data necessary for making decisions, verifying models and the usefulness of control technology, determining background levels of pollutants and existing groundwater quality, and determining the physical, chemical, or biological processes and characteristics of a particular groundwater system. The committee finds, in particular, that there are substantial gaps in the areas of quality assurance (QA), quality control (QC), methods, and protocols for handling contaminants in groundwater. The re-

port indicates the importance of developing monitoring practices and verification techniques for the 250 compounds regulated under the Resource Conservation and Recovery Act (RCRA), for which there are no proven methods, standards, QA, QC, or validation data.

## Uncertainties in information

The document identifies gaps in knowledge and the problems that can result from proceeding as quickly as this program has to protect groundwater. Like many thoughtful reviews, the committee's report concludes with as many questions as it starts: "Which sources of groundwater contamination warrant greater emphasis? Which technologies promise the best results for protection or remediation? What levels of protection or remediation are technologically feasible? To what extent can sources of contamination be reduced? Can exposure of humans to groundwater contamination be accurately determined or predicted?"

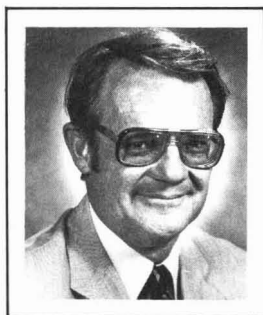
The list of questions continues: "Can present and potential health effects be quantified, and what are they? Can institutional controls be developed to safeguard against human exposure? Does a scientific basis exist to conclude that compliance with proposed laws and regulations is feasible? What will such compliance cost?"

It should not escape anyone's attention that regulatory decisions must be made under RCRA, Superfund, and the pesticides and drinking-water programs—questions or no questions. The more quickly such an expanded groundwater research program is implemented, the greater becomes the likelihood of making scientifically sound decisions.

*Richard M. Dowd, Ph.D., is a Washington, D.C., consultant to Environmental Research & Technology, Inc.*

# Jekyll Island meeting report

*George Hidy reports on the acquisition  
of reliable atmospheric data*



*George Hidy*

In May 1985, the 15th Annual Symposium on the Analytical Chemistry of Pollutants convened in Jekyll Island, Ga. As part of the meeting, a series of lectures on acid deposition and the closely allied subject of acquiring valid air quality monitoring data was presented. In last month's issue, we reported on a talk given by Courtney Riodan of EPA. This month, we report on the lecture given by George Hidy of the Desert Research Institute (DRI) in Reno, Nev. Next month, we will conclude this series of Views with a report on the talk given by James Galloway of the University of Virginia.

Hidy's lecture covered recent progress in formalizing the process of making environmental measurements. He discussed the need for atmospheric scientists to build a framework, a data base, for monitoring programs that will generate data of a defined quality and traceability. More than 100 scientists have been involved in this field; a framework has been developed and adopted for air quality measurements and monitoring, a subject closely allied to the study of acid deposition.

The ultimate reasons for making such measurements are to establish historical records of atmospheric pollutants, to explore the spatial and temporal distribution of atmospheric gradients of pollutants, to test scientific and regulatory hypotheses, and to verify mechanistic and source-receptor models.

Hidy illustrated the use of air quality data with application to each of these areas. Particular discussion was focused

Hidy illustrated the use of air quality data with application to each of these areas. Particular discussion was focused on the importance of traceability and consistency in measurements for trend analysis. It is important that atmospheric scientists know how and when such monitoring data are collected and whether they are reliable. Hidy discussed the difficulty encountered in interpreting observations of precipitation chemistry in light of changes in pollutant emissions. He also outlined the use of data to infer spatial and temporal changes in meteorology and atmospheric chemistry. Finally, he listed the data requirements for the validation of models, specifically for the determination of particulate matter source-receptor relationships (1).

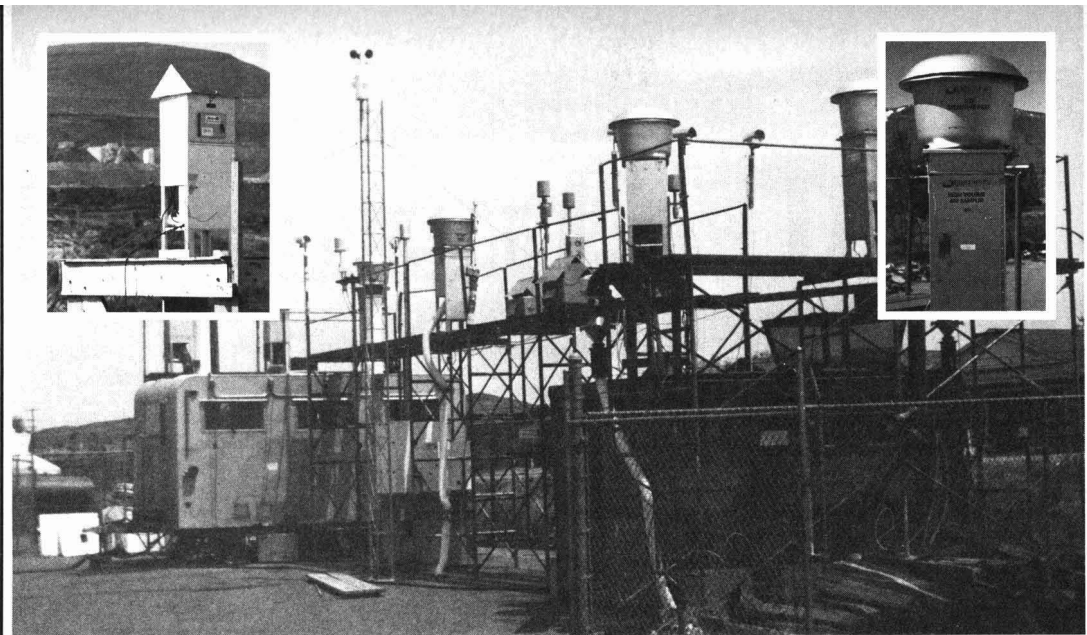
Hidy defined the details of air quality measurement processes and illustrated these aspects with recent examples of significant measurements, such as "The Sulfate Regional Experiment" (2). He also related these aspects to the process of interpreting the data collected. The evaluation of monitoring activity, which has been formalized by John Watson and others (3), involves consideration of four basic factors: the datum of the observation, the precision or reproducibil-

ity of the measurement, the accuracy of the measurement against a reference standard, and the validity of the measurement in relation to interferences.

## On the cutting edge

The development status of measurements was illustrated by three examples of current technology. First, the current established method of measuring  $\text{SO}_2$  in the atmosphere is accurate to a level of 3-5 ppb. The methodology for verifying this measurement has been described by Mueller and Hidy (2) and Mueller and Watson (3). These scientists employed the four characteristics of measurements mentioned earlier.

Second, the development of a semi-established method for size-fractionated particulate matter measurement has resulted in a proposed new ambient air quality standard. This standard involves the  $< 10\text{-}\mu\text{m}$  fraction of particulate matter; new monitoring requirements are required for this standard. In the past five years, many atmospheric scientists have been involved in the development of sampling devices. Collectively, they have arrived at new standard operating procedures, compared the sampling schemes and inlet ducts of the sampling devices for the  $10\text{-}\mu\text{m}$  fraction of particulate matter, resolved the efficiencies of the collection process, identified and quantified filter artifacts from gas adsorption and desorption on the collected particulate matter samples, established criteria for accepting the precision and accuracy of sample collection, and validated the collected data.



Comparisons of several particulate samplers have been made recently by the Electric Power Research Institute. The left inset photo shows the standard high-volume filter sampler used in U.S. air-monitoring programs since 1969. The right inset is a sampler with a size-fractionated inlet that collects particles  $< 10 \mu\text{m}$ . It may replace the older units entirely.

### Terms used in acquiring valid atmospheric data

**Measurement.** The representation of an observation at a specific time and place is characterized by the four elements proposed for verification; these include its *value*—the center of the measurement interval; its *precision*—the width of the measurement interval; its *accuracy*—the difference between measured and reference values; and its *validity*—the compliance with assumptions made in the measurement method.

**Measurement methods** require the use of a combination of equipment, reagents, and procedures to provide the value of a measurement, that is, data that are uniform and of acceptable accuracy.

**Quality control.** The periodic presentation of known or replicate quantities of an observation to a measurement method, the comparison of the measured value with the known or replicate value, and corrective action when the difference exceeds a preset tolerance. These differences are used to estimate precision.

**Quality assurance.** An independent presentation of reference quantities of an observation to a measurement method. Differences between the measurement and reference values are used to estimate accuracy.

**Validation.** The identification of deviations from standard operating procedures (SOPs) and measurement method assumptions, corrections, deletions, and quantifications of the affected measurements.

**Development status.** Methodology here can be divided into three categories—established, semi-established, or unestablished. The characteristics of each are as follows:

*Established methodology* has accepted SOPs, interferences that are identified and quantified, traceable calibration and quality assurance standards, agreement with other established methods, and acceptable levels of precision, accuracy, and validation.

*Semi-established methodology* uses different SOPs and allows for incomplete characterization of interferences, nontraceable standards, and disagreement among methods, but requires acceptable levels of precision, accuracy, and validation.

*Unestablished methodology* uses operating procedures that are incomplete or unspecified and offers little or no characterization of interferences, questionable or nonexistent calibration standards, and little or no data comparison of interlaboratory methods. It provides for unacceptable or unknown levels of precision, accuracy, and validation.

**Measurement process.** This is a combination of established and semi-established methods, including quality control, quality assurance, and validation procedures that produce measurement values of known precision, accuracy, and validity.

The third example Hidy discussed involved the unestablished method for the measurement of the amount of liquid water in suspended particles. Although research in this area is in a relatively early stage, such measurements are useful in studies of atmospheric visibility and for determining atmospheric light extinction. Light scattering, which is a function of relative humidity and filter collection of particulate matter, is measured by chromatography and microwave spectroscopy. Microwave spectroscopy appears the more promising measurement method because it is semi-continuous and free from interference. But the sampling technique and analytical method for the measurement of liquid water in suspended particles involve preconcentration on a filter, which presents significant difficulties, such as artifact formation. Nevertheless, no standard operating procedure exists for this measurement, and although limited comparisons have been made between the methods, no formal method for verifying the data by the four characteristic criteria exists.


Although Hidy's presentation revealed little new science, it did provide a thought-provoking insight on the standardization of measurement processes.

### References

- (1) Cooper, J.; Watson, J. G. *J. Air Pollut. Control Assoc.* **1980**, *30*, 1116.
- (2) Mueller, P. K.; Hidy, G. M. "The Sulfate Regional Experiment," Report EA-1901; Electric Power Research Institute: Palo Alto, Calif., 1983; Vols. 1 and 2.
- (3) Mueller, P. K.; Watson, J. "Eastern Regional Air Quality Measurements," Report EA-1914; Electric Power Research Institute: Palo Alto, Calif., 1982; Vol. 1.



# professional consulting services directory

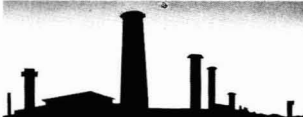


**TRADITIONAL SOURCE SAMPLING**

- Air Emissions Testing and Compliance Determination for Particulate and Gases
- Control Device Evaluation
- Particle Sizing Studies
- Resistivity Studies
- Specialized Analysis
- Method 1 Alternative
- 3-D Air Flow Studies

D. James Groves, P.E., Director  
PO Box 12291, Research Triangle Park, NC 27709 (919) 781-3550 or 1-800-ENTROPY

**ENTROPY**  
ENVIRONMENTALISTS INC.




**SPECIALIZED SAMPLING**

- (RCRA) Incinerator Testing
- Volatile Organic Compound (VOC) Testing
- Vapor Recovery Unit Compliance/Performance Testing
- Specialized Hydrocarbons Testing
- Testing of High Temperature and Pressure Sources

Walter S. Smith, P.E., Director  
PO Box 12291, Research Triangle Park, NC 27709 (919) 781-3550 or 1-800-ENTROPY

**ENTROPY**  
ENVIRONMENTALISTS INC.



**CONTINUOUS EMISSIONS MONITORING (CEM)/ENGINEERING**

- Performance Specification Tests of Opacity, SO<sub>2</sub>, NO<sub>x</sub>, O<sub>2</sub>, CO, CO<sub>2</sub> and TRS CEMS
- Stratification Tests (All Pollutants)
- CEM Performance Audits (RAA and CGA)
- Real-time Measurements Using Transportable CEM System — Boiler Tuning (NO<sub>x</sub>)
- FGD Performance Evaluation
- Combustion Efficiency Studies
- Performance Tests of Gas Turbines (Method 20)

James W. Zeller, Director  
William G. DeWees, Associate Director  
PO Box 12291, Research Triangle Park, NC 27709 (919) 781-3550 or 1-800-ENTROPY

**ENTROPY**  
ENVIRONMENTALISTS INC.

## A Cost Effective On-Site Biodegradation Process That Is Working! SOIL AND GROUNDWATER CONTAMINANTS CLEANED-UP AT COSTS OF LESS THAN 1¢ PER GALLON!

### How Does It Work?

The proprietary system is based on accelerating Nature's own process of biodegradation by utilizing naturally occurring microorganisms. This on-site process eliminates contamination in both soil and groundwater.

### Why Is It Cost Effective?

The complete system operates at your facility. There are no contaminants materials, soil or water to be hauled away to other locations.

Let KG BIO-TECHNOLOGIES EASE YOUR CONCERNS ABOUT YOUR WASTE DISPOSAL. AFTER EVALUATING CONTAMINANTS, WE GUARANTEE TO CLEAN YOUR WASTE, IN MOST CASES WITHIN WEEKS. PLEASE CALL 214-690-9451 Or 9478.

**KG BIO-TECHNOLOGIES**  
1303 Columbia Dr., Suite 221  
Richardson, Texas 75081-2936



**COMPLETE ANALYTICAL SERVICES** GC/MS CAPABILITIES

- ☐ Screening & Analysis of Industrial & Hazardous Waste.
- ☐ Superfund & RCRA Requirements.
- ☐ Sampling to EPA Protocols.
- ☐ Toxicity Studies.

(516) 334-7770  
75 URBAN AVE, WESTBURY, NY 11590  
**NYTEST ENVIRONMENTAL INC.**

**Cenref Labs**

BRIGHTON, CO (303) 659-0497  
LIBERAL, KS (316) 624-4292

**ENVIRONMENTAL TESTING**

Priority Pollutants • PCB's  
RCRA Hazardous Waste Analyses  
Drinking Water • Wastewater  
Pesticides • Sludge  
Engine Emission Monitoring

## HITTMAN EBASCO

Analytical Laboratories

- EPA Priority Pollutants - GC/MS
  - Water Monitoring
  - Hazardous Waste Characterization
  - Sampling Services
  - NPDES and RCRA Services
- EPA Approved and State Certified—

HITTMAN EBASCO ASSOCIATES INC.  
A Subsidiary of EBASCO SERVICES INCORPORATED  
9151 Rumsey Road, Columbia, MD 21045  
(301) 730-8525

### CONSULTING GROUND-WATER GEOLOGISTS

**ROUX ASSOCIATES INC.**

- RCRA Monitoring
- Superfund Response
- Site Evaluation
- Aquifer Clean-Up
- Resource Development

11 STEWART AVENUE  
HUNTINGTON, NEW YORK 11743 516 673-7200  
500 PURDY HILL ROAD  
MONROE, CONNECTICUT 06468 203 268-2846



**COMPLETE ANALYTICAL SERVICES**

- Gas Chromatography/ Mass Spectroscopy
- Trace Metal Analyses - ICAP: AA, GFAA
- Drinking Water Analyses
- Industrial Hygiene Services
- Research and Development
- Environmental Field Sampling
- EPA Priority Pollutant Analyses

Brochure and/or fee schedule available on request  
**BARRINGER MAGENTA LTD.**  
304 Carlingview Drive, Rexdale, Ont. Canada (416) 675-3870  
US Office Denver CO 80401 (303) 232-8811




**ENVIROMED**  
LABORATORIES, INC.

**Sampling, Testing, & Consulting Services**

- Priority Pollutants GC/MS, GC, AA
- RCRA-Hazardous Waste
- Animal Toxicity & Bioassay Studies
- Wastewater, Water & Sewage Analysis
- Permit Preparation, Audits
- TOX, TOC
- PCB and Chlorinated Hydrocarbon Analysis
- Industrial Hygiene & Ambient Air Monitoring
- Ground Water Monitoring

414 W. Calif. Ruston La. 71270 (318) 255-0060  
1874 Dallas Dr. Baton Rouge, La. 70806 (504) 928-0232  
La. Toll Free 1-800-421-2993



**ENVIRODYNE ENGINEERS**

a consulting engineering and sciences firm

- environmental engineering
- analytical chemistry
- priority pollutant analyses
- environmental monitoring and assessment
- hazardous waste monitoring
- hazardous waste management
- transportation engineering
- energy engineering
- construction management

12161 Lackland Road  
St. Louis, Missouri 63146  
(314) 434-6960  
Baltimore / Chicago / New York

**GYMNUMS LABORATORIES, INC.**

- HAZARDOUS WASTE-RCRA ANALYSIS
- PRIORITY POLLUTANT ANALYSIS
- INDUSTRIAL & MUNICIPAL DISCHARGE ANALYSIS INCLUDING AIR, WATER & WASTE
- OCCUPATIONAL SAFETY & HEALTH ANALYSIS
- AGRICULTURAL PESTICIDES & PCB ANALYSIS
- GUARANTEED 5-DAY ROUTINE ANALYSIS

**MODERN COMPUTERIZED INSTRUMENTS**  
1303 COLUMBIA DR., SUITE 221, RICHARDSON, TX 75081 (214) 690-9431

**USE THE  
DIRECTORY  
SECTION**

## Senior Environmental Scientist

EG&G Idaho, Inc., prime operating contractor for the Department of Energy's Idaho National Engineering Laboratory (INEL), has an immediate opening for a Senior Scientist responsible for evaluating unit processes of current and proposed nuclear and non-nuclear operations for environmental compliance. Working knowledge and experience in interpretation/application of current Federal Environmental Regulations will be required.

The successful candidate will have an advanced degree in Environmental Science or Engineering with at least three (3) years experience including environmental program auditing experience and technical knowledge in two (2) or more of the following fields: health physics, air pollution, hazardous waste and water quality.

## Engineers and Scientists

Additional openings are anticipated for Engineers and Scientists with experience in hazardous waste management. Individuals with expertise in waste treatment or remedial investigations are specifically invited to apply.

A career with EG&G Idaho, Inc., is a commitment to the future, at a work location in the heart of the western recreation areas.

If interested and qualified, please send resume, with salary history, in confidence to **Salary and Staffing Services, (BD-69), EG&G Idaho, Inc., P.O. Box 1625, Idaho Falls, Idaho 83415.** U.S. Citizenship Required. We are an equal opportunity employer, M/F/H/V.



**ANALYTICAL CHEMISTRY:** Assistant or associate professor, tenure-track position; appointment for August 1986. Ph.D. required. Primary teaching responsibility in Instrumental Analysis. Active research program expected. Qualified candidates in physical, inorganic, or environmental chemistry will also be considered. Research analytical instrumentation including nmr, HPLC, and capillary gc-mass spec available. Send vita, transcripts, and three letters of reference to: L. Keller, Department of Chemistry, Florida International University, Miami, FL 33199. Closing date is November 21, 1985, but the search will continue until the position is filled. FIU is a member of the State University System of Florida with an enrollment of 16,000 students and with anticipated expansion in science and engineering. FIU is an equal opportunity/affirmative action employer.

**PROJECT MANAGER**—EDI Engineering & Science, an equal opportunity employer, is seeking project managers for hydrogeological and multi-disciplinary projects. Minimum requirements are a degree in hydrogeology, geology or engineering, four years of professional experience and one year of relevant project management experience. Experience with hazardous waste site investigations and design of groundwater containment recovery systems, and computer skills are highly desirable. Reply in confidence to Personnel Director, EDI, 611 Cascade West Parkway, SE, Grand Rapids, MI 49506.

# HEALTH PHYSICISTS ENVIRONMENTAL ENGINEERS

UNC Nuclear Industries, a prime operating contractor to the U.S. Department of Energy at Richland, WA, is embarking upon a major multi-year program to upgrade the N Reactor. We are looking for a few top professionals to join our select technical team.

We have entry and mid-level professional positions in:

- Radioactive waste shipping and management, including DOT regulation compliance.
- Exposure reduction/ALARA efforts involving reactor operation and maintenance forces.
- Radiological support services including audit, development and presentation of radiological safety training material.
- Implementation of environmental and emergency preparedness plans, controls, procedures, and instructions in accord with all applicable standards.

The successful candidates will possess a degree and strong technical knowledge in one of the above areas, plus mature judgment and the ability to effectively interface with all levels of plant personnel.

If the above describes your background, and you are interested in being considered, please send resume, **salary history and salary requirements**, in confidence to: K.A. Bresnahan, Dept. JD, UNC Nuclear Industries, P.O. Box 490, Richland, WA 99352.

U.S. citizenship required (DOE security clearance preferred).

Equal employment opportunity is our pledge and our practice.



## UNC NUCLEAR INDUSTRIES

## Environmental Chemists

**ENVIRESPONSE** has been awarded the EPA's Environmental Emergency Response Unit (EERU) contract in Edison, New Jersey. The following openings currently exist in the sampling and analytical section:

### • GC/MS

Degree in Chemistry, Chemical Engineering, or Environmental Science plus a minimum of 3-5 years' experience for this position which offers the challenge that only a state-of-the-art GC/MS/MS toxics in air monitoring system can provide. Activities will include collection, analysis, interpretation of environmental data from wastes, soil, air and other media. Individuals will be required to support projects in the field. Extensive travel and experience in dealing with hazardous wastes are required for this position.

### • Field Chemist

Degree in Chemistry, Chemical Engineering or Environmental Science as well as a minimum of 3 years' related experience required. Duties include the development and performance of procedures for the rapid analyses of numerous samples of complex waste.

To be considered for the above positions, please send resume, including salary history, to: Kevin McDonald, Personnel Dept., Enviresponse, 110 South Orange Avenue, Livingston, New Jersey 07039. We are an equal opportunity employer m/f/h/v.

## ENVIRESPONSE

## CLASSIFIED SECTION

### HAZARDOUS WASTE RESEARCH UNIVERSITY OF SOUTHERN CALIFORNIA

The Civil Engineering Department, Environmental Engineering Program is requesting applications for a tenure-track assistant professor position from individuals with demonstrated research ability in some aspect of hazardous waste or a closely related area. Candidates should also be able to teach graduate level courses in laboratory methods and either sanitary engineering, or solid and hazardous waste management. A Ph.D. in a biological, chemical, physical or engineering discipline is required. A background in Civil Engineering is preferred, but not required. The position is available immediately. Send application letter, resume detailing research and teaching experience, a statement of proposed research and three (3) names for letters of recommendation by December 15th, to Ronald C. Henry, University of Southern California, Biegler Hall of Engineering 213M, University Park, Los Angeles, CA 90089-0231.

USC is an Equal Opportunity/Affirmative Action Employer.

### LABORATORY BUSINESS MANAGER

Opportunity for a business oriented person to lead the expansion and development of a commercial laboratory into new areas of environmental analysis. Familiarity with market development and laboratory analysis particularly in the areas of industrial waste water, soil, potable water and hazardous waste are essential. A chemical/marketing background is desirable. EOE. Apply in writing to:

**Sunohio—Personnel Manager**  
1700 Gateway Blvd., S.E.  
Canton, OH 44707

## CLASSIFIED ADVERTISING RATES

Rate based on number of insertions used within 12 months from date of first insertion and not on the number of inches used. Space in classified advertising cannot be combined for frequency with ROP advertising. Classified advertising accepted in inch multiples only.

Unit	1-T	3-T	6-T	12-T	24-T
1 inch	\$100	\$95	\$90	\$85	\$80

(Check Classified Advertising Department for rates if advertisement is larger than 10".)  
SHIPPING INSTRUCTIONS: Send all material to

**Environmental Science & Technology**  
Classified Advertising Department  
25 Sylvan Rd. South  
Westport, CT. 06881  
(203) 226-7131

## INDEX TO THE ADVERTISERS IN THIS ISSUE

### ADVERTISERS

### PAGE NO.

### SALES REPRESENTATIVES

**ABC Laboratories, Inc. . . . . OBC**  
M.R.W.

**Philadelphia, Pa. . . .** Patricia O'Donnell, CENTCOM, LTD., GSB Building, Suite 725, 1 Belmont Ave., Bala Cynwyd, Pa 19004 (Area Code 215) 667-9666

**New York, N.Y. . . .** Dean A. Baldwin, CENTCOM, LTD., 60 E. 42nd Street, New York 10165 (Area Code 212) 972-9660

**Westport, Ct. . . .** Edward M. Black, CENTCOM, LTD., 25 Sylvan Road South, P.O. Box 231, Westport, Ct 06881 (Area Code 203) 226-7131

**Anderson Laboratories, Inc. . . . . 1012**  
Dusty Crocker & Company

**Cleveland, Oh. . . .** Bruce Poorman, CENTCOM, LTD., 325 Front St., Berea, OH 44017 (Area Code 216) 234-1333

**Chicago, Ill. . . .** Michael J. Pak, CENTCOM, LTD., 540 Frontage Rd., Northfield, Ill 60093 (Area Code 312) 441-6383

**Houston, Tx. . . .** Michael J. Pak, CENTCOM, LTD., (Area Code 312) 441-6383

**Seastar Instruments, Ltd. . . . . 1025**

**San Francisco, Ca. . . .** Paul M. Butts, CENTCOM, LTD., Suite 1070, 2672 Bayshore Frontage Road, Mountainview, CA 94043. (Area Code 415) 969-4604

**Los Angeles, Ca. . . .** Clay S. Holden, CENTCOM, LTD., 3142 Pacific Coast Highway, Suite 200, Torrance, CA 90505 (Area Code 213) 325-1903

**Boston, Ma. . . .** Edward M. Black, CENTCOM, LTD., (Area Code 203) 226-7131

**John Wiley & Sons, Inc. . . . . IFC**  
Flamm Advertising

**Atlanta, Ga. . . .** Edward M. Black, CENTCOM, LTD., (Area Code 203) 226-7131

Advertising Management for the  
American Chemical Society Publications

**CENTCOM, LTD.**

*President*

**Thomas N. J. Koerwer**

*Executive Vice President* *Senior Vice President*  
**James A. Byrne** **Benjamin W. Jones**

**Alfred L. Gregory, Vice President**  
**Clay S. Holden, Vice President**  
**Robert L. Voepel, Vice President**  
**Joseph P. Stenza, Production Director**

25 Sylvan Road South  
P.O. Box 231  
Westport, Connecticut 06881  
(Area Code 203) 226-7131  
Telex No. 643310

ADVERTISING SALES MANAGER

**James A. Byrne, VP**

ADVERTISING PRODUCTION MANAGER  
**Jay S. Francis**

### United Kingdom:

Reading, England—Technomedia, Ltd. . . .  
Wood Cottage, Shurlock Row, Reading  
RG10 0QE, Berkshire, England 0734-343302

Lancashire, England—Technomedia, Ltd. . . .  
c/o Meconomics Ltd., Meconomics House,  
31 Old Street, Ashton Under Lyne, Lancashire, England 061-308-3025

**Continental Europe . . .** International Communications Inc., Rue Mallard 1, 4800 Verviers, Belgium. Telephone (087) 22-53-85. Telex No. 49263

**Tokyo, Japan . . .** Shuji Tanaka, International Media Representatives Ltd., 2-29, Toranomon 1-Chrome, Minatoku, Tokyo 105 Japan. Telephone: 502-0656

## Prediction of Multicomponent Adsorption Equilibria Using Ideal Adsorbed Solution Theory

John C. Crittenden,\*<sup>†</sup> Paul Luft,<sup>‡</sup> David W. Hand,<sup>§</sup> Jacqueline L. Oravitz,<sup>||</sup> Scott W. Loper,<sup>†</sup> and Metin Arli<sup>†</sup>

Department of Civil Engineering, Michigan Technological University, Houghton, Michigan 49931, Westvaco Corporation, Charleston, South Carolina 29406, Water and Waste Management Programs, Michigan Technological University, Houghton, Michigan 49931, and Morrison-Knudson Engineers, Inc., Denver, Colorado 80290

■ The capability of ideal adsorbed solution theory (IAST) to predict multicomponent competitive interactions between the following volatile organic chemicals was tested: chloroform, bromoform, trichloroethene, tetrachloroethene, 1,2-dibromoethane, and chlorodibromomethane. A total of seven mixtures that contained various combinations of two, three, and six solutes were tested for three commercially available activated carbons. The predictions were satisfactory for the 256 isotherm data that were collected. An error analysis was performed for various isotherms that are used to represent single solute data in IAST calculations. This analysis demonstrated that the Freundlich equation was sufficiently accurate in representing the data under certain simplifying assumptions, and the use of the Freundlich equation in IAST calculations resulted in a relatively straightforward expression to describe the multicomponent data. The multicomponent data for the mixtures were plotted as total organic halogen (TOX) and total organic carbon (TOC), and, when the mixture data were plotted in this manner, appeared to behave as a pseudo single solute.

### Introduction

A potentially useful technique for the removal of synthetic organic chemicals (SOCs) is adsorption onto granular activated carbon (GAC). The degree of removal of SOCs from drinking water or wastewater by GAC depends on the multicomponent competitive interactions of organic chemicals which are present in solution. In order to design a cost-effective system, the adsorption capacity of a solute in the presence of other solutes must be quantified. The design of GAC treatment systems using isotherm results such as those which are reported herein is discussed elsewhere (1-11).

Ideal adsorbed solution theory (IAST) has been used to predict the multicomponent equilibria of two components using their respective single-solute isotherm parameters (10-17). In this study, IAST was used to predict the multicomponent equilibria of up to six volatile organic compounds (VOCs) by using a simple algorithm. The identical algorithm has also been used to predict multicomponent equilibria of known adsorbates in unknown mixtures by using hypothetical components to represent

the adsorption strength of the background (18-21).

### Materials and Experimental Methods

**Chemicals.** All chemicals were reagent grade or better. 1,2-Dibromoethane, bromoform, and chlorodibromomethane were obtained from Aldrich Chemical Co., Milwaukee, WI. Methanol, 2,2,4-trimethylpentane, chloroform, and trichloroethene were obtained from Burdick & Jackson Co., Muskegon, MI. Tetrachloroethane and 1,1,1-trichloroethane were obtained from J. T. Baker Chemical Co., Phillipsburg, NJ. Three activated carbons were used in these studies: Calgon's (Pittsburgh, PA) Filtrasorb-400 and Westvaco's (Covington, VA) WV-G and WV-W.

**Chemical Analysis.** The VOCs were analyzed by using gas chromatography with liquid-liquid extraction (LLE) and purge and trap methods (22). The samples for LLE method were extracted by using 5-30 mL of solution with 5-10 mL of 2,2,4-trimethylpentane following the procedure which was described by Mieux (23). 1,1,1-Trichloroethane was used as the internal standard for the LLE method. Hall, electron capture, and photoionization detectors were used for identification.

To determine the total organic halogen (TOX) of the isotherm mixtures, the gas chromatograph was used to quantify each halogenated species, and the total number of halogens in the various organic molecules was summed and expressed as chloride. This analytic procedure would give similar results to the actual procedure because Billet and Lichtenberg (24) have shown high TOX recovery for many of the solutes which were used in this study.

**Isotherm Procedure.** The equilibration time that was used satisfied the requirements which were discussed by Crittenden and Hand (5), Hand et al. (6), and Randtke and Snoeyink (25). A bottle point isotherm procedure was used to conduct all equilibrium studies. Carbon dosages, generally ranging from 6 to 3000 mg/L (1-500 mg in 160-mL bottles), were added to serum bottles that were then filled head space free with water containing the VOCs. The isotherm bottles were then rotated at 25 rpm and allowed to come to equilibrium.

Initial liquid-phase concentrations were determined by running blanks, with no carbon dosage, along with the samples. VOC loss, due to volatilization, was found to be negligible by comparing samples that were analyzed immediately to those that were equilibrated along with the samples.

Solutions were prepared with distilled, deionized Milli-Q water (Millipore Corp., Bedford, MA). The six-component

<sup>†</sup>Department of Civil Engineering, Michigan Technological University.

<sup>‡</sup>Westvaco Corporation.

<sup>§</sup>Water and Waste Management Programs, Michigan Technological University.

<sup>||</sup>Morrison-Knudson Engineers, Inc.



isotherm experiment was conducted at 10–12 °C in a temperature-controlled room. The two- and three solute mixture isotherms were conducted at 20–22 °C. The solutions were buffered with a 0.001 M phosphate buffer at a pH of 6.0.

Once equilibrium was achieved, the PGAC was removed by centrifuging the isotherm bottles, and the liquid-phase concentrations were determined. The corresponding surface loadings were calculated from the following mass balance on an isotherm bottle:

$$q_i = (C_{i0} - C_i)V/M \quad (1)$$

**Carbon Preparation.** Representative samples of the GAC were obtained by mixing and splitting the GAC. Powdered granular activated carbon (PGAC) which was within U.S. no. 200 and 400 sieves was used in the isotherm studies. PGAC was obtained by crushing representative samples of the U.S. no. 12 by 40-sieve carbon such that all of the crushed GAC passed the U.S. no. 200 sieve. The PGAC that was retained on a U.S. no. 400 sieve was then washed with Milli-Q water and dried overnight at 105 °C.

### Approach

**Ideal Adsorbed Solution Theory.** In IAST, the following five basic equations are used to predict multicomponent behavior from single-solute isotherms (12):

$$q_T = \sum_{i=1}^N q_i \quad (2)$$

$$z_i = q_i/q_T \quad i = 1 \text{ to } N \quad (3)$$

$$C_i = z_i C_i^0 \quad i = 1 \text{ to } N \quad (4)$$

$$1/q_T = \sum_{i=1}^N z_i/q_i^0 \quad (5)$$

$$\frac{\pi_m A}{RT} = \int_0^{q_i^0} \frac{d \ln C_i^0}{d \ln q_i^0} dq_i^0 = \frac{\pi_i^0 A}{RT} = \int_0^{q_j^0} \frac{d \ln C_j^0}{d \ln q_j^0} dq_j^0 = \frac{\pi_j^0 A}{RT} = \dots \text{ for } j = 2 \text{ to } N \quad (6)$$

Equation 2 defines  $q_T$ , the total surface loading. Equation 3 defines  $z_i$ , the mole fraction on the surface of the carbon for component  $i$ . Equation 4 is analogous to Raoult's law, where  $C_i^0$  is the single-solute liquid-phase concentration in equilibrium with  $q_i^0$ . The single-solute surface loadings,  $q_i^0$ , are the loadings that cause the same spreading pressure, or reduction in surface tension, as the mixture. Equation 5 is the expression for no area change per mole upon mixing in the mixture from the single-solute isotherms at the spreading pressure of the mixture. Equation 6 equates the spreading pressures of the pure component systems to the spreading pressure of the mixture.

In this study, the single-solute isotherm representations which were proposed by Freundlich, Jossens et al. (13), and Singer and Yen (14, 17) were used in eq 6 to evaluate the spreading pressure.

**Ideal Adsorbed Solution Theory Using the Freundlich Isotherm Equation.** The Freundlich adsorption isotherm equation is given by the expression:

$$q_i = K_i C_i^{1/n_i} \quad (7)$$

If the Freundlich isotherm equation is used to represent single-solute behavior in eq 6, then eq 6 will simplify to the expression:

$$n_i q_1^0 = n_j q_j^0 \quad j = 2 \text{ to } N \quad (8)$$

After a great deal of algebraic manipulation, the following equation for each adsorbate was derived:

$$C_i = \frac{q_i}{\sum_{j=1}^N q_j} \left( \frac{\sum_{j=1}^N n_j q_j}{n_i K_i} \right)^{n_i} \quad \text{for } i = 1 \text{ to } N \quad (9)$$

Fritz et al. (16) reported an IAST algorithm that used a series of Freundlich parameters over various concentration ranges; accordingly, eq 9 may be considered a simplification of their IAST equations. Equation 9 was combined with the mass balance, eq 1, to eliminate the liquid-phase concentration,  $C_i$ , in IAST predictions for bottle point isotherms as shown in the equation:

$$F_i(q_1, q_2, \dots, q_i, \dots, q_N) = 0 = C_{i0} - \frac{M}{V} q_i - \frac{q_i}{\sum_{j=1}^N q_j} \left( \frac{\sum_{j=1}^N n_j q_j}{n_i K_i} \right)^{n_i} \quad \text{for } i = 1 \text{ to } N \quad (10)$$

According to eq 10, the equilibrium state in an isotherm bottle is determined by setting  $F_i$  equal to zero. Furthermore, all that is needed to define the equilibrium state are the Freundlich  $K$  and  $1/n$ , the initial concentration of each solute, and carbon dosage  $M/V$ . Since eq 10 is valid for all components,  $N$  nonlinear simultaneous equations with  $N$  unknown  $q_i$  values must be solved to estimate the final equilibrium state in the isotherm bottle.

This set of equations was solved by using a Newton–Raphson algorithm. If we let  $\bar{q}_{\text{new}}$  equal the new guesses of  $(q_1, q_2, q_i, q_N)^T$  ( $T$  is the mathematic operand known as transpose),  $\bar{F}$  equal  $(F_1, F_2, \dots, F_i, \dots, F_N)^T$ , and  $J^{-1}$  equal inverse of the Jacobian of eq 10, then the Newton–Raphson algorithm can be formulated by

$$\bar{q}_{\text{new}} = \bar{q}_{\text{old}} - J^{-1}_{\text{old}} \bar{F}_{\text{old}} \quad (11)$$

in which,  $\bar{q}_{\text{new}}$  and  $\bar{q}_{\text{old}}$  are the new and old guesses to the roots of eq 10;  $\bar{F}_{\text{old}}$  is the numerical value of eq 10 which is evaluated at  $\bar{q}_{\text{old}}$ . The off diagonal elements of the Jacobian are given by (eq 12 is valid for all  $i$  and  $k$  except when  $k$  equals  $i$ )

$$\frac{\partial \bar{F}_i(q)}{\partial q_k} = \frac{q_i}{(\sum_{j=1}^N q_j)^2} \left( \frac{\sum_{j=1}^N n_j q_j}{n_i K_i} \right)^{n_i} - \left( \frac{q_i n_i n_k}{\sum_{j=1}^N q_j} \right) \frac{(\sum_{j=1}^N n_j q_j)^{n_i-1}}{(K_i n_i)^{n_i}} \quad (12)$$

The diagonal elements of the Jacobian are

$$\frac{\partial F_i(\bar{q})}{\partial q_i} = -\frac{M}{V} - \frac{1}{\sum_{j=1}^N q_j} \left( \frac{\sum_{j=1}^N n_j q_j}{n_i K_i} \right)^{n_i} + \left[ \frac{q_i}{(\sum_{j=1}^N q_j)^2} \right] \left( \frac{\sum_{j=1}^N n_j q_j}{n_i K_i} \right)^{n_i} - \left( \frac{q_i n_i^2}{\sum_{j=1}^N q_j} \right) \frac{(\sum_{j=1}^N n_j q_j)^{n_i-1}}{(n_i K_i)^{n_i}} \quad (13)$$

To implement this algorithm, we start with an initial guess for  $\bar{q}$  and improve our guess using eq 10–12 until eq 10 is satisfied. Usually four to six iterations are required to obtain greater than 0.01% precision in the roots to eq 10.

**Table I. Summary of the Single-Component Isotherms, Experimental Conditions, and Freundlich Isotherm Parameters**

carbon type, temp	compound	equi- bration time, days and pH	$K$ , $\mu\text{g/g}$ , ( $\text{L}/\mu\text{g})^{1/n}$ best fit	95% confidence interval $K$	$K$ , $\mu\text{M/L}$ , ( $\text{L}/\mu\text{M})^{1/n}$ best fit	95% confidence interval	1/ $n$ best fit	95% confidence interval 1/ $n$	concn range, $\mu\text{g/L}$
F-400, 10–20 °C	cis-dichloroethene	7, 6.0	150.7	121.4–187.2	39.0	26.7–57.1	0.7045	0.6687–0.7402	120–1250
	trichloroethene	6.5, 6.0	3389.7	2795.6–4109.9	196.6	124.4–310.6	0.4163	0.3620–0.4706	5.6–360
	tetrachloroethene	6.0, 6.0	10388.8	9443.1–11429.2	650.6	530.1–798.9	0.4579	0.4365–0.4794	3.5–1170
	bromoform	10, 6.0	1802.0	1696.2–1914.4	160.5	142.9–180.3	0.5629	0.5528–0.5730	40.0–2000
	chloroform	7, 6.0	284.8	254.7–318.4	30.4	24.5–37.9	0.5325	0.5102–0.5549	8.0–1180
	1,2-dibromoethane	7, 6.0	1795.0	1632.6–1973.5	118.4	98.5–142.4	0.4808	0.4637–0.4979	32.0–1750
	chlorodibromomethane	7, 6.0	1265.7	951.7–1631.8	96.0	59.8–154.2	0.5170	0.4758–0.5581	92.0–1830
F-400, 20–22 °C	chloroform	2, 6.0	39.23	36.19–42.92	12.19	11.87–12.50	0.7556	0.7387–0.7725	34.5–1324
	trichloroethene	2, 6.0	1245	1012–1531	93.66	85.00–103.2	0.4696	0.4216–0.5177	3.2–528
	bromoform	2, 6.0	436.6	370.8–498.7	78.17	74.85–81.64	0.6889	0.6640–0.7139	11.8–3871
WV-G, 10–12 °C	cis-dichloroethene	7.0, 6.0	180.4	141.2–240.4	35.4	23.1–56.6	0.6441	0.6045–0.6383	143–1340
	trichloroethene	6.5, 6.0	3261.9	2986.9–3562.2	181.0	148.7–220.3	0.4073	0.3850–0.4295	5.3–120
	trichloroethene	3.0, 6.0	2847.0	2482.3–3265.3	148.4	107.3–205.1	0.3944	0.3561–0.4327	3.7–400
	tetrachloroethene	6.0, 6.0	7524.3	6700.6–8449.3	589.5	460.8–753.7	0.5017	0.4762–0.5271	7.0–910
WV-W, 20–22 °C	chloroform	2, 6.0	55.69	51.30–60.46	15.91	15.45–16.38	0.7380	0.7188–0.7571	4.2–947
	trichloroethene	2, 6.0	1062	816.7–1380.	92.84	82.12–105.0	0.5005	0.4399–0.5612	3–537
	bromoform	2, 6.0	474.6	401.8–560.6	64.82	64.60–67.28	0.6482	0.6236–0.6728	37–8092
HD 3000, 20–22 °C	chloroform	2, 6.0	92.48	88.63–96.52	19.12	18.90–19.34	0.6704	0.6612–0.6795	13.5–888
	trichloroethene	2, 6.0	712.8	479.2–1060	53.77	44.61–64.80	0.4702	0.3766–0.5637	4–585
	bromoform	2, 6.0	632.0	538.8–741.2	55.72	53.11–58.46	0.5608	0.5373–0.5843	46–8319
	chlorodibromomethane	2, 6.0	281.0	263.7–299.4	31.31	30.61–32.02	0.5890	0.5749–0.6031	14.5–510

## Results and Discussion

**Single-Solute Isotherms.** The single-solute isotherm data were fit to the Freundlich adsorption isotherm equation. The data points were transformed by taking the logarithm of  $C_i$  and  $q_i$ , and the resulting values were fit by the least-squares method. Calculated values for  $K_i$  and  $1/n_i$ , along with upper and lower 95% confidence limits, are shown in Table I for the various GACs and adsorbates. Adsorption isotherms were conducted at two temperatures, 10–12 °C, which is a typical groundwater temperature in the Northern United States, and 20–22 °C. As shown in Table I, the adsorption capacities at 10–12 °C were approximately 2–4 times as high as those that were observed at 20–22 °C.

The time it takes for an isotherm to achieve equilibrium must be considered when conducting isotherms (5, 6, 25). Dobbs and Cohen (26) reported isotherm data that had been equilibrated for 2 h at 22 °C. This was not sufficient time to achieve equilibrium (5, 6, 25). For similar temperature, carbon, and adsorbates, capacities which were measured in this study was 2–3 times higher than were reported by Dobbs & Cohen (26) for all adsorbates except for bromoform. With a decrease in temperature to 10–12 °C, trichloroethene was still not at equilibrium until after 6 days. This was demonstrated by conducting long-term isotherms for 20 days. Consequently, 20–22 and 10–12 °C isotherm experiments were conducted for at least 2 and 6 days, respectively.

The agreement of the data to the Freundlich equation was expressed in terms of the average percent error (APE) in the fit:

$$\text{APE} = \frac{100}{N} \sum \frac{|X_{\text{observed}} - X_{\text{predicted}}|}{X_{\text{observed}}} \quad (14)$$

The isotherm data for 1,2-dibromoethane were described with excellent precision by the Freundlich isotherm with an APE of 3.9% in  $C$  and 1.1% in  $q$ . The isotherm data for trichloroethene had the most scatter of the single-solute isotherms with an APE of 14.9% in  $C$  and 1.5% in  $q$ . The single-solute isotherm data for 1,2-dibromomethane and trichloroethene are shown in Figures 1 and 2, respectively.

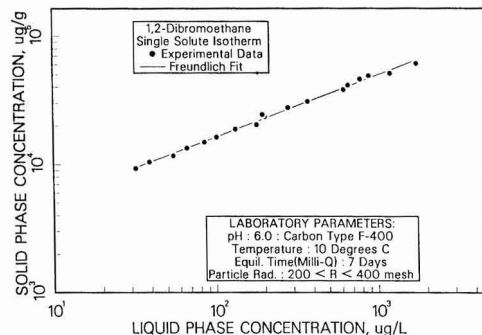


**Figure 1.** 1,2-Dibromoethane isotherm data and the Freundlich isotherm fit for F-400 carbon.

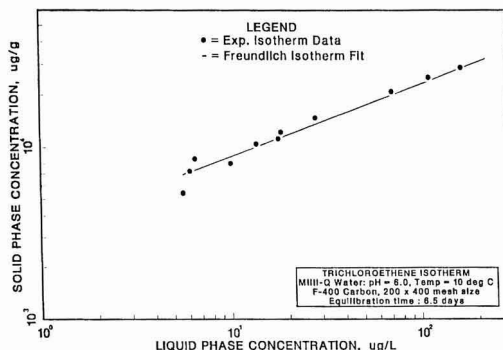


**Figure 2.** Trichloroethene data and the Freundlich isotherm fit for F-400 carbon.

The dots are the experimental data and the solid lines are the Freundlich isotherm fits.

**Analysis of Errors Associated with Using Ideal Adsorbed Solution Theory To Predict Multicomponent Equilibrium Using Various Single Solute Isotherms.** Errors that arise from utilizing IAST are caused

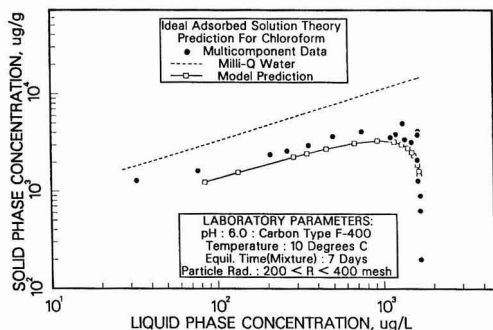


**Figure 3.** Chloroform isotherm data in the six-component mixture 7, IAST predictions using eq 10, and the single-solute isotherm.

from extrapolating the single-solute isotherm data to zero and high concentrations. As shown in eq 6, a plot of  $d \ln C_i^0 / d \ln q_i^0$  vs.  $q_i^0$  may be used to evaluate the importance of the single-solute isotherm on IAST predictions. Singer and Yen (14, 17) have proposed an isotherm that extrapolates the isotherm to low concentrations by assuming the isotherm is linear at a zero surface loading. However, IAST calculations that were made in this study using Singer and Yen's isotherm had a negligible effect on IAST calculations. Consequently, it was not used in IAST calculations because Freundlich IAST calculations which are given by eq 9 are much simpler to use.

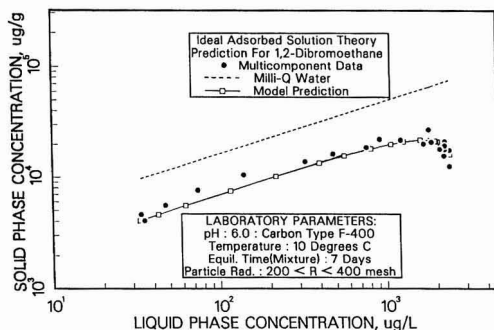
With respect to extrapolation of single isotherms to high concentrations, IAST predictions often required single-solute surface loadings that were much higher than experienced in multisolute systems, particularly for the weakly adsorbed components. In spite of the fact that the single-solute isotherms were extrapolated, it is interesting to note that the IAST predictions for high surface concentrations were not any further off than the low concentration predictions.

Since no curvature was found in the single-solute isotherms when plotted on a log-log scale, the representations of the single-solute isotherms that account for curvature (10, 11, 13, 16) were not used to predict the VOC data.

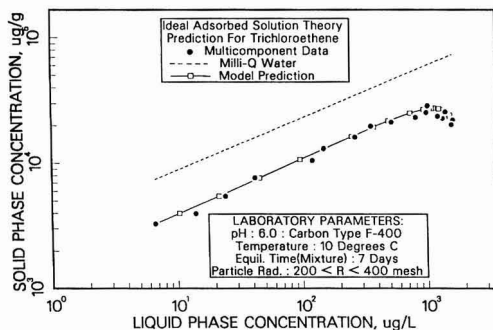
**Comparisons between Ideal Adsorbed Solution Theory Predictions and Multicomponent Volatile Organic Chemical Isotherm Data.** As shown in Table II, isotherms were conducted for four bisolute mixtures, two ternary mixtures, and one six-component mixture to verify that IAST could predict multicomponent equilibria. All the raw isotherm data and IAST predictions for mixture 7 were presented by Luft (20). The information that is required for an IAST prediction using eq 9 is the Freundlich isotherm parameters, initial concentrations which are given in Table II, and the bottle volume and carbon dosages. For all the isotherm mixtures, the initial concentrations in the isotherm bottles were held constant, and the carbon dosages were varied to obtain the results. This procedure was used because this would be the situation that analysts would face in the field when they are estimating the capacity of GAC.

Table II also displays the APE in predicting  $C$  and  $q$  by using IAST. If all the 256 data are included, the APE which is defined by eq 14 was 29% and 16% for  $C$  and  $q$ , respectively. The greater precision in predicting  $q$  is expected because the isotherm slopes are close to 0.5 and errors in  $C$  would have less impact on  $q$ . Accordingly, multicomponent equilibria can be predicted satisfactorily by using eq 9.

Figures 3–5 provide a visual representation of the pre-



**Figure 4.** 1,2-Dibromoethane isotherm data in the six-component mixture 7, IAST predictions using eq 10, and the single-solute isotherm.



**Figure 5.** Trichloroethene isotherm data in the six-component mixture 7, IAST predictions using eq 10, and the single-solute isotherm.

cision of IAST predictions for three of the components in the six-component mixture (mixture 7 in Table II). The adsorbate chloroform, 1,2-dibromoethane, and trichloroethene, which are shown in Figures 3–5, are weakly, intermediately, and strongly adsorbing components in this mixture. The open boxes are the IAST predictions that correspond one to one with the data which are represented as solid dots. In cases where the prediction matches the data exactly, the dots hide the boxes. This displacement of the capacity which was observed in the mixture from the single-solute capacity can be seen by comparing the dashed lines which represent the single-solute isotherms to the data. This displacement is the greatest for higher liquid-phase concentrations or for small PGAC dosages because high surface concentrations of the strongly adsorbing components caused more competitive interactions.

On the basis of sensitivity analyses that were conducted by Luft (20) and the APEs that were observed in the single-solute isotherms, the IAST predictions were as precise as the experimental methods used to determine the single-solute isotherms. For example, the APE for TCE was 14% and 1.5% in  $C$  and  $q$  for the single-solute isotherms as contrasted to 22% and 4% in mixture 7. Therefore, no improvements in IAST predictions would be necessary until better methods could be obtained to measure single-component data.

Table III displays one set of the trisolute isotherm results and IAST predictions using the Freundlich isotherm equation. Also shown are the experimental relative adsorptivities which give the preference of component  $i$  as compared to component  $j$  by the adsorbent. The relative adsorptivity is defined by

$$\alpha_j^i = q_i C_j / (q_j C_i) \quad (15)$$

**Table II. Average Percent Error between Experimental Multisolute Equilibrium Data and Ideal Adsorbed Solution Theory Predictions**

mixture no.	carbon	temp, °C	components	initial concn in mixture, μM/L	relative % error using IAS		no. of data	C range, μM/L	q range, μM/g
					C	q			
1	F-400	20-22	chloroform trichloroethene	11.8 12.4	12 44	11 4	22	1.46-10.2 0.019-3.33	12.8-29.5 15.4-182
2	F-400	20-22	chloroform trichloroethene	10.9 70.4	8 84	20 18	16	2.53-10.3 0.512-56.9	13.6-53.0 113-1151
3	WV-W	20-22	chloroform trichloroethene	9.76 45.2	21 12	21 2	22	0.276-9.03 0.0990-27.1	4.39-19.7 20.9-492
4	HD-3000	20-22	chloroform chlorodibromoethane	8.46 4.79	57 54	67 17	24	2.07-7.25 0.431-3.35	7.61-27.3 5.19-32.4
5	WV-W	20-22	chloroform trichloroethene bromoform	38.5 35.2 30.2	31 25 12	45 2 2	18	7.09-35.7 0.244-26.7 0.368-23.1	20.2-113 22.7-345 19.3-283
6	F-400	20-22	chloroform trichloroethene bromoform	38.5 35.4 30.2	22 24 27	30 2 15	23	4.16-37.4 0.102-30.6 0.198-27.0	15.7-82.1 16.2-389 13.8-256
7	F-400	10-12	chloroform trichloroethene chlorodibromoethane 1,2-dibromoethane bromoform tetrachloroethene	14.0 13.5 12.4 13.4 11.4 12.3	64 22 24 22 19 45	21 4 13 8 12 4	22 24 24 24 23 14	0.05-14 0.04-12.3 0.13-11.9 0.13-12.7 0.07-10.9 0.04-5.4	1.7-66 7.4-224 6.7-128 7.3-146 6.5-195 95.7-915
av % error for mixtures 1-7					29	16	256		
8 <sup>a</sup>	B10-I		phenol <i>p</i> -nitrophenol		3 47	8 1	50 50		
8 <sup>b</sup>	B10-I		phenol <i>p</i> -nitrophenol		21 1	44 28	50 50		

<sup>a</sup>Data of Fritz et al. (7), predicted by using the Jossens et al. (13) isotherm in IAST predictions. <sup>b</sup>Data of Fritz et al. (7), predicted by using eq 10.

According to Table III, the adsorbent prefers bromoform over chloroform by a factor of 4-18. It is interesting to note that the multicomponent Langmuir isotherm would predict a constant relative adsorptivity. Recently, Yen and Singer (17) demonstrated that the multicomponent Langmuir equation did not describe multicomponent equilibria for several phenols, whereas IAST was successful in describing the data.

Jossens et al. (13) presented IAST predictions for bisolute isotherm data that were collected by Fritz et al. (16). Since their data were collected at much higher concentrations, curvature was observed in their single-solute data, and the Jossens et al. isotherm equation was used to represent the single-solute isotherms in IAST calculations. The APE that was reported by Jossens et al. (13) was 2% in *q*; however, the APE in *C* was not reported. Bisolute data for phenol (initial concentrations 0.01, 0.02, 0.03, 0.04, 0.05, 0.06, 0.07, 0.08, 0.09, and 0.1 mM/L) and *p*-nitrophenol (initial concentrations of 0.02, 0.03, 0.04, 0.05, and 0.1 mM/L) were reanalyzed in this study by using the Jossens et al. isotherm in IAST calculations, and the APEs for *q* were 8% and 1% for phenol and *p*-nitrophenol, respectively. The APEs for *C* were 3% and 47% for phenol and *p*-nitrophenol, respectively. Jossens et al. (13) also reported 2-21% relative error for *q* in three other pairs of bisolute-substituted phenol data. Accordingly, the deviations from IAST which was found in this study were not significantly out of line with those reported by Jossens et al. (13) given the fact that this study was conducted at lower concentrations.

For the sake of mathematic expediency in fixed-bed model calculations, the curvature that is observed in the single-solute isotherm data may be ignored if less precision in the fixed-bed calculations can be tolerated. For example, the data which were predicted by Jossens et al. (13) isotherm were reanalyzed by fitting the Freundlich isotherm equation to the single-component data. Following this, eq 9 was used to predict their multicomponent isotherm data. As shown in Table II for mixture 8, the APE for *C* and *q* for phenol was 21% and 44% and for *p*-nitrophenol was 1% and 28% using the Freundlich isotherm as compared to 3% and 8% for phenol and 47% and 1% for *p*-nitrophenol, respectively, using the Jossens et al. isotherm. Consequently, one could use eq 9 to represent the data; however, the IAST predictions would not be as good.

**TOC and TOX Isotherm Representations of Multicomponent Data.** The multicomponent isotherm results for the various mixtures shown in Table II were expressed as single-component TOC and TOX isotherms, and their effective single-solute isotherms were evaluated. For example, according to these results, TOC or TOX isotherms of the various mixtures may appear to behave as pseudo single components. Figure 6 displays TOC and TOX isotherms for the trisolute mixture of chloroform, trichloroethene, and bromoform on F-400 carbon which was reported in Table II.

### Conclusions

Ideal adsorbed solution theory (IAST) satisfactorily



**Table III. Mixture 6 Equilibrium Data for Chloroform (Species 1), Bromoform (Species 2), and Trichloroethylene (Species 3), for F-400 Carbon and Initial Concentrations of 38.5  $\mu\text{M/L}$  Chloroform, 30.2  $\mu\text{M/L}$  Bromoform, and 35.4  $\mu\text{M/L}$  TCE As Compared to IAS Predictions Using Equation 10**

experimental surface concentration, $\mu\text{M/g}$			predicted surface concentration, $\mu\text{M/g}$			experimental solution concentration, $\mu\text{M/L}$			predicted solution concentration, $\mu\text{M/L}$			experimental relative adsorptivity	
$q_1$	$q_2$	$q_3$	$q_1$	$q_2$	$q_3$	$C_1$	$C_2$	$C_3$	$C_1$	$C_2$	$C_3$	$\alpha_1^2$	$\alpha_1^3$
82.1	256	389	80.8	491	353	37.4 <sup>a</sup>	27.0 <sup>a</sup>	30.6 <sup>a</sup>	37.4	24.1	31.0	4.33	5.79
60.9	289	373	80.4	420	339	37.0 <sup>a</sup>	23.2 <sup>a</sup>	26.4 <sup>a</sup>	36.5	20.0	27.1	7.58	8.58
57.7	281	323	80.0	365	322	36.4 <sup>a</sup>	19.9 <sup>a</sup>	23.7 <sup>a</sup>	35.5	16.8	23.5	8.88	8.60
73.4	242	311	79.5	320	303	34.8 <sup>a</sup>	18.2 <sup>a</sup>	20.1 <sup>a</sup>	34.5	14.2	20.2	6.32	7.33
99.8	205	287	79.0	288	286	32.4 <sup>a</sup>	17.6	17.9 <sup>a</sup>	33.6	12.4	17.7	3.78	5.21
81.0	213	272	78.4	258	268	32.5 <sup>a</sup>	14.2	15.1 <sup>a</sup>	32.5	10.8	15.2	6.02	7.20
55.7	193	238	77.5	227	296	33.3 <sup>a</sup>	12.8	13.6 <sup>a</sup>	31.2	9.09	12.5	8.98	10.5
47.2	161	206	75.8	188	212	32.7 <sup>a</sup>	10.4	10.3 <sup>a</sup>	29.1	7.02	9.16	10.7	13.9
39.5	140	176	73.6	157	182	32.5 <sup>a</sup>	8.41	8.11 <sup>a</sup>	26.9	5.49	6.67	13.7	17.8
38.1	120	156	71.4	137	161	31.4 <sup>a</sup>	7.13	6.42 <sup>a</sup>	25.0	4.52	5.14	13.9	20.0
40.0	113	141	69.1	121	143	29.8 <sup>a</sup>	5.77	4.98 <sup>a</sup>	23.3	3.80	4.06	14.6	21.1
40.9	93.1	115	64.4	97.5	116	27.1 <sup>a</sup>	4.27	3.43 <sup>a</sup>	20.3	2.80	2.65	14.5	22.3
43.8	86.8	106	62.3	89.4	107	25.0 <sup>a</sup>	3.50	2.82 <sup>a</sup>	19.1	2.47	2.22	14.2	21.5
39.5	64.3	78.9	53.9	65.8	76.7	21.5 <sup>a</sup>	2.51	1.55	15.0	1.59	1.19	13.9	27.7
34.5	46.5	56.0	44.0	46.9	55.8	17.2 <sup>a</sup>	1.48	0.890	11.0	0.977	0.589	15.6	31.2
32.1	36.6	43.7	37.1	36.6	43.4	12.9 <sup>a</sup>	1.04	0.586	8.55	0.685	0.353	14.1	29.8
28.5	31.9	38.1	33.4	31.9	37.8	11.8 <sup>a</sup>	0.779	0.388	7.37	0.561	0.264	17.0	40.6
26.3	27.4	32.6	29.6	27.3	32.3	10.1 <sup>a</sup>	0.597	0.301	6.20	0.448	0.190	17.6	41.5
24.2	24.0	28.5	26.5	23.9	28.2	8.62 <sup>a</sup>	0.494	0.213	5.33	0.370	0.144	17.3	47.7
22.0	21.6	24.9	24.2	21.5	25.3	7.42 <sup>a</sup>	0.419	0.228	4.70	0.316	0.113	17.4	36.9
20.7	19.2	22.8	21.9	19.1	22.5	6.36	0.348	0.154	4.08	0.266	0.0880	17.0	45.2
17.8	16.1	18.9	18.7	16.0	18.8	5.47	0.285	0.263	3.28	0.204	0.0586	17.4	22.2
15.7	13.7	16.2	16.2	13.6	16.0	4.16	0.198	0.102	2.70	0.163	0.0425	18.4	42.0

<sup>a</sup> Extrapolated beyond existing single-solute isotherm data for evaluation of spreading pressure.

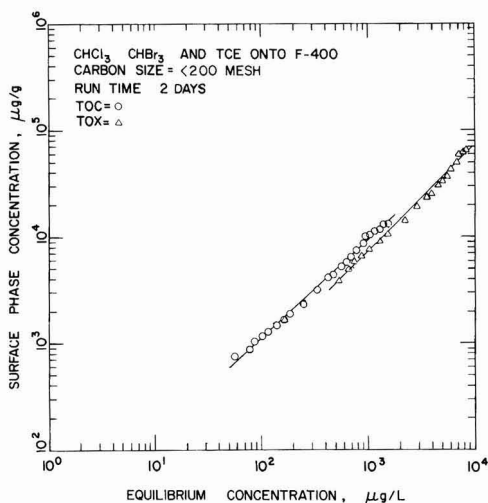


**Figure 6.** TOC and TOX (as Cl) isotherms for the trisolute mixture 6 which contains chloroform, bromoform, trichloroethene, and F-400 carbon.

predicted multicomponent competitive interactions between the following volatile organic chemicals: chloroform, bromoform, trichloroethene, tetrachloroethene, 1,2-dibromoethane, and chlorodibromomethane. A total of seven mixtures that contained various combinations of two, three, and six solutes were tested for three commercially available activated carbons. The average percent error was 29% and 16% for  $C$  and  $q$ , respectively, for the 256-multicomponent data that were collected. This amount of error is reasonable when compared to the precision of the single-solute data. However, these results are for relatively similar molecules, and more work is required to prove IAST can predict competitive interactions between

dissimilar adsorbates and adsorbates of different sizes.

An error analysis was performed for various isotherms that are used to represent single-solute data in IAST calculations. This analysis demonstrated that the Freundlich equation was sufficiently accurate to represent the data under certain simplifying assumptions, and the use of the Freundlich equations in IAST calculations resulted in a relatively simple expression to describe the multicomponent data. Accordingly, resulting IAST equilibrium expressions which are given by eq 9 can be used if two conditions are met. First, the single-solute isotherm data cannot exhibit any curvature on a log-log scale. Second, extrapolation of the Freundlich isotherm equation to high and zero surface concentration must not result in significant errors in the calculation of the spreading pressure.

The multicomponent data for the mixtures were plotted as total organic halogen (TOX) and total organic carbon (TOC). When the mixture data were plotted in this manner, the mixture appeared to behave as a pseudo single solute.

## Glossary

$A$	surface area of adsorbent per unit mass of adsorbent, $\text{L}^2/\text{M}$
$C_i$	liquid-phase concentration for component $i$ , $\text{M/L}^3$
$C_i^0$	single-solute liquid-phase concentration for component $i$ which is evaluated at the spreading pressure of the mixture, $\text{M/L}^3$
$C_{0i}$	initial liquid-phase concentration for component $i$ , $\text{M/L}^3$
$\vec{F}_{\text{old}}$	vector of values of eq 10 which are evaluated at $\vec{q}_{\text{old}}$
$\vec{F}_{\text{new}}$	vector of values of eq 10 which are evaluated at $\vec{q}_{\text{new}}$
$J$	Jacobian of eq 10
$J^{-1}$	inverse of the Jacobian of eq 10
$K_i$	Freundlich capacity parameter for component $i$ , $(\text{M/M})(\text{L}^3/\text{M})^{1/n_i}$
$M$	mass of carbon in isotherm bottle, $\text{M}$
$N$	number of components

$1/n_i$	Freundlich isotherm intensity parameter for component $i$ , dimensionless
$n_i$	inverse of $1/n_i$
$q_i$	solid-phase concentration for component $i$ , M/M
$q_i^b$	single-solute solid-phase concentration for component $i$ which is evaluated at the spreading pressure of the mixture, M/M
$\bar{q}_{\text{new}}$	vector of the new guesses to the roots of eq 10, M/M
$\bar{q}_{\text{old}}$	vector of the old guesses to the roots of equation 10, M/M
$q_T$	total surface concentration, M/M
$R$	universal gas constant
$T$	absolute temperature
$V$	volume of isotherm bottle, L <sup>3</sup>
$z_i$	mole fraction of component $i$ adsorbed on surface, dimensionless
<b>Greek</b>	
$\pi_p$	spreading pressure of the mixture
$\pi_s$	spreading pressure of the single solute $i$
<b>Symbolic</b>	
$\rightarrow$	vector of values of a variable
<b>Abbreviations</b>	
APE	relative percent error as defined in eq 14
DCE	cis-dichloroethene
EDB	1,2-dibromoethane
GAC	granular activated carbon
IAST	ideal adsorbed solution theory
LLE	liquid-liquid extraction
PGAC	powdered granular activated carbon
SOC	synthetic organic chemical
$\bar{F}^T$	transpose of vector $F$
TCE	trichloroethene
TOC	total organic carbon
TOX	total organic halogen
VOC	volatile organic chemical

**Registry No.** C, 7440-44-0; chloroform, 67-66-3; bromoform, 75-25-2; trichloroethene, 79-01-6; tetrachloroethene, 127-18-4; 1,2-dibromoethane, 106-93-4; dibromochloromethane, 124-48-1.

## Literature Cited

- (1) Crittenden, J. C.; Weber, W. J., Jr. *J. Environ. Eng. (N.Y.)* **1978**, *104*, 185-197.
- (2) Crittenden, J. C.; Weber, W. J., Jr. *J. Environ. Eng. (N.Y.)* **1978**, *104*, 433-443.
- (3) Crittenden, J. C.; Weber, W. J., Jr. *J. Environ. Eng. (N.Y.)* **1978**, *104*, 1175-1195.
- (4) Crittenden, J. C.; Wong, B. W. C.; Thacker, W. E.; Snoeyink, V. L.; Hinrichs, R. L. *J. Water Pollut. Control Fed.* **1980**, *52*, 2780-2795.
- (5) Crittenden, J. C.; Hand, D. W. *Am. Water Works Assoc., Semin. Proc. Control Trihalomethanes* **1983**, 71-111.
- (6) Hand, D. W.; Crittenden, J. C.; Thacker, W. E.; *J. Environ. Eng. (N.Y.)* **1983**, *109*, 82-101.
- (7) Hand, D. W.; Crittenden, J. C.; Thacker, W. E. *J. Environ. Eng. (N.Y.)* **1984**, *110*, 440-456.
- (8) Lee, M. C.; Snoeyink, V. L.; Crittenden, J. C. *J. Am. Water Works Assoc.* **1981**, *73*, 440-446.
- (9) Lee, M. C.; Crittenden, J. C.; Snoeyink, V. L. *J. Environ. Eng. (N.Y.)* **1983**, *109*, 631-645.
- (10) Thacker, W. E.; Snoeyink, V. L.; Crittenden, J. C. *J. Am. Water Works* **1983**, *76*, 144-149.
- (11) Thacker, W. E.; Crittenden, J. C.; Snoeyink, V. L. *J. Water Pollut. Control Fed.* **1984**, *56*, 243-250.
- (12) Radke, C. J.; Prausnitz, J. M. *AIChE J.* **1972**, *18*, 761-768.
- (13) Jossens, L.; Prausnitz, J. M.; Fritz, W.; Schlunder, E. U.; Myers, A. L. *Chem. Eng. Sci.* **1978**, *33*, 1097-1106.
- (14) Singer, P. C.; Yen, C.-Y. "Activated Carbon Adsorption of Organics from the Aqueous Phase"; Ann Arbor Science Publishers: Ann Arbor, MI, 1980; Vol. 1, pp 167-189.
- (15) Okazaki, M.; Hiroyuki, K.; Toie, R. *J. Chem. Eng. Jpn.* **1980**, *13*, 286-291.
- (16) Fritz, W.; Schlunder, E. U. *Chem. Eng. Sci.* **1981**, *36*, 721-730.
- (17) Yen, C.-Y.; Singer, P. C. *J. Environ. Eng. (N.Y.)* **1984**, *110*, 976-989.
- (18) Crittenden, J. C.; Luft, P. J.; Hand, D. W.; Friedman, G. Proceedings of the 1984 National Conference on Environmental Engineering, ASCE, Los Angeles, CA, 1984.
- (19) Crittenden, J. C.; Luft, P. J.; Hand, D. W. Proceedings of the 1984 National American Water Works Association Meeting, Dallas, TX, 1984.
- (20) Luft, P. J. "Modeling of Multicomponent Adsorption onto Granular Carbon in Mixtures of Known and Unknown Composition". submitted in partial fulfillment of a Master of Science degree in Chemical Engineering, Michigan Technological University, Houghton, University Microfilms, Ann Arbor, 1984.
- (21) Crittenden, J. C.; Luft, P. J.; Hand, D. W.; Friedman, G. *Water Res.*, in press.
- (22) Environmental Protection Agency "The Analysis of Trihalomethanes in Finished Water by the Purge and Trap Method". U.S. EPA, Environmental Monitoring and Support Laboratory, Cincinnati, OH, 1979.
- (23) Mieux, J. P., Jr. *Am. Water Works Assoc.* **1977**, *69*, 60-62.
- (24) Billets, S.; Lichtenberg, J. J. "Total Organic Halide Method 450.1". Environmental and Monitoring Support Laboratory, Cincinnati, OH, 1980.
- (25) Randtke, S. J.; Snoeyink, V. L. *J. Am. Water Works Assoc.* **1983**, *75*, 406-413.
- (26) Dobbs, Cohen, "Carbon Adsorption Isotherms for Toxic Organics". Municipal Environmental Research Laboratory, Cincinnati, OH, 1980.

Received for review January 30, 1984. Revised manuscript received January 15, 1985. Accepted June 23, 1985. This research is based upon work supported by the National Science Foundation under Grants CEE-7924589 and CEE-8300213 from the Environmental and Water Quality Engineering Program and by the Water and Waste Management Programs at Michigan Technological University. Any opinions, findings, and conclusions or recommendations which are expressed in this publication are those of the authors and do not necessarily reflect the views of the National Science Foundation or the Water and Waste Management Programs.

# Scavenging of Airborne Polycyclic Aromatic Hydrocarbons by Rain

Paul C. M. van Noort\* and Erik Wondergem

Laboratory for Ecology, Water and Drinking Water, National Institute for Public Health and Environmental Hygiene, 2260 AD Leidschendam, The Netherlands

■ The variation of the concentrations of some polycyclic aromatic hydrocarbons in rain with time during three precipitation events was determined. On all occasions these concentrations were found to decrease during the precipitation events. The apparent removal rate constants on a precipitation amount base for two of the three events were calculated to be 1.46 and ca. 3 mm<sup>-1</sup>. For the third event the concentration decrease did not allow the calculation of the apparent removal rate constant. Furthermore, concentrations of polycyclic aromatic hydrocarbons in rain sampled simultaneously at ground level and at an altitude of 200 m were determined. These measurements demonstrate that concentrations of phenanthrene and fluoranthene in rainwater at ground level are noticeably higher than those at 200 m. No significant differences in concentrations of benzo[*k*]fluoranthene, benzo[*b*]fluoranthene, benzo[*a*]pyrene, dibenz[*a,h*]anthracene, benzo[*ghi*]perylene, and indeno[1,2,3-*cd*]pyrene in rain at the two altitudes were found. It is concluded on the basis of these findings that at least on the event with sampling at two altitudes the main process responsible for the presence of phenanthrene in rain is below-cloud gas-phase scavenging and that for the other compounds except fluoranthene and benz[*a*]anthracene it holds that in-cloud scavenging is the main process; for fluoranthene and benz[*a*]anthracene below-cloud gas-phase scavenging and in-cloud scavenging are about equally important.

## Introduction

Precipitation, as one of the removal processes for air pollutants and thus responsible for fluxes of pollutants from air to soil and open waters, has gained widespread attention in the last 10 years. Extended knowledge has up to now been gathered concerning the concentrations of inorganic compounds and elements in rainwater and the mechanisms responsible for their presence. As to organic compounds less investigations have been carried out.

Polychlorinated biphenyls (PCBs) have been found to be present in precipitation in the Lake Michigan basin (1). The authors concluded from their measurements that the gas phase of PCBs is a relatively unimportant source of PCBs in precipitation, that sources of PCBs are possibly diffuse, and that residence times in the atmosphere are long. On theoretical grounds McClure arrived at a similar conclusion for the scavenging of DDT vapor (2). The long residence times for DDT in air were also found by Peakall on the basis of his measurements of DDT levels in rainwater in Ithaca, NY (3). Organic compounds identified in rainwater by Lunde (4) and by Kawamura and Kaplan (5) comprise aliphatic and aromatic hydrocarbons, phthalates, aldehydes, ketones, carboxylic acids and esters, phenols, amines, and azarenes.

Concentrations of polycyclic aromatic hydrocarbons (PAHs) in the range 10-500 ng/L were reported for precipitation in Germany by Schmitt (6), in Belgium by Quaghebeur et al. (7), and in Norway by Lunde et al. (4). In general these levels are higher in winter than in summer (6,7). Furthermore, the determination of PAHs in snow in the Frankfurt area revealed the high influence of local sources to PAH levels in snow (6).

Our institute recently has incorporated organic compounds (among which PAHs) in the existing national network also. No literature data concerning the relative contribution of local and distant sources of PAHs to their presence in rainwater are at present known to us. Knowledge about scavenging mechanisms could aid in this assessment. Therefore, some measurements were set up to study the mechanisms of scavenging PAHs in air by precipitation. Two types of experiments were carried out: (i) the sequential sampling of precipitation events and (ii) the sampling at two different altitudes.

## Experimental Section

**Sampling.** Rainwater was collected in glass bottles by using stainless steel funnels with an area of 1 m<sup>2</sup>. The funnels and bottles were cleaned before use by thoroughly rinsing with detergent and finally with tap water.

**Analysis.** Within 6 h after collection the samples were transported to the laboratory and, after addition of 15% (v/v) 2-propanol to the original collection vessel, stored in the dark at 4 °C. The samples were subsequently passed over Waters Seppak-C<sub>18</sub> cartridges. The PAHs retained on the C<sub>18</sub> phase were eluted with 4 mL of tetrahydrofuran. Additional concentration was achieved by evaporation of the solvent under a gentle N<sub>2</sub> stream down to about 0.3 mL. An aliquot of this concentrate was injected on a Waters Radial-PAK C<sub>18</sub>-PAH high-performance liquid chromatography (HPLC) column and eluted with 2 mL/min acetonitrile/water (1:1 v/v) followed by a linear gradient in 30 min to 100% acetonitrile. The effluent was monitored by using an absorbance (λ 254 and 280 nm) and fluorescence (λ<sub>exc</sub> 280 nm, λ<sub>em</sub> ≥ 389 nm) detector.

Quantitation was obtained on comparing peak areas from rainwater samples with those from calibration solutions of the PAH of interest in water containing 15% (v/v) 2-propanol.

A rinse of cleaned samplers with PAH-free tap water afforded water with no PAH present at concentrations exceeding detection limits (about 1 ng/L). Differences between duplicate rainwater samples were earlier found by us to be less than 10%.

## Results

On Dec 10, 1982, two precipitation events were sequentially sampled at Leidschendam (a suburb of The Hague). The direction of wind was southwest, thus transporting air containing PAH from automobile exhausts and perhaps domestic heating from the city of The Hague and its adjacent highways. The concentrations of some PAHs in these rainwater samples are listed in Tables I and II along with the precipitation amount (in mm), average precipitation intensity (in mm/h), and the sampling interval.

The concentration data in Tables I and II reveal a gradual decrease during the precipitation for the concentration of the PAHs investigated. From the data in table II a removal rate for PAHs can be calculated on the assumption of a first-order process by using the following equation:

$$-\ln(1 - M_t/M_\infty) = kt$$

**Table IV. PAH Levels in Rainwater (in ng/L) at the Eurotower Rotterdam at the Top (T) and at Ground Level (B), Sept 15, 1983, 10.50 h**

compound	sample							
	T1	T2	T3	T4	B1	B2	B3	B4
Phen <sup>a</sup>	53	45	46	30	133	91	89	90
Fl	110	85	66	70	180	142	120	115
Py	ND <sup>b</sup>	ND	ND	ND	37	ND	ND	ND
Chry <sup>a</sup>	ND	62	57	62	67	ND	ND	ND
BaA	33	30	9	9	30	32	20	10
BbF	53	60	60	45	48	57	70	55
BkF	23	27	22	17	22	25	30	20
BaP	37	37	22	17	30	30	29	10
DahA <sup>a</sup>	13	10	7	9	10	12	10	20
BghiP <sup>a</sup>	63	70	54	51	55	52	69	40
IP	90	110	85	70	72	77	100	50
amount, mm	0.300	0.400	0.650	0.450	0.400	0.400	0.800	0.200
rate, mm/h	1.50	4.00	13.00	9.00	2.00	3.43	16.0	4.00
sampling interval, min	12	7	3	3	12		3	3

<sup>a</sup> Phen, phenanthrene; Chry, chrysene; DahA, dibenz[*a,h*]anthracene; BghiP, benzo[*ghi*]perylene. <sup>b</sup> ND, not detected.

**Table V. Data for the Relation between PAH Deposited and the Amount of Rain**

com- pound	at 200 m		at ground level	
	<i>r</i> <sup>2</sup>	slope, ng/(m <sup>2</sup> ·mm)	<i>r</i> <sup>2</sup>	slope, ng/(m <sup>2</sup> ·mm)
Phen	0.9934	41.7	1.000	89.2
Fl	0.9976	71.2	0.9987	124.5
BaA	0.9112	13.6	0.9819	21.8
BbF	0.9966	56.2	0.9985	65.5
BkF	0.9930	21.8	0.9980	27.9
BaP	0.9765	24.0	0.9933	27.3
DahA	0.9958	8.2	0.9912	11.5
BghiP	0.9959	56.8	0.9962	62.2
IP	0.9929	86.7	0.9955	89.8

Rotterdam Eurotower, located near the center of the city at a distance of 300 m from the harbor in an area with dense traffic (see Figure 2).

On Sept 15, 1983, a precipitation event was sampled in four fractions with the results shown in Table IV. The direction of wind was about south, thus transporting PAH emitted from automobiles in the city and on nearby highways south of Rotterdam.

Contrary to the data in Tables I and II a drastic decrease in PAH during precipitation is not observed in this case. In fact, it can be calculated that the total amount of a PAH precipitated per square meter is directly proportional to the amount of rain (Table V).

In order to relate PAH levels in rainwater at the two altitudes, samples at similar time periods and hence with identical volumes are required. The combination of samples T1 and B1 does not completely meet this requirement: the volume of B1 is 4/3 of that of T1. However, because of the slight decrease in PAH levels observed for both the T1-T4 and the B1-B4 series, the difference in sample size only results in a slightly too high value for the ratio T1:B1. The sample sizes of T3 and T4 are not compatible at all with those of B3 and B4. Therefore, PAH concentration values for T3 and T4 were combined and divided by the sum of B3 and B4. The results are given in Table VI.

## Discussion

The presence of PAHs in rainwater is the result of both in-cloud and below-cloud scavenging. One of the main differences between these two processes is that the latter only occurs during precipitation events. As PAHs in air are present both in the gas phase and adsorbed on par-

**Table VI. Ratio of PAH Levels in Rainwater at the Two Altitudes**

	T1/B1	T2/B2	T(3+4)/ B(3+4)	average
Phen	0.39	0.49	0.45	0.44 ± 0.05
Fl	0.61	0.60	0.55	0.59 ± 0.03
BaA	1.10	0.94	0.45	0.83 ± 0.34
BbF	1.10	1.05	0.80	0.98 ± 0.16
BkF	1.04	1.08	0.71	0.94 ± 0.20
BaP	1.23	1.23	0.79	1.08 ± 0.25
DahA	1.30	0.83	0.65	0.92 ± 0.34
BghiP	1.14	1.35	0.84	1.11 ± 0.26
IP	1.25	1.43	0.88	1.19 ± 0.28
average <sup>a</sup>	1.18 ± 0.10	1.16 ± 0.22	0.78 ± 0.08	1.04 ± 0.23

<sup>a</sup> Excluding Phen, Fl, and BaA.

ticular matter (8), the scavenging of PAHs in air by either cloud water or rainwater is the result of dissolving of gas-phase PAHs in water and the result of scavenging of particulate bound PAHs by cloud or rain drops.

The scavenging of gas-phase PAHs below clouds is the result of gas-water partitioning. The equilibrium is described by the Henry coefficient *H*. It can easily be derived that the rate constant (in mm<sup>-1</sup>) for disappearance of gas-phase compounds in air by precipitation over a height *h* (mm) is given by 1/(*Hh*), with *H* in dimensionless units, on the assumption of equilibrium partitioning between the gas and water phase. For phenanthrene with *H* = 6.6 × 10<sup>-3</sup> (from a vapor pressure of 6.8 × 10<sup>-4</sup> mmHg (9) and a water solubility of 1 mg/L (10)), when an estimated value of 10<sup>6</sup> for *h* is used, the removal rate constant for gas-phase phenanthrene below clouds is expected to be 1.5 × 10<sup>-4</sup> mm<sup>-1</sup>.

The below-cloud scavenging by rain of PAH-containing particulate matter in air is a result of the nature of the particulate matter and not of the PAHs. In general it is believed that aerosol particles are more efficiently removed from within rather than from below clouds (11). Below-cloud aerosol particles are scavenged by gravitational collision resulting in removal of only giant particles in the coarse mode (radius ≥ 1 μm) (12, 13).

The rate constant for this aerosol removal can be estimated to be 0.07 mm<sup>-1</sup> and 0.9 mm<sup>-1</sup> for aerosol particles with diameters of 4 and 40 μm, respectively (14). A compilation of literature data on the scavenging coefficient of aerosols obtained from field data are given by McMahon and Denison (15). The data for below-cloud scavenging

(sometimes including in-cloud scavenging) lie in the range  $10^{-5}$ – $10^{-4}$  s<sup>-1</sup>, or, with a rain intensity of 5 mm/h,  $7 \times 10^{-3}$ – $7 \times 10^{-2}$  mm<sup>-1</sup>.

The in-cloud scavenging of particulates is a result of diffusion, interception, and impaction. This scavenging may occur whether a cloud is at that time precipitating or not. Furthermore, gas-phase compounds may enter cloud water before precipitation. Therefore, the rate of in-cloud scavenging of compounds does not necessarily correlate with the apparent removal rate obtained via rainwater analysis.

From our measurements on the precipitation event on Dec 10, 1982, at 16.30 h we obtained an apparent removal rate constant of  $1.46 \pm 0.20$  mm<sup>-1</sup> as the average for Py, BaA, BbF, BkF, and BaP (Table III). The rate constants for the individual PAHs are 4 orders of magnitude greater than that expected for the below-cloud scavenging of phenanthrene and do not vary substantially with the type of PAH. Accordingly, it may be assumed that on that precipitation event the gas-phase below-cloud scavenging of the PAHs does not significantly contribute to their presence in rainwater. A similar conclusion holds for the event on Dec 10, 1983, at 10.08 h with an estimated removal rate constant of 3 mm<sup>-1</sup>.

The mass median diameter for PAH-containing aerosols in The Netherlands and Belgium in 1977 was found to be ca. 1  $\mu$ m (16). Accordingly, it may be expected that the removal rate constant for PAH-containing aerosols in air below clouds will be close to the removal rate constant of 0.07 mm<sup>-1</sup> for 4- $\mu$ m aerosols (14). The two rate constants of 1.46 and ca. 3 mm<sup>-1</sup> found in our study of the precipitation event on Dec 10, 1982, are 20–40 times as high as expected for below-cloud scavenging of PAH-containing aerosols. Accordingly, we conclude that at least for these precipitation events the below-cloud scavenging of PAH-containing aerosols does not significantly contribute to the measured PAH levels in the rainwater.

By this process of elimination we arrive at the conclusion that the measured PAH levels in rainwater from the Dec 1982 events are predominantly the result of the in-cloud scavenging of PAHs.

From the measurements at the Rotterdam Eurotower we found, in contrast to the earlier measurements on Dec 10, 1982, a too little decrease in PAH levels during the precipitation event to calculate apparent removal rate constants. This could indicate below-cloud scavenging of either gas-phase or aerosol-associated PAHs. However, this mechanism is not in agreement with the dependence of the PAH concentration levels on the sampling altitude as will be discussed hereafter. Therefore, it is more likely that the observed PAH concentration variations during precipitation may very well not be the result of scavenging kinetics.

The data in Table V demonstrate that the average concentration levels of BbF, BkF, BaP, DahA, BghiP, and IP in rain during the precipitation event are the same at 0 m and at 200 m. Therefore, it can be concluded that the scavenging of these compounds by rain between 0 and 200 m does not contribute significantly to their concentration levels at 0 m. Since it is hard to imagine that (i) scavenging above 200 m, but below the cloud base, differs from that between 0 and 200 m and (ii) PAH concentration levels in urban air are higher above than below 200 m, and because cloud bases are located at ca. 1000 m, it is concluded that the presence of BbF, BkF, BaP, DahA, BghiP, and IP in rain is mainly the result of in-cloud scavenging.

The data for Phen, Fl, and BaA in Table V reveal a scavenging of PAH in air by rain between 0 and 200 m.

Most probably this scavenging is acting on gas-phase PAHs since Phen in air is mainly found in the gas phase, Fl and BaA both in the gas phase and on aerosols, and BbF, BkF, BaP, and others mainly or exclusively on aerosols (8).

The concentration of Phen in rainwater more than doubles between 200 m and ground level. This supports the theory that the presence of Phen in rain is mainly the result of below-cloud gas-phase scavenging. If for Phen below-cloud scavenging is the exclusive scavenging process, then it can be calculated from the data in Table IV that below-cloud scavenging of Fl and BaA accounts for 50 and 15%, respectively. This may perhaps explain the relatively slow decrease in concentrations of Fl compared to other PAHs in Table II to be the result of the additional below-cloud gas-phase scavenging of Fl.

In conclusion, our measurements of PAH concentration levels in rain at two different altitudes show for the event on Sept 15 that those PAHs mainly present in air on aerosols are present in rain as a result of in-cloud scavenging and that PAHs which in air are mainly present in the gas phase enter rain as a result of below-cloud scavenging. The conclusion for PAHs on aerosols is supported by the observed rate of concentration decay during the precipitation event. In a strict sense this conclusion only holds for the event at Rotterdam. However, since site-specific data were not needed to explain the observed behavior of PAH, it may well be that this scavenging model is generally applicable.

Finally, it is interesting to note that our results imply that concentrations of especially Phen in cloud water should be low relative to "higher" PAHs. A mathematical model for the description of equilibrium in-cloud partitioning of PAH is therefore currently being developed.

#### Acknowledgments

We are especially grateful to Peter Slingerland and Hans Verboom for their sampling at high altitudes and to the technical staff of the Eurotower, Rotterdam, for their assistance during the experiments.

**Registry No.** Phen, 85-01-8; Fl, 206-44-0; Py, 129-00-0; Chry, 218-01-9; BaA, 56-55-3; BbF, 205-99-2; BkF, 207-08-9; BaP, 50-32-8; DahA, 53-70-3; BghiP, 191-24-2; IP, 193-39-5.

#### Literature Cited

- (1) Murphy, Th. J.; Rzeszutko, C. P. 1978, EPA Report EPA-600/3-78-071.
- (2) McClure, V. E. *Environ. Sci. Technol.* **1976**, *10*, 1223–1229.
- (3) Peakall, D. B. *Atmos. Environ.* **1976**, *10*, 899–900.
- (4) Lunde, G.; Gether, J.; Gjøs, N.; Støbet Lande, M. B. *Atmos. Environ.* **1977**, *11*, 1007–1014.
- (5) Kawamura, K.; Kaplan, I. R. *Environ. Sci. Technol.* **1983**, *17*, 497–501.
- (6) Schmitt, G., Diplomarbeit, Frankfurt am Main, 1982; Schmitt, G. In "Deposition of Atmospheric Pollutants"; Georgii, H. W.; Pankrath, J., Eds.; D. Reidel Publishing: Dordrecht, Holland, 1982; pp 133–142.
- (7) Quaghebeur, D.; de Wulf, E.; Janssens, G.; Ravelingien, M. C.; Desmet, D. Polycyclische Aromatische Koolwaterstoffen in Regenwater, Brussel, 1982.
- (8) Yamasaki, H.; Kuwata, K.; Miyamoto, H. *Environ. Sci. Technol.* **1982**, *16*, 189–214.
- (9) Radding, S. B.; Mill, T.; Gould, C. W.; Liu, D. H.; Johnson, H. L.; Bomberger, D. C.; Fojo, C. V. 1975, EPA Report EPA 560/5-75-009.
- (10) May, W. E.; Wasik, S. P.; Freeman, D. H. *Anal. Chem.* **1978**, *50*, 175–179.
- (11) Slinn, W. G. H.; Hasse, L.; Hicks, B. B.; Hogan, A. W.; Lal, D.; Liss, P. S.; Munnich, K. O.; Sehmel, G. A.; Vittori, O. *Atmos. Environ.* **1978**, *12*, 2055–2087.
- (12) Whelpdale, D. M. In "Chemistry of the Unpolluted and Polluted Troposphere"; Georgii, H. W.; Jaeschke, W., Eds.;



D. Reidel Publishing: Dordrecht, Holland, 1982; pp 375-391.

- (13) Mészáros E., "Atmospheric Chemistry"; Elsevier: Amsterdam, 1981.
- (14) Stern, A. C.; Wohlers, H. C.; Boubel, R. W.; Lowry, W. P. "Fundamentals of Air Pollution"; Academic Press: New York, 1983; p 265.
- (15) McMahon, T. A.; Denison, P. J. *Atmos. Environ.* 1979, 13, 571-585.

(16) Van Vaeck, L.; Broddin, G.; Van Cauwenberghe, K. *Environ. Sci. Technol.* 1979, 13, 1494-1502.

Received for review June 18, 1984. Accepted April 3, 1985. This investigation was executed within the framework of the Dutch National Coal Research Programme which is managed by the Project Office for Energy Research of the Netherlands Energy Research Foundation ECN and which is financed by the Ministry of Economic Affairs.

## Effects of Silicon on the Crystallization and Adsorption Properties of Ferric Oxides

Paul R. Anderson and Mark M. Benjamin\*

Environmental Engineering and Science, Department of Civil Engineering, University of Washington, Seattle, Washington 98195

■ The effect of dissolved silicate on the bulk and surface properties of aged ferrihydrite was investigated. Under aging conditions where ferrihydrite crystallizes to goethite in less than 24 h in the absence of silicate, the solid remains noncrystalline for at least 1-2 weeks in its presence. Some of the dissolved Si associates with the solid, and the point of zero charge (PZC) of the solid decreases from about 8 to about 4 as the ratio Si/Fe in the solid increases from 0 to 0.35. Incorporation of the Si in the solid dramatically increases the solid's binding strength for Cd but has relatively little effect on its strength for Cu, Co, or Zn. The binding strength for  $\text{SeO}_3$  decreases with Si content in the solid, correlating closely with the PZC.

### Introduction

Oxides, hydroxides, and oxyhydroxides of iron are present either as discrete phases or as coatings on other solids in many soils and sediments and provide an important control on the distribution of trace elements in aquatic environments (1-4). Numerous studies of trace element adsorption onto these solids, which we will refer to collectively as ferric oxyhydroxides, have been conducted (5-9). These studies have focused primarily on single-component, pure oxides as model adsorbents.

The ferric oxyhydroxides are secondary minerals formed as the weathering products of primary minerals. Thus, the environments in which they form normally contain an array of other weathering products. The ferric oxyhydroxides and these other compounds can interact in various ways which may alter their affinity for soluble ions and the rate of formation or the identity of the solid phase formed. Examples include the inhibition of crystallization of ferric oxyhydroxides in the presence of fulvic acid (10), increased stability of ferrihydrite over lepidocrocite in the presence of Si (11), and the preferential formation of hematite over goethite in the presence of Al under certain aging conditions (12). Characterization of the solids formed under these conditions has generally been limited to analyses of their bulk physical and chemical properties, while the surface chemistry has been largely neglected.

This report describes a study of how the presence of silicate affects the solids formed when ferrihydrite is aged at elevated temperature and pH. Both the bulk crystallinity of the solids and their surface properties were characterized.

### Materials and Methods

Ferric oxyhydroxides were prepared in either glass or Teflon beakers containing a 0.1 M  $\text{NaNO}_3$  solution preheated to 50 °C. Concentrated NaOH was added to  $10^{-3}$

or  $10^{-1}$  M Fe (III) solutions to raise the pH to 10.5, and the precipitate was aged up to 2 weeks. In some experiments Si was added (as  $\text{Na}_2\text{SiO}_3$ ) either prior to, 2 h after, or 24 h after the precipitation step. All of the preparation steps were performed under a  $\text{N}_2$  atmosphere.

At the desired oxyhydroxide age, the solution was rapidly cooled to 20 °C, and concentrated  $\text{HNO}_3$  was added to attain a final pH of about 7. Batch adsorption experiments, oxalate solubility tests, and point of zero charge (PZC) determinations were conducted with subsamples from this suspension. The precipitate was washed several times with deionized water and air-dried prior to the oxalate, X-ray, and infrared absorption analyses.

The pH of the PZC was determined by the salt titration procedure of Davis and Leckie (6). The quantity of noncrystalline material in the solids was estimated by solubility in ammonium oxalate using a procedure similar to that described by Landa (13) and McKeague and Day (14). The infrared absorption spectra were obtained with samples prepared as KBr pellets. Air-dried solids crushed to pass through a 0.105-mm sieve were used for the X-ray analysis. Particulate and soluble fractions were separated by centrifugation and analyzed by atomic absorption spectrophotometry after digestion with HF.

Procedures followed in the batch adsorption experiments were similar to the methods used by several previous workers (15, 16). In all of the batch adsorption experiments the total Fe concentration was  $10^{-3}$  M, and the background electrolyte was 0.1 M  $\text{NaNO}_3$ .

### Formation and Identification of the Solid

The rate of crystallization and the identity and morphology of the crystalline phase formed when iron oxyhydroxides are aged can be affected by several factors, including the identity of the major anions in solution and the temperature and pH of the aging solution. In the systems studied, the conversion of ferrihydrite to goethite ( $\alpha\text{-FeOOH}$ ) was of interest. This conversion is accelerated by aging ferrihydrite suspensions at elevated pH and temperature (17-19). Atkinson et al. (20) reported that a 0.12 M  $\text{Fe}(\text{NO}_3)_3$  solution adjusted to pH "near 12" and aged 24 h at 60 °C yielded crystalline goethite free of other X-ray identifiable phases. The authors noted that "...no precautions were taken to prevent silicate contamination [from processing in glass beakers], which is possible at high pH". Sung and Morgan (21) tried to synthesize  $\alpha\text{-FeOOH}$  by using the same pH and temperature conditions as Atkinson et al. but reported that the precipitate was X-ray amorphous. The solid did have an infrared absorption spectrum similar to that of  $\alpha\text{-FeOOH}$ . They did not in-

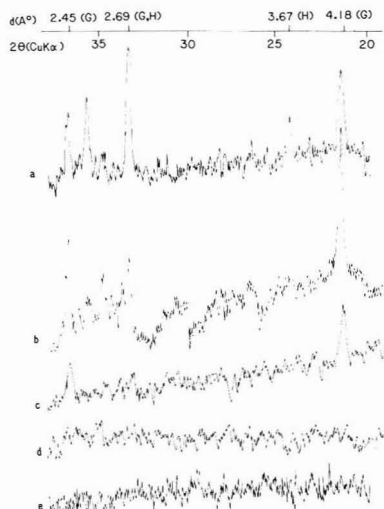


**Figure 1.** X-ray diffraction patterns for ferric oxides. All of the solids were prepared and aged in 0.1 M NaNO<sub>3</sub> at 50 °C and pH 10.5. (a) 10<sup>-3</sup> M Fe<sub>T</sub> in Teflon, aged 48 h; 20 mg/L Si added after 24 h. (b) 10<sup>-3</sup> M Fe<sub>T</sub> in Teflon, aged 24 h. (c) 10<sup>-1</sup> M Fe<sub>T</sub> in glass, aged 24 h. (d) 10<sup>-3</sup> M Fe<sub>T</sub> in glass, aged 144 h. (e) 10<sup>-3</sup> M Fe<sub>T</sub> in Teflon, aged 48 h; 20 mg/L Si added at *t* = 0. The *d* spacings indicated on the top axis are characteristic of goethite (G) or hematite (H).

**Table I.** Ratio of Oxalate-Soluble Fe to Total Fe<sup>a</sup>

Fe oxide age, h	oxalate-soluble Fe/ total Fe
24	0.99 <sup>b</sup>
48	0.96 <sup>b</sup>
144	0.80 <sup>b</sup>
288	0.74

<sup>a</sup> Fe (10<sup>-3</sup> M) aged in glass at 50 °C and pH 10.5. <sup>b</sup> Visually, it appeared that the solid dissolved completely in these tests, i.e., oxalate-soluble Fe/total Fe ≈ 1.0.

dicating the concentration of Fe<sub>T</sub> in their system.

Initially, conditions similar to those of Atkinson et al., but somewhat less severe (pH 10.5, 50 °C), were used to investigate the conversion of ferrihydrite to goethite. In addition, the suspensions were more dilute than those of Atkinson et al. (10<sup>-3</sup> M Fe<sub>T</sub> in a background electrolyte of 0.1 M NaNO<sub>3</sub>) to facilitate comparisons with previous adsorption experiments. Samples were aged from 2 h to 12 days under these conditions and were analyzed for crystallinity.

X-ray diffraction analysis, oxalate dissolution, and visual appearance of the solids indicated that none of them had crystallized to a significant extent even after aging 12 days. All these samples were X-ray amorphous (Figure 1, line d) and retained the characteristic deep red color of ferrihydrite throughout the aging period. (Goethite formed using Atkinson's method is typically a gold yellow.) They remained completely soluble in oxalate for aging times of at least several days and were predominantly so after 12 days (Table I). By contrast, suspensions containing 10<sup>-1</sup> M Fe<sub>T</sub> exposed to identical conditions (pH 10.5, 50 °C) were converted to goethite within 24 h, on the basis of X-ray pattern, oxalate solubility, and color (Figure 1, line c; Table I).

A possible explanation for the failure of the ferrihydrite to crystallize in the 10<sup>-3</sup> M suspensions is poisoning of the crystal nuclei by Si dissolving from the beaker walls. Schwertmann and Thalmann (11) had reported that Si in-

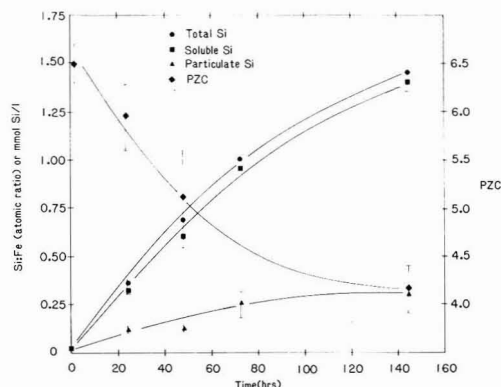


**Figure 2.** Si concentration and pH of the PZC vs. oxide age. All samples are suspensions of 10<sup>-3</sup> M Fe<sub>T</sub> aged at 50 °C and pH 10.5 in glass.

terfered with the conversion of ferrihydrite to lepidocrocite, and Schwertmann and Taylor (22) reported a similar result for conversion of lepidocrocite to goethite. Analysis of soluble and total Si in the suspensions as a function of time (Figure 2) indicated that significant amounts of Si were indeed being solubilized. Over a period of 144 h, about 61 mg of Si dissolved from approximately 600 cm<sup>2</sup> of glass surface, giving a total Si concentration (soluble plus particulate) of 41 mg/L. The majority of the Si released remained in solution. Nevertheless, Si:Fe atomic ratios in the solid phase were as high as 0.35 in some samples.

The relationship between crystallization and Si was evaluated by precipitating and aging ferric oxides in Teflon beakers under conditions identical with those aged in glass (10<sup>-3</sup> M Fe<sub>T</sub>, 0.1 M NaNO<sub>3</sub>, pH 10.5, 50 °C). In the absence of Si, the X-ray diffractogram (Figure 1, line b) indicated that goethite formed within 24 h. By contrast, solids prepared in Teflon beakers with 20 mg/L Si added to the solution prior to precipitating the Fe remained X-ray amorphous (Figure 1, line e). This confirmed the ability of Si to inhibit crystallization. The solid-phase Si:Fe ratio at which inhibition first occurs can be bracketed between approximately 0.02, the largest ratio found in a solid which crystallized (according to X-ray analysis), and 0.11, the smallest ratio found in a solid which did not.

The IR spectra of these solids are also informative (Figure 3). Two absorption peaks characteristic of goethite are observed in the solids prepared in Teflon in the absence of Si (Figure 3, line b) and are absent in the spectra of freshly prepared ferrihydrite (Figure 3, line c). The ferrihydrite aged in the presence of Si (Figure 3, line a) has a broad peak centered at 950 cm<sup>-1</sup>, which Carlson and Schwertmann (23) attribute to Si-O-Fe bonds.

As noted earlier, Sung and Morgan (21) reported that a ferrihydrite aged at high temperature and pH was X-ray amorphous but had some of the IR-absorbing characteristics of goethite. In our case, the aging apparently caused the solid to acquire some of the characteristics of goethite and some of freshly precipitated silica. This conclusion is also consistent with the surface characteristics, which are presented later.

In their study of the effects of Si on the transformation of lepidocrocite to goethite, Schwertmann and Taylor (22) reported that the conversion was affected by the time at which Si was added. To study this effect in our systems, Si was added to 10<sup>-3</sup> M Fe suspensions in Teflon at various times during the aging process. On one series of tests, 20–80 mg/L Si was added 2 h after the precipitation step,

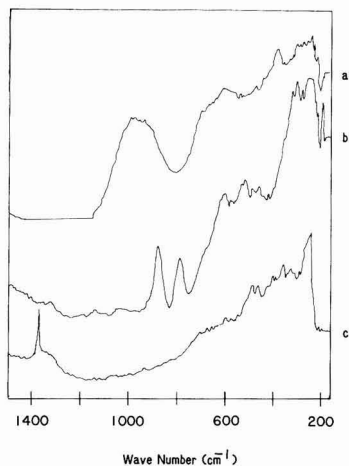


**Figure 3.** Infrared spectra of solids prepared in 0.1 M  $\text{NaNO}_3$ . (a)  $10^{-3}$  M Fe + 20 mg/L Si (added as  $\text{Na}_2\text{SiO}_3$ ) aged 24 h at 50 °C, pH 10.5, in Teflon. (b)  $10^{-3}$  M Fe aged 24 h at 50 °C, pH 10.5, in Teflon. The peaks at 890 and 797  $\text{cm}^{-1}$  are characteristic of  $\alpha\text{-FeOOH}$ . (c)  $10^{-3}$  M Fe aged 2 h at 22 °C, pH 7.5, in Teflon.

and the high temperature and pH aging conditions were maintained for 144 h. Although these solids were not analyzed by X-ray diffraction, they retained the characteristic color and texture of ferrihydrite, and the results of the batch adsorption experiments (see below) suggest that the solids were noncrystalline. However, when 20 mg/L Si was added 24 h after the precipitation step, the X-ray diffraction pattern (Figure 1, line a) indicated the presence of both goethite and hematite within 24 h of additional aging. Thus, the transformation of ferrihydrite to goethite is inhibited if Si is introduced early in the crystallization process (<2 h), while the introduction of Si at a later stage (>24 h), after significant amounts of goethite have formed, apparently favors the formation of hematite.

#### Surface Properties of the Aged Oxyhydroxides

**Changes in pH of the PZC during Aging.** The next portion of the study involved an investigation of selected surface properties of the aged oxyhydroxides. The PZCs of most iron oxyhydroxides are in the range 6.5–10, and those of silicon oxides are 1.5–3.0 (24). Thus, one might expect the PZC of a mixture of these two to decrease with increasing silicon concentration. The PZCs of the solids aged in glass beakers are presented in Figure 2. Electrophoretic mobility measurements on a few of these samples yielded values for the isoelectric points (IEP) which were always within a few tenths of a pH unit of the PZC. PZCs of Fe + Si coprecipitates have been investigated by Pyman et al. (25) and Schwertmann and Fechter (26) and show the same trend. Though there was some variation in the absolute values of the PZC among batches, the change in PZC in any given batch of oxyhydroxide followed a consistent trend, decreasing with increasing age and increasing Si concentration in the solid up to at least several weeks. Thus, while the tests for bulk crystallinity did not indicate that an identifiable crystalline phase was forming, surface properties of the solids were changing significantly during the aging process.

**Cation Adsorption.** Adsorption data for Zn, Co, Cu, and Cd onto these solids are presented in Figure 4. In these graphs the aging time listed is the time the solid was aged at pH 10.5 and 50 °C prior to starting the adsorption

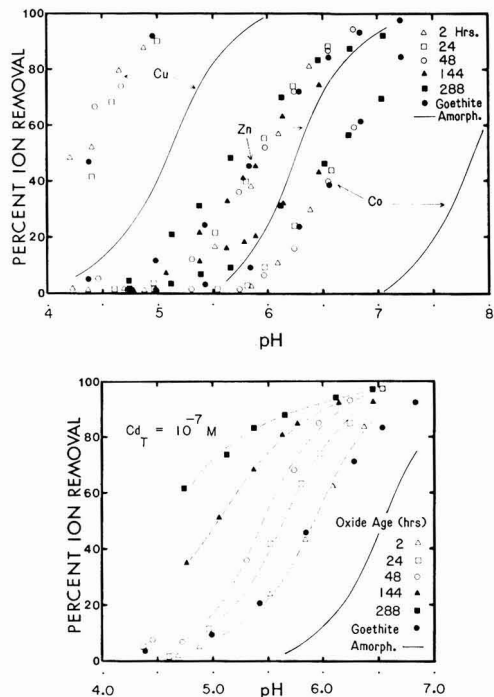


**Figure 4.** Percent metal ion removal vs. pH. Batch adsorption experiments with  $10^{-3}$  M  $\text{Fe}_T$ . The Fe oxides were prepared in glass beakers at 50 °C and pH 10.5. The solid lines are for adsorption onto ferrihydrite freshly precipitated at room temperature and are from ref 27 and 28.

experiments and is related to the Si:Fe ratio shown in Figure 2. All the solutions were adjusted to pH 7.0 and 20 °C before adsorbate was added. As is commonly observed for hydrolyzable metals, adsorption increased from near 0 to near 100% removal over a narrow pH range (the pH adsorption "edge") in all cases.

The adsorption behavior of Zn, Cu, and Co was not significantly affected by the Si concentration, the PZC, or the aging time of the oxide. The bulk crystallinity of the solids also appears to have no effect, since adsorption onto goethite and onto the X-ray amorphous, aged oxyhydroxides is quite similar.

Also shown is the adsorption edge for each metal onto ferrihydrite which was precipitated and aged for 2 h at pH 7.0 and 20 °C. These are literature data in which the Si concentration was not measured but was presumably negligible. In each case the adsorption edge on the fresh precipitate is displaced toward alkaline pH compared to that on the aged oxyhydroxides. The shift is about 1 pH unit for Co and about 0.5 pH unit for Zn and Cu (Figure 4, top). This means that Si ferrihydrite and goethite are stronger adsorbents for the metals than is fresh ferrihydrite when equal concentrations of Fe are used as the basis of comparison. Because the adsorption edge for these metals is not affected by aging times between 2 and 288 h, it appears that the change in binding strength is related to changes in the solid which occur in the very early stages of aging. For these three metals adsorption is similar on all aged ferrihydrites and goethite and significantly different on fresh ferrihydrite. This fact, along with the IR spectra presented here and those of Sung and Morgan (21), suggests that the aged ferrihydrite was microcrystalline goethite, despite lacking a clear X-ray pattern.

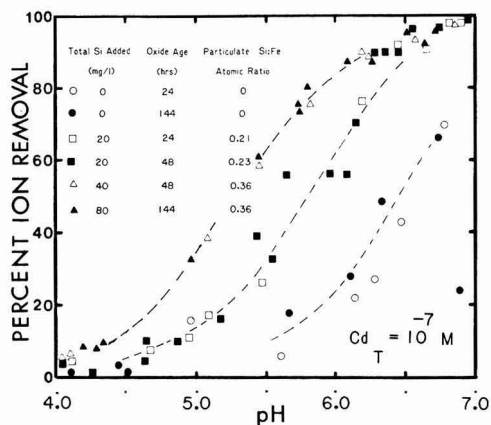


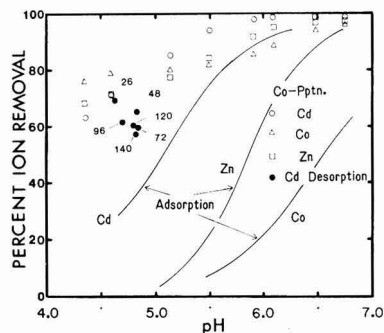
**Figure 5.** Percent Cd removal vs. pH. The Fe oxide was prepared in Teflon beakers at 50 °C and pH 10.5.  $\text{Na}_2\text{SiO}_3$  was added 2 h into the aging process.

In contrast to the other metals, Cd sorption is continuously enhanced as the Si content of the ferrihydrite increases (Figure 4, bottom). This may be due to either the changing electrostatic properties of the solid or the creation of strong Cd-specific binding sites. If the latter, the strength of these binding sites would be striking, since sorption of Cd is not particularly strong on any known pure iron or silicon oxyhydroxide (15, 29, 30).

The effect of Si on Cd sorption was confirmed in experiments using Fe + Si oxyhydroxides prepared in Teflon beakers. In these experiments Si was added 2 h after precipitating the iron, and the solids were then aged an additional 24 h. The strength of Cd sorption to these solids correlated strongly with the concentration of Si in the solid and was independent of aging time (Figure 5). Since the Cd sorption strength also correlated reasonably well with the concentration of dissolved Si in these experiments, it seemed possible that Si was affecting sorption via a reaction with Cd in solution prior to uptake. To explore this, a batch of solids was prepared as in the previous experiments and was then thoroughly washed and resuspended in Si-free electrolyte. Cadmium sorption onto these solids was similar to that on unwashed solids, indicating that it is the amount of Si associated with the oxyhydroxide, and not the Si in solution, which affects Cd sorption.

**Coprecipitation Studies.** For amorphous oxyhydroxides the process of aging is usually accompanied by dehydration and conversion to a less porous structure. The aged oxyhydroxides in this study showed little evidence of bulk crystallinity by X-ray or oxalate dissolution tests. However, other evidence (PZC and Cd sorption) indicated that significant changes were occurring in the solid during the aging process, possibly reflecting crystallization at a microscale. This possibility is supported by the results of coprecipitation experiments, in which the solid was formed and aged in the presence of the adsorbate (Figure 6).

In these experiments removal of trace metals was considerably greater than when the metals were added after the aging process was complete. The similarity of the removal curves for coprecipitation of the three metals analyzed, even though their adsorption edges are separated by  $1\frac{1}{2}$  pH units, suggests that the removal mechanism during coprecipitation is relatively nonselective. The strength of the bonding in the coprecipitation experiments is attested to by the fact that little metal was released when the pH was held near 4.7 for 6 days. Only the data for Cd release during long-term aging at low pH are shown in



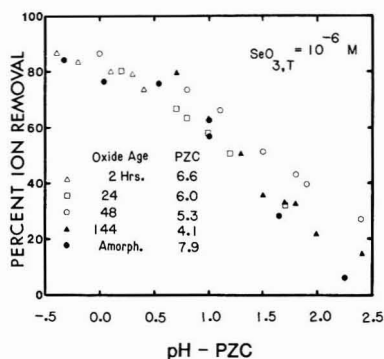
**Figure 6.** Metal ion removal vs. pH for batch coprecipitation studies. Metal and ferrihydrite were coprecipitated and aged at 50 °C and pH 10.5 for 144 h, then cooled to 20 °C, and adjusted to the pH indicated for 2 h. The data with numbers adjacent to are for samples held at that pH for the number of hours indicated. The solid lines are for adsorption onto solids aged 144 h, from Figure 4.

Figure 6, but the results for Zn and Co release were similar (Cu was not analyzed). These results contrast with those obtained when coprecipitation and aging are conducted at 20 °C and pH 7.0. In the latter case, trace metal removal is identical whether the trace metals are added before or after the solid is formed (9, 27). Although other explanations are possible, the results are consistent with the hypothesis that the solid was crystallizing during the high-temperature, high-pH aging, "trapping" metal ions in the lattice. If the crystallites were small and randomly oriented, it would be possible for a large fraction of the solid to have crystallized but not have a sharp X-ray diffraction pattern. As a practical matter, the coprecipitation data are significant in that they show the remarkable increase in removal efficiency that can be accomplished by varying the conditions under which the same reagents are mixed.

**Relative Adsorptive Strengths of Ferrihydrite and Goethite.** The relative binding strength of various solid phases for metals can be assessed in a number of ways. For instance, relative adsorptive strength can be evaluated by comparing, for identical solution conditions, the mass adsorbed per unit mass of adsorbent, per unit surface area, or per mole of adsorption sites. For the solids under consideration here, typical specific surface areas are 500  $\text{m}^2/\text{g}$  of  $\text{Fe}(\text{OH})_3$  and 30–50  $\text{m}^2/\text{g}$  of  $\alpha\text{-FeOOH}$  for fresh ferrihydrite and for goethite, respectively. Site densities for these solids also differ by more than an order of magnitude: 0.87 mol of sites/mol of Fe for ferrihydrite and 0.02 mol of sites/mol of Fe for goethite (6, 7, 31).

It has commonly been asserted that ferrihydrite may have an influence greatly out of proportion to its mass fraction in soils and sediments because of its extremely large specific surface area. However, the results presented here indicate that goethite is a stronger sorbent than fresh ferrihydrite for the four hydrolyzable metals studied on any basis of comparison. That is, given equal masses of goethite-Fe and fresh ferrihydrite-Fe in a system, metals would preferentially bind to the goethite despite the higher surface area and site availability of the ferrihydrite. In systems with equal surface areas or equal numbers of binding sites of the two solids, the preferential binding to goethite would be even more pronounced. Many adsorption models define an "intrinsic binding" constant to quantify and compare adsorptive bond strengths. The numerical value of such constants is model dependent. Our results indicate that, regardless of the model chosen, the intrinsic binding constant of goethite for Co, Cu, Cd,





**Figure 7.** Percent  $\text{SeO}_3$  removal vs. pH-PZC. Batch adsorption experiments with  $10^{-3}$  M  $\text{Fe}^{+}$ . The Fe oxide was prepared in glass beakers. For the 2-, 24-, and 48-h solids, PZCs were determined on the same batch of solids as used in adsorption experiments. For the 144-h solids, the PZC was estimated from analysis of other batches. For the fresh ferrihydrite, data were taken from ref 27.

and Zn would be larger than that of fresh ferrihydrite. Depending on the specific metal under consideration, the basis used for comparison, and the adsorption model, the difference between the two would be 1–3 orders of magnitude.

**Anion Adsorption.** When oxyanions adsorb on an oxyhydroxide surface, the binding strength often correlates strongly with average electrostatic field near the surface. That is, for a series of oxyhydroxides with a varying isoelectric point (IEP), the adsorption edge for an oxyanion such as  $\text{CrO}_4$ ,  $\text{SeO}_4$ , or  $\text{AsO}_3$  often moves up or down the pH scale as the IEP changes (32–34). This characteristic pattern for anion sorption was observed for selenite adsorption on the Si-ferrihydrites. As the Si content increased, the PZC of the solid decreased; in all cases the adsorption of  $\text{SeO}_3$  started to decrease as the pH was raised above the PZC. (As noted earlier, the PZC and IEP were quite similar for the solids under consideration.) The adsorption of  $\text{SeO}_3$  onto goethite (PZC = 8) and onto fresh ferrihydrite was also consistent with this pattern. Selenite sorption onto all the Si-ferrihydrites and fresh ferrihydrite collapses to a single narrow band when the pH is normalized to the PZC of that solid (Figure 7). Anderson et al. (34) reported a similar result for adsorption of arsenate onto amorphous aluminum hydroxide, although in that case the reduction in the IEP was caused by adsorption of the arsenate itself, rather than incorporation of another ion in the solid matrix.

The sorption experiments emphasize the very different effects of the average surface charge on adsorption of oxyanions and hydrolyzable cations. These electrostatic effects seem to be extremely important in the former cases, while they are almost totally absent in the latter. Evidence supporting this generalization has also been provided by Benjamin (35), Benjamin and Bloom (28), and Davis (36) from competitive adsorption studies. The explanation for these differences may lie in different adsorption stoichiometries for the two types of ions or in differences in the closeness of approach of the adsorbates to the surface. Whatever the explanation, the observation has significant implications for the modeling of the electrostatic contribution to ion adsorption.

### Summary and Conclusions

Iron oxyhydroxides that are prepared in the presence of Si can associate with the Si and form solids with some surface properties different from either pure ferrihydrite

or pure  $\text{SiO}_2$ . Freshly precipitated Fe oxyhydroxides prepared and aged at elevated pH and temperature in the presence of Si can reach Si:Fe molar ratios at least as high as 0.36. The presence of Si increases the stability of the amorphous oxyhydroxide. If the Si:Fe ratio in the solid is larger than about 0.1, the ferrihydrite does not crystallize for at least 144 h. Under similar aging conditions in the absence of Si, crystalline goethite forms within 24 h.

The surface chemistry of Si-containing Fe oxyhydroxides also depends on the Si content. The PZC and the IEP of the solid decreases from about pH 8 to about pH 4 as the Si:Fe molar ratio increases from 0 to 0.35. The pH adsorption edge for  $\text{SeO}_3$  correlates strongly with the change in the PZC, and it is expected that this would be true for other oxyanions as well. When the Fe oxyhydroxide is aged at high temperature and pH in the presence or absence of Si, its binding strength for Cd, Co, Cu, and Zn increases compared to that of ferrihydrite prepared at pH 7 and 20 °C. The increase in binding strength occurs within the first 2 h of aging and is independent of aging time thereafter.

The adsorption of Cu, Co, and Zn is independent of the Si content in the solid, but Cd adsorption is significantly enhanced (the pH adsorption edge becomes more acidic) with increasing Si content. Apparent binding constants for Cd can be several orders of magnitude higher on Fe + Si solids than on pure ferrihydrite or pure  $\text{SiO}_2$ .

The adsorption of metal ions to oxide adsorbents indicates that, in general, they are insensitive to electrostatic attraction or repulsion by the surface as measured by the IEP. By contrast, the IEP appears to strongly influence anion adsorption. This observation has significant implications for modeling adsorption, especially in systems containing relatively high concentrations of adsorbates.

### Acknowledgments

The authors would like to thank John Ferguson, Bruce Honeyman, and Laurie Balistrieri for reviewing the manuscript.

**Registry No.** Si, 7440-21-3; ferrihydrite, 39473-89-7; iron oxide, 1332-37-2.

### Literature Cited

- (1) Davies-Colley, R. J.; Nelson, P. O.; Williamson, K. J. *Environ. Sci. Technol.* **1984**, *18*, 491–499.
- (2) Jenne, E. A. In "Adsorption from Aqueous Solution"; Weber, W.; Matijevic, E., Eds.; American Chemical Society: Washington, DC, 1968; Adv. Chem. Ser. No. 79.
- (3) Lion, L. W.; Altmann, R. S.; Leckie, J. O. *Environ. Sci. Technol.* **1982**, *16*, 660–666.
- (4) Luoma, S. N.; Bryan, G. W. *Sci. Total Environ.* **1981**, *17*, 165–196.
- (5) Davis, J. A.; Leckie, J. O. *J. Colloid Interface Sci.* **1980**, *74*, 32–43.
- (6) Davis, J. A.; Leckie, J. O. *J. Colloid Interface Sci.* **1978**, *67*, 90–107.
- (7) Hingston, F. J.; Posner, A. M.; Quirk, J. P. In "Adsorption from Aqueous Solution"; Weber, W.; Matijevic, E., Eds.; American Chemical Society: Washington, DC, 1968; Adv. Chem. Ser. No. 79.
- (8) Kinniburgh, D. G.; Jackson, M. L.; Syers, J. K. *Soil Sci. Soc. Am. J.* **1976**, *40*, 796–799.
- (9) Swallow, K. C.; Hume, D. N.; Morel, F. M. M. *Environ. Sci. Technol.* **1980**, *14*, 1326–1331.
- (10) Kodama, H.; Schnitzer, M. *Geoderma* **1977**, *19*, 279–291.
- (11) Schwertmann, U.; Thalmann, H. *Clay Miner.* **1976**, *11*, 189–200.
- (12) Lewis, D. G.; Schwertmann, U. *Clays Clay Miner.* **1979**, *27*, 195–200.
- (13) Landa, E. R. *Clays Clay Miner.* **1973**, *21*, 121.
- (14) McKeague, J. A.; Day, J. H. *Can. J. Soil Sci.* **1966**, *46*, 13–22.



- (15) Benjamin, M. M.; Leckie, J. O. In "Contaminants and Sediments"; Baker, R. A., Ed.; Ann Arbor Science: Ann Arbor, MI, 1980; Vol. 2.
- (16) Benjamin, M. M.; Hayes, K. F.; Leckie, J. O. *J. Water Pollut. Control Fed.* **1982**, *54*, 1472-1481.
- (17) Atkinson, F. J.; Posner, A. M.; Quirk, J. P. *J. Inorg. Nucl. Chem.* **1968**, *30*, 2371-2381.
- (18) Forbes, E. A.; Posner, A. M.; Quirk, J. P. *J. Colloid Interface Sci.* **1974**, *49*, 403-409.
- (19) Schenck, C. V.; Dillard, J. G.; Murray, J. W. *J. Colloid Interface Sci.* **1983**, *95*, 398-409.
- (20) Atkinson, R. J.; Posner, A. M.; Quirk, J. P. *J. Phys. Chem.* **1967**, *71*, 550-558.
- (21) Sung, W.; Morgan, J. J. *Environ. Sci. Technol.* **1980**, *14*, 561-568.
- (22) Schwertmann, U.; Taylor, R. M. *Clays Clay Miner.* **1972**, *20*, 159-164.
- (23) Carlson, L.; Schwertmann, U. *Geochim. Cosmochim. Acta* **1981**, *45*, 421-428.
- (24) Parks, G. A. *Chem. Rev.* **1965**, *65*, 177-198.
- (25) Pyman, M. A. F.; Bowden, J. W.; Posner, A. M. *Clay Miner.* **1979**, *14*, 87-92.
- (26) Schwertmann, U.; Fechter, H. *Clay Miner.* **1982**, *17*, 471-476.
- (27) Leckie, J. O.; Benjamin, M. M.; Hayes, K.; Kaufman, G.; Altmann, S. Electric Power Research Institute, Palo Alto, CA, 1979, Final Report EPRI-RP-910.
- (28) Benjamin, M. M.; Bloom, N. S. In "Adsorption from Aqueous Solutions"; Tewari, P. H., Ed.; Plenum Press: New York, 1981.
- (29) Dugger, D. L.; Stanton, J. H.; Irby, B. N.; McConnell, B. L.; Cummings, W. W.; Maatman, R. W. *J. Phys. Chem.* **1964**, *68*, 757.
- (30) Schindler, P.; Furst, B.; Dick, R.; Wolf, P. *J. Colloid Interface Sci.* **1976**, *55*, 469-475.
- (31) Balistreri, L. S.; Murray, J. W. *Am. J. Sci.* **1981**, *281*, 788-806.
- (32) Anderson, M. A.; Malotky, D. T. *J. Colloid Interface Sci.* **1979**, *72*, 413-427.
- (33) Pierce, M. L.; Moore, C. B. *Environ. Sci. Technol.* **1980**, *14*, 214.
- (34) Anderson, M. A.; Ferguson, J. F.; Gavis, J. J. *Colloid Interface Sci.* **1976**, *54*, 391.
- (35) Benjamin, M. M. *Environ. Sci. Technol.* **1984**, *18*, 686-692.
- (36) Davis, J. A. *Geochim. Cosmochim. Acta* **1984**, *48*, 679-691.

Received for review September 7, 1985. Revised manuscript received March 8, 1985. Accepted May 16, 1985. The work was aided by financial support from the Valle Scandinavian Exchange Scholarship Fund and the University of Washington Graduate School Research Fund.

## Trace Organic Compounds in Rain. 4. Identities, Concentrations, and Scavenging Mechanisms for Phenols in Urban Air and Rain

Christian Leuenberger, Mary P. Ligocki, and James F. Pankow\*

Department of Chemical, Biological, and Environmental Sciences, Oregon Graduate Center, Beaverton, Oregon 97006

■ The gaseous and filterable air concentrations of a variety of phenols were determined for seven rain events in Portland, OR. The dissolved and filterable rain concentrations were also determined concurrently. The phenols in the air were found to exist virtually exclusively in the gaseous state as expected on the basis of their large vapor pressures. The fact that virtually all of the phenols found in the rain were present in the dissolved state is in agreement with the air data. The rain (dissolved) concentrations were quite high, in the microgram per liter range. Of all the constituents present in the rain samples, the most concentrated ones were phenols. The results indicate that gas scavenging is much more important than particle scavenging for phenols. Considering the rather low values of their Henry's law constants, gas scavenging is an efficient atmospheric removal process for these compounds.

### Introduction

The importance of the atmosphere for the distribution and degradation of organic compounds has been documented (1-4). An increasing level of effort has therefore been devoted to understanding how dry (5-7) and wet (8-18) deposition remove atmospheric organic compounds. For wet deposition, it is of interest to evaluate the roles played by gas and particle scavenging. Precipitation scavenging has been studied both theoretically and in the field. The determination of the importance of gas and particle scavenging requires a differentiation between the

dissolved and suspended particulate phases in the rain and between the gaseous and aerosol particulate phases in the case of the atmosphere. Air and rain samplers that meet these needs have been developed in our laboratory by Ligocki and Pankow (19), Pankow et al. (16), and Ligocki et al. (20, 21), respectively. They provide filtration for the collection of aerosol and rain particulate matter and for the immediate preconcentration of gaseous and dissolved organic compounds with sorbent cartridges.

If  $\phi$  is the fraction of a given compound in the atmosphere associated with aerosol particles (22), then to a first approximation gas scavenging will dominate if (16)

$$RT/H(T) \gg W_p \phi / (1 - \phi) \quad (1)$$

where  $R = 8.2 \times 10^{-5} \text{ m}^3 \cdot \text{atm} / (\text{mol} \cdot \text{K})$ ,  $T$  = temperature (K), and  $H(T)$  = temperature-dependent Henry's law constant ( $\text{atm} \cdot \text{mol} / \text{m}^3$ ).

The research described here has employed the air and rain samplers developed in our laboratory to provide concurrent, ground-level air and rain measurements of numerous phenols for seven storms sampled between Feb and April 1984 in an urban residential section of Portland, OR. Results acquired from the analysis of the same samples for a variety of nonpolar compounds are available elsewhere (20, 21). The emphasis on phenols here is a result of the fact that they can be present in rain at relatively high, microgram per liter concentrations. A main goal will be the examination of the relative roles played by gas and particle scavenging for these compounds. On the basis of their low  $H$  values ( $\sim 10^{-7} - 10^{-6} \text{ atm} \cdot \text{m}^3 / \text{mol}$ ) (23), and their relatively large vapor pressures ( $10^{-3} - 10^{-1} \text{ torr}$ ) (24) (and therefore low  $\phi$  values), low molecular

\* To whom correspondence should be addressed.

weight phenols should be exclusively gas scavenged. The experimental verification of this premise is presented in this paper.

### Experimental Section

**Air Sampling.** Sampling took place at 5824 S.E. Lafayette St. in Portland, OR. The air sampler has been described in detail (19). It was coupled electronically to the rain sampler to allow concurrent sampling. It employed primary and backup glass-fiber filters (GFFs) followed by three parallel arms containing (1) primary and backup Tenax-GC cartridges for sampling ~30 L of air at 40 mL/min with subsequent analysis by thermal desorption (air desorption cartridges, "ADC-1s"), (2) primary and backup Tenax-GC cartridges for sampling ~400 L of air at 500 mL/min with analysis by thermal desorption (ADC-2s), and (3) primary and backup polyurethane foam plugs (PUFPs) for sampling ~100 m<sup>3</sup> of air with analysis by solvent extraction. Identical field blank filters, cartridges, and PUFPs were transported to, stored at, and recovered from the field site for each rain event.

**Rain Sampling.** The rain sampler used was that of Pankow et al. (16) as modified by Ligocki et al. (20, 21). Rainwater was forced in increments through a Teflon-membrane prefilter and a silver-membrane filter. Approximately 80% of the rain then passed through primary and backup rain extraction cartridges (RECs) for analysis by adsorption/solvent extraction (ASE). The remaining 20% passed through primary and backup rain desorption cartridges (RDCs) for analysis by adsorption/thermal desorption (ATD). The air temperature, total collection time, and the sample volumes were measured. Field blanks were employed as in the air sampling.

**Adsorbent Material and Filter Preparation.** The methods used to prepare the Tenax-GC cartridges and PUFPs are described elsewhere (21). The methods used to prepare the filters are also available (20).

**Recovery Experiments.** Tenax-GC exhibits excellent retention of many nonpolar aqueous compounds (25, 26). For phenols, however, there can be substantial breakthrough. Recovery experiments were carried out with two phenols using procedures described elsewhere for aqueous ASE with Tenax-GC (25). A standard solution of the phenols (20 µL, 4.0 ng/µL in acetone) was injected into a stream of water flowing at 1 mL/s through an injection port, a glass wool mixing cartridge, and then two RECs in series. A total of 1 L of water (pH 7.6) was then passed through the system. The analytes were recovered by solvent extraction with acetone. Other details were as described below.

**Analytical Procedures.** After sampling, all units were resealed, then returned with the field blanks to the laboratory, and refrigerated at 4 °C. The extraction and workup of the rain filters is described elsewhere (20). An additional pertinent detail is that the 50 µL volume of internal standard (IS) (in acetone) added to the filters prior to extraction also contained 4.0 ng/µL 2,4-dibromophenol and 2,4,6-tribromophenol. A 1.5 µL volume of the concentrated extract was injected on-column into a 30 m × 0.32 mm i.d., 0.25-µm film thickness SE-54 DB-5 fused silica capillary column (J & W Scientific, Rancho Cordova, CA). The column was mounted in a Finnigan 9610 or a Hewlett-Packard 5790A GC interfaced (27) to a Finnigan 4000 mass spectrometer/data system (MS/DS; Finnigan-MAT, Sunnyvale, CA). The temperature program used was 80° to 320° at 10°C/min. The MS was scanned from 60 to 450 amu in 0.5 s. Electron impact (EI) ionization was employed. The transfer line, source, MS manifold,

**Table I. Per Cartridge Field Blank Amounts (ng) with ADC-1s and ADC-2s (N = 7)**

compound	ADC-1s	ADC-2s
phenol	11 ± 5.4	10 ± 2.8
2-methylphenol	0.13 ± 0.079	0.11 ± 0.08
3- + 4-methylphenol	1.1 ± 0.95	0.64 ± 0.49
2-methoxyphenol	0.073 ± 0.042	0.15 ± 0.19
2,6-dimethylphenol	0.005 ± 0.007	0.55 ± 1.1
2,4- + 2,5-dimethylphenol	0.18 ± 0.21	2.0 ± 4.0
3,5-dimethylphenol	0.52 ± 0.57	0.47 ± 0.94
3,4-dimethylphenol	0.030 ± 0.040	2.8 ± 5.6

and electron multiplier were at 240 °C, 250 °C, 100 °C, and 1400 V, respectively.

The extraction and workup of the air GFFs is described elsewhere (20). An additional pertinent detail is that the 50 µL volume of internal standard (IS) (in acetone) that was added to the filters prior to extraction also contained 4.0 ng/µL 2,4-dibromophenol and 2,4,6-tribromophenol. The resulting 10-mL extract was then separated into acid and base/neutral fractions as described elsewhere (19). The acid fraction contained the phenols. The final volume reduction, ES addition, and GC/MS/DS analysis steps were carried out as with the rain filter extracts.

The RECs and PUFPs were extracted and analyzed as described elsewhere (see ref 21 and 19, respectively). As above, however, the 50 µL volume of internal standard (IS) (in acetone) added to the RECs and PUFPs prior to extraction also contained 4.0 ng/µL 2,4-dibromophenol and 2,4,6-tribromophenol. In addition, the workup of the PUFP acid fraction extracts involved a cleanup on 5 mL of 15% deactivated silica gel and then recovery in 20 mL of methylene chloride prior to the N<sub>2</sub> blowdown step.

The thermal desorption analysis of the RDCs, ADC-1s, and the ADC-2s was as described elsewhere (21). In addition to the IS compounds cited there, the 2.0 µL volume of IS solution (in methanol) contained phenol-d<sub>5</sub> (10 ng/µL), 2,4-dibromophenol (2 ng/µL), and 2,4,6-tribromophenol (2 ng/µL). Both 0.25- and 1.0-µm film thickness capillary columns were used. The MS conditions were as described for the rain filter analyses.

The water that passed through the RECs was spiked with the same IS solution as the rain filters and then extracted 3 times with 200 mL of methylene chloride. The extracts were reduced in volume as with the rain filter extracts, cleaned up on 5 mL of 15% deactivated silica gel, and then recovered in 20 mL of methylene chloride. They then were concentrated again and then analyzed by GC/MS/DS as with the rain filter extracts.

The identifications of the target compounds in sample runs were carried out as described earlier (16). Quantitation was performed by analysis of standards containing varying amounts of the target and internal and external standard compounds. Relative response factors (RRFs) were calculated by using the GC/MS/DS software, taking nonlinearity into consideration. The phenol IS compounds were used in the RRF calculations in their respective chromatographic regions.

### Results and Discussion

**Phenols in Air: Gaseous.** Breakthrough was small (<1%) on the ADCs in good agreement with other information on the air sampling of phenols with Tenax-GC (28). The average nanogram amounts of the ADC blank values (Table I) were comparable to the corresponding values for rain sampling. 2-Nitrophenol and the C<sub>3</sub>-phenols could not be found in the ADC blanks. The chlorinated phenols were not present in either the ADC or PUFP blanks. The

**Table II. Gas-Phase Phenol Concentrations ( $c_{g,t-b}$ , ng/m<sup>3</sup>)<sup>a</sup> and Average Concentrations (ng/m<sup>3</sup>)<sup>b</sup> during Seven Rain Events in Portland, OR**

compound	sampling days							average
	2/12/84- 2/13/84, Sun-Mon	2/14/84- 2/15/84, Tues-Wed	2/20/84- 2/21/84, Mon-Tues	2/23/84- 2/24/84, Fri-Sat	2/29/84- 3/01/84, Wed-Thurs	3/16/84- 2/20/84, Fri-Tues	4/11/84- 4/12/84, Wed-Thurs	
phenol	220	430	350	270	410	280	250	320
2-methylphenol	52	88	88	51	130	46	51	71
3- + 4-methylphenol	87	170	160	89	230	86	100	130
2-methoxyphenol	110	190	170	89	290	91	130	150
2,6-dimethylphenol	8.4	11	14	8.0	24	6.4	8.3	11
2-nitrophenol	17	15	39	11	28	34	24	24
2,4- + 2,5-dimethylphenol	24	30	37	26	70	15	29	33
2,4-dichlorophenol	0.60	1.3	1.7	0.93	2.3	1.9	2.0	1.5
3,5-dimethylphenol	13	26	23	15	42	9.7	13	20
3,4-dimethylphenol	ND <sup>c</sup>	ND	5.4	ND	ND	ND	3.5	4.0
2,6-dichlorophenol	0.009	0.15	0.14	0.12	0.31	0.12	0.13	0.14
C <sub>9</sub> -phenols	20	40	34	21	57	7.5	8.8	27
2,4,6- + 2,4,5-trichlorophenol	0.023	ND	0.31	0.061	0.13	0.11	0.29	0.15
2,3,4,6-tetrachlorophenol	ND	ND	0.38	0.069	0.62	0.23	0.064	0.27

<sup>a</sup> Individual data are averages of ADC-1 and ADC-2 values. <sup>b</sup> Averages were computed by using only detected values. <sup>c</sup> ND = not detected at statistically significant levels.

magnitudes of the ADC blanks may be compared to the observed air concentrations (see below) by assuming average ADC-1 and ADC-2 sample volumes of 30 and 400 L, respectively.

Although the ADC blank levels were low in absolute terms, the small air volumes sampled in some cases required a careful comparison of sample and blank levels prior to calculating blank-corrected concentrations. The required *t*-test criterion for a 95% confidence level difference between a sample and a blank was  $(A - A_b)/(1/n + 1/n_b)^{0.5} > t_{s_b}$ , where *A* was the amount (ng) on either a given primary or backup cartridge, *A<sub>b</sub>* was the amount (ng) on the field blank for that event, *n* = 1, *n<sub>b</sub>* is the number of blanks, and *s<sub>b</sub>* was the standard deviation of the *A<sub>b</sub>* values for the rain events. If both the primary and backup concentrations were significant, a *c<sub>g,t-b</sub>* (total minus blank) value was calculated as their sum minus twice the equivalent concentration for the blank (*A<sub>b</sub>*/sample volume). If only the primary cartridge value was significant, *c<sub>g,t-b</sub>* was calculated by subtracting (*A<sub>b</sub>*/sample volume) directly. If neither was significant, then the phenol was not detected (ND) at statistically significant levels in that event.

There was very good agreement between the data obtained with the ADC-1 cartridges and those obtained with the ADC-2 cartridges. The means and standard deviations of the ADC-1/ADC-2 ratios for the several rain events were the following: 2-methylphenol,  $1.07 \pm 0.22$ ; 3- + 4-methylphenol,  $1.08 \pm 0.08$ ; 2-methoxyphenol,  $0.70 \pm 0.11$ ; 2,6-dimethylphenol,  $1.04 \pm 0.38$ ; 2-nitrophenol,  $0.91 \pm 0.38$ ; and 2,4- + 2,5-dimethylphenol,  $1.03 \pm 0.34$ .

The *c<sub>g,t-b</sub>* values for 11 specific phenols and four multimer phenol classes are given in Table II. The major compounds were phenol, the methylphenols, and 2-methoxyphenol. The data for the nonchlorinated phenols are the averages of the ADC-1 and ADC-2 results where the phenol was determined on both types of cartridges. When a phenol was found at a statistically significant concentration on only one type of cartridge, the significant value was selected. The chlorinated phenols were determined on the PUFFs with multiple ion detection (MID), or "selected ion monitoring" since their lower concentrations prevented their detection in the lower air volume ADC sampling. The average gas-phase concentrations were computed by using only those storms in which a given compound was detected. ND values were not included as zeroes in the averaging since detection limits varied from

storm to storm due to variable sample volumes and variable background in the quantitation ion signals.

**Phenols in Air: Particulate.** Particulate matter-associated phenols were only found in the samples collected during two storms (2/23/84-2/24/84 and 2/29/84-3/1/84). The compounds included phenol, the methylphenols, 2-methoxyphenol, and two dimethylphenols. They were <5% of the gas-phase values in every case, and generally <1%. No phenols were found on the backup GFFs: sorption on the filters from the gas phase was not a problem.

**Aqueous Phenol ASE/Tenax-GC Recovery Studies.** The amounts of 2,4-dimethylphenol and 2,3,5-trimethylphenol found on the first cartridge (*A<sub>1</sub>* ± 1s) were  $22 \pm 1\%$  and  $34 \pm 6\%$ , respectively (three replicates). The amounts on the second cartridge (*A<sub>2</sub>*) were  $18 \pm 3\%$  and  $17 \pm 1\%$ , respectively (three replicates). The sums of the two amounts were 40% and 51%, respectively. Since the pH was 7.6, and since the *pK<sub>a</sub>* values of these two phenols are ~10, ~100% of both were present in the neutral form, and so this breakthrough was a result of simple polarity, and not ionization. Indeed, the recoveries were less than the ~85% observed for strongly retained, nonpolar compounds with a single cartridge under identical conditions (25). As in that prior study, however, the fractions of the phenols that passed into cartridge 2 and were retained there ( $R_2 = A_2/(100\% - A_1)$ ) were similar to the corresponding values for the first cartridge ( $R_1 = A_1/100\%$ ).

Such behavior is expected if sorption on the bed is diffusion limited, though under the conditions used here if such mass transport in the bed was the only factor influencing sorption, *R<sub>1</sub>* should have been near 0.85 as expected for strongly sorbing compounds (25, 26). Under diffusion limitation, the fraction *R* of the analyte that passes onto a cartridge and is retained is constant for each cartridge and is set by the bed hydrodynamics (26). If [*X*] is the total concentration in the sample and [*P*] and [*S*] are the concentrations found with the primary and secondary (backup) cartridges, respectively, then

$$[P] = R[X] \quad [S] = R(1 - R)[X] \quad (2)$$

$$R = 1 - [S]/[P] \quad [X] = [P]/(1 - [S]/[P]) \quad (3)$$

may be used to estimate [*X*]. A lower bound *B* (%) on the breakthrough from the first cartridge is  $B = [S]100/([P] + [S])$ .

Table III. Dissolved Phenol Concentrations in Rain ( $c_{d,t-b}$ , ng/L)<sup>a</sup> and Average Concentrations (ng/L)<sup>b</sup> for Seven Events in Portland, OR

compound	sampling days									average
	<i>B</i> (N) <sup>c</sup>		2/12/84- 2/13/84, Sun-Mon	2/14/84- 2/15/84, Tues-Wed	2/20/84- 2/21/84, Mon-Tues	2/23/84- 2/24/84, Fri-Sat	2/29/84- 3/01/84, Wed-Thurs	3/16/84- 3/20/84, Fri-Tues	4/11/84- 4/12/84, Wed-Thurs	
	RDCs	RECs								
phenol	56 (7)	58 (2)	>110	1200	>93	>210	>100	>75	>150	>280
2-methylphenol	56 (7)	46 (7)	240	1200	1500	770	2800	>260	>370	>1000
3- + 4-methylphenol	56 (7)	46 (7)	380	1900	2000	1300	1000	460	>610	>1100
2-methoxyphenol	56 (7)	42 (7)	790	1900	5400	2300	2300	710	1100	>2100
2,6-dimethylphenol	47 (7)	32 (7)	84	110	280	150	92	91	160	140
2-nitrophenol	24 (7)	28 (6)	26	51	130	41	78	43	46	59
2,4- + 2,5-dimethylphenol	47 (7)	36 (7)	300	710	1300	810	750	940	940	820
2,4-dichlorophenol	35 (2)	8 (1)	5.0	13	7.4	3.2	2.8	2.9	7.0	5.9
3,5-dimethylphenol	47 (7)	40 (7)	160	410	640	440	600	680	500	490
3,4-dimethylphenol	33 (7)	39 (7)	54	82	140	160	190	140	140	130
2,6-dichlorophenol	45 (1)	NA <sup>d</sup>	0.56	ND <sup>e</sup>	1.1	0.83	1.5	ND	2.5	1.3
C <sub>3</sub> -phenols	31 (7)	32 (7)	250	480	1100	1000	790	430	400	640
2,4,6-trichlorophenol	32 (4)	NA	0.81	ND	1.9	ND	1.9	0.98	1.2	1.4
2,4,5-trichlorophenol	29 (4)	NA	0.69	ND	0.92	ND	1.8	1.1	ND	1.1
tetrachlorophenol	24 (4)	NA	1.9	ND	2.8	1.8	4.6	2.0	ND	2.6
2,3,4,6-tetrachlorophenol	31 (7)	NA	14	16	34	23	10	21	25	20
pentachlorophenol	43 (7)	24 (6)	71	20	54	84	72	44	35	54

<sup>a</sup> Individual data are RDC and REC averages or best values. <sup>b</sup> Averages were computed by using only detected values. <sup>c</sup> *N* = number of replicates. <sup>d</sup> NA = not available. <sup>e</sup> ND = not detected at statistically significant values (95% confidence level).

While eq 2 and 3 will be most accurate for strongly retained compounds, they may also provide rough estimates of  $[X]$  for phenols which are at least moderately retained and for which retention is perhaps partially diffusion limited. When applied to the recovery experiments, the results are  $[X] \pm 1s = 120 \pm 80\%$  and  $68 \pm 18\%$  for 2,6-dimethylphenol and 2,3,5-trimethylphenol, respectively. While not fully satisfying, they are moderately close to 100%. The *s* values were calculated on the basis of standard error propagation procedures. As  $B \rightarrow 50\%$  ( $R \rightarrow 0$ ), the model breaks down rapidly since retention on the bed is far from diffusion controlled.

**Phenols in Rain: Dissolved.** The pH of the bulk rain samples averaged 5.2 and ranged between 4.9 and 5.6. The 15 specific phenols and the three multimember phenol classes found in the rain are given in Table III. According to the identification criteria of Christman (29, 30), a methylnitrophenol, a methoxymethylphenol, and a dimethylmethoxyphenol were also tentatively identified in some of the samples on the basis of mass spectral data alone. The sensitivity of the aqueous ATD (31) with the RDCs allowed some of the minor phenols to be determined. Six of the phenols are U.S. EPA priority pollutants (32).

For the RDCs, the average amounts of phenol, 2-methylphenol, and 3- + 4-methylphenol detected on the blank cartridges were 5.2, 0.06, and 0.37 ng, respectively. No others were detected. For the REC, only 2-methoxyphenol and 3,5-dimethylphenol were detected on the blank cartridges (phenol itself was not examined), and the amounts were 0.78 and 4.0 ng, respectively. When normalized to the average sample volumes (RDCs, 2.0 L; REC, 10.0 L) and compared to the rain concentrations (see below), these blank levels were very low: a statistical comparison of sample and blank values was not required.

The average *B* values ( $\bar{B}$ ) are given in Table III. They were in the 24–56% range for the RDCs and in the 8–58% range for the REC. The compounds with  $\bar{B} \geq 50\%$  were those with the lowest degree of nonpolar substitution. The REC  $\bar{B}$  values for 2,6-dimethylphenol and the C<sub>3</sub>-phenols (32% and 32%, respectively) were similar to the recovery study *B* values. The relative acidity (i.e., anion formation) of pentachlorophenol ( $pK_a = 4.8$ ) was probably the cause

of its substantial breakthrough on the RDCs. The individual *B* values did not appear to depend upon the rain sample volume. Thus, for the more retained compounds, the use of eq 2 and 3 may allow the estimation of the actual rain concentrations to within a factor of 2–3.

Whenever possible ( $B < 50\%$ ), the total, dissolved, blank-corrected concentration  $c_{d,t-b} ([P] + [S] - 2c_{d,b})$  values were corrected for breakthrough. Table III presents the resulting best estimates with their averages. When both RDC and REC data were available, any preference of one value over another was based on the minimal *B* value; when characterized by comparable *B* values, the two were averaged. In a few cases (marked with a greater than sign), *B* was  $>50\%$ , correction for breakthrough was not possible, and the actual concentrations were certainly greater than the values reported. In the case of 2-methylphenol, the analysis of the REC effluent water alone resulted in an average concentration of 1300 ng/L.

2,4- and 2,5-dimethylphenol were incompletely separated on the GC column. Nevertheless, both concentrations were approximately equal (their peak sizes and RRFs were always approximately equal). Thus, estimates of their average individual concentrations are half the 2,4- + 2,5-dimethylphenol numbers in Table III. 3- and 4-methylphenols were not separated at all. At least eight separate C<sub>3</sub>-phenols contributed to the values given for "C<sub>3</sub>-phenols". Their values were based on the assumption that the RRFs for the contributing C<sub>3</sub>-phenols were similar to those for 2,3,5-trimethylphenol. The concentration data given for the unknown tetrachlorophenol are based on the assumption that its RRF was equal to that for 2,3,4,6-tetrachlorophenol. Other information on specific phenols is limited to a study in Hawaii where average pentachlorophenol concentrations of 60 ng/L were observed (33). For this study, the average was 54 ng/L.

The methylphenols, 2-methoxyphenol, and the unidentified methylmethoxyphenol were the largest peaks in the GC/MS/DS chromatograms of the RDC and REC samples. As described above, even the concentrations in Table III may underestimate the actual levels. In previous work (27), we have demonstrated that neutral gas-phase compounds such as PAHs are scavenged by rain according to Henry's law partitioning. The same is likely to be true of the phenols. The dissolved rain concentrations ( $c_d$ , ng/L)

**Table IV. Vapor Pressures and Solubilities of Phenols and Resulting Henry's Law Constants ( $H$ , atm•m<sup>3</sup>/mol) and Rain/Air Partition Coefficients ( $\alpha$ )**

compound	vapor pressure, torr			solubility, g/L			$H$ , atm•m <sup>3</sup> /mol 8 °C	$\alpha$ , 8 °C
	25 °C	8 °C	ref	25 °C	8 °C	ref		
phenol	0.34	0.064	24	82	74	36	$1.1 \times 10^{-7}$	$2.2 \times 10^5$
2-methylphenol	0.29	0.045	24	26	23	36	$2.8 \times 10^{-7}$	$8.2 \times 10^4$
3-methylphenol								
liquid <sup>a</sup>	0.14	0.032	24	23		36		
solid		0.029	24		21	36	$2.0 \times 10^{-7}$	$1.2 \times 10^5$
4-methylphenol	0.12	0.020	24	18	13	36	$2.2 \times 10^{-7}$	$1.1 \times 10^5$
2-methoxyphenol	0.13	0.022	34	16 <sup>d</sup>	15 <sup>b</sup>	37	$2.4 \times 10^{-7}$	$9.6 \times 10^4$
2,6-dimethylphenol	0.18	0.029	24	5.9	2.9	36	$1.9 \times 10^{-6}$	$1.2 \times 10^4$
2-nitrophenol	0.12	0.019	35	1.4 <sup>e</sup>	1.0 <sup>b</sup>	7	$3.5 \times 10^{-6}$	$6.6 \times 10^3$
2,4-dimethylphenol								
liquid <sup>c</sup>	0.098	0.020	24	6.2		36		
solid		0.013	24		3.3	36	$6.3 \times 10^{-7}$	$3.6 \times 10^4$
2,5-dimethylphenol	0.030	0.0038	24	4.6	2.3	36	$2.6 \times 10^{-7}$	$8.8 \times 10^4$
2,4-dichlorophenol	0.089	0.015	34	4.5	3.0 <sup>b</sup>	37	$1.1 \times 10^{-6}$	$2.2 \times 10^4$
3,5-dimethylphenol	0.020	0.0027	24	4.8	2.7	36	$1.6 \times 10^{-7}$	$1.4 \times 10^5$
2,3-dimethylphenol	0.027	0.0035	24	4.7	2.9	36	$2.0 \times 10^{-7}$	$1.2 \times 10^5$
3,4-dimethylphenol	0.014	0.0018	24	5.1	3.0	36	$9.3 \times 10^{-8}$	$2.5 \times 10^5$
2,4,5-trichlorophenol	0.022	0.0035	34	1.2	0.7 <sup>b</sup>	37	$1.3 \times 10^{-6}$	$1.8 \times 10^4$
2,4,6-trichlorophenol	0.017	0.0025	34	0.80	0.5 <sup>b</sup>	37	$1.3 \times 10^{-6}$	$1.8 \times 10^4$

<sup>a</sup> Melting point ( $T_m$ ) is 12 °C. Solid vapor pressure at 8 °C calculated from the equation  $P_s(T) = P_1 \exp[6.8(1 - T_m/T)]$ . <sup>b</sup> Estimated by analogy to the other phenols. <sup>c</sup> Melting point is 24.5 °C. <sup>d</sup> At 15 °C. <sup>e</sup> At 20 °C.

**Table V. Mean Measured Air Concentrations and Predicted and Measured Mean Rain (Dissolved) Concentrations**

compound	mean air concn, ng/m <sup>3</sup>	$\alpha$ (8 °C)	predicted mean rain concn, µg/L	measured mean rain concn, µg/L
phenol	320	$2.1 \times 10^5$	68	>0.28
2-methylphenol	71	$8.2 \times 10^4$	5.8	>1.0
3- + 4-methylphenol	130	$1.1 \times 10^5$	15	>1.1
2-methoxyphenol	150	$9.6 \times 10^4$	14	>2.1
2,6-dimethylphenol	11	$1.2 \times 10^4$	0.14	0.14
2-nitrophenol	24	$6.6 \times 10^3$	0.16	0.059
2,4- + 2,5-dimethylphenol	33	$(3.6-8.8) \times 10^4$	1.2-2.9	0.82
2,4-dichlorophenol	1.5	$2.2 \times 10^4$	0.033	0.006
3,5-dimethylphenol	20	$1.4 \times 10^5$	2.9	0.49
3,4-dimethylphenol	4.0	$2.5 \times 10^5$	0.99	0.13
2,4,5- + 2,4,6-trichlorophenol	0.15	$1.8 \times 10^4$	0.0028	0.0025

may then be estimated from the gas-phase concentrations ( $c_g$ , ng/m<sup>3</sup>) (16):

$$c_d = 10^{-3} c_g RT / H(T) = 10^{-3} c_g \alpha \quad (4)$$

$$c_d \approx 10^{-3} c_g RTS / P \quad (5)$$

where  $\alpha$  is the rain/air partition coefficient,  $S$  is the solubility (mol/m<sup>3</sup>), and  $P$  is the vapor pressure (atm). The use of the  $\approx$  sign applies to compounds whose solubilities lie above Henry's law limiting range. Table IV presents a compilation of literature vapor pressure and solubility data for the phenols at 25 and 8 °C. The latter value was the average temperature during sampling. The  $\alpha$ (8 °C) values range from  $6.6 \times 10^3$  to  $2.5 \times 10^5$ . They are high enough to result in significant depletion of the gas-phase concentrations of phenols during a single rainstorm.

On the basis of the air data in Table II, the  $\alpha$ (8 °C) values in the Table IV have been used to predict the average rain concentrations. The results are presented in Table V and also compared to the average measured concentrations. Both the predicted and the measured values for the nonchlorinated phenols are quite high (microgram per liter levels) compared to the nanogram per liter levels of neutral compounds found in the same samples (21). The predicted and measured concentrations tend to agree more closely for the compounds with the lowest  $\alpha$  values since they are the least polar and tend in general to be retained somewhat better on Tenax-GC. Overall, these results indicate that the total concentration

of phenols in the rain samples may have been  $\sim 100$  µg/L, two-thirds due to phenol itself. Total phenol concentrations in Los Angeles rainwater have been reported to be in the 2–8 µg/L range (17).

**Phenols in Rain: Filterable.** The analyses of the rain filters showed only phenol, the methylphenols, a dimethylphenol, and pentachlorophenol to be present. Moreover, the levels of these compounds were very low,  $\leq 1.0\%$  of the  $c_{d,t-b}$  concentrations in every case. It is possible that sorption on the filters from the dissolved state was responsible for at least a portion of these low levels.

### Conclusions

The phenols determined in the air samples were found to exist virtually exclusively in the gaseous state. This is in agreement with the large vapor pressures of the phenols studied. It is also supported by the fact that virtually no phenols were found on the rain filters, even though substantial amounts were found dissolved in the rain. Despite the fact the rain (dissolved) data only provided estimates of the actual concentrations, the air and rain data together clearly demonstrate that gas scavenging was much more important than particle scavenging for these phenols. Considering their rather low Henry's law constant values, it is evident that even in absolute terms, gas scavenging will be an efficient removal process for these compounds. This efficiency is reflected clearly in their high rain (dissolved) concentrations.



## Acknowledgments

The donation of a portion of the Tenax-GC used in this study from Alltech Associates, Inc., Deerfield, IL, is gratefully acknowledged. The assistance of Lorne M. Isabelle in a portion of the work is also appreciated.

**Registry No.** Phenol, 108-95-2; 2-methylphenol, 95-48-7; 3-methylphenol, 108-39-4; 4-methylphenol, 106-44-5; 2-methoxyphenol, 90-05-1; 2,6-dimethylphenol, 576-26-1; 2-nitrophenol, 88-75-5; 2,4-dimethylphenol, 105-67-9; 2,5-dimethylphenol, 95-87-4; 2,4-dichlorophenol, 120-83-2; 3,5-dimethylphenol, 108-68-9; 3,4-dimethylphenol, 95-65-8; 2,6-dichlorophenol, 87-65-0; 2,4,6-trichlorophenol, 88-06-2; 2,4,5-trichlorophenol, 95-95-4; 2,3,4,6-tetrachlorophenol, 58-90-2; tetrachlorophenol, 25167-83-3; pentachlorophenol, 87-86-5.

## Literature Cited

- (1) Graedel, T. E. In "Chemical Compounds in the Atmosphere"; Academic Press: New York, 1978; pp 256-265.
- (2) Atlas, E.; Giam C. S. *Science (Washington, D.C.)* **1981**, *211*, 163-165.
- (3) Eisenreich, S. J.; Looney, B. B.; Thornton, J. D. *Environ. Sci. Technol.* **1981**, *15*, 30-38.
- (4) Altshuller, A. P.; Buffalini, J. J. *Environ. Sci. Technol.* **1971**, *5*, 39-64.
- (5) Christensen, E. J.; Olney, C. E.; Bidleman, T. J. *Bull. Environ. Contam. Toxicol.* **1979**, *23*, 196-202.
- (6) McClure, V. G. *Environ. Sci. Technol.* **1976**, *10*, 1223-1229.
- (7) Tucker, W. A.; Lyman, W. J.; Preston, A. L. *Precip. Scavenging, Dry Deposition, Resuspension, Proc. Int. Conf., 4th* **1983**, 1243-1257.
- (8) Slinn, W. G. N.; Hasse, L.; Hicks, B. B.; Hogan, A. W.; Lal, D.; Liss, P. S.; Munnich, K. O.; Sehmel, G. A.; Vittori, O. *Atmos. Environ.* **1978**, *12*, 2055-2087.
- (9) Lee, R. N.; Hales, J. M. In "Precipitation Scavenging of Organic Contaminants". Durham, NC, final reports to U.S. Army Research Office, 1974; DAH-C-04-72-C-0035, and 1975, DAH-C-04-74-0014.
- (10) Hales, J. M. *Atmos. Environ.* **1972**, *6*, 635-659.
- (11) Atkins, D. H. F.; Eggleton, A. E. J. *Nucl. Tech. Environ. Pollut., Proc. Symp.* **1971**, 521-533.
- (12) Ohta, T.; Morita, M.; Mizoguchi, I.; Tada, T. *Atmos Environ.* **1977**, *11*, 985-987.
- (13) Harder, H. W.; Christensen, E. J.; Matthews, J. R.; Bidleman, T. F. *Estuaries* **1980**, *3*, 142-147.
- (14) Bidleman, T. F.; Christensen, E. J. *J. Geophys. Res.* **1979**, *84*, 7857-7862.
- (15) Pankow, J. F.; Isabelle, L. M.; Asher, W. E.; Kristensen, T. J.; Peterson, M. E. *Precip. Scavenging, Dry Deposition, Resuspension, Proc. Int. Conf., 4th* **1983**, 1243-1257.
- (16) Pankow, J. F.; Isabelle, L. M.; Asher, W. E. *Environ. Sci. Technol.* **1984**, *18*, 310-318.
- (17) Kawamura, K.; Kaplan, I. R. *Environ. Sci. Technol.* **1983**, *17*, 497-501.
- (18) Kawamura, K.; Kaplan, I. R. *Anal. Chem.* **1984**, *56*, 1616-1620.
- (19) Ligocki, M. P.; Pankow, J. F. *Anal. Chem.* **1985**, *57*, 1138-1144.
- (20) Ligocki, M. P.; Leuenberger, C.; Pankow, J. F. *Atmos. Environ.* **1985**, *19*, 1619-1626.
- (21) Ligocki, M. P.; Leuenberger, C.; Pankow, J. F. *Atmos. Environ.* **1985**, *19*, 1609-1617.
- (22) Junge, C. E. In "Fates of Pollutants in the Air and Water Environment"; Suffet, I. H., Ed.; Wiley-Interscience: New York, 1977; Part 1, pp 7-25.
- (23) Mabey, W. R.; Smith, J. H. Podoll, R. T.; Johnson, H. L.; Mill, T.; Chou, T.-W.; Gates, J.; Partridge, I. W.; Jaber, H.; Vandenberg, D. "Aquatic Fate Process Data for Organic Priority Pollutants", U.S. EPA, 1982, EPA Report 440/4-81-014.
- (24) Andon, R. J. L.; Biddiscombe, D. P.; Cox, J. D.; Handley, R.; Harrop, D.; Herington, E. F. G.; Martin, J. F. *J. Chem. Soc.* **1960**, 5246-5254.
- (25) Leuenberger, C.; Pankow, J. F. *Anal. Chem.* **1984**, *56*, 2518-2522.
- (26) Pankow, J. F.; Isabelle, L. M.; Kristensen, T. J. *J. Chromatogr.* **1982**, *245*, 31-43.
- (27) Pankow, J. F.; Isabelle, L. M. *Anal. Chem.* **1984**, *56*, 2997-2999.
- (28) Krost, K. J.; Pellizzari, E. D.; Walburn, S. G.; Hubbard, S. A. *Anal. Chem.* **1982**, *54*, 810-817.
- (29) Christman, R. F. *Environ. Sci. Technol.* **1982**, *16*, 143A.
- (30) Christman, R. F. *Environ. Sci. Technol.* **1984**, *18*, 203A.
- (31) Pankow, J. F.; Isabelle, L. M.; Hewetson, J. P.; Cherry, J. A. *Ground Water*, in press.
- (32) Keith, L. H.; Telliard, W. A. *Environ. Sci. Technol.* **1979**, *13*, 416-423.
- (33) Bevenue, A.; Ogata, J. N.; Hylin, J. W. *Bull. Environ. Contam. Toxicol.* **1972**, *8*, 238-241.
- (34) Weast, R. C. "Handbook of Chemistry and Physics", 54th ed.; CRC Press: Cleveland, OH, 1973-1974.
- (35) Chao, J.; Lin, C. T.; Chung, T. H. *J. Phys. Chem. Ref. Data* **1983**, *12*, 1033-1063.
- (36) Erichsen, V. L.; Dobbert, E. *Brenns-Chem.* **1955**, *36*, 338-345.
- (37) Verschuere, K. "Handbook of Environmental Data on Organic Chemicals"; Van Nostrand Reinhold: New York, 1983.
- (38) Korenman, Ya. I.; Karmaeva, I. B.; Ternovich, N. N. *Fiz-Khim. Metody Anal.* **1978**, *3*, 121-124.
- (39) Hashimoto, Y.; Tokura, K.; Kishi, H.; Strachan, W. M. J. *Chemosphere* **1984**, *13*, 881-888.

Received for review October 15, 1984. Revised manuscript received May 15, 1985. Accepted May 23, 1985. This work was funded in part with federal funds from the U.S. Environmental Protection Agency (U.S. EPA) under Grant R8113380. A portion of the financial support for C.L. came from the Swiss National Science Foundation.

# Wall Loss of Gaseous Pollutants in Outdoor Teflon Chambers

Daniel Grosjean

Daniel Grosjean and Associates, Inc., Suite 645, 350 N. Lantana Street, Camarillo, California 93010

■ Loss rates have been measured for ~20 gaseous pollutants in FEP Teflon chambers. Loss rates were  $\leq (1-4) \times 10^{-4} \text{ min}^{-1}$  for toluene, *o*-cresol, benzaldehyde, biacetyl, pyruvic acid,  $\text{SO}_2$ , and methyl nitrate. Higher loss rates,  $(10-20) \times 10^{-4} \text{ min}^{-1}$ , were measured for ammonia, benzoic acid, and nitric acid. Ozone loss rates in dry air were  $(0.5-3.0) \times 10^{-4} \text{ min}^{-1}$  in the dark and  $(2-8) \times 10^{-4} \text{ min}^{-1}$  in sunlight and increased in humid air. These loss rates are consistent with collision yields of  $\sim \leq 2 \times 10^{-8}$  (number of molecules lost per collision on the Teflon surface). Loss by chemical reactions cannot be ruled out for the most reactive compounds studied. For oxides of nitrogen, the measured loss rates reflected the competing pathways of thermal oxidation of NO (dark), photolysis of  $\text{NO}_2$  (sunlight), loss of  $\text{NO}_x$  and loss of products (e.g.,  $\text{HONO}_2$ ) to the walls, and heterogeneous hydrolysis of  $\text{NO}_2$ . The latter pathway contributes to the production of free radicals, with  $k(\text{NO}_2 + \text{wall} \rightarrow \text{HONO}) = (1.5-4.0) \times 10^{-4} \text{ min}^{-1}$  under our conditions.

## Introduction

Environmental chambers (commonly referred to as smog chambers) have been extensively used in atmospheric chemistry studies (e.g., see ref 1-5). In fact, most of the experimental information concerning hydrocarbon photochemistry, ozone production, and aerosol formation in urban air has been derived from smog chamber studies of "model" systems such as single hydrocarbon- $\text{NO}_x$  mixtures in purified air. Experimental results obtained in smog chambers are also used extensively for the formulation, testing, and validation of increasingly detailed computer kinetic models (e.g., see ref 6-8) describing the gas-phase chemistry of atmospheric pollutants.

As for any other laboratory instrument, smog chambers are not without shortcomings and limitations. Wall effects, including film contamination, heterogeneous reactions on the chamber walls, and release of reactive species including free radicals and their precursors have been the object of several reports (9-12). Wall-promoted processes are obviously related to the extent of gas-phase pollutant loss to the chamber walls. In a typical example, a net flux of free radicals may result from a sequence of processes involving diffusion of  $\text{NO}_2$  to the walls, reaction of  $\text{NO}_2$  with water on the wall to form nitrous and nitric acids, release of volatile nitrous acid from the wall to the gas phase, and subsequent photolysis of nitrous acid to form hydroxyl radicals.

While the importance of these heterogeneous effects is now well recognized, there is a paucity of data regarding the loss rates of organic and inorganic pollutants in environmental chambers. For example, current computer kinetic models take only into account measured or estimated loss rates for ozone and, in some instances, oxides of nitrogen. A more comprehensive assessment of wall loss rates for gaseous and particulate pollutants is critical to, for example, the validation of computer kinetic models, the derivation of carbon, sulfur, and nitrogen mass balances in chemically reactive mixtures, and the determination of organic aerosol formation rates from precursor hydrocarbons.

In the course of recent studies of organic aerosol formation from olefins (13), aromatic hydrocarbons (14), and

organosulfur compounds (15), we have measured loss rates for a number of pollutants in outdoor environmental chambers constructed from fluorinated ethylene-propylene copolymer film (FEP Teflon). While the chamber facility we employed no longer exists, our results are applicable to other Teflon chambers, a number of which are currently being employed for atmospheric chemistry and physics studies (e.g., see ref 16 and 17). While the emphasis of this report is on gas-phase pollutants, detailed studies of aerosol losses have also been carried out and are described elsewhere (18, 19).

## Experimental Section

The outdoor chamber facility and its dedicated instrumentation have been described in detail elsewhere (13-15), and only a summary of information relevant to this study is given below.

Outdoor chambers were constructed from panels of FEP 200A Teflon film heat sealed together, with the seams externally reinforced with 5 cm wide strips of plastic tape (mylar). Large chambers were constructed from 10 panels, each  $9.14 \times 1.22 \text{ m}$ , with a total wall area of  $111.6 \text{ m}^2$ . For a typically initial volume of  $\sim 80 \text{ m}^3$  (fully inflated chamber), the initial surface to volume ratio was  $\sim 1.4 \text{ m}^{-1}$ . Smaller chambers were constructed from four panels, each  $3.05 \times 1.22 \text{ m}$ , with a wall area of  $14.9 \text{ m}^2$ . For a typical initial volume of  $3.9 \text{ m}^3$ , the initial S/V was  $3.8 \text{ m}^{-1}$ .

Newly constructed chambers were first "conditioned" by sunlight irradiation for 6-10 h of purified air containing 1-5 ppm of ozone followed by purging several times with purified air. This protocol has been shown to minimize, in subsequent runs, contamination due to organic impurities desorbing from the Teflon film (9). Following this initial "conditioning" protocol, the chambers were purged at least once with purified air after each experiment, and sunlight irradiations of purified air were carried out at regular intervals. Detailed studies for a number of pollutant mixtures (20) have shown that "memory" effects, i.e., the possible retention of a fraction of the reactants and products from one run to the next, were reduced to negligible levels by using this cleanup protocol.

In a typical experiment, a test atmosphere was prepared by injecting the pollutant of interest into the chamber containing purified air provided by an Aadco 737-14 air purification system. Stability studies were conducted in the dark (chamber covered with opaque plastic film which removed  $\geq 99\%$  of the incident sunlight) and in sunlight (opaque cover removed after injection and mixing). Measurement methods and other pertinent information are summarized in Table I. Temperature (YSI-741-A-10 sensor), dew point (EG&G 880-C-1 hygrometer), and sunlight intensity (Eppley ultraviolet radiometer) were also monitored. While most experiments were conducted with dry matrix air (typically dew point =  $-20$  to  $-16^\circ \text{C}$  at  $T = 18-26^\circ \text{C}$ ), the stability of ozone,  $\text{NO}_x$ , and ammonia was also studied in humid air. Compounds that photolyze rapidly in sunlight such as pyruvic acid (27) and other carbonyls were obviously tested only in the dark. While most runs were carried out for 4-6 h, shorter ( $\sim 2 \text{ h}$ ) and longer runs ( $\sim 10-12 \text{ h}$ , overnight) were also included.

Control experiments were also carried out. The matrix air provided by the purified air generator contained low

Table I. Experimental Conditions

compound	source/preparation	injection	measurement method
ozone	Welsbach generator	diluted output	ultraviolet photometry, Dasibi 1003-AH <sup>a</sup>
nitric oxide	lecture bottle	<i>b</i>	chemiluminescence, Teco 14B/E <sup>a</sup>
nitrogen dioxide	gas cylinder, 100 ppm in N <sub>2</sub>	<i>b</i>	chemiluminescence, Teco 14B/E <sup>a</sup>
sulfur dioxide	gas cylinder, 50 ppm in N <sub>2</sub>	<i>b</i>	pulsed fluorescence, Monitor Labs 8550 <sup>a</sup>
ammonia	lecture bottle	<i>b</i>	collection on oxalic acid impregnated filters, ion chromatography
nitric acid	air stream through diluted aqueous solution	direct	chemiluminescence, Teco 14B/E, <sup>c</sup> and collection on nylon filters/ion chromatography (21)
<i>n</i> -butane	<i>d</i>	<i>b</i>	gas chromatography-flame ionization detection (GC-FID) (22)
<i>n</i> -pentane	<i>d</i>	<i>b</i>	GC-FID (22)
styrene	<i>d</i>	<i>b</i>	GC-PID <sup>e</sup>
$\beta$ -methylstyrene	<i>d</i>	<i>b</i>	GC-PID <sup>e</sup>
<i>o</i> -cresol	<i>d</i>	<i>b</i>	gas chromatography-photoionization detection (GC-PID) (14)
benzaldehyde	<i>d</i>	<i>b</i>	GC-PID <sup>e</sup>
biacetyl	<i>d</i>	<i>b</i>	gas chromatography-electron capture detection (GC-ECD) <sup>f</sup>
pyruvic acid	<i>d</i>	<i>b</i>	collection in impingers, ion chromatography (23)
peroxyacetyl nitrate (PAN)	synthesized (23)	diluted output, or prepared in situ <sup>g</sup>	GC-ECD (24), also chemiluminescence <sup>c</sup>
methyl nitrate	synthesized <sup>h</sup>	<i>b</i>	GC-ECD <sup>f</sup>
benzoic acid	<i>d</i>	prepared in situ <sup>i</sup>	collection in KOH impingers, ion chromatography with ultraviolet detection (25)

<sup>a</sup> Calibrated according to U.S. EPA approved methods involving NBS-traceable standards. <sup>b</sup> Diluted with pure nitrogen in 200-cm<sup>3</sup> glass bulbs. <sup>c</sup> Instrument response to nitric acid and to PAN is quantitative in NO<sub>2</sub> mode of instrument. <sup>d</sup> Commercial source, purity  $\geq 98\%$ , used without further purification. <sup>e</sup> On Teflon, TCEP, or SP 1240 packed columns. <sup>f</sup> Same column and conditions as for PAN. <sup>g</sup> From irradiated chlorine-acetaldehyde-NO<sub>x</sub> (24), propene-NO<sub>x</sub>, or biacetyl-NO<sub>x</sub> mixtures. <sup>h</sup> Synthesized according to ref 26. <sup>i</sup> From styrene-ozone or  $\beta$ -methylstyrene-ozone mixtures in the dark.

Table II. Summary of Pollutant Loss Rates in Outdoor Teflon Chambers<sup>a</sup>

compound	no. of runs	range of initial concn, ppb	chamber size <sup>b</sup>	loss rate, $\times 10^{-4}$ min <sup>-1</sup>	
				dark	sunlight
ozone	14	10-1280	L	1.3 $\pm$ 0.9	5.1 $\pm$ 2.8
	8	340-1450	S	3.4 $\pm$ 1.4	6.7 $\pm$ 2.2
NO <sup>c</sup>	11	6-590	L, S	0.4 $\pm$ 4.15	0.5 $\pm$ 1.1
NO <sub>2</sub> <sup>c</sup>	11	4-460	L, S	-1.6 $\pm$ 4.1 <sup>d</sup>	3.9 $\pm$ 3.6
NO <sub>x</sub>	11	10-710	L, S	0.7 $\pm$ 1.1	2.6 $\pm$ 1.7
SO <sub>2</sub>	3	200-500	S	1.3 $\pm$ 0.3	
NH <sub>3</sub>	7	100-420	S	4-17 <sup>e</sup>	
nitric acid	2	125	S	15 $\pm$ 1	
<i>n</i> -butane	3	25-100	L, S	$\leq 2.0$ <sup>f</sup>	$\leq 2.0$ <sup>f</sup>
<i>n</i> -pentane	1	130	S	$\leq 2.0$ <sup>f</sup>	$\leq 2.0$ <sup>f</sup>
toluene	4	300-1100	L, S	$\leq 2.5$ <sup>f</sup>	$\leq 2.5$ <sup>f</sup>
styrene	2	500-1000	S	$\leq 2.4$ <sup>f</sup>	
$\beta$ -methylstyrene	1	500	S	$\leq 2.9$ <sup>f</sup>	
<i>o</i> -cresol	4	900-1100	S	$\leq 3.4$ <sup>f</sup>	$\leq 2.0$ <sup>f</sup>
benzaldehyde	3	500-1000	S	3.4 $\pm$ 1.7	NA <sup>g</sup>
benzoic acid	1	25	S	10.8	
biacetyl	3	50-400	S	$\leq 2.5$ <sup>f</sup>	NA <sup>g</sup>
pyruvic acid	4	200-400	S	$\leq 2.5$ <sup>f</sup>	NA <sup>g</sup>
methyl nitrate	3	50-500	S	$\leq 0.8$ <sup>f</sup>	
PAN	8	15-400	L, S	$\leq 4.3$ <sup>h</sup>	3.9 $\pm$ 1.6 <sup>h</sup>

<sup>a</sup> In dry air (dew point = -20 to -16 °C at  $T = 18-26$  °C) unless otherwise indicated. <sup>b</sup> S = small ( $V = 3.9$  m<sup>3</sup>, initial  $S/V = 3.8$  m<sup>-1</sup>); L = large ( $V = 80$  m<sup>3</sup>, initial  $S/V = 1.4$  m<sup>-1</sup>). <sup>c</sup> In mixtures of NO and NO<sub>2</sub>; see Table IV for details. <sup>d</sup> Net production of NO<sub>2</sub> in some runs by thermal oxidation of NO; see text. <sup>e</sup> Includes runs with humid air (~55-50% RH). <sup>f</sup> No measurable loss was observed. The upper limit listed was calculated from the precision of the measurements and the length of the run. <sup>g</sup> NA = not applicable; compound photolyzes in sunlight. <sup>h</sup> In the presence of NO<sub>2</sub>.

levels of oxides of nitrogen (typically 6-12 ppb) and of non-methane hydrocarbons ( $\leq 10$  ppb as measured by gas chromatography analysis of individual hydrocarbons (22)). No measurable pollutant increase could be detected in chambers filled with purified air and kept in the dark for up to 6 h. This indicates negligible contamination from impurities desorbing from the walls and/or by permeation of ambient air contaminants through the Teflon film (see ref 9 for a more detailed discussion). In sunlight, only low levels of ozone were formed in either newly conditioned or older chambers (20). Maximum ozone concentrations obtained in 4-8-h sunlight irradiations of purified matrix air were in the range 2-21 ppb, with a median value of  $5.0 \pm 4.7$  (1 $\sigma$ ) ppb (22 runs). The corresponding initial NO<sub>x</sub>

concentrations were  $12.6 \pm 5.3$  ppb. Net ozone formation rates (i.e., photochemical ozone production minus loss of ozone on walls; see below) were in the range 0.3-7 ppb h<sup>-1</sup>, with a median value of  $1.34 \pm 1.56$  ppb h<sup>-1</sup> (1 $\sigma$ , 22 runs).

### Results and Discussion

Pollutant removal rate constants are summarized in Table II and are derived from measured concentrations vs. time in individual runs, as is illustrated in Figure 1 for nitric acid.

**Removal of Pollutants on Teflon Film Surfaces.** The data listed in Table II indicate that FEP Teflon film has a reasonably low efficiency with respect to removal of gaseous pollutants. Assuming that gas-phase chemical

Table III. Collision Yields on FEP Teflon Film and Other Surfaces

compound	collision rate constant $k_c$ , m s <sup>-1</sup> <sup>a</sup>	collision yields			
		FEP Teflon, this work <sup>b</sup>	FEP Teflon <sup>c</sup>	sulfuric acid <sup>d</sup>	carbon soot <sup>e</sup>
O <sub>3</sub>	91	1.75 × 10 <sup>-8</sup> / 1.65 × 10 <sup>-8</sup>	0.9 × 10 <sup>-8</sup>	<10 <sup>-6</sup>	
NO	115	0.16 × 10 <sup>-8</sup>		<10 <sup>-6</sup>	<10 <sup>-6</sup>
NO <sub>2</sub>	93	<1 × 10 <sup>-8</sup>		<10 <sup>-6</sup>	<10 <sup>-6</sup>
SO <sub>2</sub>	79	0.73 × 10 <sup>-8</sup>		<10 <sup>-6</sup>	<10 <sup>-6</sup>
NH <sub>3</sub>	153	1.2–4.8 × 10 <sup>-8</sup>		>10 <sup>-3</sup>	>10 <sup>-3</sup> <sup>g</sup>
HONO <sub>2</sub>	79	8.3 × 10 <sup>-8</sup>		≥2.4 × 10 <sup>-4</sup>	<10 <sup>-6</sup>
<i>n</i> -butane	83	<1.0 × 10 <sup>-8</sup>		<10 <sup>-6</sup> <sup>h</sup>	
<i>n</i> -pentane	74	<1.2 × 10 <sup>-8</sup>			
toluene	66	<1.7 × 10 <sup>-8</sup>			
styrene	62	<1.7 × 10 <sup>-8</sup>			
β-methylstyrene	58	<2.2 × 10 <sup>-8</sup>			
<i>o</i> -cresol	60	<2.5 × 10 <sup>-8</sup>			
benzaldehyde	61	<2.4 × 10 <sup>-8</sup>			
benzoic acid	57	8.3 × 10 <sup>-8</sup>			
biacetyl	68	<1.6 × 10 <sup>-8</sup>			
pyruvic acid	67	<1.5 × 10 <sup>-8</sup>			
methyl nitrate	72	<0.5 × 10 <sup>-8</sup>			
PAN	57	<1.5 × 10 <sup>-8</sup>			

<sup>a</sup> At 25 °C, from eq 5 and 6. <sup>b</sup> In dry air in the dark, from eq 7, with  $S/V = 3.8$  m<sup>-1</sup> unless otherwise indicated. <sup>c</sup> Data from Kelly (9). <sup>d</sup> Concentrated H<sub>2</sub>SO<sub>4</sub> (≤5% water); data from Baldwin and Golden (28, 29). <sup>e</sup> Soot from propane flame; data from Baldwin and Golden (28, 29). <sup>f</sup> Runs with large chamber,  $S/V = 1.4$  m<sup>-1</sup>. <sup>g</sup> Initially and then decreases rapidly. <sup>h</sup> Value given for unspecified paraffins and olefins.

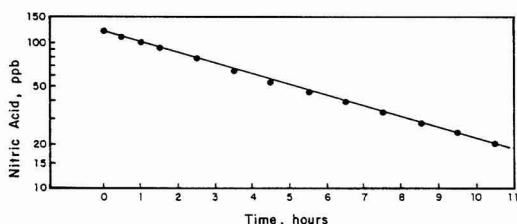


**Figure 1.** Example of loss rate measurement: nitric acid in the dark (4-m<sup>3</sup> Teflon chamber).

removal processes are negligible (see discussion in following paragraphs), collision yields, that is, the fraction of collisions on Teflon film resulting in the loss of a molecule, can be calculated from the data in Table II, the chamber surface to volume ratio, and standard gas kinetic considerations. Thus

$$cy_x = k_x/k_c \quad (1)$$

where  $cy$ ,  $k$ , and  $k_c$  are the collision yield, removal rate constant, and collision rate constant, respectively, for species  $x$ . The removal rate constant for species  $x$  on a surface of area  $S$  is given by

$$dn_x/dt = k_x[x]S \quad (2)$$

where  $n$  is the number of molecules and brackets indicate concentration. In the same way

$$d[x]/dt = k_{rx}[x] \quad (3)$$

where  $k_{rx}$  values are the removal rate constants given in Table II. Combining eq 2 and 3

$$k_x = k_{rx}(S/V)^{-1} \quad (4)$$

Collision rate constants  $k_c$  are simply calculated from the mean thermal velocity:

$$k_{cx} = v_x/4 \quad (5)$$

with

$$v_x = \sqrt{8RT/(\pi M_x)} \quad (6)$$

where  $M_x$  is the molecular weight. Mean thermal velocities increase with increasing temperature (but by only ~2% in the range 18–26 °C covered in our experiments) and decrease with increasing molecular weight, from ~610 m s<sup>-1</sup> for ammonia ( $M_x = 17$ ) to ~228 m s<sup>-1</sup> for benzoic acid ( $M_x = 122$ ). Combining eq 1 and 4–6, collision yields are given by

$$cy_x = k_{rx}(S/V)^{-1} \sqrt{RT/(2\pi M_x)} \quad (7)$$

The collision yields calculated from eq 7 are listed in Table III. For most compounds including ozone, hydrocarbons, oxygenated aromatics, aliphatic dicarbonyls, and nitrogen-containing aliphatic oxygenates, only two or fewer molecules are destroyed in 10<sup>8</sup> collisions on FEP Teflon film. Larger yields were obtained for ammonia (up to ~5 × 10<sup>-8</sup>) and for nitric acid and benzoic acid (~8 × 10<sup>-8</sup>). Also listed in Table III for comparison are collision yields reported by Baldwin and Golden (28, 29) for two substrates, sulfuric acid and soot, which are relevant to gas-aerosol interactions in the atmosphere. Collision yields on these two surfaces are in qualitative agreement with those we calculated for Teflon, i.e., lower values for ozone, NO<sub>x</sub>, SO<sub>2</sub>, and hydrocarbons and higher values for ammonia and nitric acid.

**Ozone.** Loss rates for ozone in our chambers, ~ (0.5–3.0) × 10<sup>-4</sup> min<sup>-1</sup> in the dark and ~ (2–8) × 10<sup>-4</sup> min<sup>-1</sup> in sunlight, are consistent with (although generally lower than) previous data for a number of chambers constructed from the same type of Teflon film (e.g., see ref 9, 30, and 31). In agreement with the discussion presented in the preceding paragraph, loss rates were observed to vary according to the chamber  $S/V$  ratio and to increase rapidly in partially deflated chambers (up to 14 × 10<sup>-4</sup> min<sup>-1</sup>).

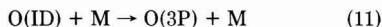
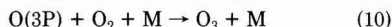
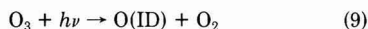
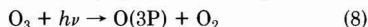
Ozone losses were 2–3 times higher in sunlight than in the dark (Table II), and this in spite of some ozone production resulting from irradiation of the purified matrix air (see Experimental Section). Ozone loss in sunlight probably is a combination of several factors including desorption of ozone-scavenging impurities from the chamber walls (chamber temperatures generally increased in sunlight), photolysis of some of these impurities to form

Table IV. NO<sub>x</sub> Stability Studies

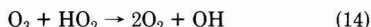
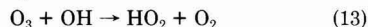
		chamber size <sup>a</sup>	time, h	initial concn, ppb			10 <sup>4</sup> × loss rate, min <sup>-1</sup> <sup>b</sup>		
				NO	NO <sub>2</sub>	NO <sub>x</sub>	NO	NO <sub>2</sub>	NO <sub>x</sub>
dark	dry air <sup>c</sup>	L	3	170	395	565	+0.7	+1.0	+0.9
		L	12	590	119	709	2.0	+8.2	0.2
		S	8	28	260	288	+5.9	2.0	1.2
		L	15	6	4	10	0	0	0
		L	17	223	40	263	1.2	+2.5	0.7
	humid air	S	6	46	190	236	5.4	1.5	2.2
		S	3	45	460	505	0	3.6	3.5
		S	4.5	33	303	336	7.8	1.6	1.1
		L	5			361			4.2
		L	3	90	100	190	1.8	+1.2	0.3
sunlight	dry air	S	7	356	210	566	0	5.0	1.8
		L	4	32	90	122	0	1.8	1.4
		L	3	114	127	241	1.5	7.9	4.8
		S	5.5	122	190	312	+0.7	6.1	3.4

<sup>a</sup>L = large and S = small; see Table II. <sup>b</sup>A (+) sign indicates that NO or NO<sub>2</sub> increased in this run; see text. <sup>c</sup>Dry air = dew point of -20 °C at T = 18–26 °C; humid air = RH = 82–86%.

species reactive toward ozone, and photolysis of ozone followed by reaction of O(ID) with water vapor:



Since ozone is rapidly regenerated from O(3P) in reaction 10, loss of ozone in the above sequence is via reactions 9 and 12, followed by additional removal of ozone by reaction with OH and HO<sub>2</sub>:



Indeed, sunlight irradiations conducted at high humidity (RH ≥ 80%) yielded substantially higher ozone loss rates (up to 65 × 10<sup>-4</sup> min<sup>-1</sup>) than those conducted with dry matrix air.

**Hydrocarbons.** Loss rates listed in Table II for hydrocarbons (HC) were typically ≤ 2 × 10<sup>-4</sup> min<sup>-1</sup>. In many instances, no measurable loss could be detected, and only upper limits could be derived from the precision of the measurement method. Kelly (32) reported loss rates of ≤ 5% per day (~0.34 × 10<sup>-4</sup> min<sup>-1</sup>) for a number of hydrocarbons stored for up to 1 week in FEP Teflon containers.

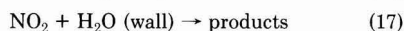
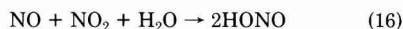
Gas-phase chemical reactions with ozone, the hydroxyl radical, and the nitrate radical may contribute to the hydrocarbon loss rates listed in Table II. Examination of the literature data for HC + O<sub>3</sub>, HC + OH, and HC + NO<sub>3</sub> reaction rate constants and for the O<sub>3</sub>–NO<sub>2</sub>–NO<sub>3</sub> system indicates that, even at the low NO<sub>x</sub> and ozone levels present in the matrix air (~6–12 ppb and detection limit of ≤ 1–2 ppb, respectively), gas-phase reactions may be of importance for at least the most reactive hydrocarbons. For example, reaction of styrene with 1 ppb of ozone in the dark (*k* ~ 3 × 10<sup>-17</sup> cm<sup>3</sup> molecule<sup>-1</sup> s<sup>-1</sup>) would result in a styrene removal rate of ~0.5 × 10<sup>-4</sup> min<sup>-1</sup>, as compared to the measured value of ≤ 2.4 × 10<sup>-4</sup> min<sup>-1</sup>. In the same way, only ~10<sup>-5</sup> ppb of NO<sub>3</sub> (~2 × 10<sup>5</sup> radicals cm<sup>-3</sup>) would be required to remove *o*-cresol in the dark at a rate of 2 × 10<sup>-4</sup> min<sup>-1</sup>. In sunlight, hydroxyl radicals are produced by photochemical reactions involving background NO<sub>x</sub> and the added hydrocarbon, as well as possibly by heterogeneous reactions of the background NO<sub>x</sub> on the chamber walls. Assuming that the observed removal rates

are entirely due to reaction with OH, upper limits of ≤ 7 × 10<sup>4</sup> radicals cm<sup>-3</sup> can be calculated for hydroxyl radical concentrations in the FEP Teflon chamber during sunlight irradiation of hydrocarbons in purified air.

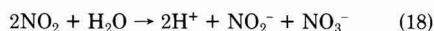
**Nitrogenous Pollutants.** Nitric acid and ammonia were rapidly lost to the chamber walls. The rapid loss of nitric acid and its implications for nitrogen mass balances in smog chamber experiments have been discussed previously (17, 33). In contrast, peroxyacetyl nitrate (PAN), methyl nitrate (Table II), and other alkyl nitrates (*n*-propyl and *n*-butyl; exploratory experiments not listed in Table II) exhibited excellent stability in our FEP Teflon chambers. Our upper limit for PAN stability in the dark is consistent with the recently measured rate constant for self-decomposition of PAN, 1.3 × 10<sup>-6</sup> s<sup>-1</sup> at ambient temperature (34).

**Oxygenated Organics.** Loss rates of oxygenated organics, aliphatic (biacetyl and pyruvic acid) or aromatic (*o*-cresol and benzaldehyde), were low and comparable to those measured for hydrocarbons. In contrast, the loss rate of benzoic acid was substantially higher and comparable to that of nitric acid. Thus, wall losses must be included in mass (or carbon) balance calculations for systems such as styrenes–O<sub>3</sub> (dark) or styrenes–NO<sub>x</sub> (sunlight) which are expected to yield benzoic acid as a major product.

**Oxides of Nitrogen.** (1) **Loss in the Dark.** Loss rates for NO, NO<sub>2</sub>, and NO<sub>x</sub> were measured in the dark and in sunlight, in dry and humid air, and over a range of NO<sub>x</sub> concentrations (~10–700 ppb) and of initial NO/NO<sub>2</sub> ratios. Results for individual experiments are listed in Table IV. In general, measured loss rates were small and comparable to those for other pollutants (see Table II), increased in the dark at high humidity, and were higher in sunlight than in the dark. In addition, NO and NO<sub>2</sub> concentrations actually increased in several runs ("negative" loss rates in Table IV) due to a number of chemical reactions including thermal oxidation of NO to NO<sub>2</sub> (e.g., see ref 35) and/or heterogeneous hydrolysis of NO<sub>x</sub> on the chamber walls (12):



Reaction 17 has been studied in the bulk liquid phase (36), where the reaction products are nitrous acid and nitric acid:





However, Sakamaki et al. (12) observed that the dark heterogeneous HO<sub>2</sub>-H<sub>2</sub>O reaction in their smog chamber was not stoichiometric and that the products were nitrous acid and nitric oxide:

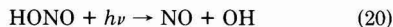


Nitric acid was probably produced as well but was not released from the chamber walls.

The data in Table IV for experiments conducted in the dark are consistent with the expected relative contributions of the several reactions discussed above. Thus, thermal oxidation of NO to NO<sub>2</sub> (reaction 15) was predominant in dry air runs with high initial NO, while some NO was produced in runs with high initial NO<sub>2</sub> (reaction 19 predominant).

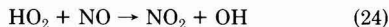
In the two dark runs with humid air, off-line samples including water impingers, alkaline impingers (5 × 10<sup>-3</sup> N KOH), and nylon filters were collected at the end of the runs and analyzed for nitric acid as nitrate by ion chromatography. No nitric acid could be detected in these samples (detection limit ≤ 1 ppb). Either nitric acid was not released from the walls, in agreement with the observations of Sakamaki et al. (12), or gas-phase nitric acid, if any, had been lost to the walls at the end of the runs (see high loss rate for HONO<sub>2</sub> in Table II).

(2) **Loss in Sunlight.** In sunlight, an additional NO<sub>x</sub> loss process is involved, namely, reaction of NO<sub>2</sub> with the hydroxyl radical formed upon photolysis of nitrous acid, i.e., reaction 19 followed by

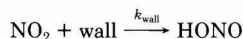


and subsequent rapid loss of nitric acid to the chamber walls. Reactions 19 and 20 account for the so-called wall source of free radicals in smog chambers. This additional supply of OH radicals includes two components, one at the onset of irradiation (photolysis of HONO formed after injection of NO<sub>x</sub> in humid matrix air) and the other taking place throughout the run and being proportional to NO<sub>2</sub>, humidity (reaction 19), and light intensity (reaction 20).

The "wall source" of radicals and its functional dependence on reactant concentrations and state parameters can be readily calculated from experimental data. In principle, OH concentrations could be calculated from nitric acid yields (reaction 21) in NO<sub>x</sub>-pure air irradiations, but this approach is severely limited owing to the rapid wall loss of HONO<sub>2</sub>. More reliable measurements can be derived from experiments in which OH can be calculated from its removal rate by reaction with other compounds, provided that  $k_i(\text{X}_i) \gg k_{\text{NO}_2}(\text{NO}_2)$ . Trace levels of hydrocarbons (11) or, conversely, high concentrations of CO (17, 37) have been employed. In the latter case, the reactions of interest, following reactions 19–21, are



From the measured NO decay rates in irradiated CO-NO<sub>x</sub> mixtures in purified air [ $T \sim$  ambient, relative humidity (RH)  $\sim$  65%], Leone et al. (17) calculated  $k_{\text{wall}} = (5.0 \pm 1.2) \times 10^{-4} \text{ min}^{-1}$  for



for an outdoor Teflon chamber similar to the one employed in this study.

The contribution of heterogeneous hydrolysis of NO<sub>2</sub> (wall source of radicals) was calculated for the NO<sub>x</sub>-purified

**Table V. Comparison of Measured and Computed NO<sub>x</sub> Loss Rates**

Experimental Conditions					
parameter	initial	final			
NO, ppb	122	125			
“NO <sub>2</sub> ”, ppb <sup>a</sup>	190	152			
“NO <sub>x</sub> ”, ppb <sup>a</sup>	312	277			
temp, °C	23	24			
dew point, °C	-19	-12			
time, PST	12:00	17:30			
Computer Simulations <sup>b</sup>					
10 <sup>4</sup> <i>k</i> <sub>wall</sub> , min <sup>-1</sup> <sup>c</sup>	NO and NO <sub>2</sub> wall loss included <sup>d</sup>	computed final concn, ppb			
		NO	NO <sub>2</sub>	HONO <sub>2</sub>	NO <sub>x</sub>
0	no	143	169	0	312
5	no	151	136	22	309
3	no	148	148	14	310
3	yes	119	141	13	273
1.5	yes	116	150	7	273
1.5	yes <sup>e</sup>	116	150	7	273
1.5	yes <sup>f</sup>	115	153	7	275

<sup>a</sup> Includes the response of the chemiluminescent NO<sub>x</sub> analyzer to nitric acid, if any. <sup>b</sup> With model described by Leone et al. (17). <sup>c</sup> For reaction NO<sub>2</sub> → (wall) HONO (17). <sup>d</sup> Loss rates of 6.6 × 10<sup>-4</sup> and 1.5 × 10<sup>-4</sup> min<sup>-1</sup> for NO and NO<sub>2</sub>, respectively. <sup>e</sup> Adding rapid loss of N<sub>2</sub>O<sub>5</sub> to walls ( $k = 8 \times 10^{-3} \text{ min}^{-1}$ ). <sup>f</sup> Reducing CO from 5.0 to 2.5 ppm (no CO was added in these runs, but the matrix air contained ~4 ppm of CO).

air irradiations (with no CO added but ~4 ppm of CO present in the matrix air) by using the computer kinetic model of Leone et al. (17). These calculations included all pertinent inorganic reactions, the appropriate time-dependent temperatures and NO<sub>2</sub> photolysis rate constants, and a wall loss term for ozone (from data in Table II). An example of calculations for a specific run is given in Table V. The wall losses of NO and NO<sub>2</sub> as determined experimentally (Table II) were included or omitted, and the parameter  $k_{\text{wall}}$  was varied incrementally in the range (0–5) × 10<sup>-4</sup> min<sup>-1</sup>. As is shown in Table V, the best agreement between computed and measured values correspond to  $k_{\text{wall}} = 3 \times 10^{-4} \text{ min}^{-1}$  when wall losses of NO and NO<sub>2</sub> are taken into account. Increasing the wall loss term for N<sub>2</sub>O<sub>5</sub> had little impact on the calculated NO<sub>x</sub> values. Varying the CO concentration in the range 2.5–5.0 ppm (CO in the matrix air was ~4 ppm) had no effect on the calculated NO<sub>x</sub> values, as expected since much higher CO concentrations would be needed for reactions 22–24 to become important. Values of  $k_{\text{wall}}$  for other runs, as well as for runs involving O<sub>3</sub>-NO<sub>2</sub> mixtures, were in the range (1.5–4.0) × 10<sup>-4</sup> min<sup>-1</sup>. These values are low (compared to other chamber facilities) and are similar to those measured by Leone et al. (17) for a similar outdoor Teflon chamber. The magnitude of the wall source for a number of indoor and outdoor chambers and the implications for computer kinetic modeling of the corresponding experiments have been discussed in detail elsewhere (7, 8, 11, 12, 17) and will not be further discussed here. It should be stressed, however, that the  $k_{\text{wall}}$  values derived from our experiments are only valid for the specific chambers employed and at a specific time in their "history". More recent, or more seasoned, chambers, even though having the same geometry (e.g., S/V ratio) and made of the same Teflon film, may yield different results. In the same way,  $k_{\text{wall}}$  values derived from "NO<sub>x</sub>-only" experiments may not be entirely applicable to NO<sub>x</sub>-organic irradiations, where other reactants and products (e.g., nitrogenous species, water-soluble carbonyls and dicarbonyls, etc.) may con-

**Table VI. Estimated Loss of Nitric Acid in NO<sub>2</sub>-O<sub>3</sub> Experiments**

	run no.			
	158	180	159	168
dark/sunlight matrix air	dark dry <sup>a</sup>	dark humid (~50% RH)	sunlight dry	sunlight dry
T, °C	31	18	23	24
initial O <sub>3</sub> , ppb	500	207	280	415
initial NO <sub>2</sub> , ppb <sup>b</sup>	470	230	340	390
length of runs, h	4.0	4.5	5.0	4.0
concn at end of run, ppb				
N <sub>2</sub> O <sub>5</sub> , calcd	75	0.7	1.0	8
HONO <sub>2</sub> , calcd	250	209	21	24
HONO <sub>2</sub> , measd	40	13	8	7
average nitric acid loss rate, % h <sup>-1</sup>	21.0	20.8	12.4	17.7

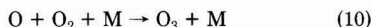
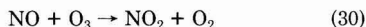
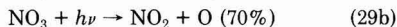
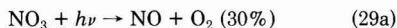
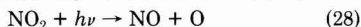
<sup>a</sup> Initial dew points of  $-17 \pm 1$  °C. <sup>b</sup> With nitric acid impurity, if any, removed from the gas cylinder source using two nylon filters in series. Matrix air contained no detectable amounts of nitric acid (<1 ppb).

tribute to free radical production as a result of their own complex wall-promoted reaction cycles.

**Loss of Nitric Acid in NO<sub>2</sub>-O<sub>3</sub> Experiments.** The loss rate of nitric acid was also estimated in several experiments involving the reaction of ozone with nitrogen dioxide in purified air. In the dark, the reaction sequence of interest is



In sunlight, the following reactions also take place:



The above reactions, along with minor reactions pertinent to the O<sub>3</sub>-NO<sub>2</sub> system, are well characterized (e.g., see ref 38-41) and are included in all computer kinetic models. Thus, estimates of nitric acid wall loss in O<sub>3</sub>-NO<sub>2</sub> experiments can be obtained by comparing computed and measured HONO<sub>2</sub> concentrations.

Table VI summarizes the nitric acid loss rates calculated in several O<sub>3</sub>-NO<sub>2</sub> experiments. The computer kinetic mechanism we employed is that described by Leone et al. (17). Included in the calculations were wall loss rates for ozone, NO, and NO<sub>2</sub> as given by Table II. Experimental data included measurements of nitric acid by ion chromatography following collection on nylon filters (27) or in alkaline impingers ( $5 \times 10^{-3}$  N aqueous KOH), as well as by difference between "NO<sub>2</sub>" readings of a chemiluminescent NO<sub>x</sub> analyzer with and without removal of nitric acid by using a nylon filter (21, 24). The three sets of measurements agreed within 20%. N<sub>2</sub>O<sub>5</sub>, which is also present in the matrix, may interfere if collected on nylon filters (this has not been verified experimentally) and/or in KOH impingers (this is likely). However, calculated N<sub>2</sub>O<sub>5</sub> concentrations listed in Table VI show that the maximum contribution of N<sub>2</sub>O<sub>5</sub> to the measured nitrate concentration is minor, i.e., 1-25%. In addition, literature data (40, 41) indicate that the wall loss rate of N<sub>2</sub>O<sub>5</sub> is substantial,  $(6-68) \times 10^{-3} \text{ min}^{-1}$  (i.e., higher than that we

measured for nitric acid). Thus, actual N<sub>2</sub>O<sub>5</sub> concentrations in our experiments may be substantially lower than the calculated values.

The wall loss rates listed in Table VI are consistent with those given in Table II for nitric acid in purified air and confirm that wall loss of nitric acid must be included in nitrogen mass balance calculations.

#### Acknowledgments

I thank Jeffrey Harrison for providing able assistance in all aspects of the outdoor chamber experiments. I also thank P. H. McMurry for useful discussions and Dr. J. S. Gaffney and Dr. J. G. Calvert for preprints of ref 34 and 41, respectively, prior to publication.

**Registry No.** PAN, 2278-22-0; NO, 10102-43-9; NO<sub>2</sub>, 10102-44-0; NO<sub>3</sub>, 11104-93-1; SO<sub>2</sub>, 7446-09-5; NH<sub>3</sub>, 7664-41-7; O<sub>3</sub>, 10028-15-6; nitric acid, 7697-37-2; n-butane, 106-97-8; n-pentane, 109-66-0; toluene, 108-88-3; styrene, 100-42-5; β-methylstyrene, 637-50-3; o-cresol, 95-48-7; benzaldehyde, 100-52-7; benzoic acid, 65-85-0; biacetyl, 431-03-8; pyruvic acid, 127-17-3; methyl nitrate, 598-58-3; FEP 200A Teflon, 25067-11-2.

#### Literature Cited

- U.S. Environmental Protection Agency, Research Triangle Park, NC, 1976, Smog Chamber Conference Proceedings, Report EPA-600/3/76-029.
- Kamens, R. M.; Jeffries, H. E.; Sexton, K. G.; Wiener, R. W. *Atmos. Environ.* **1982**, *16*, 1027-1034.
- Grosjean, D.; Friedlander, S. K. In "The Character and Origins of Smog Aerosols"; Hidy, G. M., et al., Eds.; Wiley: New York, 1978; pp 435-473.
- O'Brien, J. N., Jr.; Holmes, J. R.; Bockian, A. H. *Environ. Sci. Technol.* **1975**, *9*, 568-576.
- Pitts, J. N., Jr.; Grosjean, K.; Van Cauwenberghe, K.; Schmid, J. P.; Fitz, D. R. *Environ. Sci. Technol.* **1978**, *12*, 946-953.
- Atkinson, R.; Carter, W. P. L.; Darnall, K. R.; Winer, A. M.; Pitts, J. N., Jr. *Int. J. Chem. Kinet.* **1980**, *12*, 779.
- Killus, J. P.; Whitten, G. Z. *Atmos. Environ.* **1982**, *16*, 1973.
- Leone, J. A.; Seinfeld, J. H. *Int. J. Chem. Kinet.* **1984**, *16*, 159.
- Kelly, N. A. *Environ. Sci. Technol.* **1982**, *16*, 763-770.
- Lonneman, W. A.; Bufalini, J. J.; Kuntz, R. L.; Meeks, S. A. *Environ. Sci. Technol.* **1981**, *15*, 99-103.
- Carter, W. P. L.; Atkinson, R.; Winer, A. M.; Pitts, J. N., Jr. *Int. J. Chem. Kinet.* **1981**, *13*, 735-740.
- Sakamaki, F.; Hatakeyama, S.; Akimoto, H. *Int. J. Chem. Kinet.* **1983**, *15*, 1013-1029.
- Grosjean, D. *Sci. Total Environ.* **1984**, *37*, 195-311.
- Grosjean, D. *Atmos. Environ.* **1984**, *18*, 1641-1652.
- Grosjean, D. *Environ. Sci. Technol.* **1984**, *18*, 460-468.
- Kamens, R. M.; Rives, G. D.; Perry, J. M.; Bell, D. A.; Paylor, F., Jr.; Goodman, R. G.; Claxton, L. D. *Environ. Sci. Technol.* **1984**, *18*, 523-530.
- Leone, J. A.; Flagan, R. C.; Grosjean, D.; Seinfeld, J. H. *Int. J. Chem. Kinet.* **1985**, *17*, 177-216.
- McMurry, P. H.; Rader, D. J. *Aerosol Sci. Technol.*, in press.
- McMurry, P. H.; Grosjean, D. *Environ. Sci. Technol.*, in press.
- Grosjean, D.; McMurry, P. H. Secondary Organic Aerosol Formation: Homogeneous and Heterogeneous Chemical Pathways, Phase 2. Coordinating Research Council, Atlanta, GA, 1984.
- Grosjean, D. *Anal. Lett.* **1982**, *15*, 785-796.
- Grosjean, D.; Fung, K. J. *Air Pollut. Control Assoc.* **1984**, *34*, 537-543.
- Grosjean, D.; Nies, J. D. *Anal. Lett.* **1984**, *17*, 89-96.
- Grosjean, D.; Fung, K.; Collins, J.; Harrison, J.; Breitung, E. *Anal. Chem.* **1984**, *56*, 569-573.
- Fung, K.; Grosjean, D. *Anal. Lett.* **1984**, *17*, 475-482.
- Johnson, J. R., Ed. "Organic Synthesis", Collect. Vol. XIX, Wiley: New York, NY, 1939; p 64.
- Grosjean, D. *Atmos. Environ.* **1983**, *17*, 2379-2382.

- (28) Baldwin, A. C.; Golden, D. M. *Science (Washington, D.C.)* **1979**, *206*, 562-563.
- (29) Baldwin, A. C.; Golden, D. M. *J. Geophys. Res.* **1980**, *85*, 2888-2889.
- (30) Sickles, J. E.; Wright, R. S. Dec 1973, U.S. EPA Report EPA-600/7-79-227.
- (31) Fox, D. L.; Kamens, R.; Jeffries, H. E. *Science (Washington, D.C.)* **1976**, *191*, 1058.
- (32) Kelly, N. A. 75th Annual Air Pollution Control Association Meeting, New Orleans, LA, June 20-25, 1982, Paper 82-33.4.
- (33) Spicer, C. W.; Miller, D. F. 67th Annual Air Pollution Control Association Meeting, Denver, CO, June 9-13, 1974, Paper 74-24.7.
- (34) Senum, G. I.; Fajer, R.; Gaffney, J. S., submitted for publication in *J. Phys. Chem.*
- (35) Lindquist, A. *Atmos. Environ.* **1982**, *16*, 1957-1972.
- (36) Lee, Y. N.; Schwartz, S. E. *J. Phys. Chem.* **1981**, *85*, 840-848.
- (37) Besemer, A. C.; Nieboer, H. *Atmos. Environ.* **1983**, *17*, 1598-1600.
- (38) Malko, M. W.; Troe, J. *Int. J. Chem. Kinet.* **1982**, *14*, 399-416.
- (39) Platt, U.; Perner, D. *Geophys. Res. Lett.* **1980**, *7*, 89-92.
- (40) Cox, R. A.; Coker, G. B. *J. Atmos. Chem.* **1983**, *1*, 53-63.
- (41) Cantrell, C. A.; Stockwell, W. R.; Anderson, L. G.; Busarow, K. L.; Perner, D.; Schmeltekopf, A.; Calvert, J. H.; Johnston, H. S. *J. Phys. Chem.* **1985**, *89*, 139-146.

Received for review October 15, 1984. Revised manuscript received April 22, 1985. Accepted May 23, 1985. This work was supported by the Coordinating Research Council, CAPA 20-80 Project Group, through an agreement with ERT, Inc.

## Activation and Reactivity of Calcareous Sorbents toward Sulfur Dioxide

Jerald A. Cole,\* John C. Kramlich, W. Randall Seeker, and Michael P. Heap

Energy and Environmental Research Corporation, Irvine, California 92718

Gary S. Samuelsen

Department of Mechanical Engineering, University of California, Irvine, California 92717

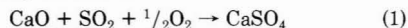
■ The reactivity of several calcareous sorbents to SO<sub>2</sub> absorption is assessed in a laboratory-scale reactor under conditions representative of those encountered in the radiant zones of pulverized-coal-fired utility boilers. Rate of calcination, surface area development, regeneration of gas-phase sulfur species, and SO<sub>2</sub> capture ability are examined as a function of gas-phase environment and sorbent type. The sulfation reaction was experimentally decoupled from the calcination process, and over 50% conversion of calcium to sulfate was observed for one sorbent in 0.6 s. Sorbent reactivity to SO<sub>2</sub> is principally governed by specific surface area of the calcined sorbent, although sorbent type is a secondary influence. Peak sorbent temperature during calcination is the dominant factor governing surface area development for a given sorbent. The results demonstrate that (1) sorbent injection into the combustion zone ( $T > 1200^\circ\text{C}$ ) for SO<sub>2</sub> control is not optimal, and (2) a significant increase in sorbent reactivity will be attained by calcination at temperatures below  $1200^\circ\text{C}$ , the lowest value assessed in the present experiment.

### Introduction

The injection of pulverized limestones into the radiant section of a pulverized-coal-fired boiler has been proposed as a method for the control of sulfur dioxide (SO<sub>2</sub>) emissions through the EPA-defined process of limestone injection into multistaged burners (LIMB). Development efforts are in progress to elucidate the principal controlling parameters of SO<sub>2</sub> capture in a flame environment (1, 2). The present paper reports on the first phase of this effort in which the activation and sulfation of pulverized limestones are assessed at the high temperatures ( $>1100^\circ\text{C}$ ) representative of those found in the combustion zone of commercial coal-fired utility boilers.

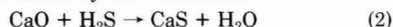
Limestones injected into a high-temperature, sulfur-laden environment follow a series of processes: heat-up, calcination/activation, sulfation, deactivation, and/or regeneration. Calcination encompasses the process of CO<sub>2</sub> evolution from the sorbent as a result of particle heating. The surface area increases, thereby increasing the number

of active sites for SO<sub>2</sub> capture. Activation may consist merely of calcination (the escaping CO<sub>2</sub> leaving the particle open for reaction). Sulfation, the active process of SO<sub>2</sub> capture, is described by the following general reaction under oxidizing conditions:

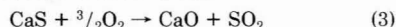


Although the physical process of eq 1 remains unknown, data from several laboratory experiments have been correctly predicted by a model incorporating zero-order intrinsic kinetics (3). Due to diffusional resistances, however, the apparent, or global, reaction order with respect to SO<sub>2</sub> has been observed as zero (4), one-half (5), and one (6). Several limestone-sorbent properties—specific surface area, pore size, total porosity, and crystallite size—influence the sulfation reaction rate (7, 8). However, the latter three of these properties manifest themselves in the specific surface area. As a result, the specific surface area is a physical property of special interest in evaluating the ability of sorbents to uptake SO<sub>2</sub>.

Deactivation and regeneration of the sorbent also are important. Deactivation is associated with sintering, a process that reduces the active surface area of the material. This may occur thermally or be augmented by interaction with other minerals (e.g., coal ash) that lower the melting point (hence, the Tammann temperature) of the solids. Regeneration is the desorption of sulfur species. This may leave the particle active for sorption but does so at the expense of sulfur release. Regeneration is mainly a concern for fuel-rich capture systems (e.g., low NO<sub>x</sub> burners) where initial capture occurs by the mechanism



followed by the regeneration reaction



Early failures of the LIMB process resulted from overburning the sorbents upon high-temperature injection. In addition, the thermodynamics of sulfation (eq 1) becomes unfavorable above about  $1200^\circ\text{C}$ . Many subsequent studies of calcination and sulfation have therefore been limited to nonflame environments and relatively low tem-

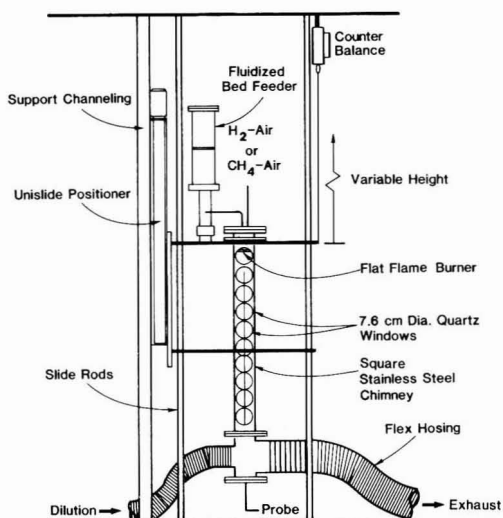


**Figure 1.** Flat-flame reactor chimney (1.2 m long) with optical access ports.

peratures, generally below 1100 °C (9). Higher temperature (>1100 °C) studies of surface areas, calcination, sulfation, and petrographic properties (10–12) have been restricted to relatively long times of 0.5 s to several hours. The simplicity and practicality of flame-zone-sorbent injection has sustained the interest in high-temperature sorbent injection. As a result, this study originated to examine transient phenomena (i.e., calcination) occurring under flame-zone conditions but in shorter times than previously explored and to relate these phenomena to subsequent SO<sub>2</sub> capture at lower temperatures.

The objectives of the present study were to (1) investigate the processes of sorbent heat-up, calcination/activation, and sulfation in a well-controlled laboratory-scale system in the range of temperature ( $T > 1100$  °C) and time (0.5 s) representative of the combustion zone of a full-scale utility boiler and (2) correlate changes in sorbent physical and chemical properties during calcination with the ability of the sorbent to uptake SO<sub>2</sub>. This was accomplished by injecting pulverized calcareous sorbents into the high-temperature region of a laboratory flame and studying the processes occurring at times as short as 10 ms.

### Apparatus

The gas-flame reactor, described in detail elsewhere (13), consisted of a 7.6-cm diameter, water-cooled sintered-

bronze flat-flame burner down fired into a 10 cm × 10 cm square stainless steel chimney. The burner was fired on both methane/air and hydrogen/air mixtures. Limestone sorbents were injected into the flat flame through a 6.4 mm i.d. copper tube mounted through the burner axis. Two chimneys were employed for this study. One of these, shown in Figure 1, is 1.2 m long and is equipped with optical windows that are removable for solids sampling probe access. A second chimney, 0.6 m long with viewing windows, was used for sulfur-capture testing with a dispersed-phase quartz reactivity probe. Gas temperatures within the reactor were measured with a 0.2-mm diameter, butt-welded type-S thermocouple and monitored by an Omega 199 readout. Temperatures reported are corrected for radiation.

Sorbent particle injection was accomplished with a Smith-type fluidized-bed feeder (14, 15). Solids feed rates from 0.2 to 2.0 g/min were attained by using transport gas flow rates of 4–60 cm<sup>3</sup>/s. Batch samples of solids for physical and chemical analysis were collected with an isokinetic water-cooled stainless steel probe (Figure 2). The solids were collected in a large volume 47-mm Nuclepore filter holder (with 0.8-μm pore size Nuclepore polycarbonate, or Gelman triacetate filter elements). This probe was operated above the dew point of the sampled gas (70 °C) by restricting the cooling water flow rate. The filter was maintained at 100 °C by keeping it in an electrically heated oven. Absorption and reaction of CO<sub>2</sub> and H<sub>2</sub>O with the sample CaO was determined to be negligible. Samples were analyzed after exposure to the reactive gases over intervals from 5 to 30 min and showed no change in composition or specific surface area.

Sorbent reactivity toward SO<sub>2</sub> was determined by using a dispersed-phase "SO<sub>2</sub>-reactivity probe" constructed of quartz (Figure 3). The probe was designed to provide a direct, relative measure of the sorbent sulfur capture decoupled from calcination and independent of the thermal environment in the flame. A sample from the flame is extracted, quenched, and then drawn into an isothermal heated reaction zone maintained at a temperature of 1100 ± 10 °C at its midpoint. The sample was drawn through the probe at 33 N cm<sup>3</sup>/s. At the entrance to the isothermal zone, SO<sub>2</sub> is mixed with the entraining gas stream to 6 vol %. Probe dimensions provide a nominal residence time in the isothermal zone of 0.6 s, estimated by jet penetration theory (16). At the furnace exit, the sample stream is cooled to 150 °C and collected on a microporous glass-fiber filter. Additional SO<sub>2</sub> uptake in the filter holder was negligible (<2.4% conversion). Sulfated samples were analyzed for total sulfur (sulfate and sulfide), carbon (carbonate), and hydrogen (water and hydroxide) by instrumental methods using a Leco SC-32 and Perkin-Elmer

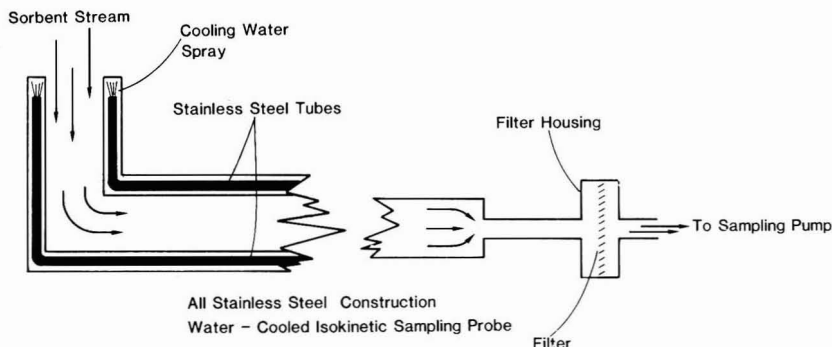


**Figure 2.** Water-cooled isokinetic sampling probe for solids collection in the flame reactor chimney.

**Table I. Physical and Chemical Properties of Test Materials**

sorbet	composition	physical properties		chemical analysis, wt %					
		mean size, $\mu\text{m}$	surface area, $\text{m}^2/\text{g}$	Ca	Mg	Al	Si	Na	Fe
Vicron 45-3	$\text{CaCO}_3$	11.0	0.6	39.2	0.49	0.07	0.07	0.02	0.04
Michigan marl	$\text{CaCO}_3$	18.0	1.52	25.0	0.93	1.09	9.29	0.19	0.87
dolomite	$\text{CaCO}_3\cdot\text{MgCO}_3$	34.0	0.9	21.0	12.1	0.09	0.37	0.03	0.10
calcium hydroxide	$\text{Ca}(\text{OH})_2$	12.5	12.2	54.0	0.3				0.02

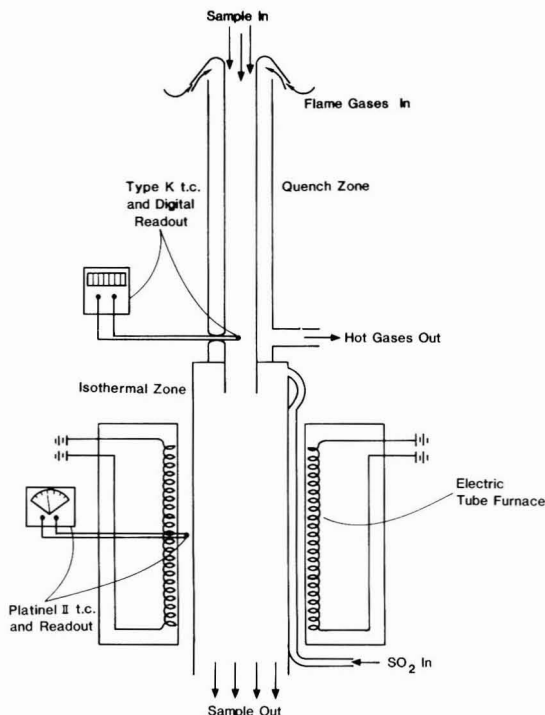


**Figure 3.** Schematic of the quartz "SO<sub>2</sub> reactivity probe".

240B. Calcium was determined by using ASTM D2795, a chelometric titration. Specific surface areas were measured by N<sub>2</sub> adsorption using the BET method.

Injection and sampling systems were tested for particle size discrimination. Mean size and specific surface area of the starting materials were compared with those of samples that were injected and collected raw. No discernible change was noted.

### Experimental Section

Physical and chemical properties of the sorbents under study are shown in Table I. Vicron 45-3 and the dolomite were locally available stones obtained from the Minerals and Pigments Division of Pfizer. They and the Michigan marl were chosen for study because of the relatively small mean size and prior successful use in larger scale studies (2). The calcium hydroxide (Fisher, reagent grade) was chosen for its chemical purity. In all, this set of four sorbents provided a cross-section of calcareous sorbet properties for investigation.

The flame conditions used in this study are listed in Table II. The center line temperature of the reactor was perturbed because the sorbet carrier gas, although a mixture of CH<sub>4</sub>-air in all cases, was not stabilized by the water-cooled burner. Therefore, the carrier-gas methane was adjusted so that the center line temperature matched

**Table II. Flame Conditions**

fuel	equivalence ratio, $\phi^a$	cold gas velocity, <sup>b</sup> cm/s	peak center line temp, °C (7 cm)
methane	0.99	48	1830
methane	0.85	47	1630
methane	0.77	47	1515
methane	0.66	23	1360
hydrogen	0.60	49	1200

<sup>a</sup>  $\phi = (\text{fuel}/\text{air})_{\text{actual}}/(\text{fuel}/\text{air})_{\text{stoichiometric}}$  <sup>b</sup> Gas velocity normal to burner corrected to 298 K.

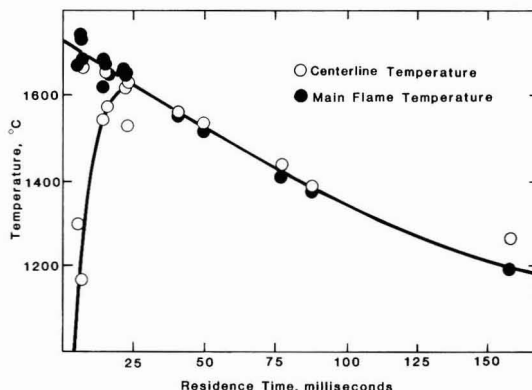


**Figure 4.** Time-temperature profiles for the burner flame and the sorbet carrier gas. 1630 °C peak temperature condition.

the main flame temperature at a convenient but arbitrary distance 7 cm from the burner surface. This gas temperature, reported in Table II, was the peak temperature experienced by the injection solids.

A typical time-temperature profile for both the main flame and the center line is shown in Figure 4. Residence times were calculated on the basis of the face velocities of the main burner flames. Heating rates of the particles were determined experimentally by two-color pyrometry to be  $5 \times 10^4$  K/s.

### Results and Discussion

**Calcination and Surface Area Development.** Vicron 45-3 was injected into several methane and hydrogen flames and sampled at varying distances in order to investigate the rates of calcination and surface area development at elevated temperatures. Data from three methane flames are provided in Table III and are averaged for clarity and plotted in Figure 5. (Data for the fourth methane flame, 1515 °C, are tabulated and presented later with data for additional sorbents.)

At all three temperatures, significant extents of calcination (mole percent CaCO<sub>3</sub> converted to CaO) are attained in times less than 100 ms. Although 100% calcination of limestones is rarely attained (17), the curves in Figure 5b all approach asymptotic values well below 100%. Recarbonation of the calcined lime during sampling was



**Table III. Surface Area and Mole Percent Calcination of Vicron 45-3**

axial peak, temp, °C	residence time, ms	total specific surface area, m <sup>2</sup> /g	% calcination
1830	20	4.6	37.4
1830	30	4.3	53.5
1830	30	5.1	85.9
1830	53	5.5	82.5
1830	53	6.9	88.1
1830	61	6.1	75.7
1830	120	5.0	76.0
1630	23	5.1	33.1
1630	33	3.7	78.3
1630	33	3.9	80.0
1630	59	6.3	78.0
1630	59	9.3	74.9
1630	68	7.9	84.4
1630	134	7.2	81.3
1360	54	7.6	31.6
1360	79	10.7	65.9
1360	161	9.4	77.1

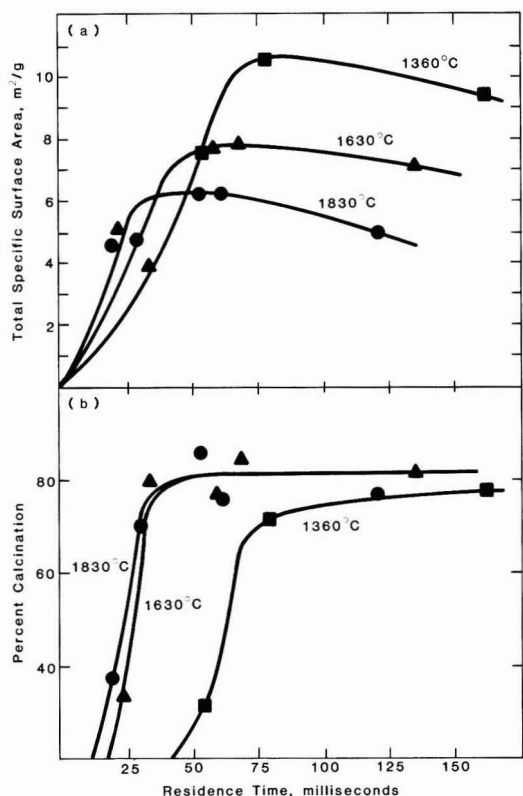


**Figure 5.** Surface area and mole percent calcination profiles for Vicron 45-3 sampled from three methane flames.

considered an explanation. Samples collected from hydrogen/air flames at similar temperatures attained as much as 95% calcination in 150 ms. However, no significant changes in sample surface areas were observed (1).

The inability to achieve 100% calcination has a twofold explanation. For all of these flames, the temperature dropped to 1200 °C by 200 ms. A model of the calcination kinetics (1) predicts that this rapid decline in flame temperature quenches the calcination reaction. In addition, internal diffusion resistance slows calcination after about

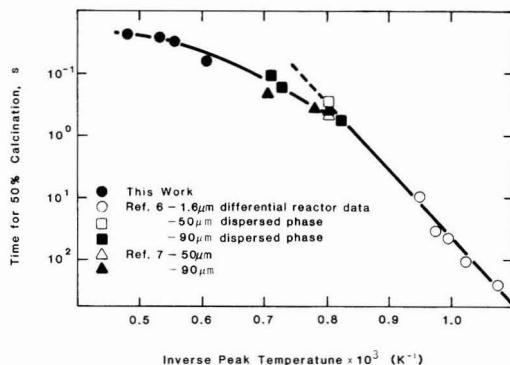


**Figure 6.** Time for 50% calcination of pulverized limestones.

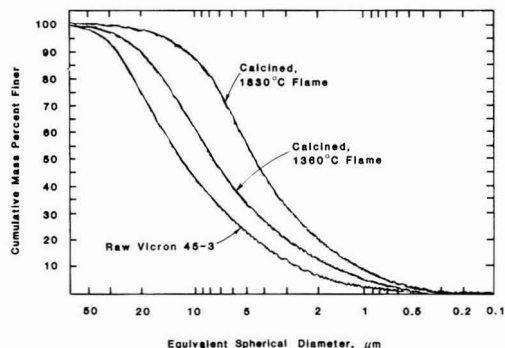


**Figure 7.** X-ray sedimentation (sedigraph) particle-size distributions of raw and calcined Vicron 45-3.

80% conversion to CaO is reached (18).

Three major observations stem from the surface area data. First, the surface areas (5–10 m<sup>2</sup>/g) are low relative to those reported for similar stones calcined at cooler temperatures (1000–1200 °C) (10). Second, surface area develops more rapidly in the higher temperature flames. Third, the ultimate surface area attained is highest after lower temperature calcination.

Calcination rate increases with increasing temperature in Figure 5. These data are compared in Figure 6 with lower temperature calcination rate data from other studies (9, 10) on an Arrhenius-type plot of time for 50% calcination vs. inverse temperature. At the higher temperatures, however, a significant portion of the calcination occurs during particle heat-up and, therefore, at lower-than-peak temperature. Nonetheless, calcination is shown to be (1) fast at the high temperatures of practical interest and (2) not an impediment to the sulfur-capture process. Only at temperatures below those typical of radiant zone exhausts (1150–1350 °C) are the times to calcine significant in comparison to the available residence time for sulfation (2–3 s). These observations demonstrate a trade off between faster calcination at higher temperatures and higher surface areas (reactivity) at lower temperatures.

Surface area increases as a result of an increase in porosity during calcination. However, thermal comminution also can contribute to specific surface area increase. Fracturing of limestones has been observed and attributed to thermal stresses and internal pressure buildup due to CO<sub>2</sub> release (10, 11). To assess the contribution of thermal comminution to surface area increase, samples of Vicron 45-3 were collected raw and from two methane-air flames (1830 and 1360 °C) at relatively long times (>250 ms). The

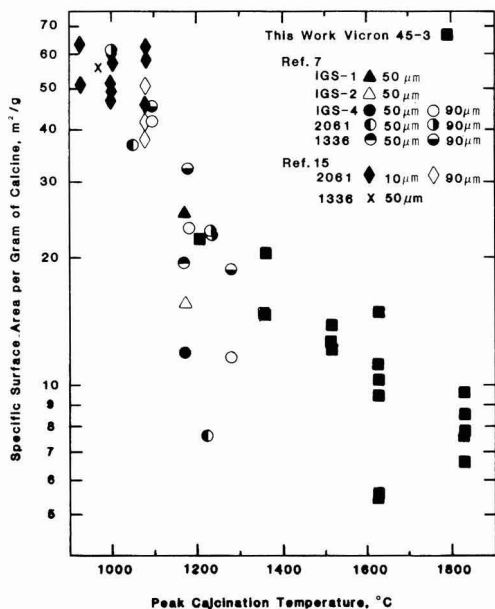


Figure 8. Effect of calcination temperatures on surface area development by calcitic limestones.

samples were analyzed for particle size by X-ray sedimentation. The results are shown in Figure 7. In both flames comminution occurred and, to a greater extent, in the higher temperature flame where nearly a factor of 3 reduction in mean diameter occurred. Numerical integration of the size distributions, however, gives specific surface areas of 0.54, 0.65, and 0.91 m<sup>2</sup>/g compared, respectively, with the measured BET surface areas of 0.6, 7.0, and 6.5 m<sup>2</sup>/g. Most of the surface area therefore is not external but resides in the interior pore structure of the particles.

In Figure 8, surface area data from other studies employing limestones similar to Vicron 45-3 are shown along with results from this study at five peak flame temperatures. (Data available from ref 15 at temperatures lower than those shown in Figure 8,  $T < 900$  °C, indicate little change in initial surface area with temperature.) Surface area development at low-temperature (nonflame) conditions occurs in concert with porosity development during calcination. As temperatures are increased, the rate of sintering increases as evidenced by coalescence of pores and some loss of surface area but with no apparent decrease in porosity (11). Above 1100 °C, the Tammann temperature for CaO, an abrupt decline in peak surface area is indicated by Figure 8. The increased variance in the data may reflect differences in sorbent types and calcination conditions. At 1100 °C, the sintering rate has become important with respect to the calcination rate, resulting in rapid growth of CaO crystallites (11). Particle shrinkage resulting from collapse of the pore structure has also been reported at these temperatures (11, 17). Although there is variance, a trend of decreasing surface area with increasing temperature is unmistakable over an order of magnitude in surface area. Similar behavior has also been observed at lower temperatures ( $T < 1100$  °C) but only over periods of several hours (19).

In summary, sorbent activation due to calcination is fast (<100 ms) at temperatures (>1100 °C) representative of boiler radiant zones and results from increased porosity

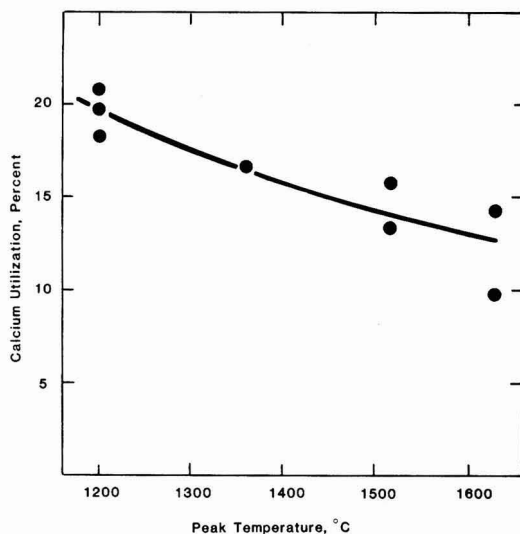


Figure 9. SO<sub>2</sub> capture by Vicron 45-3 in the SO<sub>2</sub> reactivity probe. 0.6 s, 6% SO<sub>2</sub>.

as CO<sub>2</sub> is expelled from the particles. Pore size and crystallite size, though not measured in the present experiment, are reflected in the specific surface area of the sorbent which, in turn, is a function of time and the calcination temperature. Sorbent fragmentation can also occur but is not sufficient to affect surface area development.

**SO<sub>2</sub> Capture.** By use of the SO<sub>2</sub> reactivity probe, Vicron 45-3 samples were collected from the four flames having peak temperatures of 1200, 1360, 1515, and 1630 °C. The probe entrance was situated 9 cm from the burner surface. Although residence time in the flame varied with the flame condition, the sampling location was coincident with the maxima in the surface area profiles and just beyond the point of maximum sorbent particle temperature. Results of these tests are shown in Figure 9 as calcium utilization (S/Ca × 100) vs. peak calcination temperature.

Sulfur capture improved as the calcination temperature decreased. In addition, comparison of average calcium utilization values at 1360 and 1630 °C (16.6 and 12.0 percent) with peak surface areas from Figure 5 (10.7 and 7.9 m<sup>2</sup>/s) shows a relationship between specific surface areas and SO<sub>2</sub> sorption ability. As such, surface area may be useful as an indirect measure of the sorbent reactivity.

**Additional Sorbents.** Three additional sorbents (Table I) were tested to (1) determine their SO<sub>2</sub> sorption capabilities relative to Vicron 45-3 and (2) seek a general correlation between specific surface area and sulfur capture. Samples of dolomite, calcium hydroxide, Michigan marl, and Vicron 45-3 were collected at different residence times from the 1515 °C peak temperature flame and analyzed to determine specific surface area and percent calcination. (Calcination data for calcium hydroxide were omitted because even small levels of H<sub>2</sub>O uptake during sampling and handling caused large errors in the calcination determination. Because of its low decomposition temperature relative to calcite, 580 vs. 950 °C, and because of its lower endothermicity of calcination, 65 vs. 178 kJ/mol, the calcium hydroxide was assumed to have been at or near complete calcination at all times prior to sampling.) Results are presented in Table IV and Figure 10.

Trends in calcination and surface area development were different for the additional sorbents when compared with

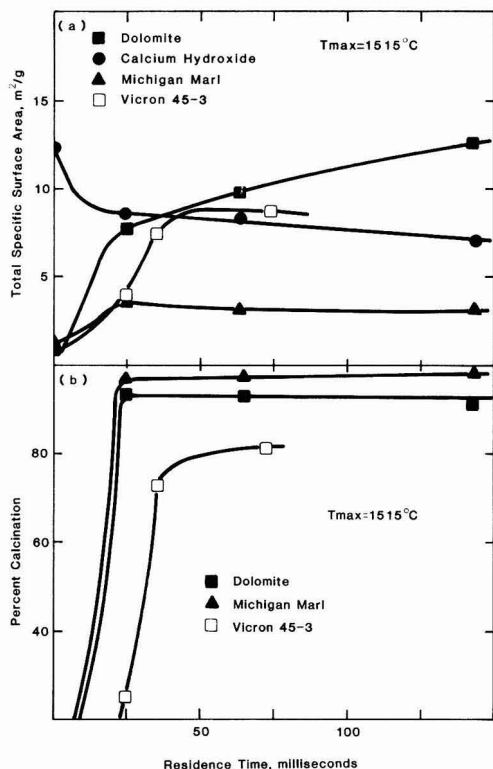


**Figure 10.** Calcination and surface area profiles for dolomite, Vicron 45-3, Michigan marl, and calcium hydroxide in a 1515 °C peak temperature flame.

**Table IV. Surface Area and Percent Calcination of Sorbents Calcined in a CH<sub>4</sub>-Air Flame-Peak Temperature 1515 °C**

sorbent	residence time, ms	total specific surface area, m <sup>2</sup> /g	% calcination <sup>a</sup>
Vicron 45-3	24	3.9	24
	36	7.5	72
	73	8.6	82
Michigan marl	24	3.5	98
	63	3.1	97
	142	3.1	99
calcium hydroxide	24	8.5	
	63	8.2	
	142	7.2	
dolomite	24	7.7	93
	63	9.7	93
	142	12.6	92

<sup>a</sup> Calcium basis.

Vicron 45-3. The behavior of the dolomite surface area is attributed to the MgO which is more refractory than CaO and stabilizes the dolomitic lime (CaO-MgO) against sintering (17). Also, dolomite and marl calcine faster and, in general, display higher extents of calcination than the other sorbents. For dolomite, the reason is that the MgCO<sub>3</sub> component decomposes at a much lower temperature than CaCO<sub>3</sub>. For marl, it is believed that the rapid calcination may be due to combustion of the organic component contained in the stone. The organic component is essentially a coal matrix which upon combustion could overheat the particles. Upon injection, the marl visually appeared

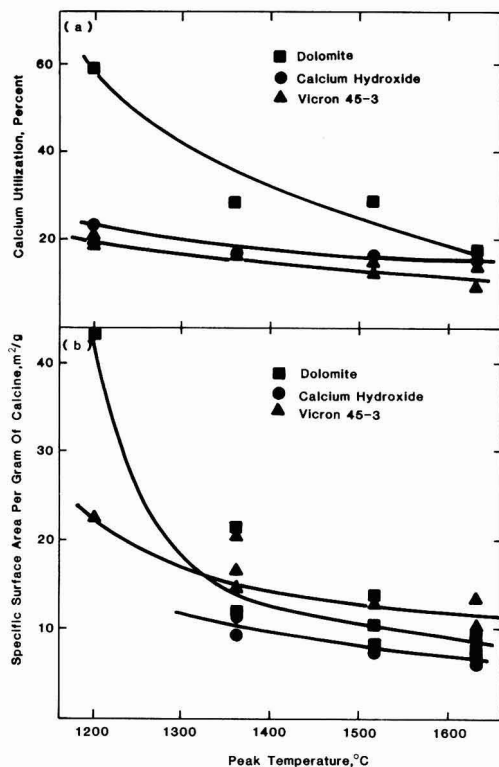


**Figure 11.** Change in surface area and calcium utilization with temperature for dolomite, calcium hydroxide, and Vicron 45-3.

to burn in a fashion similar to pulverized coal.

Calcium hydroxide has a relatively high initial surface area which decreased during calcination under all of the conditions tested. Calcination of Ca(OH)<sub>2</sub> produces a metastable hexagonal oxide structure (20), and decomposition to the stable cubic oxide at high temperatures may account for the decay of surface area. In addition, there is some indication that water vapor catalyzes sintering of CaO (20, 21) so the internal supply of water vapor may promote surface area decay during high-temperature calcination.

In terms of specific surface area, the dolomite displayed the greatest potential for SO<sub>2</sub> capture in the 1515 °C flame. Calcium hydroxide proved to be comparable to Vicron 45-3, although changes in sulfur capture due to its loss, rather than gain, of specific surface area upon calcination have not been taken into account. The Michigan marl produced very low-specific surface areas in spite of its ability to completely calcine very rapidly. Because of its poor surface area development, further tests on the marl were not completed.

Limited additional surface area measurements were performed on dolomite, Vicron 45-3, and calcium hydroxide calcined in the 1200, 1360, and 1630 °C flames in order to provide data for comparison with the SO<sub>2</sub>-capture tests also conducted in these flames. Both the surface area and sulfur-capture data are shown in Figure 11. The surface areas in Figure 11 are normalized to account for the degree of calcination. This simplifies the comparison with the sulfur-capture data, especially for the 1200 °C flame condition where the extents of calcination were generally low (less than 80%). The trends of increasing surface area and reactivity with decreasing calcination

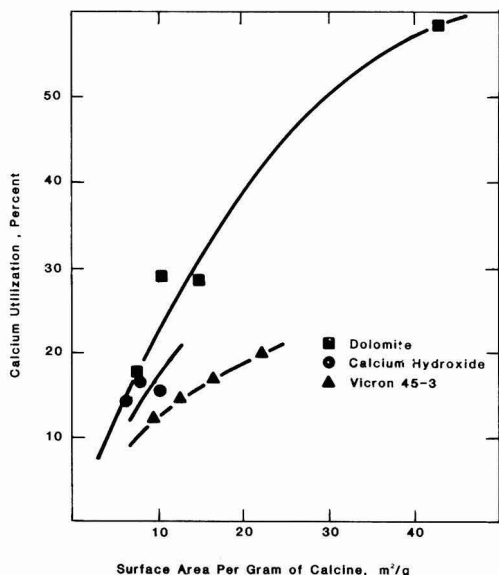


**Figure 12.** Correlation between calcium utilization and specific surface area for dolomite, calcium hydroxide, and Vicron 45-3 calcined in flames at 1200, 1360, 1515, and 1630 °C.

temperature match those observed for Vicron 45-3 in Figures 5 and 9. Dolomite, however, dramatically increased in both reactivity and surface area at 1200 °C.

The normalized surface areas of Vicron 45-3 exceeded those of the dolomite at the higher temperatures. This was due in part to the lower extents of calcination for Vicron, but the generally poor repeatability in the dolomite data also contributed to uncertainty in interpretation of the surface area-temperature curve. The calcium hydroxide surface areas, which are not normalized, fell below those of Vicron 45-3 and dolomite. Differences in surface areas were not directly reflected in the SO<sub>2</sub>-capture data. Material properties, as explained below, affect the capture efficiency. For example, Vicron 45-3, which had the highest normalized surface area at all but the 1200 °C condition, showed the lowest calcium utilization at all temperatures. Calcium hydroxide was slightly more reactive than Vicron 45-3, but the dolomite showed significantly greater calcium utilization at all except the highest temperature.

The exceptionally high reactivity of dolomite to sulfur capture is attributable to physical aspects of the mineral after calcination. The magnesium component begins to calcine first, and as the CaCO<sub>3</sub> is calcined, the MgO provides a barrier to agglomeration and growth of the CaO crystallites. This follows from the low intersolubility of the oxides (22). This, in turn inhibits sintering and keeps the pore structure open. In addition, SO<sub>2</sub> sorption by MgO does not occur at elevated temperatures (8), and so the magnesium component also serves to slow the pore plugging process which otherwise occurs during CaSO<sub>4</sub> formation. On the basis of the molar volumes of calcite (37 cm<sup>3</sup>/mol), dolomite (64.2 cm<sup>3</sup>/mol), calcium sulfate (46 cm<sup>3</sup>/mol), and periclase (11.26 cm<sup>3</sup>/mol), 100% calcium utilization is possible for dolomite compared with only 67% for Vicron 45-3.

The calcium utilization of calcium hydroxide was also disproportionate relative to its specific surface area and that of Vicron 45-3. Two plausible explanations exist. The sensitivity of the product calcine to ambient moisture

during handling and analysis may have biased the surface area measurements. Alternatively, the different crystal structure of the calcine may have resulted in an enhanced reactivity.

For all three stones, a general correlation between surface area and reactivity was observed. Figure 12 provides an indication of the surface area-activity relationship for each material. Normalized surface areas and calcium utilization data were averaged for each flame condition to provide the data in Figure 12. Because of the small change with temperature in both surface area and reactivity for calcium hydroxide the correlation is weak. The line drawn through the data merely suggests a trend. Results for the dolomite and Vicron 45-3 are clearer. Dolomite not only generates higher specific surface areas but also is more reactive for the same surface area.

### Summary

Times required for calcination of pulverized calcareous sorbents at high temperatures (>1100 °C) are short (<100 ms). Surface area development occurs in concert with calcination, and it was found that higher surface areas were attained at lower calcination temperatures. The measured surface areas were also a function of sorbent type. Thermal comminution of the sorbents did not contribute to the measured specific surface areas.

Reactivity of the calcined sorbents toward SO<sub>2</sub> was found to be related to specific surface area, although sorbent type also had a strong influence. On the basis of CaO content, dolomite was the most reactive sorbent studied followed by calcium hydroxide and Vicron 45-3. The high reactivity of dolomite was attributed to the MgO component which inhibits sintering (surface area loss) and helps keep the pore structure open.

### Conclusions

Dry sorbent injection remains a viable possibility for SO<sub>2</sub> emissions control. In the short residence times (<1.0 s) assessed in the present experiment, calcium utilization in excess of 50% was achieved with a dolomitic sorbent. The data reaffirm that sorbent reactivity decreases with increasing calcination temperature. However, they also suggest that substantial gains in reactivity may be realized by sorbent injection below 1200 °C. Future laboratory-scale flame-mode studies should investigate these lower temperatures as well as evaluate the effects of large furnace parameters such as thermal gradients and environments laden with molten fly ash particles. However, it has yet to be shown whether the idealized conditions of the laboratory reactor can be adapted to existing utility boilers.

### Acknowledgments

We are grateful to R. K. La Fond for performing the analytical work.

### Literature Cited

- (1) Cole, J. A.; Clark, W. D.; Heap, M. P.; Kramlich, J. C.; Samuelsen, G. S.; Seeker, W. R. June 1985, EPA-600/7-85-027.
- (2) Case, P. L.; Ho, L.; Clark, W. D.; Kau, E.; Pershing, D. W.; Payne, R.; Heap, M. P. Jan 1984, Final Report, EPA Contract 68-02-3921.
- (3) Silcox, G. D.; Slaughter, D. M.; Pershing, D. W. presented at the 20th International Symposium on Combustion, Ann Arbor, MI, Aug 1984.
- (4) Borgwardt, R. H. *Environ. Sci. Technol.* **1972**, *6*, 59-63.
- (5) Coutant, R. W.; Barrett, R. E.; Simon, R.; Campbell, B. E.; Lougher, E. H. Nov 1970, Final Report, NAPCA Contract PH86-67-115.

- (6) Ishihara, Y., presented at the Dry Limestone Injection Process Symposium, Gilbertsville, KY, June 1970.
- (7) Borgwardt, R. H.; Harvey, R. D. *Environ. Sci. Technol.* 1972, 6, 350-360.
- (8) Bhatia, S. K.; Perlmutter, D. D. *AIChE J.* 1981, 27, 226-234.
- (9) Borgwardt, R. H.; Gillis, G. R.; Roach, N. F., presented at the Joint EPA/EPRI Symposium on Stationary Source Combustion NO<sub>x</sub> Control, Dallas, TX, Nov 1982.
- (10) Coutant, R. W.; Simon, R.; Campbell, B.; Barrett, R. E. Oct 1971, EPA APTD-0802.
- (11) McClellan, G. H., presented at the Dry Limestone Injection Process Symposium, Gilbertsville, KY, June 1970.
- (12) Harvey, R. D. July 1971, EPA APTD-0920.
- (13) Seeker, W. R.; Samuelsen, G. S.; Heap, M. P.; Trolinger, J. D. 18th Symp. (Int.) Combust. [Proc.] 1981, 18th, 1213-1226.
- (14) Hamor, R. J.; Smith, I. W. *Fuel* 1970, 50, 394-404.
- (15) Altenkirch, R. A.; Peck, R. E.; Chen, S. L. *Powder Technol.* 1978, 20, 189-196.
- (16) Beer, J. M.; Chigier, N. A. "Combustion Aerodynamics"; Applied Science Publishers, Ltd.: London, 1972; p 18.
- (17) Boynton, R. S. "Chemistry and Technology of Limestone", 2nd ed.; Wiley: New York, 1980.
- (18) Borgwardt, R. H. *AIChE J.* 1985, 31, 103-111.
- (19) Glasson, D. R. *J. Appl. Chem.* 1967, 17, 91-96.
- (20) Beruto, D.; Barco, L.; Searcy, A. W.; Spinolo, G. *J. Am. Chem. Soc.* 1980, 63, 439-443.
- (21) Beruto, D.; Barco, L.; Belleri, G.; Searcy, A. W. *J. Am. Chem. Soc.* 1981, 64, 74-80.
- (22) Levin, E. M.; Robbins, C. R.; McMurdie, H. F. "Phase Diagrams for Ceramists"; Reser, M. K., Ed.; American Ceramic Society: Columbus, OH, 1964; p 102.

Received for review November 2, 1984. Revised manuscript received June 13, 1985. Accepted June 27, 1985. This research was supported by the U.S. Environmental Protection Agency under Contract 68-02-3633. Although the research described in this article has been funded by the Environmental Protection Agency, it has not been subjected to Agency review and therefore does not necessarily reflect the views of the Agency, and no official endorsement should be inferred.

## Interactions between Polycyclic Aromatic Hydrocarbons and Dissolved Humic Material: Binding and Dissociation

John F. McCarthy\* and Braulio D. Jimenez

Environmental Sciences Division, Oak Ridge National Laboratory, Oak Ridge, Tennessee 37831

■ Binding of polycyclic aromatic hydrocarbons (PAH's) to dissolved humic material (DHM) was examined by using equilibrium dialysis and fluorescence techniques. There was a direct relationship between the hydrophobicity of the PAH and the affinity for binding to DHM. The binding affinity  $P_b$  for benzo[a]pyrene (BaP), benzanthracene, and anthracene decreased slightly as the concentration of DHM increased. The binding of BaP to DHM was completely reversible and the extent of reversibility was unrelated to the sorption time. The rate of binding of BaP to DHM, measured by the quenching of BaP fluorescence, was very rapid and was completed within 5-10 min. The results suggest that the presence of DHM, or other sorptive components of the dissolved organic pool, may affect binding to sediment or suspended particles and thus alter the fate and transport of organic contaminants in aquatic systems.

### Introduction

The partitioning of hydrophobic organic contaminants within the environment is of fundamental importance in determining their fate and transport. A number of studies have examined the adsorption of organic contaminants to sediments or to suspended particulates and have shown that the affinity for association of a contaminant with a sediment is well correlated both with the hydrophobicity of the contaminant (expressed as the octanol-water partition coefficient,  $K_{ow}$ ) and with the organic content of the sediment (1, 2). Another potentially important, but less obvious, sorbent for organic contaminants is naturally occurring dissolved organic matter (DOM) such as dissolved humic material (DHM). DHM has been shown to form stable complexes with several trace organic contaminants (3-5). More recently, the binding of contaminants such as polycyclic aromatic hydrocarbons (PAH's), insecticides, and herbicides to DHM has been measured quantitatively (6-9). Binding of PAH's to DHM has been shown to greatly reduce the availability of the PAH's for uptake and bioaccumulation by aquatic organisms (10-13).

Very little is known, however, about the interaction between contaminants and DHM or about the influence of this interaction on the binding of contaminants to particles.

In this study, the association of a series of PAH's with DHM and the reversibility of that association are examined by using equilibrium dialysis and fluorescence techniques. There is continuing discussion in the literature as to whether association of organic contaminants with sediment involves a process of adsorption or partitioning (14, 15); we attempt to avoid that controversy by referring to "binding" or "association", without suggesting any specific mechanism. We refer to the humic material used in this study as "dissolved" since it is resistant to centrifugation and passes through a 0.3- $\mu$ m filter. This is a functional definition and is not intended to address the physicochemical distinction between dissolved and colloidal material.

### Materials and Methods

Humic acid was obtained from Aldrich Chemical Co. (Milwaukee, WI). Before it was used in any experiment, the humic acid was dissolved in water, centrifuged at 10000g for 30 min, and then filtered through precombusted glass-fiber filters (type A-E, nominal retention of 0.3  $\mu$ m; Gelman Sciences, Inc., Ann Arbor, MI) to remove any particulate material. The silica content of the DHM solution was measured by atomic absorption (Perkin-Elmer Model 603 equipped with a Model 2200 graphite furnace) and by ICP (Instruments SA) to determine if substantial amounts of clay microparticles were present. The organic carbon content of the DHM stock solutions was measured with an OI carbon analyzer (OI Corp., College Station, TX). DHM concentrations are expressed as grams of organic carbon per liter. Water used in these experiments either was dechlorinated tap water that was passed through a bed of activated charcoal to remove any DOM or was deionized distilled water free of DOM; both types of water were filtered through precombusted Gelman type A-E glass-fiber filters to remove particulates.



Radiolabeled ( $^{14}\text{C}$ ) PAH's [naphthalene (NPH), anthracene (ANTH), benzantracene (BA), 3-methylcholanthrene (MC), and benzo[a]pyrene (BaP)] were obtained from Pathfinder Laboratories, Inc. (St. Louis, MO) and California Bionuclear (Sun Valley, CA). [ $^{14}\text{C}$ ]PAH's were repurified by high-performance liquid chromatography (10) before their use in experiments since the presence of radiolabeled polar impurities can produce underestimates of the association coefficient. Nonradioactive PAH's were obtained from Aldrich (gold label) or from Mallinckrodt Chemical Co. Radioactive and nonradioactive PAH's were dissolved in a carrier (acetone, methanol, or dioxane), and a small volume of the carrier stock solution ( $<0.1\text{ mL/L}$ ) was added to water and stirred overnight to achieve the desired aqueous concentration and specific activity. All experiments were conducted under gold fluorescent lights ( $>500\text{ nm}$ ) to minimize photodegradation of the PAH's.

Dialysis tubing (Spectra/Por 6; molecular weight cutoff of 1000) was washed in distilled water,  $1\text{ M Na}_2\text{CO}_3$ ,  $1\text{ M NaHCO}_3$ , and distilled water to remove the sodium benzoate preservative. Some of the tubing was packed in sodium azide; this tubing was washed in distilled water. Equilibrium dialysis experiments to measure the binding of PAH's to DHM were performed by placing 4 or 8 mL of a DHM solution in dialysis tubing and clamping the ends of the tubing with dialysis tubing clamps (Fisher Scientific). The dialysis bag was then placed in a 100-mL glass jar containing an aqueous solution of a PAH (80 mL). Sodium azide (0.02%) was added to prevent bacterial transformation of the PAH. The jar was sealed with a Teflon-lined cap and shaken in the dark at  $23^\circ\text{C}$  for at least 4 days unless otherwise noted. Control experiments demonstrated that equilibration was complete within 24–48 h. A sample of the solutions inside and outside the dialysis bag was analyzed for  $^{14}\text{C}$  radioactivity by using ACS scintillation cocktail (Amersham) and a CD460 liquid scintillation counter (Packard). Data are expressed as moles of PAH on the basis of the specific activity of the PAH stock solutions. The radioactivity outside the dialysis tubing represents the PAH that is dissolved in the water (free), and the radioactivity inside the tubing represents the sum of dissolved PAH and PAH bound to the DHM. The concentration of PAH bound to DHM (mol of PAH/g of C) was calculated by subtracting the PAH concentrations inside and outside the dialysis bag (mol of PAH/mL) and dividing by the concentration of DHM within the bag (g of C/mL).

The dissociation of PAH from DHM was also measured by equilibrium dialysis. After equilibration of the PAH and DHM as described above, the dialysis bag was rinsed in distilled water and transferred to a jar containing 80 mL of uncontaminated water with sodium azide. The jar was covered and shaken in the dark at  $23^\circ\text{C}$  for at least 4 days unless otherwise noted (dissociation equilibrium was completed within 24–48 h).

The time course of binding of PAH to DHM was analyzed by measuring the quenching of the fluorescence of BaP on a SPF-500 spectrofluorometer (American Instrument Co., Silver Spring, MD). BaP was excited at 380 nm, and emission was measured at 405 nm. A small volume of DHM solution (10–100  $\mu\text{L}$ ) was added to a cuvette containing a solution of BaP and rapidly mixed. Fluorescence data were corrected for the contribution of DHM fluorescence to the observed fluorescence and for the inner filter effect resulting from the absorption of excitation and emission light by the DHM (16, 17). Both of these corrections were minimal since relatively low

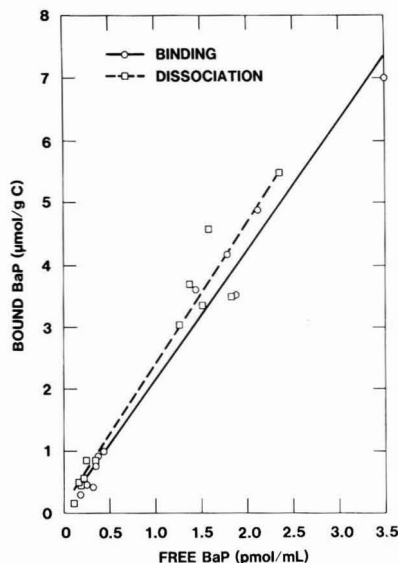


**Figure 1.** Isotherms describing the association (circles and solid line) and dissociation (squares and dashed line) of BaP and DHM (2.5 mg of C/L). Association continued for 7 days, and dissociation lasted 4 days. The slopes, ( $P_a = 1.8 \times 10^6$ ,  $r^2 = 0.97$ ;  $P_d = 2.16 \times 10^6$ ,  $r^2 = 0.98$ ) were not significantly different ( $p > 0.05$ ).

concentrations of DHM were used in these experiments.

The quenching of BaP fluorescence is quantified as the ratio of  $F_0/F$ , where  $F_0$  is the fluorescence of BaP when no DHM is present and  $F$  is the observed fluorescence when DHM is present. Quenching results in a decrease in the value of  $F$  relative to  $F_0$  and is measured as an increase in the ratio  $F_0/F$ .

Results were analyzed by linear regression and analysis of variance using SAS (Statistical Analysis System, Carey, NC).

### Results and Discussion

**Binding Affinities of PAH's.** Organic carbon constituted 50.2% of the DHM used in these experiments, and the silica content of the DHM was 2.6 mg of Si/g of C. The association of PAH's to DHM was measured by equilibrium dialysis. Isotherms were linear up to the solubility limit of the PAH. A typical association curve is illustrated in Figure 1. The association coefficient,  $P_a$ , is calculated as the ratio of the concentration of free vs. DHM-bound PAH after equilibration or as the slope of the association curve estimated by a linear least-squares fitting procedure. It should be noted that sorption onto the glassware and onto the dialysis membrane does not affect the results of the equilibrium dialysis experiments. When the system is at equilibrium, the free and DHM-bound PAH's are in equilibrium with each other and with PAH bound to the glass or to the membrane. Binding to the glass and membrane decreases the total amount of PAH in solution (free or bound to DHM) but does not affect the final equilibrium between these components of interest (6).

The possibility that a low molecular weight component of the DHM passed through the dialysis bag and bound PAH outside the bag was considered. The DHM solution was predialyzed for 4 days against several changes of distilled water before the bag was transferred to a jar with radiolabeled PAH. It is assumed that any portion of the DHM that could pass through the bag would have been removed by the predialysis step. There was no significant

**Table I. Effect of Association Time on Reversibility of Binding of BaP to DHM (2.5 mg of C/L)<sup>a</sup>**

association time, days	dissociation time, days	$P_a \times 10^6$	$P_d \times 10^6$	$(P_a - P_d) \times 10^6$
2	2	$2.02 \pm 0.30$ (4)	$2.59 \pm 0.55$ (4)	-0.24
7	2	$1.95 \pm 0.12$ (4)	$2.36 \pm 1.20$ (4)	-0.41
7	4	$1.94 \pm 0.36$ (12)	$2.22 \pm 0.59$ (12)	-0.45
		$2.03 \pm 0.43^b$	$2.42 \pm 0.66^b$	$-0.41 \pm 0.69^b$

<sup>a</sup> $P_a$  and  $P_d$  are calculated from the ratio of bound and free BaP after association or dissociation equilibration, respectively, and are expressed as the mean  $\pm$  standard deviation. The number of replicates is indicated in parentheses. See text for results of statistical analyses. <sup>b</sup>Mean  $\pm$  SD.

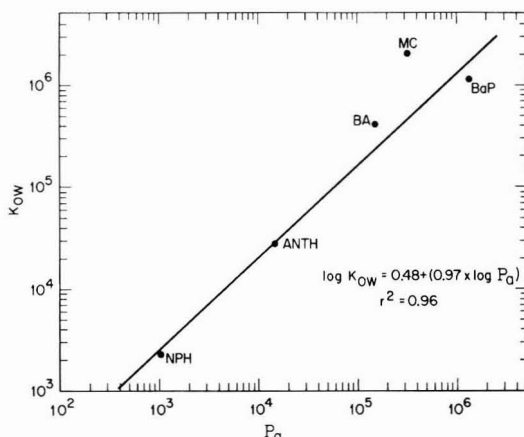


**Figure 2.** Relationship between the  $K_{ow}$  of the PAH's and their affinity for binding to DHM, expressed as the association coefficient,  $P_a$ .

difference ( $p > 0.1$ ) between the results of association experiments with or without predialysis of DHM.

The affinity for binding to the DHM was related to the hydrophobicity of the PAH, expressed as the  $K_{ow}$  (Figure 2). In fact, the  $P_a$  is approximately equal to the  $K_{ow}$ . The  $P_a$ 's for binding of BaP, BA, and ANTH to DHM reported here agree within a factor of 2 of those measured by a reverse-phase technique using the same DHM from Aldrich (8). These  $P_a$ 's are approximately an order of magnitude lower than those reported for the binding of NPH and ANTH to natural marine colloids, which was measured by using a hollow fiber technique (9). This discrepancy may reflect variability in the binding affinities of different sources of DOM.

The  $P_a$ 's for the binding of PAH's to Aldrich DHM agree well with the partition coefficients describing the binding of the PAH's to sediment, when those coefficients are corrected for the organic content of the sediment [i.e., expressed as the  $K_{oc}$  or  $K_{om}$  (1, 2)]. This result is consistent with the hypothesis that the binding of nonionic organic contaminants such as PAH to the sediment is controlled primarily by interaction of the contaminant with the organic coating on the sediment particle. Because most sediments have a low organic carbon content relative to DHM (100% organic matter when expressed on a gram of C per liter basis), DHM can have a much higher capacity for binding PAH's in the water column than will the same mass of suspended sediment particles. For example, equivalent amounts of PAH would be bound by a solution containing 10 mg of C/L of DHM, or 200 mg/L suspended sediment particles with an organic content of 5%.

**Reversibility of Binding.** The dissociation of BaP bound to DHM was examined quantitatively by using equilibrium dialysis. The equilibrium dialysis method would be invalid for measuring dissociation of the BaP-

DHM complex if substantial amounts of BaP bound to the dialysis membrane were released into the water during the dissociation equilibration or if substantial amounts of freed BaP were removed from the system due to sorption to the glassware. Although there was undoubtedly reequilibration among all these components, there was no net change in the mass of BaP associated with the equilibration between the free BaP and the BaP bound to DHM. The total mass of BaP transferred when the dialysis bag was introduced into uncontaminated water at the beginning of the dissociation (free and DHM-bound BaP, exclusive of any radiolabeled material associated with the dialysis membrane) was within 98% (+7%,  $n = 13$ ) of the total mass of free and DHM-bound BaP in the dialysis system after dissociation equilibrium (exclusive of any radiolabeled material associated with the dialysis membrane or glassware).

A partition coefficient for dissociation,  $P_d$ , is defined as the ratio of the concentration of PAH bound to the DHM vs. that dissolved in the water at dissociation equilibrium or as the slope of the dissociation isotherm (Figure 1). The binding of BaP to DHM is fully reversible, since the slopes of the association and dissociation curves ( $P_a$  and  $P_d$ , respectively) were not significantly different ( $p > 0.05$ ).

The length of time that BaP and DHM associated did not affect the reversibility of the binding (Table I).  $P_a$  was not affected by the association time ( $p > 0.20$ ), and  $P_d$  was not affected by either the association or dissociation times ( $p > 0.66$  or  $0.92$ , respectively). Evaluation of the differences between  $P_a$  and  $P_d$  ( $P_a - P_d$  reflects the reversibility of binding under the different combinations of time) showed that there was no significant effect due to association or dissociation time ( $p > 0.85$ ). However, analysis of  $P_a - P_d$  did reveal that there was a tendency for  $P_d$  to be greater than  $P_a$  at all combinations of time ( $0.02 < p < 0.05$ ). On the basis of the lack of significant differences in the slopes of the isotherms in Figure 1 and the marginal differences between  $P_a$  and  $P_d$  in Table I, it seems reasonable to conclude that the binding of BaP to DHM is fully reversible.

**Effect of DHM Concentration on Binding Affinity.** The effect of the DHM concentration on the binding affinity,  $P_a$ , was examined for a series of PAH's (Figure 3).  $P_a$  decreased slightly at increasing concentrations of DHM for BaP, BA, and ANTH. The  $P_a$  for NPH increased, but at DHM concentrations that were much higher than those used with the other PAH's. Although the change in  $P_a$  at increasing concentrations of DHM is statistically significant ( $p > 0.1$ ) for the four PAH's, the magnitude of the change is quantitatively small;  $P_a$  did not change by more than a factor of 2 over the range of DHM concentrations examined. Similar results have been reported for BaP and ANTH (8).

**Time Course of Binding.** The time course of the quenching of BaP fluorescence due to the addition of DHM is shown in Figure 4. The quenching of fluorescence by DHM followed the classic Stern-Volmer relationship with the ratio  $F_0/F$  being linearly related related to the

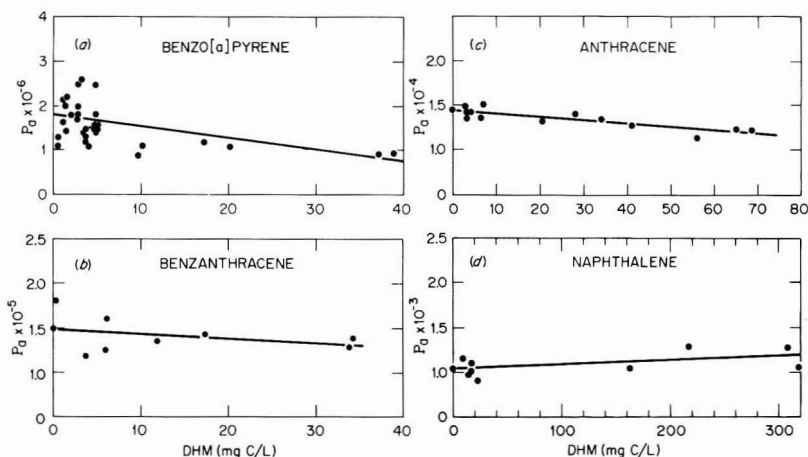


Figure 3. Effect of DHM concentration on the  $P_a$  for four PAH's. Note the different scales for DHM concentration.

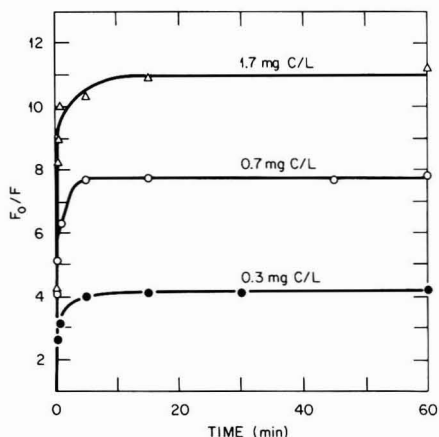


Figure 4. Time course of quenching of BaP fluorescence following the addition of DHM at time zero. DHM concentrations are indicated.  $F_0/F$  is the ratio of fluorescence in the absence of DHM to that in the presence of DHM.

concentration of quencher (DHM). Since the quantum yield of the BaP-DHM complex is not known, no attempt was made to directly quantify the extent of binding by fluorescence measurements.

The association of BaP with DHM was very rapid. Quenching is complete within 5-10 min after the addition of DHM (Figure 4).

Karickhoff (18) has proposed that there are two kinetically distinct components associated with the binding of contaminants to sediment, a "fast" and a "slow". The latter component is postulated to reflect migration of the contaminant to less accessible sites within the sediment matrix. The data in Figure 4 suggest that binding of BaP to DHM exhibits only a fast kinetic component (or, arguably, a very fast and fast component). The apparent speed with which BaP binds to DHM would be consistent with the smaller molecular distances involved in migrating into the interior of a DHM molecule, rather than to a sediment particle. The possibility that further binding to DHM may occur over long periods of time cannot be excluded on the basis of these short-term fluorescence data. However, dissociation of BaP from DHM is equally reversible regardless of the association time (Table I). This behavior

contrasts with that for desorption of contaminants from sediment. In the latter system, recovery of sorbed pollutants depends on the incubation time of the pollutant in the sediment system. Longer incubation times are postulated to result in migration of an increasingly large fraction of the pollutant into the less readily desorbed slow compartment within the sediment particles (18). Comparison of the results in the two sorbent systems suggests that binding to DHM does not involve a slow component comparable to that postulated in sediment systems.

**Environmental Implications.** The results of the present study demonstrate that DHM can reversibly bind organic contaminants with an affinity comparable to that of the organic coating of sediment particles [ $K_{oc}$  (1, 2)]. Furthermore, binding to DHM appears to be more rapid than comparable binding to sediment (1, 2). It should be noted that different sources of DHM in natural waters can have different affinities for binding organic contaminants (6-9) and that the quantitative relationships developed in this study cannot be applied universally. Nevertheless, our results suggest that the presence of DHM or other sorptive components of the dissolved organic carbon pool can affect the environmental transport and fate of organic contaminants by competing with sediment or suspended particles for the binding of contaminants. Hassett and Anderson (19) have shown that binding of cholesterol and a PCB by particles from river water or treated sewage was less efficient when the aqueous phase consisted of concentrated DOM from sewage or river compared to unconcentrated samples or to distilled water. Voice et al. (20) have postulated that the decrease in binding affinity of organic contaminants with sediment at increasing solids concentrations is due to release of solute-binding material, in the form of DOM or microparticulates, to the liquid phase. Thus, it would appear that DHM (and possibly other components of DOM) have the potential to affect the partitioning of contaminants to the sediment. The presence of DHM might be expected to decrease the amount of hydrophobic contaminant that will bind to suspended particles or be sequestered in the sediment and increase the amount of contaminant that will remain stabilized within the water column. In lotic systems, contaminants could be transported much further downstream from their source since settling of particles will have less effect in limiting their transport. The increased amount of contaminant in the water column (nonparticulate) could be a source of biological concern since, in

general, contaminant bound to sediment or particles is much less available for uptake by aquatic organisms than is contaminant dissolved in the water (10, 21, 22). Such concerns appear to be unnecessary, however, since contaminants bound to DHM are largely unavailable for uptake by aquatic organisms (10-13).

Our studies on the interactions of DOM with organic contaminants have demonstrated that DOM is an important factor to be considered to understand processes controlling the transport, fate, and biological effect of hydrophobic contaminants in aquatic systems.

#### Acknowledgments

We thank D. K. Whitmore and M. C. Black for technical assistance, J. J. Beauchamp for help with the statistical analyses, and G. R. Southworth for valuable discussions and suggestions.

Registry No. NPH, 91-20-3; ANTH, 120-12-7; BA, 56-55-3; MC, 56-49-5; BaP, 50-32-8.

#### Literature Cited

- (1) Karickhoff, S. W.; Brown, D. S.; Scott, T. A. *Water Res.* 1979, 13, 241-248.
- (2) Means, J. C.; Wood, S. G.; Hassett, J. J.; Banwart, W. L. *Environ. Sci. Technol.* 1980, 14, 1524-1528.
- (3) Warshaw, R. L.; Burcar, P. J.; Goldberg, M. C. *Environ. Sci. Technol.* 1969, 3, 271-273.
- (4) Boehm, P. D.; Quinn, J. G. *Geochim. Cosmochim. Acta* 1973, 37, 2459-2477.
- (5) Poirrier, N. A.; Bordelot, B. R.; Laseter, J. L. *Environ. Sci. Technol.* 1972, 6, 1033-1035.
- (6) Carter, C. W.; Suffett, I. H. *Environ. Sci. Technol.* 1982, 16, 735-740.
- (7) Means, J. C.; Wijayarathne, R. *Science (Washington, D.C.)* 1982, 215, 968-970.
- (8) Landrum, P. F.; Nihart, S. R.; Eadie, B. J.; Gardner, W. S. *Environ. Sci. Technol.* 1984, 18, 187-192.
- (9) Wijayarathne, R.; Means, J. C. *Mar. Environ. Res.* 1984, 11, 77-89.
- (10) McCarthy, J. F. *Arch. Environ. Contam. Toxicol.* 1983, 12, 559-568.
- (11) Levesee, G. J.; Landrum, P. F.; Giesy, J. P.; Fannin, T. *Can. J. Fish. Aquat. Sci.* 1983, 40 (Suppl. 2), 63-69.
- (12) McCarthy, J. F.; Jimenez, B. D. *Environ. Toxicol. Chem.* 1985, 4, 511-521.
- (13) McCarthy, J. F.; Jimenez, B. D. *Aquat. Toxicol.*, in press.
- (14) Chiou, C. T.; Porter, P. E.; Schmedding, D. W. *Environ. Sci. Technol.* 1983, 17, 227-31.
- (15) Mingelgrin, U.; Gerstl, Z. J. *Environ. Qual.* 1983, 12, 1-11.
- (16) Parker, C. A. "Photoluminescence of Solutions"; Elsevier: New York, 1968; pp 220-232.
- (17) Lloyd, J. B. "Standards in Fluorescence"; Miller, J. N., Ed.; Chapman Hall: New York, 1981; pp 33-35.
- (18) Karickhoff, S. W. "Contaminants and Sediments"; Baker, P. A., Ed.; Ann Arbor Science: Ann Arbor, 1980; Vol. 2, pp 193-205.
- (19) Hassett, J. P.; Anderson, M. A. *Water Res.* 1982, 16, 681-686.
- (20) Voice, T. C.; Rice, C. P.; Weber, W. J. *Environ. Sci. Technol.* 1983, 17, 513-518.
- (21) Landrum, P. F.; Scavia, D. *Can. J. Fish. Aquat. Sci.* 1983, 40, 298-305.
- (22) Muir, D. C. G.; Townsend, B. E.; Lockhart, W. L. *Environ. Sci. Technol.* 1983, 2, 269-281.

Received for review November 5, 1984. Accepted June 10, 1985. This research was sponsored by the Office of Health and Environmental Research, Ecological Research Division, U.S. Department of Energy, under Contract DE-AC05-84OR21400 with Martin Marietta Energy Systems, Inc. Publication No. 2534, Environmental Sciences Division, Oak Ridge National Laboratory.

## Seasonal Variations in Weathering and Toxicity of Crude Oil on Seawater under Arctic Conditions

Leiv K. Sydes,\* Tor H. Hemmingsen, Solvi Skare, and Sissel H. Hansen

Department of Chemistry, University of Tromsø, N-9001 Tromsø, Norway

Inger-Britt Falk-Petersen and Sunniva Lønning†

Institute of Biology and Geology, University of Tromsø, N-9001 Tromsø, Norway

Kjetill Østgaard

Institute of Marine Biochemistry, University of Trondheim, N-7034 Trondheim NTH, Norway

■ The present study shows that oil in Arctic marine environment is modified by several processes. From October to February the oil composition is mainly affected by evaporation. During the rest of the year the composition is considerably influenced by photooxidation and subsequent dissolution of polar oxidation products in the water phase. These products are toxic and may represent a hazard to marine organisms in the Arctic spring and summer.

#### Introduction

Oil discharged into the marine environment is affected by a number of processes that change its chemical and

physical characteristics (1-9). One of the processes is photochemical oxidation, which is capable of transforming a variety of oil components into oxygenated derivatives (5, 10-13). Many of these products are fairly water soluble and show significant toxicity to algae (14, 15), bacteria (16, 17), marine invertebrates, and fish (18, 19).

Most of the studies performed to assess the importance of photochemical weathering of oil have been carried out under laboratory conditions with various light sources (2, 10, 11, 20-26). Although some experiments have been performed with simulated sunlight, it is of importance that the conditions prevailing in nature are studied directly. This is particularly the case in the Arctic area where the influx of solar radiation shows great seasonal changes in total energy as well as wavelength distribution. The purpose of this study was to observe how the natural

\*Deceased July 12, 1985.

**Table I. Conditions during the Weathering Experiment at 69°30'N with Each Experiment Lasting 14 Days (336 h)**

date	ambient temp, °C		water temp, °C	sunshine, h	global radiation, J/cm <sup>2</sup>
	range	average			
1983					
Feb 14-28	-8.9/2.8	-2.1	4	5.41	1.222
March 12-26	-4.8/3.3	-1.5	4	54.41	13.005
April 11-25	-2.5/5.9	2.9	4	69.08	15.406
May 10-24	5.9/9.6	8.2	6-9	84.25	21.457
June 7-21	3.3/12.8	8.3	4-11	62.37	17.987
July 6-20	7.5/13.4	10.2	7.5-12	14.30	13.066
Aug 15-29	3.8/12.0	7.9	4-11	10.75	8.395
Sept 12-26	1.5/11.1	7.8	4-10	35.70	7.059
Oct 10-24	0.4/6.6	3.3	4	28.32	2.415
Nov 7-21	-7.1/2.3	-2.5	4	2.97	122
Dec 5-19	-7.8/0.6	-4.4	4	0	0
1984					
Jan 2-16	-10.4/0.9	-4.1	4	0	0

variation in solar energy influx in an Arctic area (69°30'N) would influence the formation of photoproducts with respect to oxygen content, water solubility, and toxicity. Experiments, lasting for 14 days, were carried out each month from Feb 1983 to Jan 1984.

#### Experimental Section

Ekofisk crude oil, containing 85.9% C, 13.3% H, 0.6% O, and 0.15% S, was used in all experiments.

**Weathering Experiments.** The experiments were carried out on the roof of the chemistry building at the University of Tromsø, Tromsø, Norway, which is situated at 69°30'N.

A glass tank (35 cm × 22 cm × 26 cm), located on a magnetic stirrer in an open, wooden box, was filled with 5.00 L of filtered seawater taken from a depth of 20 m in a practically unpolluted area. The water surface was at the level of the edge of the box. The tank was equipped with a magnetic stirring bar and a thermostat system which ensured that the water temperature did not drop below 4 °C during the winter experiments (Table I). The water surface was then completely covered with 16.0 g of a 3:1 mixture of crude oil and hexane, and the tank was kept under a black cover until all the solvent had evaporated (24 h). A thin film of oil was left behind. Gentle stirring was then started; i.e., no deformation of the oil-water interface was observed. The wooden box was covered with a thin sheet of transparent polyethylene in such a way that the experimental setup was protected from rain and snow whereas air could pass easily. The setup then remained under natural light conditions for 2 weeks (336 h).

An identical sample of crude oil on gently stirred seawater kept in the dark at 6 °C for 14 days served as reference.

The weathering experiments with artificial light were carried out essentially as the outdoor experiments except that the tank was placed in a cooling bath and that an Osram dysprosium lamp, placed 70 cm above the oil sur-

face, was used as the light source. The effect of the lamp (HQI-T 400 W/DH) was 400 W, and its spectral distribution was similar to the solar spectrum. Experiments were carried out with a water temperature of 5, 15, and 23 °C.

The dissolved material was isolated as described below.

**Analysis.** The weathered mixture of oil and seawater was analyzed as follows.

The aqueous phase was removed through a siphon, and a fraction of the solution (1025 mL) was continuously extracted with ethyl acetate under vacuum (60 mmHg), first 4 h without pH adjustment and then 3 h after adjustment to pH 3 by using a HCl (27). The extract was dried (Na<sub>2</sub>SO<sub>4</sub>) for 48 h, filtered, and concentrated to 0.5 mL. The concentrate was diluted to 5.00 mL with dry dichloromethane, membrane filtered (0.45-μm pore size; Millipore), and analyzed by gas chromatography/mass spectrometry (GC/MS) (VG Analytical Micro Mass 7070H; Hewlett-Packard 5710A; SE-54, 0.22 mm i.d.). A part of the sample (0.50 mL) was evaporated to constant weight on a microbalance (Cahn 29 analytical electrobalance) at room temperature. The oxygen content of the residues was determined by elemental analysis (Ilse Betz, Kronach, West Germany).

IR spectra were recorded on a Shimadzu IR 420 spectrophotometer. The samples were dissolved in CCl<sub>4</sub>.

Synchronous excitation of emission spectra were obtained on a Perkin-Elmer LS-5 luminescence spectrometer (28). The instrument was operated with synchronous scan with 5-mm slits and Δλ 23 nm.

Treatment with iodide was carried out according to Herbes and Whitley (29).

The oil remaining in the tank was dissolved in dichloromethane (10 mL). Some of this solution was evaporated to constant weight, and the oxygen content was then determined. The solution was also analyzed by GC/MS before and after silylation with *N,O*-bis(trimethylsilyl)-trifluoroacetamide (BSTFA) according to Poole (30). The reference sample was analyzed in the same way.

In order to determine the influence of the extraction procedure on the oxygen analysis, various organic compounds of known composition, viz., indanone, naphthalene, 2-phenylethanol, and 1-methylphenanthrene, were dissolved in seawater and isolated as described above. Subsequent oxygen analysis gave values that were consistently 0.9-1.5% higher than the true value. On an average the discrepancy was 1.2%, and this value was used to obtain the true oxygen contents of the organic material extracted from seawater.

**Phytotoxicity Testing.** The seawater samples were tested immediately after the termination of the weathering period. Cultures of the marine diatom *Skeletonema costatum* (Grev.) cleve clone Skel-5, isolated by S. Myklestad, Institute of Marine Biochemistry, Trondheim, were grown at 14 °C and a photosynthetically active radiation (400-700 nm, spherical distribution) of approximately 70 m<sup>-2</sup> s<sup>-1</sup>. Nutrients corresponding to the f/10 medium of Guillard and Ryther (31) were added to all seawater samples prior to inoculation of the alga.

Toxicity testing of seawater samples was performed as generally described previously (15). Briefly, 1 mL of a concentrated algal suspension was inoculated to give a 100-mL closed batch culture with an initial biomass of 1 μg of C/mL (approximately (10-16) × 10<sup>4</sup> cells/mL) (see ref 32). The aqueous oil solutions were tested both undiluted (100%) and diluted to 30% of the original dose. Algal growth was followed for 3 days, with sampling at 0 h, 3 h, and 3 days. In vivo fluorescence without (FL) and



**Table II. Oxygen Content of Surface Oil and Concentration and Oxygen Content of Organic Material Dissolved in the Seawater at the End of the Weathering Experiments**

month	oxygen content, %		dissolved organic material, mg/L
	surface oil	dissolved organic material <sup>a</sup>	
1983			
Feb	1.07	<i>b</i>	2.5
March	1.52	17.3	9.7
April	1.85	19.9	15.8
May	2.95	21.8	44.1
June	2.74	18.8	27.1
July	3.14	16.2	30.3
Aug	2.23	18.7	16.1
Sept	1.84	20.8	16.8
Oct	1.26	19.8	6.7
Nov	0.93	<i>b</i>	3.8
Dec	0.64	<i>b</i>	3.8
1984			
Jan	0.67	<i>b</i>	4.2

<sup>a</sup>The experimental values have been reduced 1.2% to correct for contaminants accumulating during the workup (see Experimental Section). <sup>b</sup>The oxygen content was not determined because of the very small amount of dissolved organic material.

with addition of DCMU (FL<sub>DCMU</sub>) was recorded (33), and the ratio (FL<sub>DCMU</sub> - FL)/FL<sub>DCMU</sub> used as a measure of photosynthetic capacity (34, 35). After being stained with Evans blue (36), living and dead cells were counted in a hemocytometer.

**Toxicity Tests with Eggs.** The seawater samples obtained in January and February were tested immediately after the termination of the weathering period, and those obtained in March, April, and May were tested in May, whereas testing of the June and July samples was carried out in July.

Fertilized sea urchin eggs from *Strongylocentrotus droebachiensis* (O. F. Müller) and *S. pallidus* (G. O. Sars) were used as test organisms (19). Seawater and test solution, total volume 100 mL, and a single layer of eggs were used in each test. The experiments were performed at 5 °C and were started 2 h after fertilization (19). Each test lasted for 4 days. The embryos were studied in microscope after 4 h and 1, 2, and 4 days and the number of abnormal and dead embryos were recorded (19).

### Results and Discussion

The visible effects of the weathering processes were quite similar from month to month. After a couple of days the oil had become considerably more viscous, and this was mainly due to evaporation of volatile components according to GC/MS analysis. Approximately 1–2 days later the oil film started to break up and form separate streaks. At the end of each experiment there were no visible slicks; the remaining oil stayed along the wall of the tank. However, the oil surface had not become crusty, although it appeared to be somewhat harder in May–August than during the rest of the year. No visible material settled to the bottom of the reaction vessel, in contradiction to laboratory experiments using filtered light ( $\lambda > 270$  nm) from a medium-pressure mercury lamp (10). This can be due to the type of oil used, but it can also illustrate some of the limitations in using artificial light sources in studies of oil weathering under natural conditions.

The oxygen content of the oil changed very little during the dark period (October–January) but increased steadily from 1.07% in February to 3.14% in July (Table II). This increase is reflected in increasing carbonyl absorptions (1680–1730  $\text{cm}^{-1}$ ) in the IR spectra from February to July.

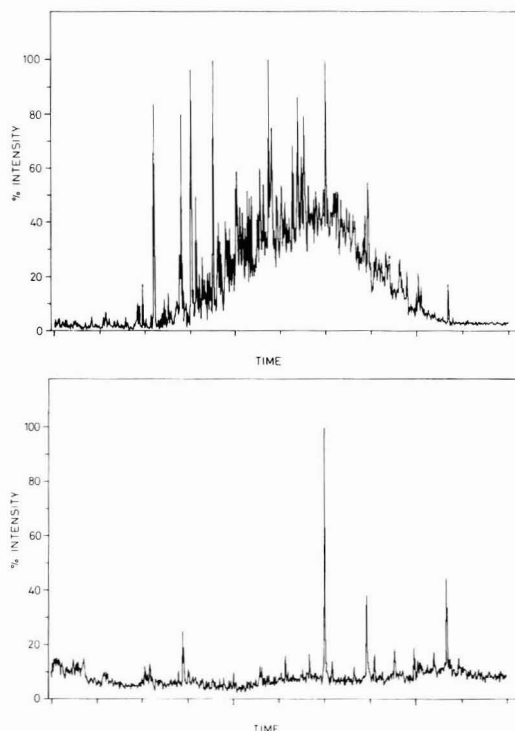


**Figure 1.** Gas chromatogram of the water-soluble fraction obtained in August (top) and November (bottom).

Isolation and analysis of water-soluble organic material showed that the amount and composition of this fraction was strongly influenced by the seasonal changes in solar radiation (Tables I and II). Whereas the aqueous phase contained less than 7 mg/L dissolved organic material from October to February, the amount exceeded 40 mg/L in May (Table II), the month with the highest influx of solar energy (Table I). The oxygen content also varied and reached a very high level, 21.8%, for the May sample (Table II). Simultaneously, the complexity of the water-soluble organic material varied as borne out by GC/MS analysis; representative chromatograms are shown in Figure 1.

The detailed structures of compounds in the water-soluble fractions are not known, but broad IR absorptions in the 1680–1730- and 2400–3500- $\text{cm}^{-1}$  regions indicated that the water-soluble material contained carboxylic acids and hydroxylated hydrocarbons. Furthermore, rapid oxidation of iodide to iodine by the same material indicates that hydroperoxides were also present (11, 29). Such structural features are compatible with the very high oxygen contents ( $>17\%$ ) of the samples. Synchronous excitation of emission spectra also indicated that the material contained aromatic compounds with two to four rings (6).

The toxicity of the seawater solutions was tested at the end of the weathering experiments. Batch cultures of *Skeletonema costatum* were tested with respect to survival and photosynthetic capacity. Figure 2 shows the concentrations of living cells in the cultures after 3 days of exposure to the seawater solutions. The control cultures had a growth rate of approximately one doubling per day; a level of 0.10–0.15 corresponds to practically zero net growth. In Figure 3 the photosynthetic capacity of the cultures exposed to the same solution is depicted. Arrows

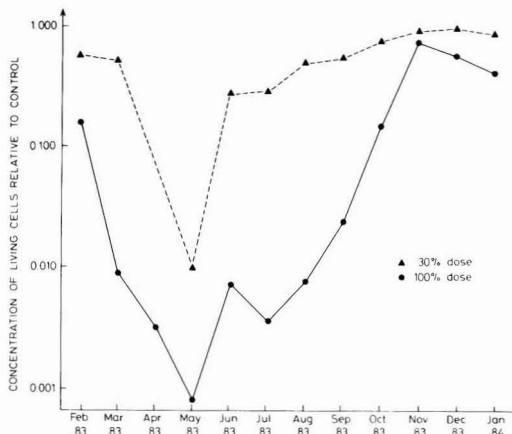


**Figure 2.** Concentration of living cells of *Skeletonema costatum*, relative to that of control cultures, after 3 days of incubation with aqueous oil solutions obtained by 14 days of weathering of oil on seawater each month from Feb 1983 to Jan 1984. No measurement was carried out with the 30% dose in April.

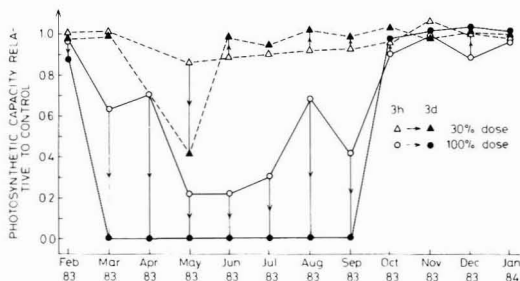


**Figure 3.** Photosynthetic capacity of cultures of *Skeletonema costatum*, relative to that of control cultures on the basis of in vivo fluorescence measurements after 3 h and 3 days of incubation. Results are shown for aqueous oil solutions prepared once a month throughout the year under natural light conditions; cf. Figure 2.

indicate the change from 3 h to 3 days of incubation. All cultures that reached a value below 80% of the control within 3 h were completely blocked after 3 days. On the other hand, cultures having a value above 85% after 3 h generally recovered within 3 days.

It should be noted that *Skeletonema costatum* is relatively sensitive to aqueous oil solutions when compared to other species (15). The recorded effect in batch cultures is very dependent on initial biomass, dose, and illumination of the oil during preparation of solutions (32). Batch culture experiments performed under standardized conditions showed a good correlation both to experiments with continuous dosage in a cage culture turbidostat (37) and in situ dialysis culture studies under field conditions (15, 38). These studies strongly support that batch culture experiments are highly relevant for effects occurring under natural conditions. The effects of changes in irradiation of the surface oil reported here in growth (Figure 2) and photosynthetic capacity (Figure 3) closely resemble those observed when solutions prepared in the laboratory under artificial illumination were studied (15, 32).

The effects on sea urchin (*Strongylocentrotus droebachiensis* and *S. pallidus*) eggs of the seawater solutions from February–July and January are shown in Figure 4. In January and February only the highest concentrations of the test medium produced abnormal embryogenesis during the experimental period. The March and April

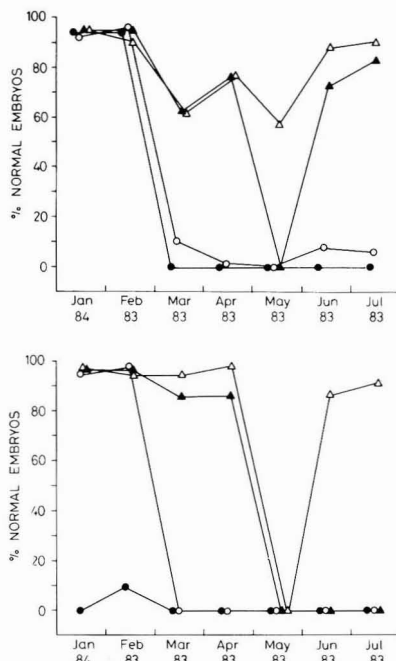


**Figure 4.** Effects on sea urchin embryos of seawater solutions obtained once a month from Feb to July 1983 and in Jan 1984 by 14 days of weathering of oil on seawater. The effect is presented as percent normal embryos after 4 h (top) and 4 days (bottom) of treatment in 100% (●), 50% (○), 25% (▲), and 12.5% (△) of seawater solutions. Control = 90–98% normal embryos.

solutions were rather toxic as effects were observed immediately for most concentrations. In samples from the solutions obtained in May, June, and July most embryos were dead after 2 days except in the lowest concentration tested. However, even in the most diluted solutions delayed cleavage rates were noted during the test period.

Sea urchin eggs have been used successfully in many toxicological studies (19, 39, 40). Eggs and larvae are generally considered to be more sensitive to environmental changes than the adult organisms. The embryology is well-known, and each female may deliver millions of transparent eggs that are easily fertilized in the laboratory to 100% and that develop normally into self-maintaining larvae in about a week. We have never detected a systematic change in sensitivity of the test organisms during the spawning season. Similarly, we have often used both sea urchin species employed in this study, but we have not found any systematic differences in sensitivity between the species.

A detailed analysis of the data compiled in Tables I and II reveals that the weathering of the oil is influenced by several factors. From October to April, a period with constant test-water temperature and a modest variation in the ambient average temperature (Table I), the amount of dissolved organic material (Table II) increased with increasing total radiation (Table I). The same observation is made when the data for June and August are compared. The oil weathering is therefore significantly influenced by the natural variation in the total radiation. The oil oxidation also seems to be affected by the temperature. This is indicated by the data for the April and July experiments; although the total amount of radiation is higher in April than in July (Table I), the total amount of dissolved or-

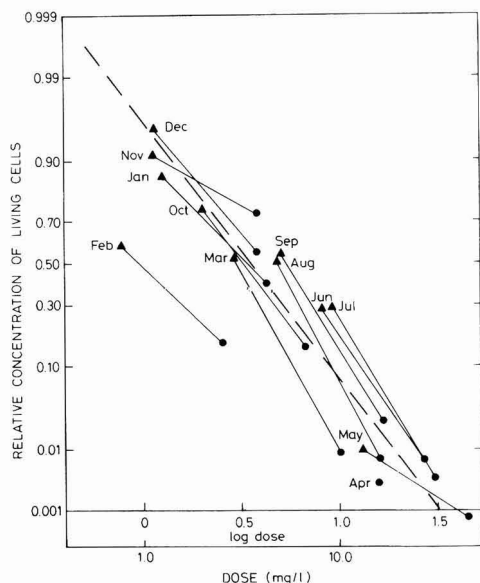


**Figure 5.** Effects of aqueous oil solutions after 3 days of incubation on *Skeletonema costatum*, shown as concentration of living cells, relative to that of control cultures, as a function of dissolved organic material on probit log scale. Doses obtained by dilution of the same sample are connected by straight lines; cf. Figure 2.

ganic material is considerably higher in July, the month with the highest ambient and water temperatures, than in April. One complicating factor in this comparison, however, is the fact that the solar zenith angle increases from April to July. Simultaneously, the solar spectrum extends toward the UV region (41) and increases the potential for radiation-induced weathering to take place. More extensive oxidation processes should therefore conceivably occur in July than in April, and this trend is confirmed by the much higher oxygen content of the surface oil in July (3.14%) than in April (1.85%) (Table II). The same trend is also obvious from the results of the weathering experiments performed in March and July: although the total radiation is the same in the two experiments, the oxygen content of the surface oil and the amount of dissolved organic material are much higher in July than in March. In order to assess the temperature influence on the oil oxidation, we therefore performed weathering experiments under accurate control. When such experiments were carried out at several water and ambient temperatures from 5 to 23 °C under otherwise identical conditions, using a dysprosium lamp with a spectral distribution resembling that of sunlight, the amount of dissolved organic material only changed from 6.6 to 8.1 mg/L whereas the oxygen content of the surface oil was essentially identical irrespective of the temperature as long as the time of illumination was the same. This indicates that the temperature primarily influences the oil weathering by affecting the evaporation and the water solubility of the oil.

The biological tests clearly show that the toxicity of the water-soluble oil fraction depends on the conditions persisting during the weathering. The more favorable the conditions are for formation and dissolution of oxidation products, the more toxic is the seawater phase. This conclusion is further substantiated by comparing the toxicity of the April–August samples with the toxicity of various seawater extracts from oil weathered in darkness.

The former group of extracts is much more toxic than those obtained in darkness both before and after the light fraction had evaporated (42).

A direct quantitative correlation between weathering and toxicity is more difficult to establish. The toxicity test involving *S. costatum* measures effects ranging from 0 to 100% when normalized relative to control values, and a sigmoidal dose–response curve should be expected on a linear response vs. logarithmic dose representation. Correspondingly, a linear dose–response connection on probit log scale is a reasonable model for evaluation of the actual results. Figure 5 illustrates the results of the phytotoxicity tests in a probability diagram when taken as a function of log dissolved organic material.

The results for *Skeletonema costatum* (cf. Figure 2) shown in Figure 5 are, with the exception of the February sample, all grouped along a straight line tentatively suggested by a dotted line in the figure. This implies that the specific toxicity (toxicity/dose) of the dissolved material should be considered as essentially constant throughout the year. The smaller tendencies toward a systematic deviation from month to month cannot be proved to be of significance. Moreover, the variation in oxygen content between different samples analyzed (Table II) is too small to verify whether the oxidation of the dissolved material is of significance for its specific toxicity or not.

The results recorded after 4 days of incubation of sea urchin eggs (Figure 4, bottom) are largely an “all or none” type of effect and therefore unsuitable for a similar treatment.

## Conclusion

Our experiments clearly suggest that oil weathering under natural conditions in the Arctic region is considerably influenced by the variation in the global radiation. However, a few remarks are appropriate. First, it should be emphasized that the experiments were carried out with the water/oil mixtures in a fairly small tank so that the primary photoproducts were unable to escape as they will do under natural conditions. The toxicity of the aqueous extracts may therefore in part be due to secondary photooxidation products that are not formed under natural conditions. Second, only one type of oil has been used, which represents a limitation because photooxidation of oil is sensitive to the oil composition (10, 12, 29, 43). Particularly the presence of sulfur compounds may interrupt the reactions taking place in the oil during weathering (10–12, 43). In spite of this we feel it is safe to conclude that the seasonal variation in global radiation, in terms of both total energy and spectral distribution, is of vital importance for the weathering and the toxic effects of oil in Arctic regions.

## Acknowledgments

We are grateful to Anne Andrews for skilful technical assistance and to Arne Jensen for valuable discussions.

Registry No. O<sub>2</sub>, 7782-44-7.

## Literature Cited

- Berridge, S. A.; Dean, R. A.; Fallows, R. G.; Fish, A. J. *Inst. Pet.* **1968**, *54*, 300–309.
- Freegarde, M.; Hatchard, C. G.; Parker, C. A. *Lab. Pract.* **1971**, *20*, 35–40.
- Boyland, D. B.; Tripp, B. W. *Nature (London)* **1971**, *230*, 40–47.
- Boehm, P. D.; Quinn, J. G. *Mar. Pollut. Bull.* **1974**, *5*, 101–105.
- Burwood, R.; Speers, G. C. *Estuarine Coastal Mar. Sci.* **1974**, *2*, 117–135.

- (6) Gordon, D. C., Jr.; Keizer, P. D.; Hardstaff, W. R.; Aldous, D. G. *Environ. Sci. Technol.* **1976**, *10*, 580-585.
- (7) McAuliffe, C. D. In "Fate and Effects of Petroleum Hydrocarbons in Marine Organisms and Ecosystems"; Wolfe, D. A., Ed.; Pergamon Press: Oxford, 1978; Chapter 3.
- (8) Payne, J. R.; Jordan, R. E. "The Fate and Weathering of Petroleum Spilled in the Marine Environment: A Literature Review and Synopsis"; Ann Arbor Science: Ann Arbor, MI, 1980.
- (9) Reinjhart, R.; Rose, R. *Water Res.* **1982**, *16*, 1319.
- (10) Larson, R. A.; Hunt, L. L.; Blankenship, D. W. *Environ. Sci. Technol.* **1977**, *11*, 492-496.
- (11) Larson, R. A.; Bott, T. L.; Hunt, L. L.; Rogenmuser, K. *Environ. Sci. Technol.* **1979**, *13*, 965-969.
- (12) Zafiriou, O. C. "Auto-oxidation and Photo-oxidation of Petroleum in the Marine Environment: A Critical Review". presented at the meeting for Petroleum in the Marine Environment, Clear Water Beach, 1982.
- (13) Tjessem, K.; Aaberg, A. *Chemosphere* **1983**, *12*, 1373-1394.
- (14) Lacaze, J. C.; Villedon de Naide, O. *Mar. Pollut. Bull.* **1976**, *7*, 73-76.
- (15) Østgaard, K.; Hegseth, E. N.; Jensen, A. *Bot. Mar.* **1984**, *27*, 309-318.
- (16) Griffin, L. F.; Calder, J. A. *Appl. Environ. Microbiol.* **1977**, *33*, 1092-1096.
- (17) Pengerud, B.; Thingstad, F.; Tjessem, K.; Aaberg, A. *Mar. Pollut. Bull.* **1984**, *15*, 142-146.
- (18) Scheier, A.; Gominger, D. *Bull. Environ. Contam. Toxicol.* **1976**, *16*, 595-603.
- (19) Falk-Petersen, I.-B.; Lønning, S. In "Ecotoxicological Testing for the Marine Environment"; Persoone, G.; Jaspers, E.; Claus, C., Eds.; State University Ghent: Belgium, 1984, Vol. 2, pp 197-217.
- (20) Baier, R. E. *J. Geophys. Res.* **1972**, *77*, 5062-5075.
- (21) Frankenfeld, J. W. "Factors Governing the Fate of Oil at Sea: Variations in the Amounts and Types of Dissolved or Dispersed Materials during the Weathering Process". In Proceedings of Joint Conference on Prevention and Control of Oil Spills, American Petroleum Institute, 1973.
- (22) Majewski, J.; O'Brien, J.; Barry, E. *Environ. Lett.* **1974**, *7*, 145-161.
- (23) Klein, A. E.; Pilpel, N. *Water Res.* **1974**, *8*, 79-83.
- (24) Hansen, H. P. *Mar. Chem.* **1975**, *3*, 183-195.
- (25) Gesser, H. D.; Wildman, T. A.; Tewari, Y. B. *Environ. Sci. Technol.* **1977**, *11*, 605-608.
- (26) Tjessem, K.; Kobberstad, O.; Aaberg, A. *Chemosphere* **1983**, *12*, 1395-1406.
- (27) Aaberg, A.; Pedersen, D.; Tjessem, K. *Water Res.* **1985**, *19*, 169-173.
- (28) Lloyd, J. B. F. *J. Forensic Sci. Soc.* **1971**, *11*, 83-94.
- (29) Herbes, S. E.; Whitley, T. A. *Environ. Pollut., Ser. B* **1983**, *6*, 221-240.
- (30) Poole, C. F. In "Handbook of Derivatives for Chromatography"; Blaw, K.; King, G. S., Eds.; Heyden & Son: London, 1979; pp 152-200.
- (31) Guillard, R. R. L.; Ryther, J. H. *Can. J. Microbiol.* **1962**, *8*, 229-239.
- (32) Østgaard, K.; Jensen, A. *Environ. Sci. Technol.* **1983**, *17*, 548-553.
- (33) Østgaard, K.; Jensen, A. *Mar. Biol.* **1982**, *66*, 261-268.
- (34) Samuelson, G.; Oquist, G. *Physiol. Plant.* **1977**, *40*, 315-319.
- (35) Kulandaivelu, G.; Daniell, H. *Physiol. Plant.* **1980**, *48*, 385-388.
- (36) Crippen, R. W.; Perrier, J. L. *Stain Technol.* **1974**, *49*, 97-104.
- (37) Østgaard, K.; Eide, I.; Jensen, A. *Mar. Environ. Res.* **1984**, *11*, 183-200.
- (38) Hegseth, E. N.; Østgaard, K. *Water Res.* **1985**, *19*, 383-391.
- (39) Kobayashi, N. *Publ. Seto Mar. Biol. Lab.* **1971**, *18*, 379-406.
- (40) Hagström, B. E.; Lønning, S. *Acta Pharmacol. Toxicol., Suppl.* **1973**, *32*, 1-49.
- (41) Henderson, S. T. "Daylight and Its Spectrum"; Adam Hilger: London, 1970.
- (42) Sydnes, L. K.; Burkow, I. C.; Stene, A.; Lønning, S. *Mar. Environ. Res.*, in press.
- (43) Sydnes, L. K.; Hansen, S. H.; Burkow, I. C. *Chemosphere* **1985**, *14*, 1043-1055.

*Received for review December 10, 1984. Accepted May 20, 1985. This work was supported by the Norwegian Marine Pollution Research and Monitoring Programme (Projects 312, 406, and 505) and the Norwegian Research Program for Marine Arctic Ecology, administered by the Norwegian Research Council for Science and the Humanities.*

# Determination of Organic Acids ( $C_1$ - $C_{10}$ ) in the Atmosphere, Motor Exhausts, and Engine Oils<sup>†</sup>

Kimitaka Kawamura,<sup>‡</sup> Lai-Ling Ng, and Isaac R. Kaplan\*

Institute of Geophysics and Planetary Physics, University of California, Los Angeles, California 90024

■ A method is described for the determination of volatile organic acids in the atmosphere, motor exhausts, and engine oils. Atmospheric organic acids were collected on a KOH impregnated quartz filter and derivatized to *p*-bromophenacyl esters. The derivatives were analyzed by high-resolution capillary gas chromatography and gas chromatography-mass spectrometry.  $C_1$ - $C_{10}$  aliphatic organic acids and benzoic acid were detected in Los Angeles air. Acetic and formic acids are dominant followed by propionic acids. Total concentrations measured were 0.37-7.45 ppb. Organic acids ( $C_1$ - $C_{10}$ ) were also detected in the motor exhaust from a single automobile at idle conditions and showed that the distribution of individual acids was similar to that in the air, but the concentration was 17 times higher than for the average atmospheric content. Formic, acetic, and benzoic acids were detected as major species of used engine oil, but their content is negligible in new oil.

## Introduction

Volatile organic acids ( $C_1$ - $C_7$ ), including formic and acetic, have been found to be the most abundant species among organic compounds identified in Los Angeles rain (1, 2). These acids probably originate from both anthropogenic and biogenic sources on the ground as well as in situ photochemical oxidation of organic compounds in the atmosphere. However, with the exception of a few isolated reports on formic and acetic acids, the distribution of volatile organic acids has not been studied in the atmosphere.

Atmospheric organic acids were first reported in downtown Los Angeles by using a bubbler in NaOH solution followed by silica gel column chromatography-titration (3). The concentration of formic acid ranged from 0.0 to 0.41 ppm, but that of acetic acid was not described. The reported concentration range is extremely wide, probably because the method is not sufficiently discriminating and analyzed inorganic acids also. A long-path Fourier transform infrared spectroscopy (FTIR) method has been applied to measure atmospheric pollutants, and formic acid has been reported at levels of 0-19 ppb in the Los Angeles area (4-6). However, acetic and higher acids were not reported in these studies cited above. Ion chromatography has been also used for measuring formic and acetic acids in the atmosphere of Tucson, AZ, after the collection with water film (7). The reported concentrations were 1-6 ppb. Activated charcoal trap followed by high-performance liquid chromatography (HPLC) analysis has been used for the determination of formic acid in air samples (8). Although studies cited are useful, they have not detected organic acids longer than  $C_2$ , which, according to our research on rainwater (2), should be present in the atmosphere, and furthermore, they do not discriminate between gaseous and particulate phases.

In this paper, we describe a sensitive capillary gas chromatography method for the determination of volatile

organic acids ( $C_1$ - $C_{10}$ ) in the atmosphere and motor exhausts which were trapped on an alkaline-treated quartz-fiber filter. A scavenging method employing bubbling into KOH solution was initially tried for the trapping of atmospheric organic acids. However, the efficiency of trapping was found to be inadequate as more than 55% of the organic acids were captured in the second trap. Engine oils (new and used) were also analyzed for organic acids.

## Materials and Methods

A volatile acid mixture ( $C_1$ - $C_7$ , 10 mM each in water) and benzoic acid were purchased from Supelco (Bellefonte, PA) and Sigma Chemical Co. (St. Louis, MO), respectively.  $\alpha$ ,*p*-Dibromooacetophenone and dicyclohexyl-18-crown-6 were purchased from Aldrich Chemical Co. (Milwaukee, WI) and purified on a silica gel column (2). KOH was used after heating at 500 °C for 4 h. Pure water was prepared by oxidizing organic impurities in distilled water with  $KMnO_4$ /KOH in a boiling flask. Organic solvents were distilled in all-glass apparatus prior to use. Quartz-fiber filters (25 cm  $\times$  21.5 cm) were purchased from Pallflex Products Corp. (Putnam, CT) and were cut into 47-mm diameter disks. The trapping efficiency of 0.3  $\mu$ M dioctyl phthalate on the filter quoted by Pallflex products Corp. is 99.77%. The filters were heated at 500 °C for 3 h to remove organic contamination, rinsed in 0.18 N KOH solution, and then dried in an oven at 80 °C.

**Sampling.** Air samples were collected on the roof of the Geology Building on UCLA campus, Los Angeles, CA. KOH-impregnated filters were set in Nuclepore filter holders (47 mm), which were each connected to a flow-meter and pump with a short (50-cm) Tygon tube, as shown in Figure 1a. To discriminate particulate and gaseous phases, a nonimpregnated filter was used together with an alkaline filter (Figure 1a). Samples were collected on the filter by pumping the air at flow rates of 10 L/min for times ranging from 4 to 24 h. During sampling, each filter holder was protected with aluminum foil from sunlight, which may cause photooxidation reactions on the trapped material. A Thomas air pump (Sheboygan, WI) was used.

Automobile exhaust was collected by using a Toyota Corolla model engine on the KOH-impregnated quartz filter, which was set in a Millipore holder (SWINNEX-47, 47 mm) as shown in Figure 1b. The filter was connected to a glass tube (5.5 mm o.d., 30 cm long), whose other end was introduced in the muffler of the car. Sampling was performed while the engine was idling for 30 min, at a flow rate of 10 L/min.

**Recovery Test.** Recovery tests were examined by using a U-shaped glass tube (5.5 mm o.d., 30 cm long), as shown in Figure 1c. An organic acid standard solution (20  $\mu$ L) was injected in the U-tube. Immediately following, pumping was started at a flow rate of 1.0 L/min for the first 30 min and then 10 L/min to trap the authentic acids on a KOH filter. In order to remove organic acids from the air stream, two KOH-impregnated filters in Nuclepore holders were attached to the top of the U-tube with Teflon tubing. Because Tygon tubing was found to release acetic acid as a contaminant, it should not be used in front of

<sup>†</sup>Institute of Geophysics and Planetary Physics Contribution No. 2601.

<sup>‡</sup>Present address: Chemistry Department, Woods Hole Oceanographic Institution, Woods Hole, MA 02543.



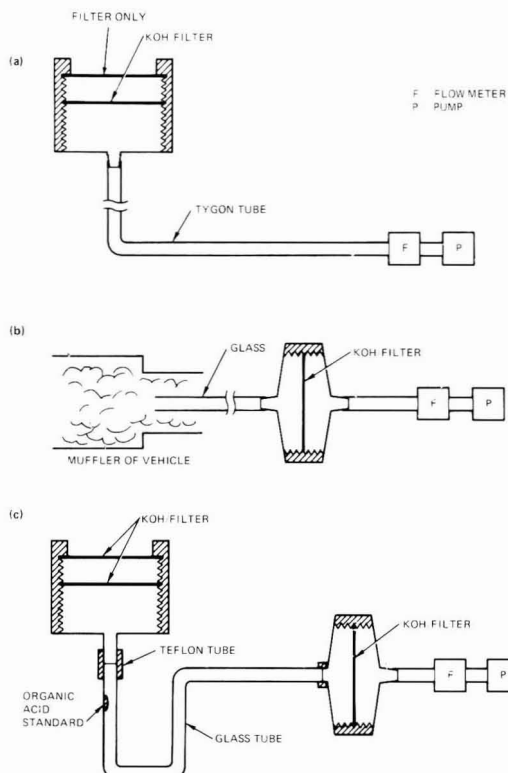


**Figure 1.** Sampling apparatus for the air (a), motor exhausts (b), and authentic organic acids (c).

the filter. Pumping time was varied from 90 min to 12 h.

**GC Analysis of *p*-Bromophenacyl Esters of Volatile Acids.** After the solutions were sampled, filters were extracted with pure water (5 mL  $\times$  3) under ultrasonification. The combined extracts were centrifuged and passed through a cation-exchange column (Bio-Rad AG 50W-X4, 100–200 mesh,  $K^+$  form) (2). The solution was pH adjusted to 8.0–8.5 with 1 N HCl for the KOH/filter extracts and with 1 N KOH for the non-KOH/filter extracts, and organic acids were determined by a method of Kawamura and Kaplan (2). Briefly, the solution was dried in a rotary evaporator followed by nitrogen gas blow down, and carboxylates ( $RCOO^-K^+$ ) were esterified in acetonitrile solution with  $\alpha$ ,*p*-dibromoacetophenone (reagent, 50  $\mu$ L of 0.2  $\mu$ mol/mL in benzene) and dicyclohexyl-18-crown-6 (catalyst, 50  $\mu$ L of 0.02  $\mu$ mol/ $\mu$ L in acetonitrile) at 80  $^\circ$ C for 1 h. The esters were purified on a silica gel column and analyzed by capillary gas chromatography using a DB 5 column. Table I lists gas chromatographic conditions. A Finnigan Model 4000 gas chromatography-mass spectrometry (GC-MS) was used with the same column to obtain the mass spectra of volatile acid phenacyl esters.

Engine oils (Chevron 15/50) were also analyzed for organic acids. One milliliter of new and used (ca. 5000 km) oils was diluted with 4 mL of  $CH_2Cl_2$  and then extracted with 0.005 N KOH solution (5 mL  $\times$  3). The extracts were combined, pH adjusted to 8.0–8.5, and analyzed as described above.

$C_1$ – $C_7$  organic acids and benzoic acid in the samples were identified by comparing gas chromatographic retention times and mass spectra of their phenacyl esters with those of authentic standards (2).  $C_8$ – $C_{10}$  acids were tentatively

**Table I. Gas Chromatographic Conditions for Determining Phenacyl Esters of Volatile Acids**

GC	Hewlett-Packard Model 5840 gas chromatograph
integrator	Hewlett-Packard Model 18850A GC terminal
column	fused silica capillary (DB 5) 0.25 mm $\times$ 30 m
column temperature	programmed from 40 (6 min) to 160 $^\circ$ C at 30 $^\circ$ C/min and then to 295 $^\circ$ C at 8 $^\circ$ C/min
injection temperature	200 $^\circ$ C
FID temperature	300 $^\circ$ C

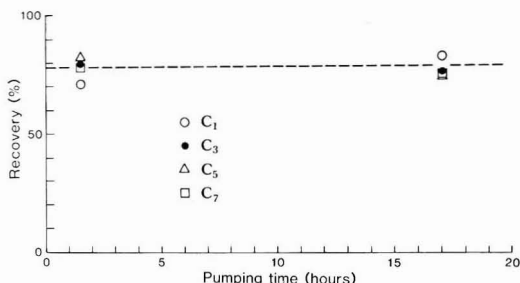


**Figure 2.** Recoveries of authentic organic acids ( $C_1$ ,  $C_3$ ,  $C_5$ , and  $C_7$ ) from a KOH-impregnated filter during pumping.

identified by a characteristic mass fragment ( $M - 213$ ) of the homologous series of volatile acid phenacyl esters.

## Results and Discussion

**Trap Efficiencies of Authentic Organic Acids on KOH Filter.** Figure 2 shows recoveries of  $C_1$ ,  $C_3$ ,  $C_5$ , and  $C_7$  acids, as example, which were trapped on the KOH-impregnated filter. Recoveries are 71–82% (average  $78 \pm 5\%$ ) at 90 min and 74–82% (average  $77 \pm 4\%$ ) at 17 h. They did not decrease with time, indicating that the organic acids, once trapped on the KOH filter, can remain there during the sample collection. During collection, no significant fractionation was obtained among  $C_1$ – $C_7$  acids.

**Trap Efficiencies of Atmospheric Organic Acids on Stepwise Filters.** In order to check trap efficiencies for atmospheric organic acids, air samples were collected on three filters which were set in the combined filter holders. The first filter was prewashed with pure water to make the filter surface neutral and to separate fine particles on the filter. The second and third were impregnated with KOH. Table II gives the concentrations of atmospheric organic acids trapped on three filters. The first (neutral) filter shows low concentrations of organic acids, whereas the second (KOH-impregnated) filter shows high concentrations. Total concentrations of  $C_1$ – $C_9$  organic acids on the first filter are less than 17% of that of total recovered acids. These results indicate that organic acids in the atmosphere can mostly pass through the neutral filters but are trapped on alkaline filters, suggesting that atmospheric organic acids are largely present in the vapor phase. However, as the amount captured on the first filter range from 2% to 17% of the total recovered organic acids, the particulate to gaseous phase ratios of organic acids may change depending on atmospheric conditions.

The organic acid concentrations for the third filter are low compared with that of the second filter. The percentage of organic acids trapped on the third filter to those on the second filter is less than 25%, except for  $C_3$ ,  $C_9$ , and benzoic acids. For the total organic acids, the percentage is within 10%. This result indicates that organic acids in

Table II. Concentrations of Atmospheric Organic Acids (C<sub>1</sub>-C<sub>9</sub>) Trapped in Stepwise Quartz Filters with and without KOH<sup>a</sup>

samples (time PDT)	organic acids, ppb											total
	C <sub>1</sub>	C <sub>2</sub>	C <sub>3</sub>	iC <sub>4</sub>	C <sub>4</sub>	C <sub>5</sub>	C <sub>6</sub>	C <sub>7</sub>	C <sub>8</sub>	C <sub>9</sub>	Benz	
6/10-11/84(1925-1032)												
1st filter (no KOH)	BB	0.009	0.001	ND	0.0004	0.0004	0.001	ND	0.001	0.001	BB	0.014
2nd filter (KOH)	0.206	0.545	0.035	0.005	0.012	0.006	0.011	0.004	0.005	0.007	0.004	0.840
3rd filter (KOH)	0.002	0.003	0.003	0.0004	0.001	0.0004	0.001	0.001	0.002	0.003	0.002	0.019
1st/total, %		2	3		3	6	8		13	10		2
3rd/2nd, %	1	1	9	8	8	7	9	25	40	43	50	2
9/20/84(1057-1757)												
1st filter (no KOH)	0.059	BB	ND	ND	ND	ND	ND	ND	0.0002	ND	ND	0.059
2nd filter (KOH)	0.349	0.612	0.051	0.006	0.015	0.008	0.008	0.004	0.005	0.003	0.007	1.068
1st/total, %	14								4			5
9/21/84(1045-1815)												
1st filter (no KOH)	0.161	0.147	0.003	ND	ND	ND	0.004	ND	0.003	0.002	ND	0.320
2nd filter (KOH)	0.428	0.842	0.068	0.001	0.018	0.009	0.016	0.006	0.007	0.006	0.008	1.409
3rd filter (KOH)	0.017	0.095	0.007	ND	0.003	0.002	0.004	0.001	0.002	0.001	0.003	0.135
1st/total, %	27	14	4				17		25	22		17
3rd/2nd, %	4	11	10		17	22	25	17	29	17	40	10

<sup>a</sup> Benz, benzoic acid; BB, below blank; ND, not detected.

Table III. Triplicate Analysis of Atmospheric Organic Acids Collected on Sept 24-25 (1215-1344), 1984, at Los Angeles

sample no.	organic acids, ppb											Benz <sup>a</sup>	total
	C <sub>1</sub>	C <sub>2</sub>	C <sub>3</sub>	iC <sub>4</sub>	C <sub>4</sub>	C <sub>5</sub>	C <sub>6</sub>	C <sub>7</sub>	C <sub>8</sub>	C <sub>9</sub>	C <sub>10</sub>		
1	1.34	2.49	0.154	0.024	0.045	0.019	0.028	0.010	0.012	0.009	0.003	0.015	4.15
2	1.06	2.11	0.126	0.021	0.042	0.019	0.029	0.010	0.015	0.008	0.004	0.014	3.46
3	1.27	2.44	0.138	0.022	0.043	0.019	0.030	0.010	0.013	0.009	0.003	0.015	4.00
mean ( $\bar{x}$ )	1.22	2.35	0.139	0.022	0.043	0.019	0.029	0.010	0.013	0.009	0.003	0.015	3.87
SD (Sx)	0.15	0.21	0.014	0.002	0.002	0	0.001	0	0.002	0.001	0.001	0.001	0.36
Sx/ $\bar{x}$ , %	12	9	10	9	4	0	3	0	11	6	17	4	9

<sup>a</sup> Benz, benzoic acid.

Table IV. Organic Acids in the Los Angeles Atmosphere, Motor Exhausts, and Engine Oils<sup>a</sup>

samples	organic acids, ppb												total
	C <sub>1</sub>	C <sub>2</sub>	C <sub>3</sub>	iC <sub>4</sub>	C <sub>4</sub>	C <sub>5</sub>	C <sub>6</sub>	C <sub>7</sub>	C <sub>8</sub>	C <sub>9</sub>	C <sub>10</sub>	Benz	
atmosphere													
7/16/84 (1205-1825)	0.896	1.16	0.125	0.011	0.038	0.021	0.024	0.014	0.014	0.009	0.004	0.008	2.32
7/23/84 (1030-1655)	0.101	0.287	0.034	0.003	0.014	0.008	0.008	0.005	0.004	0.003	0.001	0.001	0.469
7/23-24/84 (1655-0945)	0.066	0.262	0.019	0.003	0.006	0.004	0.006	0.002	0.002	0.0009	ND	0.001	0.372
9/24-25/84 (1215-1344)	1.22	2.35	0.139	0.022	0.043	0.019	0.029	0.010	0.013	0.009	0.009	0.015	3.88
9/27/84 (1310-1731)	0.395	0.600	0.054	0.007	0.016	0.008	0.011	0.004	0.005	0.002	0.001	0.004	1.11
9/27-28/84 (1734-1006)	0.497	1.58	0.111	0.014	0.029	0.014	0.025	0.008	0.010	0.005	0.002	0.012	2.31
9/28/84 (1008-1901)	2.98	3.90	0.305	0.031	0.083	0.033	0.044	0.017	0.021	0.011	0.003	0.026	7.45
9/28-29/84 (1925-1800)	1.69	1.01	0.055	0.005	0.016	0.008	0.019	0.006	0.011	0.006	0.002	0.014	2.84
motor exhaust <sup>b</sup>	9.30	31.81	1.22	0.056	0.123	0.045	0.063	0.047	0.078	0.052	0.020	0.164	43.0
engine oil, nmol/mL <sup>c</sup>													
used	836	145	19	2.3	3.4	2.4	ND	ND	ND	ND	ND	45.3	1050
new	1.9	5.3	5.6	ND	1.0	ND	ND	ND	ND	ND	ND	ND	13.9

<sup>a</sup> Benz, benzoic acid; ND, not determined. <sup>b</sup> Toyota Corolla 1982 model (gasoline engine). <sup>c</sup> Chevron 15/50 motor oil.

the atmosphere are trapped mostly on a single KOH-impregnated filter. On the basis of a method of Smith (9), overall trapping efficiencies of gaseous organic acids on the second and third KOH filters combined are estimated to be 99.9% (6/10-11/87 air) and 99.1% (9/21/84 air), whereas for the second filter alone, they are 98% and 91%, respectively.

**Reproducibility and Blank.** To check the reproducibility of this air sampling technique, triplicate samples were collected on KOH-impregnated filters. The results are shown in Table III. Relative standard deviation to average concentrations of total organic acids are within  $\pm 9\%$  (up to 17% for individual acids), indicating that this method is reproducible.

Procedural blanks were run together with the samples. Formic and acetic acids have appeared as major contamination on the gas chromatogram and propionic acid as a

minor contaminant. However, their amounts are usually less than 5% of the samples. Other organic acids were not detected in the blanks. Data presented here are corrected for the procedural blanks.

**Distribution of Organic Acids in the Atmosphere.** Figure 3 shows a gas chromatogram of *p*-bromophenacyl esters for volatile acids in the atmosphere. C<sub>1</sub>-C<sub>10</sub> aliphatic organic acids and benzoic acid were identified and/or tentatively identified by retention times and mass fragmentation patterns of authentic standards. Generally, acetic acid is the most abundant species followed by formic and propionic acids. Concentrations appear to decrease with an increase in chain length. Qualitative distribution of atmospheric organic acids is quite similar to that of rain and fog samples collected in Los Angeles (2), except that formic acid is always more abundant than acetic acid in fog samples.

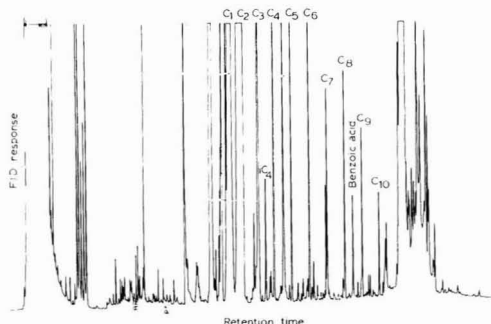


**Figure 3.** Gas chromatogram of *p*-bromophenacyl esters for organic acids in the atmosphere. Sample: 7/6/1984, air (3.8 m<sup>3</sup>). One microliter was injected from 50  $\mu$ L of ester solution in hexane.

Table IV gives concentrations of organic acids in the atmosphere and motor exhausts as well as motor engine oils. The concentrations in Los Angeles atmosphere ranged from 0.37 to 7.45 (average  $2.59 \pm 2.30$ ) ppb (parts per billion), which correspond to 1000–19 600 ng/m<sup>3</sup> (average of  $6800 \pm 6000$  ng/m<sup>3</sup>). These values are extremely high compared with long-chain (C<sub>10</sub>–C<sub>30</sub>) carboxylic acids. Simoneit and Mazurek (10) reported that atmospheric concentrations of C<sub>12</sub>–C<sub>30</sub> fatty acids were 217–308 ng/m<sup>3</sup> (average  $260 \pm 50$  ng/m<sup>3</sup>) in urban Los Angeles areas. The average concentration of short-chain organic acids is more than 25 times higher than that of long-chain fatty acids in the atmosphere. Kawamura and Kaplan (2) by comparison observed in the rain samples of Los Angeles that volatile organic acids were 40–300 times higher than long-chain fatty acids.

The concentrations of formic acid in Los Angeles air which we measured are lower (0.07–3.0 ppb) than those (0–19 ppb) measured at downtown Los Angeles and Riverside by spectroscopic (long-path FTIR) methods (4–6). The difference may be caused by a difference in sampling location. Downtown Los Angeles and Riverside areas are much more polluted than the west Los Angeles area (UCLA campus). Dawson et al. (7) measured formic and acetic acids in the air at a site 16 km NW of Tucson, AZ, at levels of 1.5–3.5 and 1–6 ppb, respectively. These values are higher than our results (see Table IV). There is a possibility that Dawson et al. have overestimated the true concentration because the collection methods capture both free organic acids and other gaseous compounds that hydrolyze or oxidize to the acids upon collection or analysis, such as formaldehyde and acetaldehyde which are abundantly present in the air (11, 12). On the other hand, the KOH-impregnated filters we use probably do not trap aldehydes; thus, they will not be oxidized to the acids when the filter is extracted with water.

**Presence of Organic Acids in Motor Exhaust and Engine Oil.** Organic acids (C<sub>1</sub>–C<sub>10</sub>) were detected in motor exhausts, as shown in Table IV. Their distribution is similar to that for air samples, except for a relatively high amount of benzoic acid. Acetic acid is predominant followed by formic acid and propionic acid. These acids are probably produced by incomplete combustion of gasoline. Their concentration in the exhaust is 43 ppb, which is 17 times higher than the average concentration of atmospheric organic acids. Because the exhaust sample in this study was collected at idling conditions of the engine, it may not be representative of exhausts from road-running vehicles. However, these results suggest that motor exhausts are important sources of organic acids in the atmosphere, in addition to possible photochemical production of organic

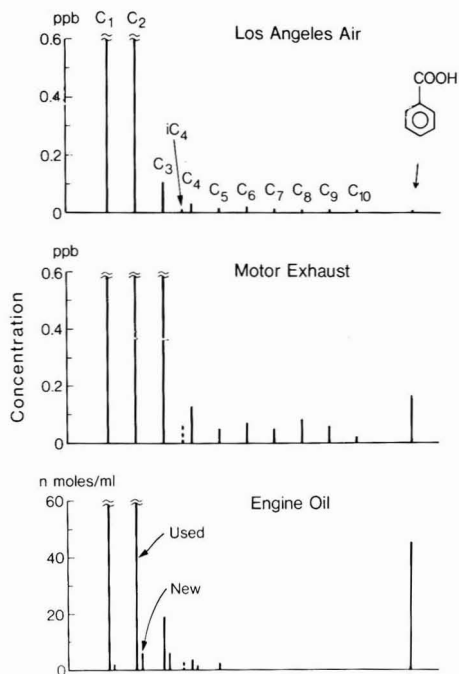


**Figure 4.** Distributions of C<sub>1</sub>–C<sub>10</sub> organic acids and benzoic acid in Los Angeles air (average of eight samples), motor exhaust, and engine oil (new and used) samples.

acids from atmospheric organic compounds such as aldehydes (6).

C<sub>1</sub>–C<sub>4</sub> organic acids were identified in both new and used engine oils. However, benzoic acid and C<sub>5</sub> acid were only detected in used oil. Furthermore, total concentration of organic acids is very high (ca. 1000 nmol/mL) in used oil but low (ca. 14 nmol/mL) in new oil, as shown in Table IV. These results clearly indicate that large amounts of organic acids are produced from engine oil and/or gasoline in the combustion chamber during engine use and then scavenged to some degree into the film of lubricating oil. The organic acids produced in engines are probably released to the atmosphere as motor exhausts or by fugitive escape. Although formic acid is more abundant than acetic acid in used engine oil, it is less abundant than acetic acid in the motor exhaust sample (see Table IV). Such a difference could be associated with vehicle operating conditions; that is, the motor exhaust was collected in an idling mode, whereas the used engine oil had been largely produced under driving conditions. It is also possible that formic acid in the exhausts may not be effectively collected on the KOH-impregnated filter because the high temperature of the exhausts may decrease the trap efficiency of formic acid on the KOH-impregnated filter. Further tests are being conducted with automobiles that simulate driving conditions by use of chassis dynamometers.

Figure 4 compares the distributions of C<sub>1</sub>–C<sub>10</sub> organic acids and benzoic acid in the air, motor exhausts, and engine oil samples. Although benzoic acid was detected in all the samples except for new engine oil, its distribution is different among the samples. In the air samples, benzoic acid is less abundant than C<sub>1</sub>–C<sub>6</sub> acids, whereas it is more abundant than C<sub>4</sub>–C<sub>8</sub> acids in the motor exhausts and C<sub>3</sub>–C<sub>8</sub> acids in the used engine oil (Figure 4). Benzoic acid is probably produced in motor engines by oxidation of

toluene and other aromatic structures in gasoline and engine oil and released to the atmosphere.

**Advantages of This Method.** Because the present KOH filter/capillary GC method is very sensitive, several hours sampling or a few cubic meters of an air sample is enough for the determination of  $C_1$ - $C_{10}$  organic acids and benzoic acid in the atmosphere. This method has advantages over previously reported methods (FTIR and water film/ion chromatography) that cannot detect organic acids longer than  $C_2$  due to their low sensitivity and/or analytical limitation. Furthermore, organic acids in the atmosphere can be easily identified as their *p*-bromophenacyl esters by using gas chromatography-mass spectrometry, due to their characteristic fragmentation patterns.

**Conclusions.** Short-chain aliphatic monocarboxylic acids ( $C_1$ - $C_{10}$ ) and benzoic acid were identified in Los Angeles air by capillary GC and GC-MS methods employing *p*-bromophenacyl esters of the acids. Their distributions are characterized by a predominance of acetic and formic acids followed by propionic acid. They were found to be present mostly in vapor phase. The particulate forms were less than 17% of the total (particulate plus gaseous) organic acids for the samples of air tested. Total concentrations of organic acids ranged from 0.37 to 7.45 ppb in the Los Angeles atmosphere. The wide range of concentrations (over an order of magnitude) suggests that the concentration levels may be largely controlled by meteorological conditions and/or time of day. Motor exhaust is suggested as being one of the major sources of atmospheric organic acids; however, this does not preclude an importance of the secondary production of organic acids in the atmosphere by photochemical reactions.

#### Acknowledgments

We appreciate the critical reviewing and helpful com-

ments on the manuscript by B. R. Appel (Department of Health Services, State of California, Berkeley, CA) and R. Gordon (Global Geochemistry Corp., Canoga Park, CA).

**Registry No.** Acetic acid, 64-19-7; formic acid, 64-18-6; propionic acid, 79-09-4; butyric acid, 107-92-6; isobutyric acid, 79-31-2; benzoic acid, 65-85-0.

#### Literature Cited

- (1) Kawamura, K.; Kaplan, I. R. *Environ. Sci. Technol.* **1983**, *17*, 497.
- (2) Kawamura, K.; Kaplan, I. R. *Anal. Chem.* **1984**, *56*, 1616.
- (3) Mader, P. P.; Cann, G.; Palmer, L. *Plant Physiol.* **1955**, *30*, 318.
- (4) Tuazon, E. C.; Graham, R. A.; Winter, A. W.; Easton, R. R.; Hanst, P. L. *Atmos. Environ.* **1978**, *12*, 865.
- (5) Tuazon, E. C.; Winter, A. M.; Pitts, J. N., Jr. *Environ. Sci. Technol.* **1981**, *15*, 1232.
- (6) Hanst, P. L.; Wong, N. W.; Bragin, J. *Atmos. Environ.* **1982**, *16*, 969.
- (7) Dawson, G. A.; Farmer, J. C.; Mayers, J. L. *Geophys. Res. Lett.* **1980**, *7*, 725.
- (8) Variotolo, S.; Pfattli, P.; Zitting, A. J. *Chromatogr.* **1983**, *258*, 207.
- (9) Smith, J. R. *J. Air. Pollut. Control Assoc.* **1979**, *29*, 969.
- (10) Simoneit, B. R. T.; Mazurek, M. A. *Atmos. Environ.* **1982**, *16*, 2139.
- (11) Graedel, T. E. "Chemical Compounds in the Atmosphere"; Academic Press: New York, 1978; pp 1-440.
- (12) Grosjean, D. *Environ. Sci. Technol.* **1982**, *16*, 254.

Received for review December 11, 1984. Accepted April 8, 1985. Although the information in this document has been funded wholly or in part by the U.S. Environmental Protection Agency under Assistance Agreement CR-807864-01 to NCITR at UCLA, it does not necessarily reflect the views of the Agency, and no official endorsement should be inferred.

## Microbial Degradation of Chlorolignins

Karl-Erik Eriksson\* and Marie-Claude Kolar

Swedish Forest Products Research Laboratory, S-114 86 Stockholm, Sweden

■ Sulfate pulping and conventional bleaching of spruce wood, which had been labeled with  $^{14}C$  in the lignin component, gave rise to  $^{14}C$ -labeled chlorolignins. High relative molecular mass fractions of both the chlorination (C) and alkali extraction (E) stages were obtained by ultrafiltration (cutoff at 1000 daltons). The degradation of these labeled chlorolignins was studied by measuring evolved  $^{14}CO_2$  using two different bacterial mixtures, isolated from aerated lagoons receiving spent bleach liquors, and the white-rot fungus *Sporotrichum pulverulentum*. The results obtained showed that the bacterial consortia degraded high molecular mass chlorolignins only very slowly, less than 4% of the  $^{14}C$  material being converted to  $^{14}CO_2$  within 3 months. However, the fungus degraded the same material much more rapidly, 35-45% of available  $^{14}C$  being converted to  $^{14}CO_2$  within 2 months.

#### Introduction

In the most commonly used process for chemical pulp production, the wood is treated at elevated temperature with a mixture of sodium hydroxide and sodium sulfide (the kraft process). This treatment removes approximately

90% of the lignin, leaving a fibrous residue which, for bleaching purposes, is further delignified in chlorination and alkaline extraction stages.

In recent years, a comprehensive investigation of the chemical composition of waste waters from pulp bleach plant effluents has taken place (1). From an environmental viewpoint, compounds with a relative molecular mass of less than 1000 daltons are of particular interest. Such compounds can penetrate the cell membranes of aquatic organisms and are both acutely toxic and genotoxic (2). However, high relative molecular mass material in spent bleach liquors, i.e., chlorolignins, will adversely affect the environment only if such chlorolignins are first degraded to low molecular mass units. It should be noted that a major part of the organic material in spent bleach liquors is of high relative molecular mass.

In a recent investigation, Neilson et al. (3) found that monocultures of bacteria, isolated from waters subjected to discharge of spent bleach liquors, generated various chlorinated veratroles from spent bleach liquor material. Eriksson et al. (4) reported that the high molecular mass material in spent liquors from both the chlorination and alkali extraction stages was chemically unstable and slowly decomposed to yield various chlorinated catechols and guaiacols. The same authors (4) also observed the for-

\* To whom all correspondence should be addressed.

mation of chlorinated veratroles when these chlorolignins were incubated with mixtures of bacteria or with the white-rot fungus *Sporotrichum pulverulentum*.

Following the observation that phenolic degradation products of high molecular mass chlorolignins are methylated to the more persistent chlorinated veratrole compounds, it seems desirable also to eliminate the polymeric parts of the organic materials in spent bleach liquors. Purification of such wastewaters is normally achieved using biological systems, and aerated lagoons are used most often for handling spent bleach waters.

Although such information is important, to our knowledge, no studies have been undertaken on the microbial degradation of high molecular mass chlorinated lignins. However, it is neither easy to analyze differences in the polymeric material nor to study the low molecular mass products formed since these are either consumed or converted to veratroles by the microorganisms. Therefore, we have investigated the complete metabolism of the polymers by labeling the lignin with  $^{14}\text{C}$  and measuring  $^{14}\text{CO}_2$  evolution from cultures of microorganisms where the  $^{14}\text{C}$ -labeled chlorolignins were used as carbon sources.

#### Materials and Methods

**$^{14}\text{C}$ -Labeling of Lignin in Spruce Wood.** Cut stems of two spruce plants (*Picea abies*), approximately 2 years old, were each fed 25  $\mu\text{Ci}$  of L-[U- $^{14}\text{C}$ ]phenylalanine according to Odier et al. (5). The labeled wood from these two plants was used in the cooking and bleaching experiments.

**Production of  $^{14}\text{C}$ -Labeled Chlorolignins.** (1) **Sulfate Pulping.** Twenty grams (b.d. = bone-dry) of laboratory chips prepared from the  $^{14}\text{C}$ -labeled spruce wood was mixed with 220 g (b.d.) of normal unlabeled laboratory spruce chips. The mixture was pulped under the following cooking conditions: wood:liquor of 1:4 using a white liquor with 17% effective alkali and 40% sulfidity, vacuum impregnation, temperature increase from 70 to 170  $^{\circ}\text{C}$  at 1  $^{\circ}\text{C}/\text{min}$ , and pulping time at 170  $^{\circ}\text{C}$  = 120 min. Due to the radioactive nature of the material, pulp yield and kappa number were not determined. However, when normal (unlabeled) laboratory spruce chips were pulped under these conditions, a total pulp yield of 48.5% and a kappa number of 32 were obtained.

(2) **Bleaching.** The  $^{14}\text{C}$ -labeled kraft pulp produced was bleached with chlorine under the following conditions: 6.7% active chlorine, 3% pulp consistency, and 20  $^{\circ}\text{C}$ . After 60 min, the pulp was filtered off and the chlorination (C-) stage liquor collected and stored in a refrigerator until required.

After being washed with water, the chlorinated pulp was extracted with alkali under the following conditions: 2.5% NaOH, 8% pulp consistency, and 60  $^{\circ}\text{C}$ . After 120 min, the pulp was filtered off and the alkaline extraction-(E-) stage liquor collected and stored in a refrigerator until required.

(3) **Ultrafiltration of the C and E Liquors.** The C-stage liquor was adjusted to pH 4.0 with 2 M NaOH and the E-stage liquor to pH 7.0 with 1 M  $\text{H}_2\text{SO}_4$ . To remove low relative molecular mass compounds, the liquors were passed through a Diaflo ultrafiltration membrane, Um 2, with a cutoff at 1000 daltons (Amicon Corp., Lexington, MA). The C-stage liquor was reduced to  $1/10$  of the original volume and washed with 15 volumes of distilled water. The efficiency of the washing was controlled by measuring the radioactivity in the washing water penetrating the membrane.

The E-stage liquor was treated in the same way, but due to higher amounts of polymeric material in this liquor, the

volume was reduced to only  $1/3$  of the starting volume before washing with 10 volumes of distilled water. The efficiency of the washing was controlled as before.

**Organisms.** Mixed cultures of bacteria were isolated from sludges of the community waste purification plant, K ppala, Stockholm, and from the aerated pond at Fiskeby Papermill, Sk rblacka, Sweden. The bacteria were adapted to a C-stage mill effluent as described in ref 6.

The fungus used in these studies was the white-rot fungus *Sporotrichum pulverulentum* Nov. (ATCC 32629), anamorph of *Phanerochaete chrysosporium* (7).

**Cultivation Conditions.** To obtain material for inoculation, the mixed bacterial suspensions (K ppala and Fiskeby 1) were grown in a medium consisting of mill C-stage liquor, adjusted to pH 4.0, which contained 0.04%  $\text{NH}_4\text{H}_2\text{PO}_4$ , 0.02%  $\text{MgSO}_4$ , and trace elements according to ref 8. A total of 40 mL of 1 M sodium phosphate buffer, pH 6.0, was added to each liter of C-stage liquor.

The following medium was used to study  $^{14}\text{CO}_2$  evolution from the  $^{14}\text{C}$ -labeled high relative molecular mass fractions of the C (HM-C) and E stages (HM-E) by the mixed bacterial populations:

To one liter of C- or E-stage liquor, adjusted to pH 4.0 or 7.0, respectively, and sterile filtered, were added 40 mL of 1 M sodium phosphate buffer, pH 6.0,  $\text{NH}_4\text{H}_2\text{PO}_4$  (0.04%), peptone (0.02%), glucose (0.05%), and trace elements according to ref 8 to a final pH value of 6.2. Two different concentrations of HM-C and HM-E, i.e., 0.1 and 0.2% (dry weight per volume), were used in the final medium. Cultivations were carried out at 28  $^{\circ}\text{C}$  in 125-mL Ehrlenmeyer flasks under shaking conditions with 20 mL of medium in each flask. Uninoculated flasks, held under the same conditions, served as controls. The amount of radioactivity in the HM-C substrate was 17 300 (0.1%) and 36 100 dpm (0.2%) per flask, respectively. The corresponding amount in the HM-E per flask was 15 000 (0.1%) and 29 000 dpm (0.2%), respectively. Triplicate flasks were used in these experiments.

DMS medium (9), pH 4.5, with trace elements according to ref 8 and with 0.1% yeast extract, was used for cultivation of *S. pulverulentum*. The concentrations, based on dry weight of HM-C and HM-E, were 0.1 and 0.2%, and the amount of radioactivity in each flask was the same as in the bacterial cultures. Flasks were inoculated with  $2.8 \times 10^6$  spores/mL and incubated at either 28 or 38  $^{\circ}\text{C}$  for 98 days in standing culture. Triplicate flasks were used in these experiments.

**Determination of Evolved  $^{14}\text{CO}_2$ .** Evolved  $^{14}\text{CO}_2$  from the HM-C and HM-E stages was absorbed in 1 M NaOH and quantified as described in ref 10. Samples were taken every third or fourth day.

#### Results and Discussion

**Microbial Degradation of  $^{14}\text{C}$  Ring Labeled High Relative Molecular Mass Chlorolignins and  $^{14}\text{C}$  Ring Labeled DHP.** Only a very low degradation was obtained when two mixed bacterial cultures (Fiskeby 1 and K ppala) were cultivated on the high relative molecular mass fraction of the chlorination (C) stage (HM-C) (Figure 1a). Less than 3% of the total  $^{14}\text{C}$  in the HM-C was converted to  $^{14}\text{CO}_2$  after more than 3 months of incubation. However, considerable degradation of labeled HM-C occurred in static cultures of the white-rot fungus *Sporotrichum pulverulentum*. After 6 weeks almost 40% of the total  $^{14}\text{C}$  in the HM-C was converted to  $^{14}\text{CO}_2$ . As seen in Figure 1b, degradation of the HM-C was dependent upon both substrate concentration and temperature. Although the fungus grows optimally at 38  $^{\circ}\text{C}$ , HM-C was degraded most rapidly at 28  $^{\circ}\text{C}$ . This may be related to



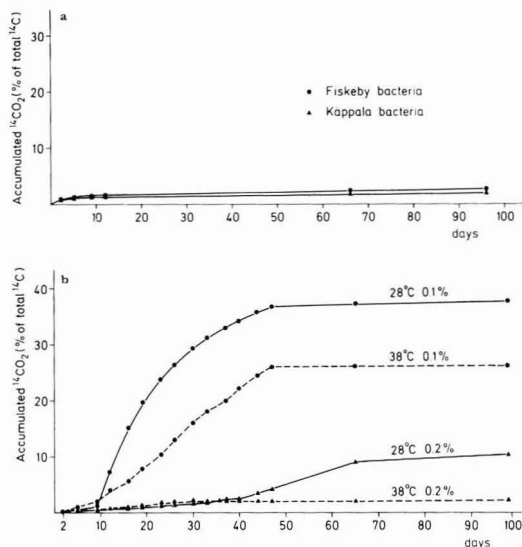


**Figure 1.** (a) Evolution of  $^{14}\text{CO}_2$  from the  $^{14}\text{C}$ -labeled high molecular mass fraction (0.2%) of the chlorination stage (HM-C) by two mixed bacterial cultures. (b) Evolution of  $^{14}\text{CO}_2$  from the  $^{14}\text{C}$ -labeled high molecular mass fraction (0.1 or 0.2%, respectively) of the chlorination stage (HM-C) by the white-rot fungus *Sporotrichum pulverulentum*.

lower  $\text{O}_2$  solubility at the higher temperature.

Bacterial and fungal degradation of the  $^{14}\text{C}$ -labeled high relative molecular mass fraction of the E stage (HM-E) is shown in parts a and b of Figure 2, respectively. Although  $^{14}\text{CO}_2$  evolution from the HM-E is higher than that from the HM-C, bacterial degradation of the HM-E is also limited and amounted to only 4% in 3 months. On the other hand, the fungus converted up to 50% of the total  $^{14}\text{C}$  to  $^{14}\text{CO}_2$  within 2 months. As before, higher  $^{14}\text{CO}_2$  yields were obtained at the lower temperature, although the concentration of the HM-E did not appear to influence degradation as much as in the case of HM-C. All values are corrected for  $^{14}\text{CO}_2$  evolution in uninoculated controls. It should be noted that  $^{14}\text{CO}_2$  evolution in uninoculated controls containing bacterial or fungal medium amounted to between 4 and 5% of total radioactivity in both cases.

To investigate if the observed low rate of degradation of lignin polymers is a common feature of bacterial mixtures obtained from aerated lagoons receiving spent bleach liquors, three additional bacterial mixtures (Frövifors, Fiskeby 2, and Korsnäs-Marma) were used in degradation studies.  $^{14}\text{C}$  ring labeled synthetic lignin (DHP) was used in these experiments due to the exhaustion of stocks of  $^{14}\text{C}$ -labeled HM-C and HM-E. It was clear from these experiments that the used bacteria degraded also synthetic lignin very slowly. Furthermore, the DHP (11) may be of considerably lower relative molecular mass than the HM-C and HM-E fractions. The chlorine in these fractions is most likely an additional obstacle to rapid degradation.

In view of this, it seems safe to predict that the  $^{14}\text{CO}_2$  produced from the HM-C and HM-E fractions by the bacteria may emanate from residual low molecular mass compounds in the ultrafiltered fractions. The rates for bacterial degradation of HM-C and HM-E are probably too low to make such degradation a feasible process under technical conditions. The residence time of water in aerated lagoons is normally less than 1 week.

What potential exists for using fungi, i.e., white-rot fungi, in technical processes designed for the degradation of

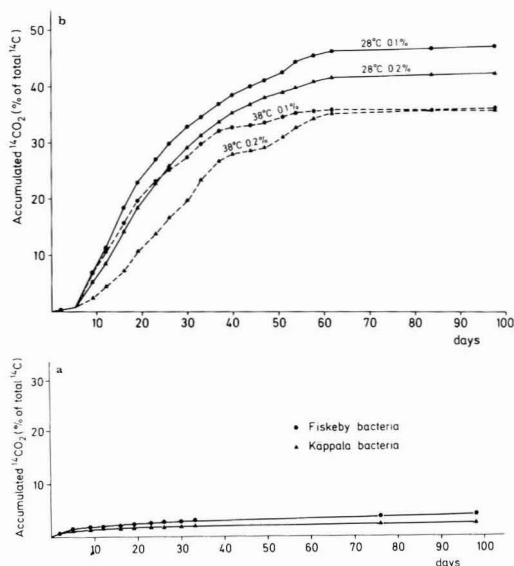


**Figure 2.** Evolution of  $^{14}\text{CO}_2$  from the  $^{14}\text{C}$ -labeled high molecular mass fraction of (0.2%) of the alkaline extraction stage (HM-E) by two mixed bacterial cultures. (b) Evolution of  $^{14}\text{CO}_2$  from the  $^{14}\text{C}$ -labeled high molecular mass fraction (0.1 or 0.2%, respectively) of the alkaline extraction stage (HM-E) by the white-rot fungus *Sporotrichum pulverulentum*.

HM-C and HM-E and for purification of spent bleach liquors? Clearly, the fungus used in this study, *S. pulverulentum*, degrades chlorolignins very much faster than bacteria. Before answering this question, it is necessary to examine the physiological requirements for the degradation of lignins by white-rot fungi. Lignin degradation is energy demanding, this energy being supplied by sugars derived from wood polysaccharides through the action of polysaccharide-hydrolyzing enzymes (12). Oxidation of these sugars may also supply most of the hydrogen peroxide which is essential for lignin degradation to take place (13–15). Degradation of wood polysaccharides occurs when the fungus *S. pulverulentum* (*Phanerochaete chrysosporium*) is in primary growth phase whereas lignin metabolism ( $[^{14}\text{C}]\text{lignin} \rightarrow ^{14}\text{CO}_2$ ) is a feature of secondary metabolism (11, 16). Ligninolytic activity is "triggered" under conditions of nitrogen starvation (16) and, under laboratory conditions, occurs only in static cultures (11). This latter feature has been interpreted as a need for physical contact between the lignin and the fungal cell wall. Since lignin degradation mechanisms are highly oxidative in nature (11, 17, 18), it is not surprising to find also that degradation is also markedly stimulated by a high  $\text{O}_2$  concentration in the medium.

Although systems may be designed where these physiological demands are satisfied (19), achieving such conditions is not without problems. We are currently studying various possibilities aimed at developing efficient fungal systems for the purification of spent bleach water, with particular emphasis on the degradation of the polymeric material.

#### Acknowledgments

We thank E. Odier, Institut National Agronomique, Paris, for labeling the lignin in growing spruce plants and T. K. Kirk, Forest Products Laboratory, Madison, WI, for

generously supplying the synthetic  $^{14}\text{C}$  ring labeled lignin (DHP). We gratefully acknowledge the skillful technical assistance from Inger Nordh.

**Registry No.** Chlorolignin, 8068-02-8.

# Literature Cited

- (1) Kringstad, K. P.; Lindström, K. *Environ. Sci. Technol.* **1984**, *8*, 236A.
- (2) Kringstad, K. P.; Stockman, L. G.; Strömberg, L. H. *J. Wood Chem. Technol.* **1984**, *3*, 389.
- (3) Neilson, A. H.; Allard, A.-S.; Hynning, P.-Å.; Remberger, M.; Landner, L. *Appl. Environ. Microbiol.* **1983**, *45*, 774.
- (4) Eriksson, K.-E.; Kolar, M.-C.; Ljungquist, P.; Kringstad, K. P. *Environ. Sci. Technol.*, in press.
- (5) Odier, E.; Janin, G.; Monties, B. *Appl. Environ. Microbiol.* **1981**, *41*, 337.
- (6) Eriksson, K.-E.; Kolar, M.-C.; Kringstad, K. P. *Sven. Papperstidn.* **1979**, *82*, 95.
- (7) Burdsall, H. H., Jr. *Mycologia* **1981**, *73*, 675.
- (8) Ander, P.; Eriksson, K.-E. *Arch. Microbiol.* **1976**, *109*, 1.
- (9) Fenn, P.; Kirk, T. K. *Arch. Microbiol.* **1979**, *123*, 307.

- (10) Ander, P.; Hatakka, A.; Eriksson, K.-E. *Arch. Microbiol.* **1980**, *125*, 189.
- (11) Kirk, T. K.; Schultz, E.; Connors, W. J.; Lorenz, L. F.; Zeikus, J. G. *Arch. Microbiol.* **1978**, *117*, 277.
- (12) Eriksson, K.-E. *Biotechnol. Pulp Pap. Ind., Proc.* **1983**, *63*.
- (13) Eriksson, K.-E.; Pettersson, B.; Volc, J.; Musilek, V. *Appl. Microbiol. Biotechnol.*, in press.
- (14) Reddy, C. A.; Forney, L. J.; Kelley, R. L. In "Recent Advances in Lignin Biodegradation Research"; Higuchi, T.; Chang, H.; Kirk, T. K., Eds.; Uni Publishing Co. Ltd.: Tokyo, 1983; p 153.
- (15) Ander, P.; Eriksson, K.-E. *Appl. Microbiol. Biotechnol.* **1985**, *21*, 96.
- (16) Jeffries, T. W.; Choi, S.; Kirk, T. K. *Appl. Environ. Microbiol.* **1981**, *42*, 290.
- (17) Bar-Lev, S. S.; Kirk, T. K. *Biochem. Biophys. Res. Commun.* **1981**, *99*, 373.
- (18) Faison, B. D.; Kirk, T. K. *Appl. Environ. Microbiol.* **1983**, *46*, 1140.
- (19) Joyce, T. W.; Chang, H.; Campbell, A. G., Jr.; Gerrard, E. D.; Kirk, T. K. *Biotechnol. Pulp Pap. Ind., Proc.* **1983**, *30*.

Received for review December 26, 1984. Accepted May 13, 1985.

## Fluorescence Spectroscopic Study of Kinetics of Gas-Surface Reactions between Nitrogen Dioxide and Adsorbed Pyrene

Ching-Hsong Wu\* and Hiromi Niki

Research Staff, Ford Motor Company, Dearborn, Michigan 48121

■ The kinetics of reactions between gaseous  $\text{NO}_2$  and pyrene adsorbed on silica plates was studied at  $25^\circ\text{C}$  in  $\text{N}_2$  or  $\text{O}_2/\text{N}_2$  diluent by using a fluorescence spectroscopic method. The temporal behavior of the fluorescence signal of pyrene, excited at 325 nm with a He/Cd cw laser, was monitored as a function of wavelength, excitation light intensity, and the concentrations of gaseous  $\text{NO}_2$ ,  $\text{O}_2$ , and adsorbed pyrene. For monodispersed samples, the fluorescence signals followed first-order kinetics with respect to  $\text{NO}_2$  concentrations from 0 to 180 ppm. Apparent bimolecular rate constants were determined to be  $(8.2 \pm 1.0) \times 10^{-3}$  and  $(1.1 \pm 0.23) \times 10^{-3} \text{ ppm}^{-1} \text{ min}^{-1}$  in  $\text{N}_2$  and in air, respectively. Possible explanations for an  $\text{O}_2$  inhibition effect were discussed.

### Introduction

Reactions between surface-adsorbed polycyclic aromatic hydrocarbons (PAH) and gaseous  $\text{NO}_2$  have been the subject of numerous studies for the purposes of assessing the atmospheric fate and the biological effects of particulate PAH and their reaction products (1-10). Although several products such as mononitro- and dinitro derivatives of PAH have been qualitatively identified, the reported reaction rates or PAH half-lives varied over a wide range. This large variation is presumably due to the differences in experimental conditions, e.g., substrate surface, reactant concentration, and exposure time. However, an apparent decreasing trend in reported conversion rates can be noted in recent years. For example, this trend can be illustrated by the  $\text{NO}_2$  reactions with one of the most widely studied PAH, i.e., benzo[a]pyrene (BaP). In the earliest work, Kotin et al. (3) made a qualitative observation although the detailed experimental conditions were not given. They found a substantial (60%) loss of BaP deposited on filter papers and exposed to  $\text{NO}_2$ . Subsequently, Pitts et al. (4)

reported 19-40% conversions of BaP deposited on glass-fiber filters and exposed to  $\text{NO}_2$  (0.25-1.0 ppm) for 8 h. From these results the BaP half-lives normalized to 1 ppm of  $\text{NO}_2$  were determined to be 7-14 h. The effects of substrate on PAH nitration was first studied by Jagar and Hanus (6). They reported 8-26% conversion of BaP deposited on alumina, fly ash, or silica gel and exposed to  $\text{NO}_2$  (1.33 ppm) for 4 h corresponding to BaP half-lives of 12-44 h. More recently, Grosjean and co-workers (9) reported that they could not detect any reactions between  $\text{NO}_2$  and BaP or other compounds deposited on the substrates, e.g., glass or Teflon filters with or without coating with coal fly ash or diesel particulates, after exposing to 0.1 ppm of  $\text{NO}_2$  for 3 h.

Such a wide variation in the reported rates of reactions between  $\text{NO}_2$  and PAH is commonly found in the literature and cannot be accounted for simply by the differences in experimental conditions. One possible source of error, as pointed out by Pitts et al. (4) and others (5, 8, 9), was that the trace  $\text{HNO}_3$  impurity in  $\text{NO}_2$  gas mixtures might be responsible for catalyzing the PAH nitration. Additional sources for the large variation might be the analytical procedures and sample preparation. In previous studies, the surface-adsorbed PAH were determined by the extraction of the compounds from the solid substrates with various solvents followed by concentration and analysis of the compounds by various analytical methods, e.g., high-performance liquid chromatography (HPLC), thin-layer chromatography (TLC), and gas chromatography/mass spectrometry (GC/MS). Because of the variation in reported extraction efficiencies (11, 12) and possible chemical transformation during analytical processes, these results may be uncertain. Besides, due to the destructive nature of these analytical techniques, several samples and runs were required for obtaining a single concentration-time profile. Therefore, the accuracy of rate measurements

depended greatly on the reproducibility of sample preparation and on the surface conditions. These potential problems associated with analytical technique and sample preparation could be more pronounced at low NO<sub>2</sub> concentrations and short exposure time when the yields are low.

For the kinetic study of these gas-surface reactions involving PAH, it is desirable to use a direct in situ analytical method to reduce some of the experimental uncertainties. Since many PAH are efficient fluorophores and their fluorescence spectra has been well characterized, fluorescence spectroscopy has been extensively used for identifying and quantifying minute quantities of PAH (13, 14). The application of this detection technique to the kinetic study of reactions between gaseous O<sub>3</sub> and two surface-adsorbed PAH, perylene and BaP, has been demonstrated recently in this laboratory (15). This paper describes a study of the kinetics of gas-surface reactions between NO<sub>2</sub> and PAH adsorbed on silica plates using the fluorescence spectroscopic method. For this study, a He/Cd continuous wave (cw) laser was used as the excitation light source, and pyrene was chosen as the surrogate PAH because its absorption band matched well with the laser wavelength of 325 nm. Special efforts were made to further reduce the potential uncertainties mentioned earlier by preparing the PAH samples on silica plates in a reproducible manner and by exposing these samples to uncontaminated NO<sub>2</sub>/diluent gas mixture at concentrations high enough to provide good rate measurements. Due to the strong dependence of the fluorescence spectra on several parameters, the temporal behavior of the fluorescence intensity of pyrene was monitored as a function of wavelength, excitation light intensity, and concentrations of gaseous NO<sub>2</sub> and O<sub>2</sub> and adsorbed pyrene. O<sub>2</sub> molecules were found to reduce the reaction rates substantially. The results and the pathways to explain the O<sub>2</sub> inhibition effect are presented in some detail.

### Experimental Section

The main features of the fluorescence detection system, reaction cell, sample preparation, and experimental procedures are similar to those described previously (15). This study was carried out using an improved fluorescence system that incorporated a He/Cd laser, a good stray light rejection monochromator, and an on-line minicomputer. The essential features of the fluorescence detection system and the experimental procedures are described below.

**Fluorescence Detection System and Sample Preparation.** A He/Cd cw laser (Liconix, 4050), tuned at 325 nm (~5 mW) and passed through a narrow-band filter (Melles Griot, 03D1U006), was used as the excitation light source. This new light source eliminated the interference from the scattered or reflected light that was present previously (15) when an arc lamp was used. The beam diameter was 0.15 cm near the edge of the sample plate where the light was incident. The intensity was adjusted by using UV transmission neutral density filters (ESCO Products). A double monochromator (SLM-Aminco, MC640-M, stray light rejection ratio 10<sup>-10</sup>–10<sup>-12</sup>/nm) was placed perpendicularly to the excitation beam for monitoring the fluorescence signals. A photon counter (PRA 1770) coupled to a discriminator (PRA 1763) and a cooled photomultiplier tube (EMI 9558Q) was used for measuring the fluorescence signals. Real time data acquisition/display and subsequent analysis/storage were performed with an on-line minicomputer (IBM System 9000).

The optically polished fused silica plate (Suprasil II, 5 × 1.3 × 0.16 cm) was used as the substrate upon which pyrene was deposited. The cleanliness of the surface was

critical to obtain homogeneous sample deposition. Thus, the plates were washed with a series of solvents, i.e., phosphate-free cleaning solution (Pierce Chem, RBS-pf), distilled water, 2-propanol (Baker, reagent grade), distilled water, occasionally with 2% HF solution (Baker, reagent grade), and distilled water in an ultrasonic bath for 30–60 min each. Solutions of pyrene (Aldrich, 99.9+%) in *n*-hexane (Burdick & Jackson, UV grade) at concentrations of 2–10 µg/mL were prepared freshly for each series of runs. Monodispersed samples of pyrene on the silica plates were prepared by evenly spreading a known quantity (20–40 µL) of solution and evaporating the solvent at room temperature for 3–5 min. The average coverage (100–200 Å<sup>2</sup>/molecule) was estimated from the geometric surface area of the plate and the amount of pyrene deposited. The homogeneity of the deposited layer was routinely checked by observing the fluorescence spectrum and the absolute intensity. The variation in intensity from run to run was typically within ±15%. As mentioned previously (15), the presence of monomeric emission and the absence of excimer emission were taken as an indication of monodispersed samples. A cylindrical quartz cell (6 × 4 o.d. cm) was used as the reactor for encasing sample plates and for gas exposure and fluorescence measurements. It was mounted on a four-way adjustable base for optical alignment.

**Gas Handling and Experimental Procedures.** The NO<sub>2</sub> gas mixtures at various concentrations were prepared by mixing a certified gas mixture of [NO<sub>2</sub>] = 180 ppm in N<sub>2</sub> (Air Products) with diluent gases, i.e., pure N<sub>2</sub> gas (Matheson, UHP 99.999%) and/or ultra zero air (Air Monitoring) with mass flowmeters (Teledyne-Hastings-Raydist). Total gas flow rate was maintained typically at 400 mL/min. To remove the HNO<sub>3</sub> impurity possibly present in the gas mixture, the gas stream was passed through a nylon trap (25 × 0.6 o.d. cm Teflon tubing filled with nylon fibers (Monsanto, type 1878)) since nylon filters are widely used as HNO<sub>3</sub> traps (16, 17). The NO<sub>2</sub> concentration downstream of the reactor was measured by using a chemiluminescence NO/NO<sub>x</sub> detector (CSI, 1600).

To begin an experiment, a freshly prepared sample plate was placed vertically at the center of the reactor with the set diluent gas flow and aligned optically for fluorescence measurements. As in the previous work (15), the optimal arrangement was accomplished by adjusting the plate nearly parallel (~15 deg) to the excitation beam, and the exciting light was incident on the edge of the plate. With this configuration, the background decay of pyrene fluorescence in diluent gases was minimal because the excitation light was internally reflected in the silica plate and diffused over a large area.

A fluorescence spectrum in the wavelength range between 350 and 550 nm was recorded in diluent gas before each kinetic measurement to check the extent of the sample dispersion. The temporal behavior of the fluorescence intensity at 394 nm was then monitored continuously before and after introduction of the reaction gas mixture. At the end of each run, another complete spectrum was recorded to establish the base line and to inspect spectral features attributable to reaction products.

### Results and Discussion

#### Fluorescence Spectra of Surface-Adsorbed Pyrene.

The fluorescence spectrum of the adsorbed pyrene was found to be affected by several factors such as the extent of sample dispersion and quenching or chemical conversion by the gaseous molecules. In Figure 1, curve A is a typical fluorescence spectrum of pyrene monodispersed on a silica plate in N<sub>2</sub> atmosphere. The estimated surface coverage

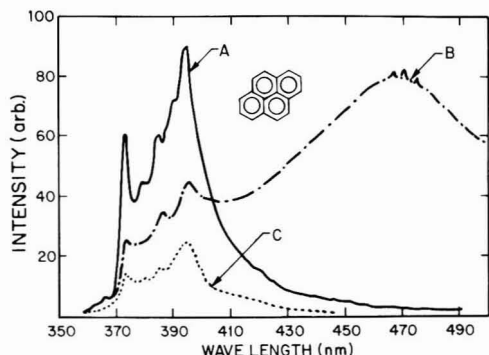


**Figure 1.** Fluorescence spectra of pyrene adsorbed on silica plates: (A) monodispersed sample in  $N_2$ ; (B) aggregated sample in  $N_2$ ; (C) monodispersed sample in air.

of the sample was about  $6.7 \times 10^{13}$  molecules/cm<sup>2</sup> which corresponded to roughly one-third of a monolayer. Vibrational structures at 374, 380, 385, 390, and 394 nm are observed. The wavelengths of these bands are nearly identical with the fluorescence bands observed from monomers in a diluted cyclohexane solution (18). This spectrum suggests no significant perturbation due to substrate interaction. The 394-nm band is the most intense and is used for monitoring the temporal variation of the pyrene concentration.

Curve B in Figure 1 corresponds to a fluorescence spectrum of pyrene adsorbed on a sample plate with a 5-fold increase in surface concentration. Compared with curve A, the intensity and the resolution of the vibrational bands between 374 and 394 nm decreased, and a new broad band with a maximum near 470 nm was observed. This broad feature of the fluorescence spectrum indicates the formation of excited dimers (excimers) via the Förster-Kasper mechanism (19). The formation of the excimers is commonly observed in concentrated solutions (20), crystals (21), and aggregated films (22) where the molecules are in close proximity.

Curve C in Figure 1 shows a fluorescence spectrum obtained in air from the same monodispersed pyrene sample from which curve A was obtained. Although the spectral features, e.g., band locations and their relative intensities are similar in these two spectra, the absolute fluorescence intensity of curve C is lower than that of curve A by a factor of more than 4. The amount of reduction in the fluorescence intensity decreased with the decrease of the  $O_2$  concentration in diluent gas, and the reduction is reversible. Curve A in Figure 2 shows a temporal fluorescence profile as the  $N_2$  and air diluent gases were alternately admitted into the reactor. It is seen that the fluorescence intensity of pyrene decreased sharply as  $N_2$  was replaced by air and recovered gradually as air, or specifically,  $O_2$  was purged from the reactor by  $N_2$ . This effect is consistent with the fluorescence quenching by  $O_2$  molecules via intersystem crossing of pyrene in the excited single-triplet states (23).

In the case of chemical reactions with  $NO_2$ , the fluorescence loss is not reversible. Curve B in Figure 2 shows that the fluorescence signal of a monodispersed pyrene sample in  $N_2$  decreases rapidly upon exposure to 90 ppm of  $NO_2$  in  $N_2$ . The decay of fluorescence signal ceases when pure  $N_2$  is readmitted. This loss of fluorescence signal is not recovered even after 5 min (>20 changes of reactor gas volume) when  $NO_2$  gas is expected to be almost totally removed from the reactor. The irreversible

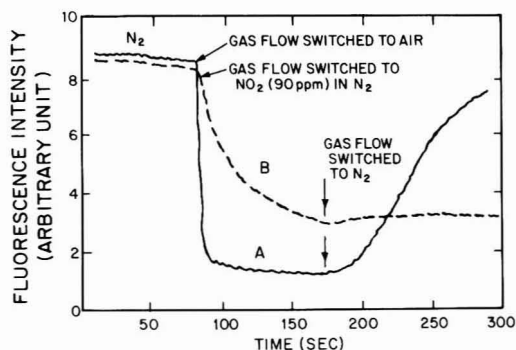


**Figure 2.** Effect of gas composition on fluorescence signals of monodispersed pyrene: (A) reversible fluorescence quenching in  $N_2$  and in air; (B) irreversible fluorescence decay in  $NO_2$ .

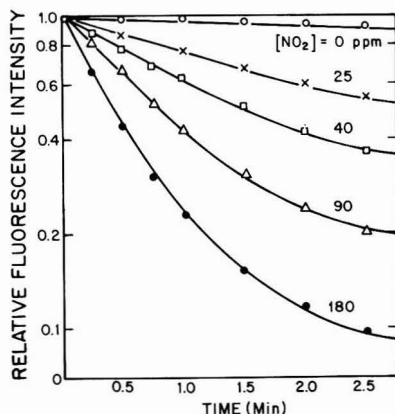


**Figure 3.** Decays of fluorescence signals of monodispersed pyrene at various  $NO_2$  concentrations.

loss of the fluorescence can be attributed to the chemical reactions between  $NO_2$  and pyrene. Further evidence for chemical reactions of adsorbed pyrene with  $NO_2$  obtained by product analysis will be discussed later.

**Kinetic Study of Reactions between  $NO_2$  and Pyrene.** The kinetics of chemical reactions between gaseous  $NO_2$  and monodispersed pyrene samples was studied at room temperature. The temporal behavior of the fluorescence signal was measured for various  $[NO_2]$  in pure  $N_2$  or in  $O_2/N_2$  diluent gas. Figure 3 shows a semilog plot of the fluorescence intensity vs. exposure time at different  $[NO_2]$  in  $N_2$  diluent. The fluorescence decays are observed to be exponential from the beginning to a substantial portion of the reactions with somewhat slower decreases at the end. These first-order decay rates are proportional to the  $NO_2$  concentrations ranging from 0 to 180 ppm as shown in Figure 4. The linear relationship indicates that the major reacting species in the gas mixture is  $NO_2$  rather than its dimer ( $N_2O_4$ ) since the reactions with  $N_2O_4$  will yield a square dependence on concentrations. The results in Figure 4 were analyzed by using pseudo-first-order rate eq 1 as described in the previous paper (15)

$$-d \ln [Py]/dt = k[NO_2] \quad (1)$$

where  $[Py]$  = pyrene concentration (molecule cm<sup>-2</sup>),  $[NO_2]$  = gaseous  $NO_2$  concentration (ppm), and  $k$  = apparent bimolecular rate constant (ppm<sup>-1</sup> min<sup>-1</sup>).

A rate constant,  $k = (8.2 \pm 1.0) \times 10^{-3}$  ppm<sup>-1</sup> min<sup>-1</sup>, was derived from the slope of the least-squares fitted straight

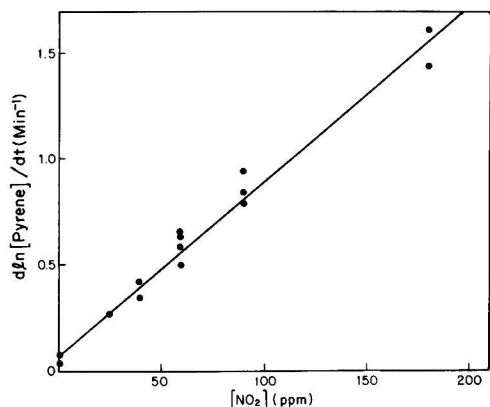


Figure 4. First-order decay rates of pyrene plotted as a function of  $\text{NO}_2$  concentration.

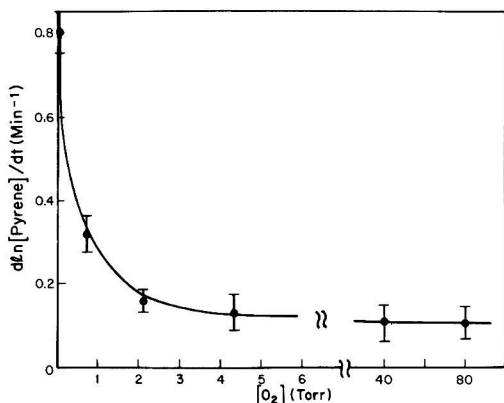


Figure 5. Effect of  $\text{O}_2$  concentration on the decay rates of pyrene fluorescence at  $[\text{NO}_2] = 90$  ppm.

line in Figure 4. On the basis of this rate constant, a half-life ( $0.639/k$ ) of 1.4 h was calculated for pyrene adsorbed on silica plates exposed to  $[\text{NO}_2] = 1$  ppm in  $\text{N}_2$ .

With the  $\text{O}_2/\text{N}_2$  diluent, the pyrene fluorescence signals decreased as mentioned above, and the  $\text{NO}_2$ -pyrene reaction rates were markedly reduced. Figure 5 shows the first-order decay rates plotted vs.  $[\text{O}_2]$  at  $[\text{NO}_2] = 90$  ppm. It should be noted that only a small amount, e.g., 0.5 torr of  $\text{O}_2$  in  $\text{N}_2$  diluent, reduces the pyrene decay rate to half of that in pure  $\text{N}_2$ . For  $[\text{O}_2] > 4$  torr, the reaction rate reached essentially a constant value. From this value, a bimolecular rate constant in air,  $k = (1.1 \pm 0.23) \times 10^{-3} \text{ ppm}^{-1} \text{ min}^{-1}$ , was derived. This corresponds to a half-life = 10.5 h, about a factor of 8 longer than that in  $\text{N}_2$ .

This apparent  $\text{O}_2$  inhibition effect on the reactions between  $\text{NO}_2$  and adsorbed pyrene was not reported previously and required further investigation. Because fluorescence spectroscopy was used in this study, it is possible that this inhibition effect was caused by artifact introduced by this analytical method, e.g., laser-induced photochemistry. Two laser-induced pathways (A and B) which have the potential of causing such an  $\text{O}_2$  effect are discussed and examined below.

**(A) Reactions of O Atoms with Pyrene.** In diluent  $\text{N}_2$ ,  $\text{O}(^3\text{P})$  atoms can be generated by photodissociation of  $\text{NO}_2$  (24) near the sample surface by the UV excitation light. These O atoms may react with surface-adsorbed

Table I. Effect of Excitation Light Intensity on Rate Measurement of Surface-Adsorbed Pyrene Reactions with Gaseous  $\text{NO}_2$  at  $[\text{NO}_2] = 60$  ppm in  $\text{N}_2$ <sup>a</sup>

% intensity excitation light	$R_0$ , $\text{min}^{-1}$	$R_1$ , $\text{min}^{-1}$	$R_1 - R_0$ , $\text{min}^{-1}$
100	0.083	0.63	0.55
100	0.090	0.65	0.56
100	0.070	0.58	0.51
50	0.037	0.65	0.61
50	0.040	0.61	0.57
30	0.030	0.63	0.60

<sup>a</sup>  $R_0$ , first-order decay rates in  $\text{N}_2$ .  $R_1$ , first-order decay rates in  $[\text{NO}_2] = 60$  ppm in  $\text{N}_2$ .

pyrene and be responsible for the fast reactions observed in  $\text{N}_2$ . However, in the presence of  $\text{O}_2$  molecules O atoms can be removed via the reaction  $\text{O} + \text{M} \rightarrow \text{O}_3 + \text{M}$ ; thus, the observed reaction rates are reduced. The steady-state O atom concentration can be shown to be proportional to the excitation light intensity and  $[\text{NO}_2]$ , and it decreases with the increase of  $[\text{O}_2]$ . This pathway qualitatively predicts the kinetic behaviors of the pyrene reactions with respect to  $\text{NO}_2$  and  $\text{O}_2$  as shown in Figures 4 and 5. And the slower rates in the high  $[\text{O}_2]$  region presumably are due to the reactions of pyrene with  $\text{O}_3$  which is in a steady concentration. In addition, it also predicts a linear relationship between the observed rate and the excitation light intensity.

**(B) Reactions of Photoexcited Pyrene with  $\text{NO}_2$ .** The observed fluorescence signals of pyrene originate from molecules in the electronically excited singlet state excited by the laser light. These energetic pyrene molecules may react more rapidly with  $\text{NO}_2$  than those in the ground state to cause faster observed rates in  $\text{N}_2$ . However, in the presence of  $\text{O}_2$ , the excited pyrene molecules may be quenched by  $\text{O}_2$  which is known to be an efficient fluorescence quencher (23); hence, the reaction rates are reduced. This pathway also qualitatively explains the experimental results that the reaction rates are proportional to  $[\text{NO}_2]$  and decrease with the increase of  $[\text{O}_2]$  until reaching a constant value where the reactions between the ground-state pyrene and  $\text{NO}_2$  become dominant. This mechanism, again, predicts the linear relationship between the observed rates and light intensities.

Since both mechanisms predict a linear dependence of reaction rates on the excitation light intensity, a series of rate measurements was made at different light levels to test this relationship. The results of six runs at three intensity levels obtained at  $[\text{NO}_2] = 60$  ppm in  $\text{N}_2$  are shown in Table I. It is seen that the background decay rates in diluent  $\text{N}_2$ ,  $R_0$ , show dependence on the light intensity; nevertheless, the net reaction rates due to reactions with  $\text{NO}_2$ ,  $R_1 - R_0$ , remain approximately constant with the light intensity changed by a factor of 3. From these results both pathways A and B were ruled out as the cause of the  $\text{O}_2$  inhibition. In order to account for the  $\text{O}_2$  inhibition effect, pathway C is proposed.

**(C) Reactions between  $\text{NO}_2$  and Pyrene Hindered by the Formation of  $\text{O}_2$ -Pyrene Complexes.** This mechanism assumes that the rates of reactions between pyrene and  $\text{NO}_2$  are reasonably fast in  $\text{N}_2$ . But in the presence of  $\text{O}_2$ , the adsorbed pyrene interacts with  $\text{O}_2$  molecules to form metastable complexes which are less reactive to  $\text{NO}_2$  molecules. Therefore, the rates of reactions decrease with the increase of  $[\text{O}_2]$  until reaching a constant value where most of the adsorbed pyrene is presumably associated with  $\text{O}_2$  molecules. This mechanism is consistent with the experimental results of the linear rela-



Table II. Summary of Literature Kinetic Data on Reactions of Surface-Adsorbed Pyrene with Gaseous NO<sub>2</sub>

investigators	substrate	NO <sub>2</sub> concn, ppm	exposure time	conversion, %	half-life <sup>a</sup>
Jager and Hanus (6)	fly ash	2.0	3 h	60	5 h
	fly ash	10.0	3 h	90	9 h
	Al <sub>2</sub> O <sub>3</sub>	4	4 h	7	150 h
Butler and Crossley (7)	soot	10.0	5-31 days	16-90	140 days
Tokiwa et al. (5)	filter	1.0	24 h	0.02	3500 days
this work	silica plate	10-180	0.1 h	10-90	1.4 h (N <sub>2</sub> ) 10.5 h (air)

<sup>a</sup>Half-life =  $0.693/k$ , where  $k = \ln ((100/(100 - C))/([NO_2]t))$ ,  $C$  = percent conversion,  $[NO_2]$  = concentration of NO<sub>2</sub>, and  $t$  = exposure time.

tionship with [NO<sub>2</sub>], the O<sub>2</sub> inhibition, and independence of the light intensity.

In fact, the formation of complexes between O<sub>2</sub> and aromatic compounds adsorbed on porous glass and silica gel has been reported by Ishida et al. (25, 26). They observed new adsorption spectra with distinct band structures (red shifted from the regular absorption spectra) when samples of aromatic amines were exposed to O<sub>2</sub> at 200 torr at room temperature or in liquid O<sub>2</sub> at liquid N<sub>2</sub> temperature. These authors reported that the absorbance increased with the increase of O<sub>2</sub> pressure and gradually decreased with evacuation. Similarly, the absorbance was found to increase with the decrease of temperature and to be reversible with temperature. No such absorption bands were observed in the presence of N<sub>2</sub> gas. From these observations and a model calculation, they concluded that these additional absorption bands were due to the formation of charge-transfer complexes between adsorbed aromatic compounds (electron donors) and O<sub>2</sub> molecules (electron acceptors) which adsorbed nearby. This direct evidence of complex formation provides further support for pathway C.

In order to demonstrate that the decay of the fluorescence signal in the presence of NO<sub>2</sub> was indeed due to chemical consumption of pyrene by NO<sub>2</sub> rather than physical quenching by NO<sub>2</sub>, a brief product study was carried out. To produce enough products for chemical analysis, a high surface area substrate, i.e., silica gel, was used for sample deposition. The sample of monodispersed pyrene on silica gel was exposed to NO<sub>2</sub> at 90 ppm in N<sub>2</sub>, and the products were analyzed by GC. The consumption of pyrene corresponding to the decrease of fluorescence intensity was determined, and several reaction products including 1-nitropyrene and 2-nitropyrene were tentatively identified. More detailed description of product analysis will be given elsewhere. Nevertheless, the results of this study further confirm the occurrence of chemical reactions between pyrene and NO<sub>2</sub>.

A comparison of the half-lives of adsorbed pyrene in the presence of NO<sub>2</sub> as estimated from the previous studies and the present results is summarized in Table II. Again, it is seen that the experimental conditions differ considerably and that the values of half-lives vary over several orders of magnitude. The half-life of pyrene, 10.5 h, determined from this study in air falls within the values of 5 and 150 h obtained by Jager and Hanus (6) for pyrene adsorbed on fly ash and alumina. But it is out of the range of 140 and 3500 days determined by Butler and Crossley (7) and Tokiwa et al. (5) on soot and filter paper, respectively.

To determine the effect of HNO<sub>3</sub> impurity in NO<sub>2</sub> gas mixtures on reaction rates, several related experiments were performed. One test was the comparison of the pyrene decay rates before and after the removal of the nylon filter from the gas stream. The results showed no

noticeable difference in the measured rates. Furthermore, the rates of reactions between gaseous HNO<sub>3</sub> and pyrene on silica plates were determined by using the same fluorescence detection technique. The results showed the reaction rates between pyrene and HNO<sub>3</sub> up to 10 ppm in air were slow with or without 100% humidity. The upper limit of the rate constant was estimated to be a factor of 2 higher than that of NO<sub>2</sub> in air. This study concluded that HNO<sub>3</sub> did not substantially enhance the rate of nitration of pyrene under the present experimental conditions.

In summary, this study clearly demonstrates the occurrence of chemical reactions between gaseous NO<sub>2</sub> and pyrene adsorbed on silica plates. The fluorescence signals followed first-order kinetics with respect to NO<sub>2</sub> concentrations from 0 to 180 ppm. The apparent bimolecular rate constants were obtained in both N<sub>2</sub> and air atmospheres. The presence of O<sub>2</sub> reduces the pyrene-NO<sub>2</sub> reaction rates substantially, and pathways for this O<sub>2</sub> inhibition effect were discussed. The observation of faster reaction rates at low O<sub>2</sub> concentrations suggests that the nitration of pyrene is more favorable under O<sub>2</sub>-deficient conditions such as in aged samples of exhaust gases from fuel-rich combustions. In addition, if the formation of PAH-O<sub>2</sub> charge-transfer complexes is indeed responsible for the deactivation of pyrene in NO<sub>2</sub> reactions, it is likely that this O<sub>2</sub> inhibition effect is applicable to all electrophilic reactions of surface-adsorbed PAH.

**Registry No.** NO<sub>2</sub>, 10102-44-0; O<sub>2</sub>, 7782-44-7; silica Si, 7631-86-9; pyrene, 129-00-0.

#### Literature Cited

- (1) Biologic Effects of Atmospheric Pollutants "Particulate Polycyclic Aromatic Organic Matters"; National Academy of Sciences: Washington, DC, 1972.
- (2) Committee on Pyrene and Analogues, National Research Council "Polycyclic Aromatic Hydrocarbons: Evaluation of Sources and Effects"; National Academy Press: Washington, DC, 1983.
- (3) Kotin, P.; Falk, H. I.; Mader, F.; Thomas, M. *AMA Arch. Ind. Hyg. Occup. Med.* **1954**, *9*, 153-163.
- (4) Pitts, J. N., Jr.; van Cauwenberghe, K. A.; Grosjean, D.; Schmid, J. P.; Fitz, D. R.; Belser, W. L., Jr.; Knudson, G. B.; Hynds, P. M., *Science (Washington, D.C.)* **1978**, *202*, 515-519.
- (5) Tokiwa, H.; Nakagawa, R.; Morita, K.; Ohnishi, Y. *Mutat. Res.* **1981**, *85*, 195-205.
- (6) Jager, J.; Hanus, V. *J. Hyg., Epidemiol., Microbiol., Immunol.* **1980**, *24*, 1-12.
- (7) Butler, J. D.; Crossley, P. *Atmos. Environ.* **1981**, *15*, 91-94.
- (8) Brorstrom, E.; Grennfelt, P.; Lindskog, A. *Atmos. Environ.* **1983**, *17*, 601-605.
- (9) Grosjean, D.; Fung, K.; Harrison, J. *Environ. Sci. Technol.* **1983**, *17*, 673-679.
- (10) Hughes, M. M.; Natusch, D. F. S.; Taylor, D. R.; Zeller, M. V., in "Polycyclic Aromatic Hydrocarbons: Chemistry and Biological Effects"; Bjorseth, A.; Dennis, A. J., Eds.; Battelle

- Press: Columbus, OH, 1980; pp 1-8.
- (11) Lee, F. S. C.; Pierson, W. R.; Ezike, J. *Polynucleot. Aromat. Hydrocarbons: Chem. Biol. Eff., Int. Symp., 4th* 1980, 1979, 543-563.
  - (12) Griest, W. H.; Caton, J. E. In "Handbook of Polycyclic Aromatic Hydrocarbons"; Bjorseth, A., Ed.; Marcel Dekker: New York, 1983; pp 95-148.
  - (13) Lee, M. L.; Novotny, M. V.; Bartle, K. D. "Analytical Chemistry of Polycyclic Aromatic Hydrocarbons"; Academic Press: New York, 1981.
  - (14) Sawicki, E.; Hauser, T. R.; Stanley, T. W. *J. Air Pollut. Control* 1980, 2, 253-272.
  - (15) Wu, C. H.; Salmeen, I.; Niki, H. *Environ. Sci. Technol.* 1984, 18, 603-607.
  - (16) Grosjean, D. *Anal. Lett.* 1982, 15, 783-796.
  - (17) Sanhueza, E.; Plum, D. N.; Pitts, J. N., Jr. *Atmos. Environ.* 1984, 18, 1029-1031.
  - (18) Berlman, I. B. "Handbook of Fluorescence Spectra of Aromatic Molecules", 2nd ed.; Academic Press: New York, 1971.
  - (19) Förster, T.; Kasper, K. Z. *Elektrochem.* 1954, 59, 976-988.
  - (20) Parker, C. A.; Hatchard, C. G. *Trans. Faraday Soc.* 1963, 59, 284; *Nature (London)* 1961, 190, 165.
  - (21) Uchida, K.; Takahashi, Y. *J. Lumin.* 1981, 24/25, 453-456.
  - (22) Takahashi, Y.; Kitamura, T. *J. Lumin.* 1980, 21, 425-433.
  - (23) Birks, J. D. "Photophysics of Aromatic Molecules"; Wiley-Interscience: New York, 1970.
  - (24) Wu, C. H.; Niki, H. *Environ. Sci. Technol.* 1975, 9, 46-52.
  - (25) Ishida, H.; Takahashi, H.; Sato, H.; Tsubomura, H. *J. Am. Chem. Soc.* 1970, 92, 275-280.
  - (26) Ishida, H.; Takahashi, H.; Tsubomura, H. *Bull. Chem. Soc. Jpn.* 1970, 43, 3130-3136.

Received for review January 8, 1985. Accepted May 10, 1985.

## The Mutagenic Activity of the Products of Ozone Reaction with Propylene in the Presence and Absence of Nitrogen Dioxide

Paul B. Shepson,\* Tadeusz E. Kleindienst, and Edward O. Edney

Northrop Services, Inc.—Environmental Sciences, Research Triangle Park, North Carolina 27709

Larry T. Cupitt

Atmospheric Sciences Research Laboratory, United States Environmental Protection Agency, Research Triangle Park, North Carolina 27711

Larry D. Claxton

Health Effects Research Laboratory, United States Environmental Protection Agency, Research Triangle Park, North Carolina 27711

■ This study was performed to determine if propylene reaction with ozone could account for the large mutagenic activity we have observed in irradiated propylene/NO<sub>x</sub> mixtures. In a 22.7-m<sup>3</sup> flow mode smog chamber, 5.4 ppm of propylene was allowed to react with 0.9 ppm of ozone either in the presence or in the absence of 0.2 ppm of nitrogen dioxide (at 25 °C in the dark). The steady-state reactant and product distribution was then tested for total mutagenic activity by exposing *Salmonella typhimurium* strain TA100 to the gas-phase chamber effluent. The total product dosage in the test plates was varied by exposing them for 0, 5, 10, 15, and 20 h. *Salmonella typhimurium* survivor levels were obtained at each length of exposure. The number of revertants per plate increased at a rate of ~4-5 per hour, while the survivor level decreased throughout the exposure. Most of the total mutagenic activity can be accounted for by the presence of formaldehyde. The total mutagenic activity observed was, however, much smaller than that observed in the irradiated propylene/NO<sub>x</sub> system, for comparable amounts of propylene consumed.

### Introduction

There has been increased concern in recent years that the photochemical conversion of gas-phase pollutants can lead to the production of atmospheric mutagens (1). We have recently demonstrated that a simulated urban air mass can be tested for total mutagenic activity using an adapted version of the Ames test (2), by allowing gas-phase pollutants to dissolve into the test medium during a gas-phase exposure. We have also recently reported that a relatively simple atmospheric hydrocarbon, propylene

(C<sub>3</sub>H<sub>6</sub>), can be photochemically converted into fairly strong gas-phase mutagens (3). In the case of C<sub>3</sub>H<sub>6</sub>, we have found that an exposure of *Salmonella typhimurium* strain TA100 to the products of an irradiated C<sub>3</sub>H<sub>6</sub>/NO<sub>x</sub> mixture at a long extent of reaction, in which reactions of ozone (O<sub>3</sub>) and NO<sub>3</sub> with C<sub>3</sub>H<sub>6</sub> occur, leads to a substantially increased mutagenic activity. At shorter reaction times, where the dominant C<sub>3</sub>H<sub>6</sub> reaction path is with OH radicals, moderate mutagenic activity was observed. In addition, we have recently found that C<sub>3</sub>H<sub>6</sub> reaction with NO<sub>3</sub> could not account for a significant fraction of the total response at long extents of reaction (3). The major reaction products, i.e., ozone, formaldehyde, acetaldehyde, nitric acid, hydrogen peroxide, and peroxyacetyl nitrate, were also shown to contribute only a small fraction of the total response. We, therefore, have turned our attention toward reactions of O<sub>3</sub> with C<sub>3</sub>H<sub>6</sub>, with the idea that some unidentified ozonolysis product might be found to be a strong mutagen.

To assess the extent that the products of the C<sub>3</sub>H<sub>6</sub>/O<sub>3</sub> reaction are mutagens, we mixed ~5.4 ppm of C<sub>3</sub>H<sub>6</sub> and 0.9 ppm of O<sub>3</sub> in a continuously stirred tank reactor (in the dark) at a reactor residence time of  $\tau = 2.7$  h (where  $\tau = \text{chamber volume}/\text{total flow rate}$ ). The steady-state distribution of reactants and products was allowed to flow through exposure chambers loaded with Petri plates containing *S. typhimurium* strain TA100. The bacteria were then exposed to the effluent for 0, 5, 10, 15, and 20 h by covering the plates at these times. A possibility that we also wished to address was whether or not the intermediate free radicals present from the ozonolysis reactions could react with NO<sub>2</sub> to yield mutagenic products. We have

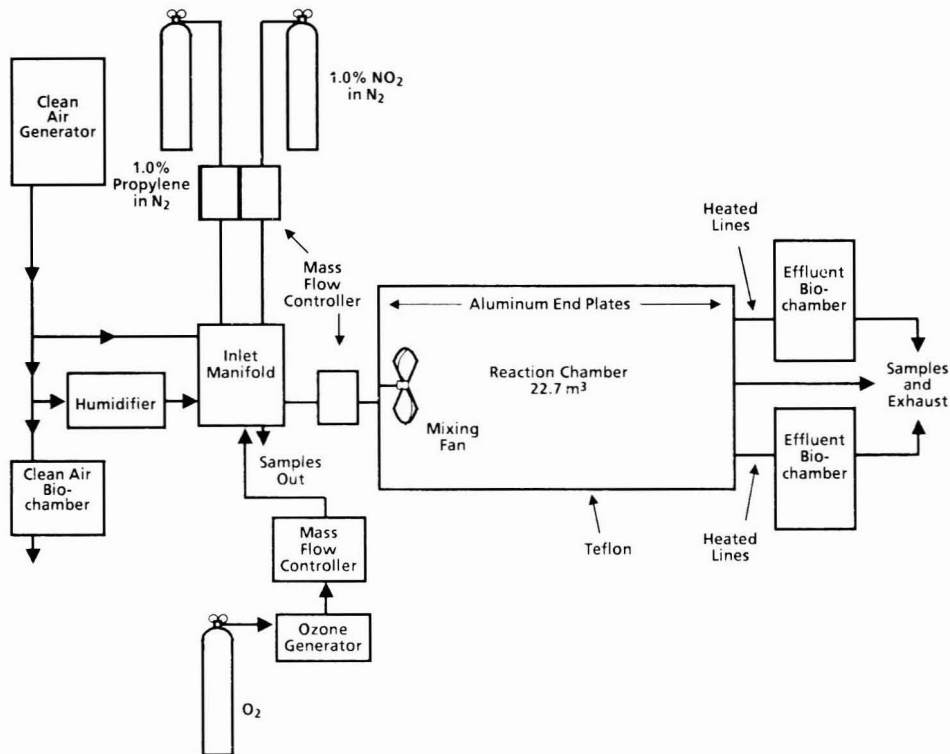


Figure 1. Schematic diagram of the reaction chamber and exposure apparatus.

shown that some organic nitrates and peroxy nitrates (such as PAN) are mutagenic (3).

In this paper, we present the results of the bioassays conducted with the products of the  $O_3$  reaction with  $C_3H_6$  in the presence and absence of  $NO_2$ . It is shown that most of the response can be accounted for by the presence of formaldehyde (HCHO), which is a weak mutagen. We will also discuss the extent to which the  $O_3$  reaction can account for the observed mutagenic activity in the irradiated  $C_3H_6/NO_x$  mixtures. The technique employed is shown to be an effective means of obtaining dose-response curves for volatile compounds.

#### Experimental Section

These experiments were conducted in a 22.7-m<sup>3</sup> Teflon smog chamber, at 25 °C. (A schematic diagram of the experimental apparatus is presented in Figure 1.) The reactant gases were metered through mass flow controllers into a 150-L stainless steel input manifold, where they were mixed and diluted to their final concentrations. The total input flow was controlled with a 150 L/min mass flow controller. Ozone was produced with a Welsbach Model T-408  $O_3$  generator supplied with zero grade  $O_2$  (MG Scientific). The  $NO_2$  and  $C_3H_6$  were obtained from MG Scientific as 1% mixtures in  $N_2$ . Clean air was provided by an AADCO clean air generator supplied with compressed air. The reaction chamber air did not contain added humidity, although there was some water present due to diffusion through the bag.

During these experiments, the following reactant and product concentrations were periodically measured:  $C_3H_6$ ,  $O_3$ ,  $NO_x$ , HCHO, peroxyacetyl nitrate (PAN), acetaldehyde ( $CH_3CHO$ ), propylene glycol dinitrate (PGDN), 2-hydroxypropyl nitrate (2-HPN), and 2-(nitrooxy)propyl

alcohol (2-NPA). The analytical procedures employed have been described previously in detail (2, 4).

The exposures were conducted by bringing the reactant (as measured in the inlet manifold) and product concentrations to steady-state values at a reactor residence time of 2.7 h. The reactor effluent was then continuously transferred (at 14 L/min) through heated ( $\sim 50$  °C) Teflon lines (9.5 mm i.d.) to two 190-L exposure chambers. The Teflon lines are heated to maximize transfer efficiency of products to the exposure chambers. Heating of the lines does not significantly increase the exposure chamber temperature (25 °C). The clean air was tested for mutagenic activity (as a control) by passing it through a clean air exposure chamber, as shown in Figure 1.

The biological assay used in this work employs the bacteria *S. typhimurium*, strain TA100. The plates were prepared by adding 0.1 mL of the *S. typhimurium* culture to 3 mL of an agar overlay at 45 °C. This mixture was then poured onto  $\sim 45$  mL of plate agar in a glass Petri plate. The *S. typhimurium* tester strain TA100 was provided by Dr. Bruce Ames (University of California, Berkeley, CA). Colony counting was done with an Artec 880 automatic colony counter using previously published guidelines (5). The test procedures used were those of Ames et al. (6), except for the following modifications: (1) glass Petri dishes were used, (2) 45 mL of base agar per plate was used, (3) minimal histidine at the same final total concentration was placed in the bottom agar rather than the top agar, and (4) 3 mL of overlay agar with  $\sim 1 \times 10^8$  bacteria was used.

The exposures were conducted by loading each exposure chamber with 35 covered glass Petri dishes containing the *S. typhimurium* test plates and also 10 covered "survivor" plates, diluted by  $\sim 10^4$ , to which additional histidine was

**Table I. Average Reactant and Product Concentrations**

species	C <sub>3</sub> H <sub>6</sub> /O <sub>3</sub> , ppm <sup>a</sup>		C <sub>3</sub> H <sub>6</sub> /O <sub>3</sub> /NO <sub>2</sub> , ppm <sup>a</sup>	
	inlet	effluent	inlet	effluent
C <sub>3</sub> H <sub>6</sub>	5.41 (0.12)	4.39 (0.10)	5.34 (0.09)	4.39 (0.08)
O <sub>3</sub>	0.895 (0.035)	0.076 (0.004)	0.894 (0.032)	0.069 (0.002)
NO <sub>2</sub> <sup>b</sup>		(0.229 (0.020)) <sup>d</sup>	0.212 (0.012)	0.210 (0.014)
HCHO		0.588 (0.013)		0.599 (0.030)
CH <sub>3</sub> CHO		0.355 (0.006)		0.348 (0.007)
PAN		0		0.032 (0.002)
2-HPN <sup>c</sup>		0		10.5 (3.3)
2-NPA <sup>c</sup>		0		2.8 (0.9)
PGDN <sup>c</sup>		0		0.15 (0.02)

<sup>a</sup>Standard deviation in parentheses. <sup>b</sup>NO<sub>2</sub> was added to one of the two effluent biochambers in the C<sub>3</sub>H<sub>6</sub>/O<sub>3</sub> exposure. <sup>c</sup>Concentrations in ppb. <sup>d</sup>Effluent NO<sub>2</sub> biochamber.

added (the approximate 10<sup>4</sup> dilution brings the total plate bacteria concentration to ~500 per plate; therefore, in the absence of toxicity, 500 colonies per plate would form due to the added histidine). Once the exposure chambers were loaded and sealed, the exposure chamber product concentrations were allowed to approach their steady-state values. Once steady state was achieved, 28 of the bioassay test plates and eight of the survivor plates were uncovered, effectively starting the exposures for these plates. The remaining seven test and two survivor plates were covered throughout the exposure, representing a zero dose level. Then, after 5, 10, 15, and 20 h, seven test plates and two survivor plates in each exposure chamber were covered, effectively stopping the exposure at that time. There were, therefore, five different exposure levels in these experiments. At the end of the 20-h exposure period, the covered plates were removed from the exposure chambers and incubated at 37 °C for 48 h, and the final revertant and survivor colonies were counted.

In addition to the test plates, five plates containing deionized water were placed in each chamber. One of the five plates was then exposed for the same time period as the test plates (0, 5, 10, 14, and 20 h). These plates were analyzed at the end of the exposures for nitrite ion (NO<sub>2</sub><sup>-</sup>), HCHO, PGDN, 2-HPN, and 2-NPA. Formaldehyde was measured by using the chromotropic acid technique (7), and NO<sub>2</sub><sup>-</sup> was measured by ion chromatography as described previously (2). PGDN, 2-HPN, and 2-NPA were analyzed by direct injection of a small sample from the water plates into a gas chromatograph (described in ref 4).

Two experiments were conducted: one without added NO<sub>2</sub> and one with 0.2 ppm of NO<sub>2</sub> introduced into the inlet manifold. We have found that NO<sub>2</sub> solubilizes into water to yield, principally, NO<sub>2</sub><sup>-</sup>. Therefore, in the experiment in which NO<sub>2</sub> was not added to the inlet manifold, we added ~0.2 ppm of NO<sub>2</sub> directly to one of the two effluent exposure chambers. In this way, comparison of the results for these two exposure chambers would indicate whether or not reactions of the products with NO<sub>2</sub><sup>-</sup> in the test medium to produce mutagens were occurring. In the experiment with added NO<sub>2</sub>, the two effluent exposure chambers were identical.

## Results

The average reactant (inlet) and product concentrations measured during the C<sub>3</sub>H<sub>6</sub>/O<sub>3</sub> and C<sub>3</sub>H<sub>6</sub>/O<sub>3</sub>/NO<sub>2</sub> 20-h exposures are presented in Table I. The bioassay results are presented in Table II as averages of the seven plates for each of the five exposure periods. In addition, as a measure of toxicity, we report the results of the average of two survivor plates at each exposure level. The survivor plates are a measure of the surviving bacteria concentration

**Table II. Bioassay Results (*S. typhimurium* TA100)**

chamber	t, h	revertants/plate <sup>a</sup>			
		C <sub>3</sub> H <sub>6</sub> /O <sub>3</sub>		C <sub>3</sub> H <sub>6</sub> /O <sub>3</sub> /NO <sub>2</sub>	
		test plates	survivors	test plates	survivors
clean air	0	265 (38)	364	181 (19)	774
	5	235 (18)	430	198 (21)	650
	10	264 (55)	451	207 (21)	790
	15	237 (20)	426	208 (31)	720
	20	244 (23)	424	187 (27)	636
effluent "A" (or effluent + NO <sub>2</sub> )	0	206 (24)	411	174 (20)	679
	5	243 (49)	358	262 (29)	222
	10	244 (50)	196	230 (15)	0
	15	253 (56)	0	235 (43)	0
	20	290 (71)	0	244 (39)	0
effluent "B"	0	217 (12)	464	184 (30)	423
	5	246 (20)	187	189 (31)	154
	10	264 (16)	46	241 (78)	108
	15	249 <sup>b</sup>	51	288 (28)	0
	20	307 (28)	0	302 (50)	0
spontaneous		215 (27)		200 (18)	
NaN <sub>3</sub>		559		484	
laboratory survivors			535		785

<sup>a</sup>Standard deviation in parentheses for seven plates at each exposure time. <sup>b</sup>One plate only.

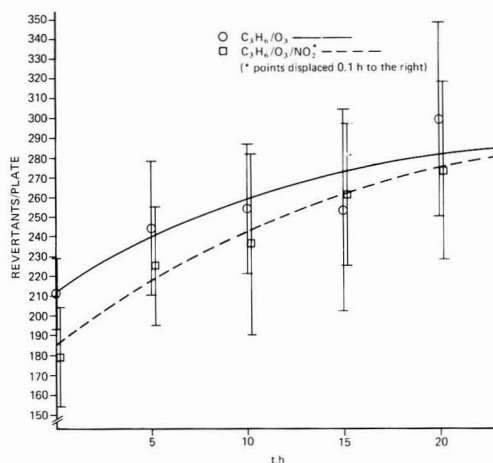


**Figure 2. Ames testing data.**

(after ~10<sup>4</sup> dilution) at the end of each exposure time. However, since the bacteria concentrations in the survivor plates are different (~10<sup>4</sup> lower) than in the test plates, the survivor data are only an indication of the possibility

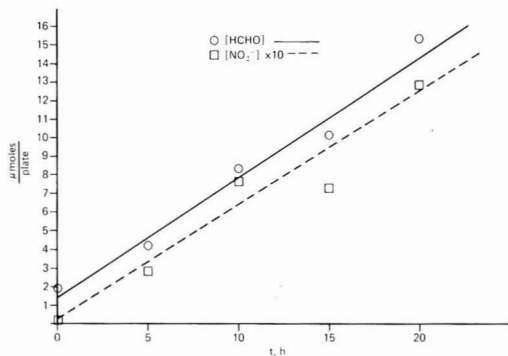


Figure 3. Water plate data, HCHO and  $\text{NO}_2^-$ .

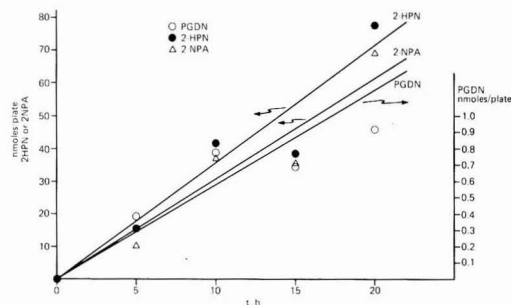


Figure 4. Organic nitrate water plate concentrations.

of toxicity effects, and do not necessarily measure the actual toxicity to the test plate bacteria (8). The bioassay data vs. exposure time is presented graphically in Figure 2, along with error bars indicating the  $\pm 1$  standard deviation uncertainties. Since, from inspection of the data in Table II, it can be seen that there is no significant difference between the results for the two effluent exposure chambers in both experiments, the data in Figure 2 are averages for the two chambers. The experiment in which  $\text{NO}_2$  was added directly to one effluent exposure chamber indicates that, in these experiments, reactions of the products with  $\text{NO}_2^-$  in the test media are not important. As shown in Figure 2, the number of revertants per plate increases measurably (but nonlinearly) with exposure time. In addition, it can be seen from Table II that the survivor levels decrease throughout the exposure and that there is no measurable increase in the clean air response with exposure time.

To determine the rate of deposition of various products into the plates during the exposures, we measured the HCHO,  $\text{NO}_2^-$ , PGDN, 2-HPN, and 2-NPA concentrations in the surrogate water plates at each exposure time. These data are presented graphically for the  $\text{C}_3\text{H}_6/\text{O}_3/\text{NO}_2$  exposure for HCHO and  $\text{NO}_2^-$  in Figure 3 and for the organic nitrates in Figure 4. Since the effluent HCHO concentrations were essentially identical in the two experiments, the HCHO data in Figure 3 are averages of the two. The data in Figures 3 and 4 demonstrate that the loading of each chemical into the water plates is linear with exposure time (with the possible exception of PGDN). We assume this is also the case with the test plates.

### Discussion

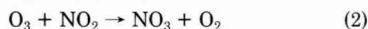
The  $\text{C}_3\text{H}_6$  concentration for these experiments was chosen to favor  $\text{O}_3$  reaction with  $\text{C}_3\text{H}_6$  rather than with  $\text{NO}_2$ , in the case of the  $\text{C}_3\text{H}_6/\text{O}_3/\text{NO}_2$  exposure. Under

Table III. Reactant and Product Mutagenic Activities, TA100

species mutagenic activity, revertants/ $\mu\text{mol}$ per plate		species mutagenic activity, revertants/ $\mu\text{mol}$ per plate	
$\text{C}_3\text{H}_6$	BD <sup>a</sup>	PAN	35
$\text{O}_3$	BD	2-HPN	3
$\text{NO}_2$	BD	2-NPA	3
HCHO	12	PGDN	BD
$\text{CH}_3\text{CHO}$	BD		

<sup>a</sup>  $\leq 2$  revertants/ $\mu\text{mol}$

the conditions of this experiment, the initial rates of reactions 1 and 2 are 71 ppb/min and 10 ppb/min, respec-



tively, using  $k_1 = 1.0 \times 10^{-17} \text{ cm}^3 \cdot \text{molecule}^{-1} \cdot \text{s}^{-1}$  and  $k_2 = 3.7 \times 10^{-17} \text{ cm}^3 \cdot \text{molecule}^{-1} \cdot \text{s}^{-1}$  (9). In this way, the extent of  $\text{NO}_3$  reaction with  $\text{C}_3\text{H}_6$  is minimized. Comparison of the organic nitrate yields with those found in a  $\text{C}_3\text{H}_6/\text{N}_2\text{O}_5$  study conducted in our laboratory (4) indicates that  $\text{NO}_3$  reaction with  $\text{C}_3\text{H}_6$  occurred to the extent of  $\sim 0.05$  ppm in the  $\text{C}_3\text{H}_6/\text{O}_3/\text{NO}_2$  exposure (or only  $\sim 5\%$  of the total reacted  $\text{C}_3\text{H}_6$ ).

The reaction of  $\text{O}_3$  with  $\text{C}_3\text{H}_6$  can produce various free radicals (e.g.,  $\text{HO}_2$  and  $\text{CH}_3\text{O}_2$ ) (10) that may then react with  $\text{NO}_2$  to produce peroxy nitrates (e.g.,  $\text{CH}_3\text{O}_2\text{NO}_2$ ). From a comparison of the results (Figure 2) for the  $\text{C}_3\text{H}_6/\text{O}_3$  and  $\text{C}_3\text{H}_6/\text{O}_3/\text{NO}_2$  exposures, it appears that either these are not significantly mutagenic at these concentrations or they are not effectively transported to the exposure chambers.

As shown in Figure 2, the number of revertants per plate increases throughout the exposure at  $\sim 4$ –5 revertants/plate per hour. The "dose-response" curves are, however, nonlinear presumably due to increasing toxicity effects with time, as indicated by the decreasing survivor levels. We can, however, attempt to account for the observed response by comparing the initial slope of the curve with the known mutagenic activities of the products present. We have conducted standard plate incorporation tests and/or gas-phase exposures for each of the reactants and products listed in Table I, and the data from these tests are presented in Table III, as revertants per micromole per plate. From the data in Figure 4 and Table III, it appears that 2-HPN and 2-NPA could account for less than 1 revertant/plate each at 20 h. To determine the contribution to the total response from PAN, we need to estimate the total quantity of PAN that deposits into the plates. In a previous paper, we reported that under these conditions  $\sim 15\%$  of the PAN passing through the exposure chambers dissolves into the media (2). The PAN concentration deposited into the plates over each exposure period can be estimated from eq 1 where  $C_p$  is the con-

$$C_p = 0.15 C_g F_c T_e (1/N_p) \quad (1)$$

centration in the plates,  $C_g$  is the molar gas-phase concentration,  $F_c$  is the flow rate through the exposure chambers (840 L/h),  $T_e$  is the exposure time, and  $N_p$  is the total number of exposed plates. Using this equation, we calculate an initial PAN deposition rate of 4.1 nmol/plate per hour, which leads to a potential contribution from PAN of  $\sim 0.14$  revertant/plate per hour, or  $\sim 3\%$  of the initial reversion rate.

We have found both by standard plate incorporation tests and by gas-phase HCHO exposures that HCHO yields



a response with TA100 of  $\sim 12$  revertants/ $\mu\text{mol}$  per plate. However, the dose-response curves tend to bend over due to toxicity effects (at  $\sim 6 \mu\text{mol/plate}$ ) yielding a maximum excess of  $\sim 70$  revertants/plate. From the slope of the curve for HCHO in Figure 3, it appears that the HCHO can account for  $\sim 8$  revertants/plate per hour, or 40 excess revertants at 5 h. This is actually greater than the observed reversion rate in the experiment. Our gas-phase exposures with HCHO have indicated essentially no decrease in the survivor level for HCHO doses up to  $6 \mu\text{mol/plate}$ . Therefore, there are probably other species present that are toxic and that lead to a reduced reversion rate. We have previously conducted experiments with  $\sim 0.5$  ppm of  $\text{O}_3$  in the exposure chambers without toxicity effects, indicating that  $\text{O}_3$  is not toxic at these levels. It does appear, however, that essentially all of the observed responses in these experiments can be accounted for based on the presence of HCHO.

The reaction of  $\text{O}_3$  with  $\text{C}_3\text{H}_6$  leads to production of several other products (10), such as  $\text{CH}_3\text{OOH}$ ,  $\text{H}_2\text{O}_2$ , and secondary ozonides. Since these are all probably soluble in the medium, these products either are not transported to the exposure chambers, or are not significantly mutagenic with this strain, at these concentrations.

The principal objective of these experiments was to attempt to determine the extent to which  $\text{C}_3\text{H}_6$  reactions with  $\text{O}_3$  could account for the large response ( $\sim 600$  excess revertants/plate) observed in the irradiated  $\text{C}_3\text{H}_6/\text{NO}_x$  system (3). Computer simulations of the irradiated  $\text{C}_3\text{H}_6/\text{NO}_x$  system under the conditions of that exposure indicated that the  $\text{C}_3\text{H}_6$  reaction with  $\text{O}_3$  had occurred to the extent of  $\sim 0.20$  ppm of reacted  $\text{C}_3\text{H}_6$ . Since this is only  $\sim 20\%$  of the extent of  $\text{C}_3\text{H}_6/\text{O}_3$  reaction in this study, it appears that the products of the  $\text{C}_3\text{H}_6/\text{O}_3$  reaction could not have caused a significant response in the  $\text{C}_3\text{H}_6/\text{NO}_x$  irradiations.

Since we have also found (3) that the products of the  $\text{C}_3\text{H}_6/\text{NO}_3$  reaction could not have caused a significant response in the  $\text{C}_3\text{H}_6/\text{NO}_x$  irradiation, it appears that there may be some very minor product, which is probably photolytically generated, that is a very strong mutagen present in the  $\text{C}_3\text{H}_6/\text{NO}_x$ -irradiated system.

It is clear from the data in Figures 2-4 that this technique of gas-phase exposure with variable exposure times presents an effective means for obtaining dose-response curves with volatile species and complex mixtures (provided those species are water soluble). In addition, the use

of survivor plates permits us to evaluate the potential for toxicity effects experienced by the bacteria during the exposure.

#### Acknowledgments

We thank G. R. Namie and J. H. Pittman of Northrop Services, Inc.—Environmental Sciences for their assistance in conducting the experiments and E. Perry of Environmental Health and Research Testing for her valuable assistance in conducting the biotesting.

**Registry No.** PAN, 2278-22-0; PGDN, 6423-43-4; 2-HPN, 20266-65-3; 2-NPA, 20266-74-4;  $\text{C}_3\text{H}_6$ , 115-07-1;  $\text{O}_3$ , 10028-15-6;  $\text{NO}_2$ , 10102-44-0; HCHO, 50-00-0;  $\text{CH}_3\text{CHO}$ , 75-07-0.

#### Literature Cited

- (1) Schairer, L. A.; Van't Hoff, J.; Hayes, C. G.; Burton, R. M.; de Serres, F. J. In "Applications of Short-Term Bioassays in the Fractionation of Complex Environmental Mixtures"; Plenum Press: New York, 1979; p 420.
- (2) Shepson, P. B.; Kleindienst, T. E.; Edney, E. O.; Namie, G. R.; Pittman, J. H.; Cupitt, L. T.; Claxton, L. D. *Environ. Sci. Technol.* **1985**, *19*, 249-255.
- (3) Kleindienst, T. E.; Shepson, P. B.; Edney, E. O.; Cupitt, L. T.; Claxton, L. D. *Environ. Sci. Technol.* **1985**, *19*, 620-627.
- (4) Shepson, P. B.; Kleindienst, T. E.; Edney, E. O.; Pittman, J. H.; Namie, G. R.; Cupitt, L. T. *Environ. Sci. Technol.* **1985**, *19*, 849-854.
- (5) Claxton, L. D.; Toney, S.; Perry, E.; King, L. *Environ. Mutagen.* **1984**, *6*, 331-342.
- (6) Ames, B. N.; McCann, J.; Yamasaki, E. *Mutat. Res.* **1975**, *31*, 347-364.
- (7) Cares, J. W. *Am. Ind. Hyg. Assoc. J.* **1968**, *29*, 405-410.
- (8) McGregor, D.; Prentice, R. D.; McConville, M.; Lee, Y. J.; Caspary, W. J. *Environ. Mutagen.* **1984**, *6*, 545-557.
- (9) Hampson, R. F., Sr.; Garvin, D., Eds. *NBS Tech. Note (U.S.)* **1975**, No. 866.
- (10) Carter, W. P. L.; Lloyd, A. C.; Sprung, J. L.; Pitts, J. N., Jr. *Int. J. Chem. Kinet.* **1979**, *11*, 45-101.

Received for review February 25, 1985. Accepted May 31, 1985. Although the research described in this article has been funded wholly or in part by the U.S. Environmental Protection Agency through Contract 68-02-4033 to Northrop Services, Inc.—Environmental Sciences, it has not been subject to the Agency's peer and administrative review and therefore does not necessarily reflect the views of the Agency, and no official endorsement should be inferred.

# Emissions of Vapor-Phase Fluorine and Ammonia from the Columbia Coal-Fired Power Plant

Christopher F. Bauer\*

Department of Chemistry, University of New Hampshire, Durham, New Hampshire 03824

Anders W. Andren

Water Chemistry Laboratory, University of Wisconsin, Madison, Wisconsin 53706

■ Gaseous fluorine and ammonia emissions from two pulverized-coal power plants were measured over a 6-month period. In one unit, emissions contained a median 1.5 mg/scm (standard cubic meter)  $\text{NH}_3$  and 1.9 mg/scm F (86% of available F in coal). For the other unit lower levels were found: 0.042 mg/scm  $\text{NH}_3$  and 0.22 mg/scm F (4.2% of available F in coal). Ammonia varied by more than 10 times in each unit and was enhanced in Unit I by addition of ammonium carbonate to improve precipitator efficiency. Fluorine varied less than 50% in each unit. The difference in F between units was related circumstantially to ash content. Daily variation of F and  $\text{NH}_3$  was less than 20%. Neither gas was in sufficient quantity relative to  $\text{SO}_2$  to influence net acidity. Levels of F were comparable to those of other combustion sources and the aluminum industry. On a global scale, coal combustion is not a major source of either F or  $\text{NH}_3$ . Among anthropogenic sources, however, it is a significant contributor and may be important locally. In contrast,  $\text{NH}_3$  emissions are negligible.

## Introduction

Among the atmospheric emissions from coal-fired power plants are several major vapor-phase materials having important environmental impacts:  $\text{CO}_2$ ,  $\text{SO}_2$ , and  $\text{NO}_x$ . In addition, a number of trace materials in coal seem to be emitted largely as vapors, notably, Hg, Se, Cl, Br, and F (1-4). Knowledge about these trace gases has been derived indirectly from discrepancies in mass balances; particulate emissions cannot account for all of the mass that entered in the fuel. Lack of direct data for minor gas species is most often due to the necessity for individualized sampling and analysis methodology. Considerably more effort must be expended in a study of trace gases than in a particulate matter emission study. Consequently, it is not surprising that previous work has focused primarily on major gases and particulate emissions, for which integrated sampling and analysis schemes (e.g., inertial impaction and neutron activation analysis) provide data on many elements simultaneously.

Since flue gas chemistry and emission factors of minor vapor species represent gaps in our knowledge, this research studied two neglected materials, F and  $\text{NH}_3$ . Our purpose was (1) to evaluate sampling and analysis methodologies for vapor-phase fluorine and ammonia, (2) to determine flue gas concentrations for emission inventory estimates, (3) to determine short- and long-term variability, and (4) to compare coal-fired steam plant  $\text{NH}_3$  and F atmospheric emissions with other anthropogenic and natural sources.

The plant studied was the Columbia electricity generating station in Portage, WI. The station consists of two 527-MW pulverized-coal furnaces. Unit I, which came on line in the early 1970s, has a 107-m stack and was burning a western bituminous coal (Colstrip, MT) containing 9% ash and 1% S (dry coal basis). Unit II, which came on line in the mid-1970s, has a 198-m stack and was burning another bituminous coal (Gillette, WY) containing 5% ash

and 0.7% S. The Columbia station offered a unique opportunity to compare two nearly identical combustion units, differing only in type of coal burned and operating conditions.

## Experimental Section

**General Sampling Procedures.** Research Appliance Co.'s "Staksamplr" (Model 2414) with a 1.5-m heatable glass probe was used to collect gas samples. The rest of the sampling train consisted of a cyclone and filter holder encased in a heatable box, an ice bath containing four impingers in series, and the meter case, consisting of manometer, pump, and dry gas meter bracketed by thermometers. An "S" type pitot tube was used to measure flue gas velocity. All surfaces contacting the sampled gases were glass except for the filter holder, which contained a plastic support for the glass frit.

Glassware was scrubbed with Alconox, soaked in hot nitric acid, and rinsed with distilled deionized water. Nalgene linear polyethylene bottles used for impinger collection solutions were leached for a week with dilute reagent-grade HCl and rinsed with water.

Sampling was performed within one of two horizontal ducts leading to the stack. Each duct had several sampling ports, one of which was selected to obtain all samples. This port was situated away from bends in the ducts to minimize gas flow inhomogeneity. Stack gas temperature was measured by means of a thermocouple attached to the pitot tube. Stack pressure, measured by means of a water manometer, was always within  $2.5 \pm 1.2$  cm of water from atmospheric pressure. The first two impingers were each filled with 100 mL of the appropriate collection solution from sample bottles previously filled in the laboratory. The third impinger contained 3% sodium carbonate solution to protect the pump from corrosive vapors. The fourth impinger was dry. The probe and filter compartment were heated to between 60 and 80 °C. During sampling, the probe and filter case were observed to be free of condensation.

After sampling, impinger solutions were transferred quantitatively back into their storage bottles. Volumes were measured at the laboratory by using calibrated graduated cylinders. The combined volume gain for all impingers during the day was used to calculate water vapor content of the stack gas. Samples were stored at 4 °C. Even after several months of storage, volumes remeasured for selected bottles showed no changes.

**Fluorine Sampling.** Methods have been reported for distinguishing particulate and vapor-phase F in the atmosphere (5-10) and in emissions from aluminum refining (11, 12) and fertilizer production (8, 13). Coal combustion emissions have not been given much attention despite estimates indicating that they represent one of the major industrial sources of atmospheric F (10, 14).

The method of Dorsey and Kenmitz (15) was adopted after modification. It involves collection through a hot glass probe, in which HF is transformed quantitatively into

SiF<sub>4</sub> at the probe walls. Being less reactive than HF, SiF<sub>4</sub> will pass through a filter without being trapped, thus effecting separation of particulate and vapor-phase F. The gas is then bubbled through impingers containing aqueous NaOH, where SiF<sub>4</sub> is hydrolyzed to soluble fluoride. Just in case conversion to SiF<sub>4</sub> was not complete in the probe, we used a citric acid impregnated paper filter (Whatman 42) (5) instead of glass fiber (15). A rate of 0.02 m<sup>3</sup>/min was used, and probe and filter box temperatures were hot enough to keep the relative humidity below the recommended maximum (6) of 90%. Accuracy of particle/vapor separation was not tested in this laboratory. Under these conditions, approximately 1–2 m<sup>3</sup> of gas had to be collected to provide adequate fluoride for analysis.

Quantitative collection of SiF<sub>4</sub> and HF has been achieved in 0.1 M NaOH (13, 15), but we selected 0.75 M NaOH so that the major acidic gases, namely, CO<sub>2</sub>, SO<sub>2</sub>, and NO<sub>x</sub>, would be neutralized. Acidic conditions were avoided to prevent possible loss of F as HF. None of the field samples had a pH below 10 after collection.

This method does not distinguish between HF, SiF<sub>4</sub>, and H<sub>2</sub>SiF<sub>6</sub>, any of which might exist in the flue gas. All of these forms will be collectively referred to as "fluorine" or "fluoride".

**Fluoride Determination.** Fluoride was determined potentiometrically by standard additions by using an Orion F-selective electrode (Model 94-09A), an Orion double-junction Ag/AgCl reference electrode (Model 90-02), and an Orion Model 801 digital meter. Electrode response was determined each analysis day by construction of a working curve. Two different complexing buffer solutions were used with equivalent effect: cyclohexylenedinitrilotetraacetic acid in acetic acid/acetate buffer (5, 16), and citric acid/citrate in ammonium/ammonia buffer (8, 16). Dry reagent-grade NaF was dissolved in 50% buffer for stock fluoride standard. Standards and buffers were stored at 4 °C. Polyethylene labware was used.

A 25-mL aliquot of each sample solution was transferred by pipet to a beaker along with an equal volume of buffer; a measured volume of glacial acetic acid was added to bring the pH to 5.5–6.0. This acidification caused loss of CO<sub>2</sub> absorbed from the stack gas. The beakers were covered and stirred until effervescence had subsided. Fluoride response was determined in duplicate from two standard addition spikes into one aliquot of sample.

**Coal.** Lump coal was collected in kilogram quantities from all the hoppers that fed the pulverizers. Representative 30-g analytical samples were prepared (17). Fluoride determinations were performed by CDM/Acculabs in Wheat Ridge, CO, using ASTM Method D3761.

**Ammonia Sampling.** Dilute sulfuric acid (0.5 M) has been reported to be an efficient absorbent for atmospheric NH<sub>3</sub> (18). A gas sampling rate of 0.025 m<sup>3</sup>/min and a stack gas total volume of 1.4 m<sup>3</sup> were used. Two glass-fiber filters were placed in the sampling train. These were leached first with sulfuric acid to neutralize excess alkalinity (19, 20) and then with water until acid free to help avoid the conversion of ammonium salts to ammonia.

The sampling train illustrated in Figure 1 was used to determine whether ammonia would pass quantitatively through the filters. Known quantities of ammonia were generated and passed through the train under conditions similar to those used for stack gas sampling. The vapor source was 150 mL of 1.25 × 10<sup>-3</sup> M NH<sub>4</sub>Cl in 0.5 M H<sub>2</sub>SO<sub>4</sub>. The two collection impingers and the inlet impinger each contained 100 mL of 0.5 M H<sub>2</sub>SO<sub>4</sub>. When the solution in the source impinger was made basic and ambient air was pulled through the train, ammonia vapor

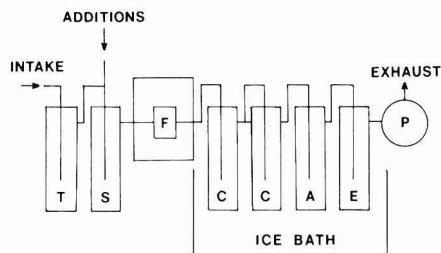


**Figure 1.** Apparatus for test of ammonia sampling train. F = filter holder in heated cabinet; P = pump; T = inlet trap, dilute H<sub>2</sub>SO<sub>4</sub>; S = source impinger, acidic ammonia solution; C = collection solutions, dilute H<sub>2</sub>SO<sub>4</sub>; A = alkaline trap for pump protection, dilute sodium carbonate; E = empty.

from the source was transported through the system. Ammonia concentrations in the source solution before and after "sampling" and in the collection impingers were measured. The inlet impinger absorbed any ammonia present in laboratory air and conditioned the air with respect to water vapor and acid vapor so that the source impinger would not be stripped of its contents.

Several different obstacles were placed between source and collection impingers: (1) a glass connector, (2) two neutralized, clean, glass-fiber filters heated to between 50 and 70 °C, or (3) a filter laden with 190 mg of fly ash from a stack sampling run, also heated to between 50 and 70 °C. Enough 10 M NaOH was added to the source impinger to raise the pH above 11 and release NH<sub>3</sub>. The pumping rate was then increased to 0.025 m<sup>3</sup>/min, the rate used for stack gas sampling. After 0.8 m<sup>3</sup> had been passed, H<sub>2</sub>SO<sub>4</sub> was added to the source to stop NH<sub>3</sub> evolution. Bubbling was continued for another 0.15 m<sup>3</sup> to purge the source of remaining ammonia.

**Ammonia Determination.** Ammonia was determined potentiometrically by standard additions with an Orion Model 95-10 NH<sub>3</sub> gas electrode and an Orion 801 meter. Electrode response was determined each analysis day. All chemicals were reagent grade. Ammonia standards were prepared from dry NH<sub>4</sub>Cl dissolved in 0.5 M H<sub>2</sub>SO<sub>4</sub>.

A 25-mL aliquot of each sample was transferred by pipet to a beaker along with an equal volume of water. After the beaker was chilled in a cold water bath (4–10 °C), 10 M NaOH was added from a buret until the pH exceeded 11.5, as determined by using a glass electrode. The beaker was then covered and placed in a room temperature water bath for 5 min. The NH<sub>3</sub> electrode was immersed in the magnetically stirred sample, and the response was recorded after 5 min. No loss of NH<sub>3</sub> was noted as indicated by absence of drift in electrode response during the time span of the measurement. Duplicate determinations were made on the basis of two standard addition spikes into a single aliquot of sample. Additional pH measurements made after these additions of acidic standard indicated that pH remained above 11.

Temperature control is necessary for reproducible response. This was especially important because entrapment of water vapor and acid gases from the stack caused varying acidities in the collection solutions. Without control, addition of base raised temperatures variably and as high as 40 °C.

## Results and Discussion

**Collected Samples.** Samples were collected 6 times in each combustion unit between April and Oct 1980. Two of these samples were collected the same day several hours apart.

Concentrations of F ranged from about  $0.3 \times 10^{-4}$  to  $5 \times 10^{-4}$  M in the first impinger and from  $0.3 \times 10^{-5}$  to  $1.5 \times 10^{-5}$  M in the second; for ammonia, the concentrations ranged between  $10^{-6}$  and  $10^{-3}$  M in the first impinger and between  $10^{-6}$  and  $10^{-4}$  in the second. Reagent blank levels were about  $10^{-6}$  M for both F and  $\text{NH}_3$ . Analytical precisions, whether F or  $\text{NH}_3$ , were about 5% relative standard deviation for the first impinger and about 20% for the second impinger. Since masses collected in the first impinger were usually much greater than those in the second, the net error in the sum is about 5%.

**Accuracy of Fluoride Method.** Loss of dissolved  $\text{F}^-$  in the glass impingers was tested by stirring a known concentration of sodium fluoride dissolved in 0.75 M NaOH collection solution in a glass beaker for 75 min. Fluoride determinations were performed on aliquots of solution before and after contact with the glass. At  $10^{-4}$  M  $\text{F}^-$  (typical of the first impinger) no losses were observed; however, at  $10^{-5}$  M (second impinger) about 15% was lost. Although significant for impinger 2, this loss was negligible for the sum of impingers 1 and 2 for all samples.

Previous literature indicated (13) that collection of water-soluble fluorine species by simple impingers should be nearly quantitative. Our field sampling results generally supported this observation; the second impinger was found to contain a median value of 3.2% F compared to the first, with a range of 0.8–17.1%.

**Accuracy of Ammonia Method.** Ionic strength of sample solutions is an important consideration in achieving stable electrode response. Addition of concentrated base to the 0.5 M  $\text{H}_2\text{SO}_4$  collection solutions to release ammonia resulted in ionic strengths of nearly 3 M. This solution required about 30 min of stabilization time apparently because osmotic pressure forced water out of the internal filling solution (about 0.1 M  $\text{NH}_4\text{Cl}$ ). Equilibration times were measured for the electrode when immersed in solutions of  $2.3 \times 10^{-4}$  M  $\text{NH}_4\text{Cl}$  containing varying ionic strengths. Ionic strengths of 0.3, 0.6, and 1.4 M required less than 5 min for equilibration, whereas an ionic strength of 2.7 M (undiluted sample solution) lengthened the time to 25 min. All sample solutions, therefore, were diluted one-to-one with water just before analysis to reduce equilibration time to 5 min.

An additional concern was the possibility that metal ions might complex  $\text{NH}_3$  irreversibly, thus causing low results. Most metals are particulate associated and should be removed by the filter. Only volatile  $\text{Hg}^0$  might penetrate substantially. Furthermore,  $\text{Hg(II)}$  forms a fairly strong ammonia complex ( $\text{p}K_1 = \text{p}K_2 = 9$ ). Ammonia responses were measured in solutions containing  $4 \times 10^{-5}$  M ammonium and  $\text{Hg(II)}$  concentrations as high as  $1.3 \times 10^{-4}$  M. There was no apparent effect. This ammonium concentration was low compared with most of the stack sample solutions, and the Hg concentrations were chosen by estimating the amount available in typical coal combustion gases (1, 2) and assuming complete oxidation to  $\text{Hg(II)}$ .

Collection efficiency of  $\text{NH}_3$  in the impingers and the effect of filtration are displayed in Table I. Each of the three treatments (no filter, clean filter, and fly ash laden filter) were duplicated, and each value listed is the average of two potentiometric determinations on each solution. The first three columns indicate where ammonia was found after the experiment had been completed. These columns should sum to 639  $\mu\text{g}$ , the initial mass in every case. Analysis of variance indicated that recoveries for the three treatments were not significantly different at the 95% probability level; the overall mean recovery was  $88 \pm 6\%$ . This 6% error can be attributed entirely to the analytical

**Table I. Efficiency of Ammonia Collection and Effect of Filtration on Recovery**

	mass of $\text{NH}_3$ found, $\mu\text{g}$			recovery, % <sup>a</sup>	impinger ratio, %
	imp 1	imp 2	used std		
no filter	506	13	76	93	2.5
	462	6	48	81	1.3
clean filter				87 <sup>b</sup>	
	446	1	79	82	0.2
	511	3	55	89	0.6
ash on filter	541	0	35	90	0.0
	557	2	50	95	0.4
grand mean				88 $\pm$ 6	

<sup>a</sup> Sum of first three columns divided by 639; as percent. <sup>b</sup> Mean.

**Table II. Comparison of Methods for Determining Stack Gas Flow Rates (in  $10^4$  dry scm/min)**

Unit I		Unit II	
plant data	this work	plant data	this work
4.3	1.7	4.0	3.6
3.8	1.8	4.0	4.0
6.7	1.7	2.8	3.6
6.1	1.7	2.5	3.6
6.0	1.7	2.3	3.9
4.2	1.8	2.2	4.0

measurement. The reason why ammonia was "lost" has not been determined; however, the size of the discrepancy was not so severe as to compromise the accuracy of results for stack samples. Calculations of ammonia content of stack gas emissions included a 12% correction for collection efficiency.

Table I also shows that the amount of ammonia reaching impinger 2 was negligible compared with the amount in impinger 1. Field sampling results, summarized above, were similar to the laboratory test results in most cases: the second impinger contained a median of 2.8% as much ammonia as the first impinger, with a range of 0.7–28%. High values were found only for those samples containing very little ammonia.

**Emissions.** Ammonia emission rates and concentration in the emitted gas were of primary interest. For F the amount appearing in the vapor phase relative to the amount input in the coal was also determined.

A factor of major importance was the means by which total stack gas flow was determined. Although stack gas velocity was measured each sampling day by means of a pitot tube, we were concerned whether this measurement was representative because Columbia plant records showed that flow velocities across the flue gas ducts were quite heterogeneous, with a variability of about 30%.

Another approach using plant records of  $\text{SO}_2$  emissions was evaluated. The average flow rate was calculated each sampling day from  $\text{SO}_2$  stack gas concentrations, measured by on-line monitors, and  $\text{SO}_2$  mass emission rates, recorded hourly in plant records. The advantage to this approach was that these emission rates were calculated from an algorithm based on the average of gas velocity measurements at many points in the stack. This algorithm had been developed when each unit was evaluated for initial compliance with emissions regulations. Table II shows that gas flow rates determined from plant data and with our pitot measurement on the same day are substantially different.

**Table III. Concentrations and Emission Rates of Ammonia at Columbia Coal-Fired Power Plant**

Unit I			
date	µg/scm	kg/h	ppm
4/17	1700	4.3	2.6
5/29	11000	25	16
9/3	6300	26	9.5
9/5	1000	3.7	1.5
9/5	1400	5.1	2.1
10/20	250	0.63	0.4
median	1550	4.7	2.3
Unit II			
date	µg/scm	kg/h	ppb
6/24	11	0.026	16
6/26	0.6	0.001	0.9
7/21	75	0.13	110
7/24	131	0.20	200
10/24	46	0.060	69
10/24	42	0.056	63
median	42	0.056	66

To determine which method was more accurate, a mass balance on carbon was calculated. Knowing the coal feed rate (hourly plant record), the percent carbon in the coal (determined daily by plant personnel using ASTM procedures), the concentration of CO<sub>2</sub> in the stack gas (hourly plant record), and the total gas flow rate, one can compare the C input and output rates. Correct gas flow rates should lead to a 100% C balance. The only assumption is that all of the C in coal be converted to CO<sub>2</sub>. This is quite reasonable since emissions of CO and of unburned coal particles are negligible. Feed rates were corrected for coal moisture content, determined by plant personnel using ASTM procedures.

By use of stack gas flow rates calculated from SO<sub>2</sub> emissions, 95% of the C in the coal was accounted for (range 91–103%), in both combustion units. These values are accurate within about 20% because of propagation of error through the various calculations. Thus, flow rates calculated from SO<sub>2</sub> emissions are indeed accurate. In contrast, if values measured by pitot (Table II) had been used, mass balances would have been incorrect by as much as a factor of 3.

Stack gas concentrations and mass emission rates for ammonia and vapor-phase fluorine are listed in Tables III and IV, respectively. On all sampling days the combustion units were operating near full capacity, consuming about  $2 \times 10^5$  kg of dry coal/h. Propagated uncertainties in the data in these tables range from 20 to 30%. Medians are displayed instead of means because shapes of the distributions of these variables were not known and individual values varied several orders of magnitude. Unit I emitted substantially higher concentrations of ammonia and vapor-phase fluoride than Unit II and at substantially greater rates. Note that samples collected the same day were much more similar to each other than those collected on different days.

Unit I had much larger emissions of ammonia because ammonium carbonate was added to improve particulate collection efficiency in the electrostatic precipitators. Ammonium carbonate decomposes at about 60 °C to NH<sub>3</sub>, H<sub>2</sub>O, and CO<sub>2</sub>. Volume concentrations were somewhat less than expected (10–20 ppm) for this type of flue gas treatment (22). Since no additions were made to Unit II, the concentrations observed here indicate that modern pulverized-coal combustion produces very little ammonia.

**Table IV. Concentrations, Emission Rates, and Mass Balance of Vapor-Phase Fluoride at Columbia Coal-Fired Power Plant**

date	mg/scm	kg/h	F emitted as vapor, %	stack temp, °C
Unit I				
4/17	2.9	7.4	87	137
5/29	1.6	3.6	50	156
9/3	1.8	7.4	85	144
9/4	2.0	7.3	94	149
9/4	2.2	8.0	102	149
10/20	1.5	3.8	22	132
median	1.9	7.4	86	
Unit II				
6/24	0.15	0.36	4.0	189
6/26	0.16	0.38	4.3	184
7/21	0.34	0.57	5.9	165
7/24	0.25	0.37	3.8	160
10/22	0.23	0.32	4.7	157
10/22	0.20	0.28	4.2	157
median	0.22	0.36	4.2	

In addition, with SO<sub>2</sub> levels typically around several hundred ppm, there was not nearly enough ammonia to achieve significant acid neutralization, even in Unit I where ammonia had been added.

For F one could hypothesize that differences arose between units because of differences in the amount or nature of F within each coal or in combustion or stack gas chemistry. No significant difference existed between the F contents of the coals: Unit I's coal contained on average 46 ppm and Unit II's, 45 ppm. With regard to the form of F, this element occurs in coals predominantly in the inorganic minerals fluorapatite, Ca<sub>5</sub>F<sub>2</sub>(PO<sub>4</sub>)<sub>6</sub>, and fluorspar, CaF<sub>2</sub> (10, 21, 23, 24). (Fluoride mineralogies of the Columbia coals were not investigated in this project.) Whereas F can be volatilized to a much greater extent from fluorspar than fluorapatite, Crossley (25) has shown that other minerals in the coals modify this behavior greatly. In particular, quartz promotes formation of gaseous SiF<sub>4</sub> (10, 26). Since Unit I coal had nearly twice the ash content of that in Unit II, the extra mineral matter may have played a role in the greater release of fluorine to the vapor phase in Unit I.

There is no indication that the higher ammonia levels in Unit I played a role in creating the higher F levels there. Tables III and IV show no apparent correlation between these two species. Table IV also shows that there was no clear relationship between flue gas temperature and amount of F in the vapor phase.

A few measurements of vapor-phase F emissions from other combustion sources are available for comparison. These are listed in Table V along with emission values from aluminum smelting operations. Columbia Unit I had emission concentrations similar to those for the other combustion sources. Levels in Unit II were somewhat lower, being more comparable to aluminum industry emissions. It should be noted that because of the significant amount of Fe released to the vapor phase by coal combustion, receptor modelers may be able to use vapor-phase F as a tracer for this source.

The form of F in the stack gas is likely to be either HF or SiF<sub>4</sub> (10). Our sampling system would have collected both species but was incapable of distinguishing between them. Upon emission to the atmosphere, the stack gas will have cooled sufficiently for water vapor to condense. Consequently, SiF<sub>4</sub> might hydrolyze to fluorosilicic acid (H<sub>2</sub>SiF<sub>6</sub>). The contribution of these two weak acid species to the overall acidity of the emissions was negligible. For



**Table V. Comparison of Fluorine Emission Sources**

source	emitted concn, mg/scm <sup>a</sup>	F emitted as vapor, %	ref
coal			
pulverized (6) <sup>b</sup>	1.9 (1.5–29)	86	Unit I
pulverized (6)	0.22 (0.15–0.34)	4	Unit II
spreader-stoker (12)		91 <sup>c</sup>	4
spreader-stoker (12)		98 <sup>c</sup>	4
fluidized-bed (5)	10		27
municipal waste			
incinerator (9)	4.7 (1.9–25)		28
incinerator (9)	2.1 (1.2–3.0)		29
aluminum			
refinery	0.33 (0.13–1.2)		11
refineries <sup>d</sup>	(0.25–1.4)	40–70	30
unspecified		0.7–96	15

<sup>a</sup>Medians or means, with ranges in parentheses. <sup>b</sup>Number of samples. <sup>c</sup>Inflated slightly by inclusion of particulate matter that escapes to atmosphere (0.18% of total particulate). <sup>d</sup>Industry-wide average.

the two units, the median concentrations of 0.22 and 1.9 mg of F/scm were equivalent to roughly 0.3–3 ppm of F, whereas SO<sub>2</sub> concentrations were typically several hundred ppm.

To place these emission measurements into perspective, one should compare F and NH<sub>3</sub> emissions from coal combustion with those from other industrial and natural sources. Given a total U.S. coal consumption by electric utilities of about  $5.4 \times 10^{11}$  kg/year (31) and multiplying by an average F content of about 70 mg/kg (21), the total amount of F liberated by coal combustion is about  $37 \times 10^6$  kg/year. Our data indicated that in typical pulverized fuel combustion as much as 95% and as little as 5% of this amount will be emitted as vapor-phase F species. This is roughly equivalent to previous estimates that place total particulate and vapor emissions from coal, based on an assumed 50% release of F to the atmosphere, at  $15 \times 10^6$  (10) and  $25 \times 10^6$  kg/year (14). At these levels coal combustion represents about 15% of the total domestic F emission (10, 14). On a global scale, coal and other anthropogenic sources are minor compared to annual natural emissions of about  $2.5 \times 10^{10}$  kg (32); consequently, F pollution effects are likely to remain a local concern, as they have in the past.

Global ammonia emissions from coal combustion have been reported previously to be less than  $2 \times 10^9$  kg/year (33), an insignificant amount compared with the dominant anthropogenic source—domestic animal feedlots at  $23 \times 10^9$  kg/year (33)—and negligible compared with natural emissions at  $1 \times 10^{12}$  kg/year (34). Our measurements confirm this situation: assuming Unit I to be typical of the U.S. coal-burning utility industry, no more than  $6 \times 10^7$  kg/year of NH<sub>3</sub> would be emitted in the U.S.

#### Acknowledgments

We express our thanks to Brad Price and Mark Knabe, who helped perform the sample collection, and to Jack Hipke and Ken Kohle at Columbia for helpful discussions and for plant operations records. This work was performed while C.F.B. was a postdoctoral research associate at the U.W. Water Chemistry Laboratory.

**Registry No.** NH<sub>3</sub>, 7664-41-7; F<sub>2</sub>, 7782-41-4.

#### Literature Cited

- (1) Kaakinen, J. W.; Jorden, R. M.; Lawasani, M. H.; West, R. E. *Environ. Sci. Technol.* **1975**, *9*, 862–869.

- (2) Klein, D. H.; Andren, A. W.; Carter, J. A.; Emery, J. F.; Feldman, C.; Fulkerson, W.; Lyon, W. S.; Ogle, J. C.; Talmi, Y.; Van Hook, R. I.; Bolton, N. *Environ. Sci. Technol.* **1975**, *9*, 973–979.
- (3) Andren, A. W.; Klein, D. H.; Talmi, Y. *Environ. Sci. Technol.* **1975**, *9*, 856–858.
- (4) Conzemius, R. J.; Welcomer, T. D.; Svec, H. J. *Environ. Sci. Technol.* **1984**, *18*, 12–18.
- (5) "Annual Book of ASTM Standards"; American Society for Testing and Materials: Philadelphia, PA, 1977; ASTM Method D3267.
- (6) Monteriolo, S. C.; Pepe, A. *Pure. Appl. Chem.* **1970**, *24*, 707–714.
- (7) Davison, A. W.; Rand, A. W.; Betts, W. E. *Environ. Pollut.* **1973**, *5*, 23–33.
- (8) Elfers, L. A.; Decker, C. E. *Anal. Chem.* **1968**, *40*, 1658–1661.
- (9) Okita, T.; Kaneda, K.; Yanaka, T.; Sugai, R. *Atmos. Environ.* **1974**, *8*, 927–936.
- (10) "Fluorides: Biologic Effects of Atmospheric Pollutants"; National Academy of Sciences: Washington, DC, 1971.
- (11) Danchik, R. S.; Obbink, R. C.; Lenz, G. F. *J. Met.* **1977**, *29* (5), 6–10.
- (12) Hrabeczy-Pall, A.; Vallo, F.; Toth, K.; Pungor, E. *Hung. Sci. Instrum.* **1977**, *41*, 55–57; *Chem. Abstr.* **1978**, *88*, 196654a.
- (13) Powell, R. A.; Stokes, M. C. *Atmos. Environ.* **1973**, *7*, 169.
- (14) Smith, F. A.; Hodge, H. C. *CRC Crit. Rev. Environ. Control* **1979**, *8*, 293–371.
- (15) Dorsey, J. A.; Kenmitz, D. A. *J. Air Pollut. Control Assoc.* **1968**, *18*, 12–14.
- (16) Nicholson, K.; Duff, E. *J. Anal. Lett.* **1981**, *14*, 887–912.
- (17) "Annual Book of ASTM Standards"; American Society for Testing and Materials: Philadelphia, PA, 1977; ASTM Method D2013.
- (18) Shendrikar, A. D.; Lodge, J. P., Jr. *Atmos. Environ.* **1975**, *9*, 431–435.
- (19) Coutant, R. W. *Environ. Sci. Technol.* **1977**, *11*, 873–878.
- (20) Felix, L. G.; Clinard, G. I.; Lacey, G. E.; McCain, J. D. "Inertial Cascade Impactor Substrate Media for Flue Gas Sampling"; Environmental Protection Agency: Washington, DC, 1977; EPA-600/7-77-060, pp 29–35.
- (21) Gluskoter, H. J.; Ruch, R. R.; Miller, W. G.; Cahill, R. A.; Dreher, G. B.; Kuhn, J. K. "Trace Elements in Coal: Occurrence and Distribution"; Illinois State Geological Survey: Urbana, IL, 1977; Circular 499.
- (22) Strauss, W. "Industrial Gas Cleaning", 2nd ed.; Pergamon: Oxford, 1975; p 441.
- (23) Crossley, H. E. *J. Soc. Chem. Ind., London* **1944**, *63*, 289–292.
- (24) Thomas, J., Jr.; Gluskoter, H. J. *Anal. Chem.* **1974**, *46*, 1321–1323.
- (25) Crossley, H. E. *J. Soc. Chem. Ind., London* **1944**, *63*, 342–347.
- (26) "Comprehensive Inorganic Chemistry"; Trotman-Dickenson, A. F., Ed.; Pergamon: Oxford, 1973; Vol. I, pp 1380–1381.
- (27) Murthy, K. S.; Howes, J. E.; Nack, H.; Hoke, R. C. *Environ. Sci. Technol.* **1979**, *13*, 197–204.
- (28) Carotti, A. A.; Kaiser, E. R. *J. Air Pollut. Control Assoc.* **1972**, *22*, 248–253.
- (29) Candrea, F.; Dams, R. *Sci. Total Environ.* **1981**, *17*, 155–163.
- (30) Rush, D.; Russell, J. C.; Iverson, R. E. *J. Air Pollut. Control Assoc.* **1973**, *23*, 98–104.
- (31) "Coal Distribution January–December 1983"; Energy Information Administration, U.S. Department of Energy: Washington, DC; p 12.
- (32) Carpenter, R. *Geochim. Cosmochim. Acta* **1969**, *33*, 1153–1167.
- (33) Robinson, E.; Robbins, R. C. *J. Air Pollut. Control Assoc.* **1970**, *20*, 303–306.
- (34) Stedman, D. H.; Shetter, R. E. *Adv. Environ. Sci. Technol.* **1983**, *12*, 412–454.

Received for review March 25, 1985. Revised manuscript received June 10, 1985. Accepted June 18, 1985. This work was supported by the U.S. EPA through Grant R806878-01-06.

# Behavior of Methyltin Compounds under Simulated Estuarine Conditions

Olivier F. X. Donard and James H. Weber\*

Chemistry Department, University of New Hampshire, Durham, New Hampshire 03824

■ A  $2^3$  factorial design is used to study the behavior of  $\text{MeSnCl}_3$ ,  $\text{Me}_2\text{SnCl}_2$ , and  $\text{Me}_3\text{SnCl}$  under laboratory-simulated estuarine conditions. The quaternary system includes methyltin ions (5 ng/L as Sn), ionic strength (0–35 g of NaCl/L) fulvic acid (0–25 mg/L), and hydrous iron oxides (0–1000 mg/L). Analysis of methyltin compounds involves hydride generation, separation by chromatographic packing material, atomization in a heated quartz furnace, and detection by atomic absorption spectroscopy. Removal of organotin compounds from solution after filtration at 0.4  $\mu\text{m}$  is from 83 to 100% for  $\text{MeSnCl}_3$ , from 28 to 66% for  $\text{Me}_2\text{SnCl}_2$ , and from 15 to 28% for  $\text{Me}_3\text{SnCl}$ . Increasing ionic strength inhibits the removal of  $\text{MeSnCl}_3$  and  $\text{Me}_2\text{SnCl}_2$ . Fulvic acid concentration contributes to increased removal of organotin compounds in saline waters but prevents adsorption of  $\text{Me}_2\text{SnCl}_2$  under freshwater-simulated conditions. Higher iron oxide concentration enhances removal of  $\text{MeSnCl}_3$  and  $\text{Me}_2\text{SnCl}_2$  but has little effect on  $\text{Me}_3\text{SnCl}$ . This study discusses mechanisms involved and relates them to estuarine processes.

## Introduction

There is widespread use of organotin compounds throughout the industrial world for stabilization of polyvinyl chloride (PVC), as biocides, in coating processes, and in antifouling paints. Two-thirds of organotin production is diorganotin compounds such as a dimethyl- and di-*n*-butyltin compounds. The ca. 27 000 tons produced worldwide in 1976 is expected to increase to 63 000 tons by 1986 (1). In 1976 approximately 4300 tons were released in the environment. About 10% of the total organotin compounds used in antifouling paints and as biocides and slimicides entered the aquatic environment including its sediment (2).

Generally for  $R = \text{alkyl}$ , toxicity is  $R_4\text{Sn} \approx R_3\text{Sn}^{3+} > R_2\text{Sn}^{2+} > \text{RSn}^{3+}$  (1, 3). Their action on living organisms is partially due to inhibition of oxidative phosphorylation and partially by mediation of anion exchange across membranes. The nature of the alkyl group determines their toxicity in regard to different species. Compounds of triethyl- and trimethyltin are toxic to mammals, whereas tri-*n*-butyltin salts are known to affect molluscs, bacteria, and fungi (4).

Estuaries are areas of high biological productivity, but they receive high inputs of pollutants due to development of harbors and leisure activities. The fate of methyltin compounds in the estuarine environment is closely linked to their partitioning in aqueous media. They either adsorb onto particulate matter and are more likely to be trapped in the estuary during transport or stay in the dissolved phase. Dissolved species are more likely to be expelled to the sea or directly ingested into the food chain and undergo bioaccumulation processes.

Adsorption studies described the fate of heavy metals in the estuarine environment (5–8). Most of these studies, because of relatively high environmental concentrations, emphasize adsorption of high concentration levels ( $\mu\text{g/mL}$ ) onto various types of surfaces. Many of these previous papers studied adsorption of heavy metals in binary systems in which the effect measured is dependent upon variation of one parameter at a time. This type of study

ignores possible synergic effects between parameters.

Several researchers reported the occurrence of organotin compounds in the aquatic environment. Mono-, di-, and trimethyltin compound concentrations are in the 10–1000 ng/L range (9–12). Saline and estuarine samples contain about 1–60 ng/L (9, 10, 12–14). Marine sediments, organisms, and shells also contain methyltin compounds (10, 13) at the 0.04–40 ng/g level.

Modeling of the fate of methyltin ions under realistic estuarine conditions requires a highly sensitive analytical technique due to their low concentrations. This paper describes studies of the partitioning of these compounds at the nanogram per milliliter level under simulated estuarine conditions with emphases on interactions of different parameters in a quaternary system including mono-, di-, or trimethyltin chloride, ionic strength, fulvic acid, and hydrous iron oxide. A  $2^3 + 1$  factorial design of experiments and analyses of variance (ANOVA) allow determination of the most important parameters contributing to removal of methyltin compounds during simulated estuarine mixing conditions and led to conclusions about removal mechanisms.

## Experimental Section

**Apparatus.** A technique derived from Andreae and Byrd (15) to determine methyltin compounds consists of several steps each of which was separately and carefully optimized. Methyltin compounds were volatilized by hydride generation, swept from the reaction vessel, trapped on a chromatographic packing material, released, atomized in a heated quartz furnace, and detected by atomic absorption spectroscopy (AAS). The electronic signal was filtered, amplified, and integrated.

The Pyrex reaction vessel was a round-bottom flask of 5-cm diameter and 7-cm height. An injection port on the side is capped by a septum. An internal standard and  $\text{NaBH}_4$  solution were injected through the septum. The flask had a 100-mL sample volume, and its design resulted in very little dead volume. There were connections for carrier gas inlet and outlet. The sample solution was stirred with a Teflon magnetic stirring bar. Methyltin hydrides were trapped after hydride generation at liquid nitrogen temperature in a U-shaped 45 cm long by 6 mm o.d. trap packed with 2.5 g of 10% SP-2100 on Chromosorb W (100–120 mesh). The trap was wrapped with a 28-gauge Nichrome wire having a 30- $\Omega$  resistance. The atomization furnace was aligned in the beam of an Instrumentation Laboratory Model 951 atomic absorption spectrophotometer (AAS). The 1.2 cm  $\times$  8 cm quartz furnace had two inlets located at its center and facing each other. It was wrapped with 26-gauge Nichrome wire, which had a 10- $\Omega$  total resistance, and was insulated by two rows of asbestos cord of 0.5-cm diameter. The electronic signal was amplified 10 times, filtered at 13 Hz, and recorded on a Hewlett-Packard Model 3392 A integrator. Methyltin compounds were identified by retention time and quantified by peak area measurements.

Careful optimization of each step resulted in the following operating conditions. A 100-mL sample was purged for 4 min prior to injection of the internal standard. Two minutes later 1.5 mL of 4%  $\text{NaBH}_4$  solution was injected.

**Table I. Percent Methyltin Compound Removal by Hydrous Iron Oxide and Its Adsorption Efficiency for the 2<sup>3</sup> + 1 Factorial Experiment<sup>a</sup>**

parameter	levels					
	MeSnCl <sub>3</sub>			Me <sub>2</sub> SnCl <sub>2</sub> , Me <sub>3</sub> SnCl		
	–	0	+	–	0	+
IS, g of NaCl/L	0	17.5	35	0	17.5	35
FA, mg/L	0	5	10	5	15	25
PM, mg/L	0	10	100	10	100	1000

expt	IS	FA	PM	% removal <sup>b</sup>			removal efficiency, <sup>c</sup> μmol/g		
				MeSnCl <sub>3</sub> <sup>d</sup>	Me <sub>2</sub> SnCl <sub>2</sub>	Me <sub>3</sub> SnCl	MeSnCl <sub>3</sub>	Me <sub>2</sub> SnCl <sub>2</sub>	Me <sub>3</sub> SnCl
1	+	+	+	98	55	28	0.413	0.023	0.012
2	–	+	+	97	66	17	0.409	0.028	0.007
3	+	–	+	93	56	18	0.392	0.024	0.007
4	–	–	+	96	60	15	0.406	0.026	0.006
5	+	+	–	ND	30	22	ND	1.30	0.921
6	–	+	–	ND	28	21	ND	1.18	0.874
7	+	–	–	ND	35	20	ND	1.50	0.861
8	–	–	–	ND	44	22	ND	1.88	0.912
9	0	0	0	91	42	23	3.83	0.175	0.097
10	0	0	0	88	45	22	3.71	0.190	0.093
11	0	0	0	93	41	22	3.92	0.175	0.094
12	0	0	0	92	39	20	3.88	0.165	0.083

<sup>a</sup> Abbreviations: IS is ionic strength (g of NaCl/L), FA is fulvic acid concentration (mg/L), PM is hydrous iron oxide concentration (mg/L), and ND is not determined. <sup>b</sup> Percent removal is the percent compound removed by filtration. <sup>c</sup> Removal efficiency is the micro-moles of compound removed per gram of hydrous iron oxide. <sup>d</sup> The percent removal is 83–100% with parameter ranges used for Me<sub>2</sub>SnCl<sub>2</sub> and Me<sub>3</sub>SnCl.

Methyltin hydrides were swept into the trap for 8 min and were desorbed from the trap during 7 min. Four gases were used in the analytical procedure. Argon blanketed the furnace from below resulting in a steadier base line and preventing oxidation of Nichrome wire. Helium was the carrier gas with a flow rate of 150 mL/min. Hydrogen and oxygen were added to the furnace at 850 °C. Hydrogen was added to the carrier gas just before the furnace, and the oxygen inlet was on the opposite side. The oxygen to hydrogen ratio strongly affected sensitivity, and a flow rate of 200 mL/min for hydrogen and 80 mL/min for oxygen was optimum. Electronic parameters were set as follows. AAS absorbance reading had a frequency of 0.2 s and scale and gain were expanded 5 times. Integrator parameters were attenuation 9, threshold 9, and peak width selection 0.16.

Because of the sensitivity of the technique and its dependence on the hydrogen/oxygen gas flow ratio, a Me<sub>3</sub>Sn internal standard was added with a 0.5-μL Hamilton syringe before reaction with NaBH<sub>4</sub>. A 68.9-ng sample (as Sn) typically gave a 1.2 × 10<sup>7</sup> peak area (arbitrary integrator units). All concentrations of tin compounds in this paper are expressed as Sn concentrations. The technique resulted in a linear calibration curve up to 3 ng/mL for each methyltin compound, a reproducibility better than 4% at the 1 ng/mL level, and a detection limit of 5 pg/mL. Retention times were SnH<sub>4</sub> (0.44 min), MeSnH<sub>3</sub> (1.59 min), Me<sub>2</sub>SnH<sub>2</sub> (2.48 min), Me<sub>3</sub>SnH (3.34 min), and Me<sub>4</sub>Sn (4.12 min).

**Reagents.** All glassware used for preparation, storage, and dilution was soaked in 10% HNO<sub>3</sub> and rinsed with deionized distilled water. Methyltin standards were purchased from Ventron and used without further purification. Stock solutions of 1000 μg/mL MeSnCl<sub>3</sub>, Me<sub>2</sub>SnCl<sub>2</sub>, and Me<sub>3</sub>SnCl were made in deionized distilled water spiked with 0.2 mL of 5 M HNO<sub>3</sub>. The Me<sub>3</sub>Sn standard was prepared in distilled methanol and kept in a sealed vial with a Teflon-coated septum. Stock standard solutions were stored in the dark at 4 °C and were shown to be stable over several months. New dilutions were made from stock solutions for each experiment. NaBH<sub>4</sub> was

purchased from Aldrich Chemical Co., and a 4% aqueous solution was made. Tin was detected in the 4% NaBH<sub>4</sub> solution (80 pg/mL) and in reagent-grade HNO<sub>3</sub>, but concentrations were small enough to be neglected. Adjustments to pH 8 were made with 0.1 M NaOH. A 5000 mg/L hydrous iron oxide stock solution was prepared by neutralization of an acidified 0.4 M iron(III) nitrate solution to pH 7 with carbonate-free 1 M NaOH solution. The precipitate was washed with deionized distilled water, centrifuged to separate solid and solution phases, and resuspended in deionized distilled water (16). The concentration of hydrous iron oxide was determined by evaporating to dryness a known volume. Solutions were aged 2 months before use. Under these conditions the cation exchange capacity was 45 mequiv/100 g and the pH of zero point of charge was 8.4 (16). Fulvic acid solutions were prepared by dissolving previously isolated fulvic acid extracted from soil (FA) in deionized distilled water and filtering at 0.4 μm prior to use. Weber and co-workers (17, 18) extensively characterized FA. Saline solutions were prepared by dissolving analytical-grade NaCl in deionized distilled water.

**Methods.** The appropriate amounts (Table I) of fulvic acid (FA), hydrous iron oxide (particulate matter, PM), and NaCl solution (ionic strength, IS) were mixed in 200-mL polycarbonate bottles and volumes increased to 95 mL with deionized distilled water. Samples were prepared in random order. Solutions were shaken for 4 h before the pH was determined with an Orion 701 A pH meter and an Orion 91-04 pH electrode. pH values in the 2.5–3.5 range were reproducible from one set of experiments to the next. Addition of 5 mL of a methyltin compound solution resulted in an initial concentration of 5 ng/mL. pH was readjusted to 8 with a 0.1 M NaOH solution, and the whole experimental set was shaken for 12 h. Each sample was filtered by 0.4-μm Nuclepore polycarbonate filters using an apparatus described by Truitt and Weber (19), and the filtrate was collected in a 100-mL volumetric flask. Final pH values were consistently in the 7–8 range. Each sample was spiked immediately with 0.2 mL of 5 M HNO<sub>3</sub> to bring the pH to 2 and decrease ad-

sorption on walls. Samples were diluted 2-fold to fit the linear part of the calibration curve and immediately analyzed by the technique described above. Calculations were made from internal  $\text{Me}_4\text{Sn}$  standards, and results were expressed as percent compound removed by filtration. One set of 12 factorial experiments was performed for each methyltin compound. The relative standard deviation for four center points was 2% for  $\text{MeSnCl}_3$ , 6% for  $\text{Me}_2\text{SnCl}_2$ , and 6% for  $\text{Me}_3\text{SnCl}$ .

Adsorption on walls was measured at the (+ + +) and (---) levels (Table I) in duplicate for each methyltin compound. After a 12-h equilibration solutions were removed from the 200-mL polycarbonate bottles, and 100 mL of deionized distilled water was added to them. The water was acidified to pH 2 with 5 M  $\text{HNO}_3$ , and the leaching solution was shaken for 4 h. Leaching solutions were analyzed as described above.

In some cases FA remaining in solution after filtration was determined by measuring absorbance at 260 nm with a Cary 14 spectrophotometer (17).

### Factorial Experimental Design

Factorial design of experiments enables us to simultaneously investigate the effects of all parameters and their combinations on removal of methyltin compounds. This experimental design was chosen for several reasons (20, 21). (1) Complexity of the system causes less meaningful results when only one variable at a time is changed. (2) Factorial experiments furnish the greatest amount of information for the fewest experiments. (3) Significant effects can be separated from nonsignificant ones. (4) The effect of one parameter on other parameters can be measured. When there are  $n$  parameters to consider,  $2^n$  experiments are necessary to measure the effects of all combinations of parameters when testing at high and low levels. Then  $n + 1$  center point experiments detect any nonlinearity in the experimental response and allow random error determination. Results of all experiments are statistically analyzed by analysis of variance (ANOVA).

Because of the complexity of estuarine processes and interactions of parameters during seaward transport, this design is most appropriate. It enables us to quantify the significance of single and multiple parameters affecting the removal of methyltin compounds at any confidence level. Validity of the experimental design lies in the choice and range of parameters chosen to realistically model a system and obtain statistically significant response. Among the important parameters in estuarine processes we chose three in belief that they and their combinations account for major nonbiological processes regulating the partitioning of heavy metals between estuarine particulate and dissolved phases. Salinity is the reference scale for estuarine processes (22, 23). Its effect is only considered here through changes in ionic strength (IS) for simplicity. We chose hydrous iron oxide as a model particulate (PM) and fulvic acid (FA) extracted from soil (18) to model riverine dissolved organic carbon. This fulvic acid from soil is very similar to that isolated from water (18). Iron oxides and organic matter are important scavengers of heavy metals in aquatic environments (24–26).

This study used parameter levels that cover ranges normally found in estuaries. The ranges were ionic strength (0–35 g of NaCl/L), fulvic acid concentration (0–25 mg/L), and particulate matter concentration (0–1000 mg/L). Saline values of 0, 17.5, and 35 g/L of NaCl, respectively, model the ionic strength, corresponding to freshwater, estuarine mixing, and seawater conditions. Varying PM concentrations on a log scale allowed us to simulate conditions found in microtidal and macrotidal

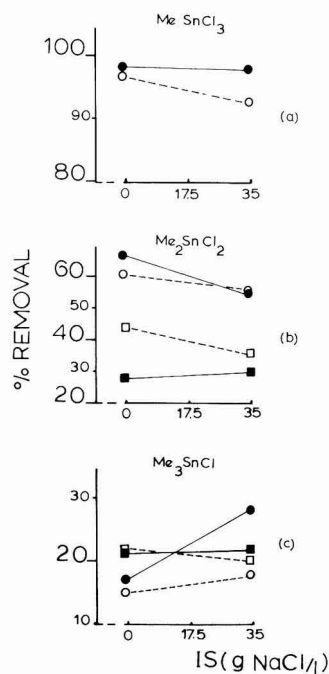


**Figure 1.** Influence of ionic strength (IS) on removal of  $\text{MeSnCl}_3$  (a),  $\text{Me}_2\text{SnCl}_2$  (b), and  $\text{Me}_3\text{SnCl}$  (c). Low PM experiments not done for  $\text{MeSnCl}_3$ . (●) +FA, +PM; (○) -FA, +PM; (■) +FA, -PM; (□) -FA, -PM.

estuaries. To achieve realistic conditions, the initial methyltin compound concentration is 5 ng/L (as Sn). This initial concentration allowed us to measure greater than 95% removal. After variable levels were established, low, center point, and high levels were, respectively, coded as (–), 0, and (+). The  $2^3 + 1$  experimental design and parameter values are shown in Table I. Experiments were done in random order to avoid systematic errors such as personal bias or aging of solutions.

### Results

**Background Losses.** To determine the validity of the results obtained, analytical losses due to clogging of the filter (27) and adsorption on container walls were assessed. Small (100 mL) sample volumes prevented clogging of the filter. To measure adsorption on walls, we did duplicate experiments for each methyltin compound at the (+ + +) and (---) levels (Table I). Adsorptive losses were less than 1% for  $\text{MeSnCl}_3$ , 2% for  $\text{Me}_2\text{SnCl}_2$ , and 1% for  $\text{Me}_3\text{SnCl}$  in all cases. These losses were smaller than percent relative standard deviation (% RSD) calculated for each center point replicate, and therefore, no adsorption corrections were necessary.

**General Results.** The results of quantitative removal of methyltin chlorides by filtration are shown in Table I and Figures 1–3. Table I indicates that each methyltin chloride has a different behavior under simulated estuarine conditions. A first set of experiments with the parameter ranges used for  $\text{Me}_2\text{SnCl}_2$  and  $\text{Me}_3\text{SnCl}$  (Table I) resulted in 83–100% removal of  $\text{MeSnCl}_3$ . Because of the narrow range of removal, we repeated the experiments using lower FA and PM (Table I). Even with these conditions, removal of  $\text{MeSnCl}_3$  was nearly complete (88–98%). The removal of  $\text{Me}_2\text{SnCl}_2$  ranged from 28 to 66% and showed a greater dependence on parameter settings.  $\text{Me}_3\text{SnCl}$  removal had

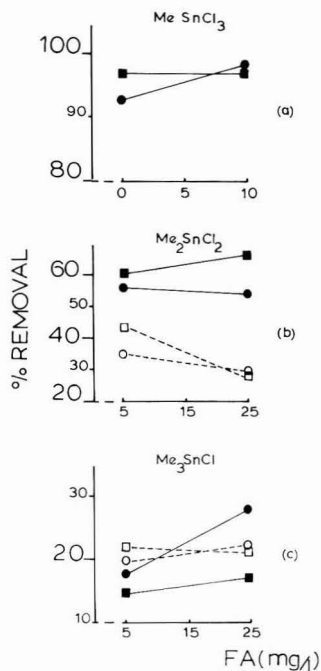


**Figure 2.** Influence of fulvic acid concentration (FA) on removal of  $\text{MeSnCl}_3$  (a),  $\text{Me}_2\text{SnCl}_2$  (b), and  $\text{Me}_3\text{SnCl}$  (c). Low PM experiments not done for  $\text{MeSnCl}_3$ . (●) +IS, +PM; (○) +IS, -PM; (■) -IS, +PM; (□) -IS, -PM.

**Table II.** Statistical Significance of Parameters<sup>a</sup>

effect <sup>b</sup>	$\text{Me}_2\text{SnCl}_2$	$\text{Me}_3\text{SnCl}$
IS	9.55	12.39
FA	5.05	10.74
PM	<u>197.37</u>	3.16
IS-PM	0.31	12.74
IS-FA	1.26	6.25
FA-PM	<u>13.34</u>	8.63
IS-FA-PM	6.39	1.91
LOF	<u>11.60</u>	2.60

<sup>a</sup> Underlined values indicate significance at the 95% confidence level. The literature *F* value for 95% confidence level is 10.13.

<sup>b</sup> Abbreviations: IS is ionic strength, FA is fulvic acid concentration, PM is hydrous iron oxide concentration, and LOF is lack of fit.

a range of 17–28%. Figures 1–3 show the separate effects of IS, FA, and PM on methyltin compound removal. The lines between pairs of points do not represent removal isotherms but indicate general trends. The slope of a line is significantly nonzero if its high and low values vary more than the % RSD for the compound determined from the center points.

Table II gives the ANOVA results of the  $2^3 + 1$  factorial experiments for  $\text{Me}_2\text{SnCl}_2$  and  $\text{Me}_3\text{SnCl}$ . ANOVA statistical analysis of data could not be applied to  $\text{MeSnCl}_3$  because of the absence of PM in vials 5–8 (see Table I). Underlined values are significant at the 95% confidence level.

Table II shows the statistical significance of IS, FA, PM, their combinations, and lack of fit for  $\text{Me}_2\text{SnCl}_2$  and  $\text{Me}_3\text{SnCl}$  experiments. PM and the FA-PM combination are significant for  $\text{Me}_2\text{SnCl}_2$  removal. The very high PM value (197.37) indicates its overwhelming importance, and the steep slopes in Figure 3b confirm this result. The high

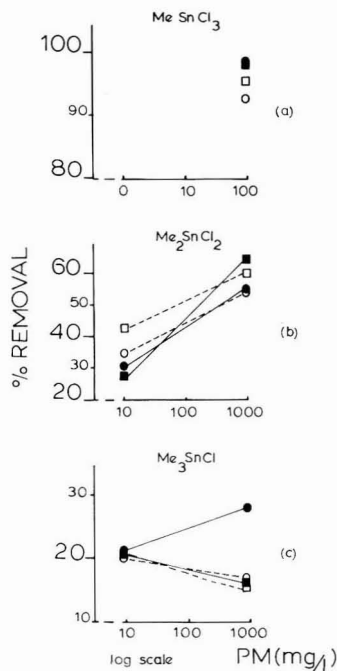


**Figure 3.** Influence of particulate matter concentration (PM) on removal of  $\text{MeSnCl}_3$  (a),  $\text{Me}_2\text{SnCl}_2$  (b), and  $\text{Me}_3\text{SnCl}$  (c). Low PM experiments not done for  $\text{MeSnCl}_3$ . (●) +IS, +FA; (○) +IS, -FA; (■) -IS, +FA; (□) -IS, -FA.

PM value also accounts for the significance of the FA-PM combination. Significant parameters for  $\text{Me}_3\text{SnCl}$  are IS, FA, and IS-PM. Low values for IS and FA in Table II indicate that these parameters are less important than PM for removal of  $\text{Me}_2\text{SnCl}_2$ .

The lack of fit, which originates from ANOVA calculations, allows a testing of the curvature of experimental response surfaces. Significance of the lack of fit term means that there is not a linear response to the parameter tested (20).  $\text{Me}_2\text{SnCl}_2$  has a significant lack of fit. This result is expected since adsorption of heavy metals is not linear with increasing IS or PM under simulated estuarine conditions (8). The reasons for the nonsignificant lack of fit for  $\text{Me}_3\text{SnCl}$  is not completely clear but might indicate a different removal mechanism or result from the small overall removal range in our experiments.

Identification of nonsignificant parameters can also be helpful, but this information must be used cautiously. A parameter might be regarded as nonsignificant either because it has no real interaction in the processes or because it has opposing responses with respect to two other variables. For example, FA is not statistically significant for  $\text{Me}_2\text{SnCl}_2$  (Figure 2b) because effects of ionic strength at high PM (● and ■) oppose those at low PM (○ and □). The result of the ANOVA calculations is a value of 5.05 for FA in the  $\text{Me}_2\text{SnCl}_2$  experiment (Table II). Interpretation of nonsignificant combined effects poses similar difficulties.

#### Influence of Parameters on Organotins Removal.

In most cases increasing NaCl concentration results in decreased methyltin compound removal (Figure 1). This trend is most pronounced for  $\text{MeSnCl}_3$  (Figure 1a) at low FA and high PM (○) and for  $\text{Me}_2\text{SnCl}_2$  (Figure 1b) at low PM and FA (□) or high PM and FA (●). However, there are statistically significant opposite trends for  $\text{Me}_2\text{SnCl}_2$



(Figure 1b) at high FA and low PM (■) and for Me<sub>3</sub>SnCl (Figure 1c) at high PM and low (○) or high (●) FA. The usual effect of increasing FA is increased removal of methyltin compounds (Figure 2). However, in some cases, e.g., for Me<sub>2</sub>SnCl<sub>2</sub> (Figure 2b) at high IS and PM (●) the trend is not statistically significant. The influence of FA on removal of Me<sub>2</sub>SnCl<sub>2</sub> (Figure 2b) is ambiguous and, as previously explained, can lead to erroneous interpretation of ANOVA results. At freshwater IS, increasing FA results in increased removal at high PM (●), but low PM and high (○) or low (□) IS result in less removal with increasing FA. As expected (8, 23) increased PM increases removal of Me<sub>2</sub>SnCl<sub>2</sub> (Figure 3b). Me<sub>3</sub>SnCl (Figure 3c) is an anomaly because only the high IS and FA data (●) agree with the general trend. The other three combinations are strongly opposed.

Table I also contains data on the removal efficiency of each methyltin compound by hydrous iron oxide. Removal efficiency is defined as micromoles of methyltin compound removed per gram of hydrous iron oxide. Several kinds of results are important. First, for all three compounds the removal efficiency decreases significantly as PM concentration increases. Second, at any PM level the efficiency of removal is not affected by IS or FA. Third, removal efficiency is MeSnCl<sub>3</sub> >> Me<sub>2</sub>SnCl<sub>2</sub> > Me<sub>3</sub>SnCl.

### Discussion

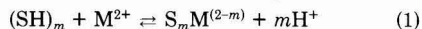
One major mechanism for removal of metal species from the dissolved phase of natural waters is adsorption onto particulate matter. A second one is coagulation in which the removed species might be adsorbed on or trapped within newly formed particulate matter. The strength and nature of interactions of methyltin species depend on the nature of the hydrolyzed compounds in water, the charge on the adsorbing surface, and the types of dissolved species—particulate matter attractive forces. In general, these forces include attractions between ions and dipoles, between dipoles and dipoles, and van der Waals forces.

**Removal Mechanisms.** Previous workers (28, 29) reported that Me<sub>2</sub>SnCl<sub>2</sub> and Me<sub>3</sub>SnCl exist, respectively, as +2 and +1 ions at low pH. However, at pH 8 it is likely that neutral Me<sub>3</sub>SnOH, Me<sub>2</sub>Sn(OH)<sub>2</sub>, and MeSn(OH)<sub>3</sub> exist in the absence of chloride ion (30, 31). The species would be hydrated to a coordination number of five or six. Cl<sup>-</sup> probably competes effectively with OH<sup>-</sup> at IS = 35 g of NaCl/L to form unknown, probably neutral, species. Omar and Bowen (28) assume that MeSnCl<sub>3</sub> reacts very weakly with humic substances and forms polymeric species, but we know of no other data on the nature of MeSnCl<sub>3</sub> in water.

The zero point of charge of hydrous iron oxide is at pH 8.4 (16). Thus, at pH 8 it will have a slight positive charge. In our experiments the mixing of hydrous iron oxide and FA results in a solution with pH 2–3. In this pH range most FA will be adsorbed (32, 33), and the FA-coated particle will have a negative charge (34, 35). In addition absorption due to increased ionic strength might induce coagulation (36) to form amorphous FA-PM particles. Therefore, in our system we are adding predominantly neutral methyltin species to negatively charged hydrous iron oxide-FA aggregates. Adjusting the pH to 8 and shaking for 12 h brings the system to a new equilibrium before filtration. At 10 mg/L PM, FA is present in excess as determined by measuring the absorbance of the filtrate at 260 nm. When PM is 1000 or 100 mg/L, however, FA is nearly 100% removed. These observations are in agreement with the adsorption capacity of FA on goethite determined by Tipping (32) to be 75 mg/g. Increasing salinity at constant FA and PM increases FA removal.

Removal of methyltin compounds in our experiments could occur by many processes. We rule out adsorption on walls on the basis of previously mentioned experiments, and precipitation is unlikely at the low concentrations used in the experiments. We assume that methyltin species removal is due to adsorption, coagulation, or both processes simultaneously. We cannot differentiate the two processes.

Davis and Leckie (37) and Bourg (38) described an adsorption model for metal ions (M<sup>2+</sup>) (eq 1). In our ex-



periments SH is –OH on hydrous iron oxide and –COOH from FA. If we assume that all FA coats the hydrous iron oxide surface or stays in solution, calculation of total available methyltin species binding sites is possible. Calculations using data such as 75 mg/g of FA adsorbed on the surface (32), 6.7 mmol/g of –COOH in FA (17), and 0.35 mmol/g of S–OH (23) lead to the result that total adsorption sites available in our experiments vary from 0.503 to 35 μmol. Thus, in our experiments micromoles of S–OH plus –COOH adsorbing sites exceed those of methyltin compounds by factors of 100–8000. Yet our results (Table I) indicate significantly incomplete removal of Me<sub>2</sub>SnCl<sub>2</sub> and Me<sub>3</sub>SnCl. Occlusion of –OH and –COOH binding sites within PM-FA aggregates may partially account for this discrepancy. In contrast experiments with alum, FA, and Cu<sup>2+</sup> result in high Cu<sup>2+</sup> removal (17).

The metal ion adsorption model clearly cannot satisfactorily explain our results. The fact that methyltin species in solution are neutral means that most likely the results are explainable on the basis of polarity of methyltin molecules rather than their ionic charges. The importance of their dipoles probably accounts for the inaccuracy of the model. Available evidence (28, 39) based on molecular shapes suggests the following polarity order: MeSnCl<sub>3</sub> > Me<sub>2</sub>SnCl<sub>2</sub> > Me<sub>3</sub>SnCl. The corresponding efficiency of removal (Table I) suggests that adsorption might occur by one or more of ion–dipole, dipole–dipole, or van der Waals forces, but our experiments do not distinguish these bonding mechanisms.

**Importance of Ionic Strength.** Usually, the metal ion adsorption model predicts less adsorption at high IS due to competition of Na<sup>+</sup> with metal ions for PM sites and competition of Cl<sup>-</sup> with PM sites for metal ions (6–8). In addition Na<sup>+</sup>, with increasing salinity, reduces the volume of the particulate matter double layer (40), saturates the PM surface, and partially neutralizes –COO<sup>-</sup> groups of FA bound to it leading to a less negative PM charge. Organotin dipoles will therefore be less attracted to PM at high NaCl concentrations. In the case of Me<sub>2</sub>SnCl<sub>2</sub> (Figure 1b), high FA and low PM (■) allow some of the FA to remain in solution. This effect is enhanced at higher ionic strength, resulting in decreased removal of Me<sub>2</sub>SnCl<sub>2</sub> since Me<sub>2</sub>SnCl<sub>2</sub> binds more strongly to free than to adsorbed FA. For Me<sub>3</sub>SnCl at high PM and high (●) or low (○) FA almost all FA is adsorbed. Na<sup>+</sup> adsorption on the PM-FA aggregate can displace weakly bound trimethyltin species, or Cl<sup>-</sup> might bind to Me<sub>3</sub>SnCl and prevent its adsorption. Second, increased IS might lead to coagulation processes involving hydrous iron oxide and FA by destabilization of the FA-coated, negatively charged colloids by seawater cations (42). At high IS and FA, the increased removal of Me<sub>3</sub>SnCl could also be accounted for by salting out of the methylated tins and partitioning into the absorbed organic phase. Coagulation might selectively remove di- and trimethyltin species. We are presently unable to distinguish these two mechanisms.

**Importance of Fulvic Acid Concentration.** FA like IS plays conflicting roles. The general trends (Figure 2)

of increasing methyltin compound removal as FA increases is caused by increased FA adsorption on PM and enhanced capacity of the PM-FA aggregate for adsorption of methyltin species. However, consideration of  $\text{Me}_3\text{SnCl}_2$  (Figure 2b) shows that adsorption is higher at high PM (● and ■) than at low PM (○ and □) for low or high FA values. Furthermore, increased FA at low PM significantly decreases removal, while the opposite trend occurs at high PM. These results suggest that excess FA in solution complexes the dimethyltin species, preventing its adsorption. Several papers (43–46) reported the same effect with  $\text{Cu}^{2+}$  and FA because of  $\text{Cu}^{2+}$ -FA complex formation. A similar phenomenon might occur for  $\text{Me}_2\text{SnCl}_2$  and FA (eq 2). (Fulvic acid has a 3- charge in eq 2 because it has



about three -COOH's per average molecule.) The resulting negative charge of  $\text{Me}_2\text{Sn}(\text{FA})^-$  prevents its adsorption on negatively charged PM-FA.

**Importance of Particulate Matter Concentration.** Increasing PM generally enhances removal of metal ions by providing more exchange sites, and the same trend might occur with methyltin compounds. The expectation is true for  $\text{Me}_2\text{SnCl}_2$  (Figure 3b) in which the percentage change is the highest for any set of data in this paper. However,  $\text{Me}_3\text{SnCl}$  (Figure 3c) shows very different behavior, as three of four cases show decreased removal with increased PM. Because anomalous trends occur with various combinations of IS and FA levels, their rationalization must lie in the difference between  $\text{Me}_2\text{SnCl}_2$  and  $\text{Me}_3\text{SnCl}$ . The answer is probably related to the nonpolar trigonal plane of the  $\text{Me}_3\text{Sn}$  group (28, 39). Apparently this group has little affinity for PM-FA except for high PM and FA values (●) at high ionic strength.

Parts b and c of Figure 3 reveal that even low PM removes significant amounts of methyltin species. Data in Table I that show increased PM removal efficiency at low values anticipate this result. Furthermore, Tipping (32) demonstrated that at low humic matter/goethite ratios, humic substances confer more negative charge on the iron oxide surface per humic matter mass adsorbed than at high ratios. Thus, low loadings have higher adsorption capacity than high loadings. As the concentration of suspended solids and ionic strength both increase, collisions among particles resulting in aggregate formation are more probable. These larger particles have less surface area per volume. The result is the adsorption efficiency of hydrous iron oxide for methyltin compounds decreases.

## Conclusions

Factorial experiments are very effective for modeling of estuarine processes. Besides quantitative percent removal values for a variety of conditions, ANOVA calculations assess the significance of all parameters and their interactions.

The range of removal of methyltin compounds under conditions identical for each compound is  $\text{MeSnCl}_3$  (83–100%) >  $\text{Me}_2\text{SnCl}_2$  (28–66%) >  $\text{Me}_3\text{SnCl}$  (15–28%). At pH 8 mono-, di-, and trimethyltin species are likely to be neutral, and FA-coated PM is negatively charged. There are probably two removal processes. First, attractive forces of adsorption are probably ion-dipole, dipole-dipole, and van der Waals ones. In agreement the percent removal is proportional to the polarity of methyltin compounds. Second, coagulation of hydrous iron oxides and FA under simulated estuarine mixing conditions can cause adsorption and entrapment of methyltin compounds.

Ionic strength, which is the most important parameter in many cases, plays an ambiguous role. Most significant

trends show less methyltin compound removal at high NaCl concentrations. Increased FA generally leads to increased removal of methyltin species. Apparently excess FA in solution complexes the dimethyltin species preventing its adsorption. High PM enhances removal of  $\text{Me}_2\text{SnCl}_2$  but generally not of  $\text{Me}_3\text{SnCl}$ . The reason for this behavior is not clear but must relate to the nonpolar nature of  $\text{Me}_3\text{SnCl}$  in water.

The first overall conclusion is that during estuarine processes  $\text{MeSnCl}_3$  will be almost completely adsorbed,  $\text{Me}_2\text{SnCl}_2$  will be in adsorbed and dissolved phases, and  $\text{Me}_3\text{SnCl}$  will be predominantly in the dissolved phase. Thus, the most toxic  $\text{Me}_3\text{SnCl}$  presents an immediate threat due to bioaccumulation. The second major conclusion is that methyltin species show a very different behavior from metal ions such as  $\text{Cu}^{2+}$  and  $\text{Cd}^{2+}$  in simulated estuarine systems.

## Acknowledgments

We thank Timothy M. Kenney and Frederick G. Hochgraf for advice on heating the quartz furnace and Spyridon Rapsomanikis and William F. Guerin for their comments.

**Registry No.**  $\text{MeSnCl}_3$ , 993-16-8;  $\text{Me}_2\text{SnCl}_2$ , 753-73-1;  $\text{Me}_3\text{SnCl}$ , 1066-45-1; hydrous iron oxide, 1309-33-7.

## Literature Cited

- (1) World Health Organization "Environmental Health Criteria. 15. Tin and Organotin Compounds". Geneva, 1980.
- (2) Craig, P. J. In "Comprehensive Organometallic Chemistry"; Wilkinson, G., Ed.; Pergamon Press: Oxford, U.K., 1983; Vol. 2, pp 979–1020.
- (3) Smith, P. J. "Toxicological Data on Organotin Compounds". Greenford, Middlesex, England, 1978, International Tin Research Institute Publication 538.
- (4) Alzieu, C.; Thibaud, Y. *Bull. Acad. Natl. Med. (Paris)*, 1983, 167, 473–482.
- (5) Millward, G. E. *Environ. Technol. Lett.* 1980, 1, 394–399.
- (6) Bourg, A. C. M. In "Trace Metals in Seawater"; Wong, C. S.; Boyle, E.; Bruland, K. W.; Burton, J. D.; Goldberg, E. D., Eds.; Plenum Press: New York, 1983; pp 195–208.
- (7) Van der Weijden, C. H. *Mar. Chem.* 1976, 377–387.
- (8) Salomons, W. *Environ. Technol. Lett.* 1980, 1, 356–365.
- (9) Hodge, V. F.; Seidel, S. L.; Goldberg, E. D. *Anal. Chem.* 1979, 51, 1256–1259.
- (10) Braman, R. S.; Tompkins, M. A. *Anal. Chem.* 1979, 51, 12–19.
- (11) Maguire, R. J. *Environ. Sci. Technol.* 1984, 18, 291–294.
- (12) Byrd, J. T.; Andreae, M. O. *Nature (London)* 1982, 218, 565–569.
- (13) Tugrul, S.; Balkas, T. I.; Goldberg, E. D. *Mar. Pollut. Bull.* 1983, 14, 297–303.
- (14) Jackson, J. A.; Blair, W. R.; Brinckman, F. E.; Iverson, W. P. *Environ. Sci. Technol.* 1982, 16, 110–119.
- (15) Andreae, M. O.; Byrd, J. T. *Anal. Chim. Acta* 1984, 156, 147–157.
- (16) Page, F. W. Ph.D. Thesis, University of New Hampshire, Durham, 1982.
- (17) Truitt, R. E.; Weber, J. H. *Water Res.* 1979, 13, 1171–1177.
- (18) Saar, R. A.; Weber, J. H. *Environ. Sci. Technol.* 1982, 16, 510A–517A.
- (19) Truitt, R. E.; Weber, J. H. *Anal. Chem.* 1979, 51, 2057–2059.
- (20) Cochran, W. G.; Cos, G. M. "Experimental Design", 2nd ed.; Wiley: New York, 1957.
- (21) Box, G. E. P.; Hunter, W. G.; Hunter, J. S. "Statistics for Experiments"; Wiley: New York, 1978.
- (22) Donard, O. F. X. These Doct. en Sciences, University of Bordeaux I, No. 1887, 1983.
- (23) Bourg, A. C. M. These Doct. es Sciences, University of Bordeaux I, No. 689, 1983.
- (24) Lion, L. W.; Altmann, R. S.; Leckie, J. O. *Environ. Sci. Technol.* 1982, 16, 660–666.

- (25) Lyons, W. B.; Gaudette, H. E. *Oceanol. Acta* 1979, 2, 477-481.
- (26) Houba, C.; Remacle, J.; Dubois, D.; Thorez, J. *Water Res.* 1983, 17, 1281-1286.
- (27) Laxen, D. P. H.; Chandler, I. M. *Anal. Chem.* 1982, 54, 1350-1355.
- (28) Blunden, S. B. *J. Organomet. Chem.* 1983, 248, 149-160.
- (29) Omar, M.; Bowen, H. J. M. *J. Radioanal. Chem.* 1982, 74, 273-282.
- (30) Baes, C. F., Jr.; Mesmer, R. E. "The Hydrolysis of Cations"; Wiley: New York, 1976.
- (31) Tobias, R. S. In "Organometals and Organometalloids"; Brinckman, F. E.; Bellama, J. M., Ed.; American Chemical Society: Washington, DC; 1978, ACS Symp. Ser. No. 82, pp 130-148.
- (32) Tipping, E. *Geochim. Cosmochim. Acta* 1981, 45, 191-199.
- (33) Tipping, E. *Chem. Geol.* 1981, 33, 81-89.
- (34) Hunter, K. A.; Liss, P. S. *Nature (London)* 1979, 282, 823-825.
- (35) Loder, T. C.; Liss, P. S. *Thalassia Jugosl.* 1982, 18, 433-446.
- (36) Sholkovitz, E. R.; Boyle, E. A.; Price, N. B. *Earth Planet. Sci. Lett.* 1978, 40, 130-136.
- (37) Davis, J. A.; Leckie, J. O. *J. Colloid Interface Sci.* 1978, 67, 90-107.
- (38) Bourg, A. C. M. *C.R. Seances Acad. Sci., Ser. 2* 1982, 294, 1091-1094.
- (39) McGrady, M. M.; Tobias, R. S. *Inorg. Chem.* 1964, 3, 1157-1163.
- (40) Preston, M. R.; Riley, J. P. *Estuarine Coastal Shelf Sci.* 1982, 14, 567-576.
- (41) Mayer, L. M. *Geochim. Cosmochim. Acta* 1982, 46, 2527-2535.
- (42) Shen, G. T.; Sholkovitz, E. D.; Mann, D. R. *Earth Planet. Sci. Lett.* 1983, 64, 437-444.
- (43) Davis, J. A.; Leckie, J. O. *Environ. Sci. Technol.* 1978, 12, 1309-1315.
- (44) Sholkovitz, E. R.; Copland, D. *Geochim. Cosmochim. Acta* 1981, 45, 181-189.
- (45) Bourg, A. C. M.; Schindler, P. W. *Inorg. Nucl. Chem. Lett.* 1979, 15, 225-229.
- (46) Dalang, F.; Buffle, J.; Haerdi, W. *Environ. Sci. Technol.* 1984, 18, 135-141.

Received for review July 20, 1984. Revised manuscript received January 2, 1985. Accepted May 28, 1985. This project was funded in part by the Office of Sea Grant, National Oceanic and Atmospheric Administration, U.S. Department of Commerce, through Grant R/PMR-84-D to the University of New Hampshire. This is contribution UNH-MP-JR-8G-84-7 from the University of New Hampshire Sea Grant program. Although the research described in this article has been funded in part by the U.S. EPA by Grant R 809416, it has not been subjected to the Agency's required peer and administrative review and, therefore, does not necessarily reflect the view of the Agency, and no official endorsement should be inferred.

## Microcomputer-Controlled Two Size Fractionating Aerosol Sampler for Outdoor Environments

Hans-Christen Hansson\* and Stefan Nyman

Department of Nuclear Physics, Lund Institute of Technology, S-223 62 Lund, Sweden

■ A microcomputer-controlled aerosol sampler has been constructed to give an optimized sampling system for measurements in outdoor environments compatible with particle-induced X-ray emission (PIXE) analysis. Aerodynamic, mechanic, and electronic principles of this sampler are discussed. The sampler has a capacity of 70 samples at the maximum flow rate of 5 L/min. The larger particles are collected on an impactor stage, and the smaller particles are deposited on a filter after the impactation stage. It is easy to vary the cutoff diameter from 1 to 5  $\mu\text{m}$  and the deposition area on the filter to suite the demands of the specific sample situation or to obtain the best possible detection limits. Tests carried out to investigate internal losses, impactor characteristics, and filter efficiency are presented. At the maximum flow rate the total losses, including wall losses, bounce off, and filter leakage, are of the 5-15% range for particle sizes between 0.05 and 10  $\mu\text{m}$ .

### Introduction

During the last decade, extensive development of increasingly sophisticated aerosol samplers for outdoor environments has taken place. The early types of simple total aerosol samples (e.g., the high volume samplers) were found to be poorly suited to new analytical methods. The requirements for certain standards for sampling aerosols grew with increasing knowledge of physical and chemical properties of the aerosol.

Different X-ray spectrometric analytical methods such as X-ray fluorescence (XRF) and particle-induced X-ray emission (PIXE) proved to be very useful tools in the field

of research on the atmospheric aerosol (1, 2). In particular PIXE has been used in studies of the elemental composition of the atmospheric aerosol with high time and size resolution, yielding new knowledge about the transport, transformation, and deposition of heavy-metal containing aerosols (3-5).

Several aerosol samplers suitable for these analytical techniques have been used in studies concerning the atmospheric aerosol. The dichotomous sampler (6) for XRF and the continuous filter sampler (the streaker) (7) and the Battelle cascade impactor for PIXE are some of the most frequently and successfully used instruments.

Investigations concerning the physical properties of the atmospheric aerosol gave strong evidence for a trimodal log-normal particle size distribution. The components of the mass distribution containing most of the mass are the accumulation and coarse modes (8), with the two modes often having different origins. The latter is mostly connected with mechanical processes such as sea-spray generation and soil resuspension while the former contains particles from the high- and low-temperature condensation processes, e.g., combustion and gas to particle conversion. Hence, the chemical compositions of these modes differ. Together, this makes separate collection necessary. The minimum of mass concentration between the coarse and the fine mode is usually found to be in the region of 1.0-2.5  $\mu\text{m}$  (8, 9).

Exposure of humans and deposition on, for example, vegetation are other important processes to be considered in the sampling of aerosols. The deposition rates on different kinds of vegetation are not well-known, since other

parameters besides particle size distributions influence the deposition processes such as surface characteristics and meteorological factors.

The deposition processes in the human lung have been measured and calculated in many different studies (10, 11). As a result of these and other similar reports a convention has been proposed by the Ad hoc Working Group appointed to International Standards Organization (ISO) technical committee 146 (12) for application in the sampling of airborne particles. The convention is thoroughly discussed by, for example, Ogden (13) and Lippmann et al. (14). The 50% cutoff of the ambient particles (not inspired) for the alveolar convention of the British Medical Research Council (BMRC) is 4.5  $\mu\text{m}$  and for the American Conference of Governmental Industrial Hygienists (ACGIH) is 3.2  $\mu\text{m}$ . For groups other than healthy adults, all the diameters are reduced 29% for the alveolar convention, which gives the cutoff diameter 2.2  $\mu\text{m}$  for the ACGIH alveolar convention.

For the thoracic convention we have 8.7  $\mu\text{m}$  according to both the BMRC and the ACGIH (=10  $\mu\text{m}$  in case of 50% cutoff of the inspired fraction).

By compiling this knowledge about the requirements for concentration data in specific particle size fractions, it can be concluded that, for most applications, two fractions are needed: one fine particle fraction with no lower cutoff and a cutoff toward the coarse fraction. The cutoff between the fractions can be chosen to be between 1 and 5  $\mu\text{m}$  depending on the specific purpose of the sampling. To be able to sample according to the alveolar and thoracic convention discussed above, the sampler has to be able to handle particles up to 10  $\mu\text{m}$  without significant internal losses. The study of the total coarse mode or particles under consideration in the extra thoracic convention (5–150  $\mu\text{m}$ ) (12) is very complicated due to the great difficulties in sampling particles with aerodynamic diameters larger than 15–20  $\mu\text{m}$  in an unknown wind field.

Aerosol concentration can vary over several decades in different atmospheric environments, e.g., when going from the Arctic to urban air. Therefore, it is very convenient if the sample mass per unit area can be controlled, in order to maintain lowest possible detection limits in the analysis, by changing the flow rate and/or changing the deposition area.

Other properties of importance in an "all-round" sampler are facilities for automatic sequential sampling and control and/or recording of the flow rate during sampling. The degree of automation should be high enough for the sampling strategy to be as free as possible from constraints caused by the sampler. Of course, high reliability is also of great importance.

#### Technical Description

**Principles.** As a consequence of the considerations discussed above, a sampler was constructed to collect two size fractions and up to 10- $\mu\text{m}$  size particles without significant internal losses.

To define the cutoff between the coarse and fine fractions, an impactor was chosen on the grounds of its well-known characteristics (15). When a change in cutoff is required, it is relatively easy to modify the impactor without causing any significant change in the particle losses. Conventional impactors are often rejected due to the problem of particle bounce off. This problem cannot be completely solved by using an adhesive grease, because particle to particle bounce will increase during the sampling. If the aerosol is dry, bounce off can cause very large errors (16). A good solution to this problem has been proposed and experimentally verified by Reischl and John

(16). They used an oil with low viscosity that was continuously fed to a porous impaction plate during sampling. The oil did not only wet the impaction plate but also the particles, due to its low viscosity. With this system the bounce off was reduced to below 1%. In a basic study Dahneke (17) has shown that the particle bounce off is directly related to the particle velocity and can be reduced by decreasing the impaction jet velocity.

For the fine particle collection a filtration stage was chosen. To facilitate repositioning for a new sample and later analysis, it is favorable to use a strong thin membrane filter. Nuclepore has been found to suit both the analysis as well as the sampling procedures (7). In the "streaker" sampler, the Nuclepore filter is used with a simple mechanical device, which makes it possible to collect many samples on one filter (7).

A major drawback of the Nuclepore filter is significant pore clogging caused by aerosols with high particle concentrations within certain size fractions, especially very fine particles (18). The flow rate has to be monitored and, if possible, controlled during sampling. The strategy used for the present sampler is to compare the flow rate with a preset value. If necessary the sampling is stopped and continued on the next fresh sampling area on the filter. The time at which the sample was changed is recorded.

The maintenance of the sampler, manual changing of filters, and manual checking of flow rate, pumps, and so forth are today often the most expensive and limiting part of sampling programs. Therefore, we made the filter strips large enough to accommodate many sample positions. To utilize the filters as efficiently as possible, the sample area for each sample, as well as the distance between different samples, can be changed for different flow rates.

**Mechanics.** Figure 1 shows the essential features of the sampler. The aerosol enters through the impactor nozzle which is an eight-hole multijet nozzle for the maximum flow rate of 5 L/min. The jet holes are 1.1 mm in diameter. At a flow rate of 5 L/min the nozzle will give a cutoff at about 2- $\mu\text{m}$  aerodynamic diameter. The multijet is preferred due to the lower air jet velocity and the larger area of deposition to decrease bounce-off effects. A Nuclepore filter is chosen as deposition foil. The filter strip is glued on to a plastic frame (2.5  $\times$  20 cm). Four frames with impaction foils together form a ring and are mounted on the side of a cylinder. The parts of this surface underneath the foils are made of porous plastic, which can be soaked in low viscosity silicone oil. The oil is then drawn out to the deposited aerosol through the foil by capillary forces. Inside the cylindrical impaction surface there is a second concentric cylinder supporting the four plastic filter frames of the filtration stage. This supporting cylinder has a diameter 2 cm smaller than the cylinder supporting the impaction substrate. Underneath the filtration stage a Teflon mouthpiece streaks along the filter surface. This mouthpiece is connected to a pump and has an 8-mm diameter allowing a maximum flow of 5 L/min. This reduces the pressure by 270 mmHg (relative to atmospheric pressure) for a filter with 0.3- $\mu\text{m}$  pore size. As a result of this reduction in pressure, the filter is sucked close to the mouthpiece without significant leakage. To measure the flow rate, an electronic pressure gauge downstream of the filter is used to measure the pressure drop over a valve. The two concentric cylindrical surfaces, carrying the impaction and filter surfaces, are attached to the same circular disk. The disk is connected through a gear to a stepping motor. When this disk is turned, a new sampling position is obtained with fresh impaction and filtration surfaces. At the maximum flow of 5 L/min the maximum



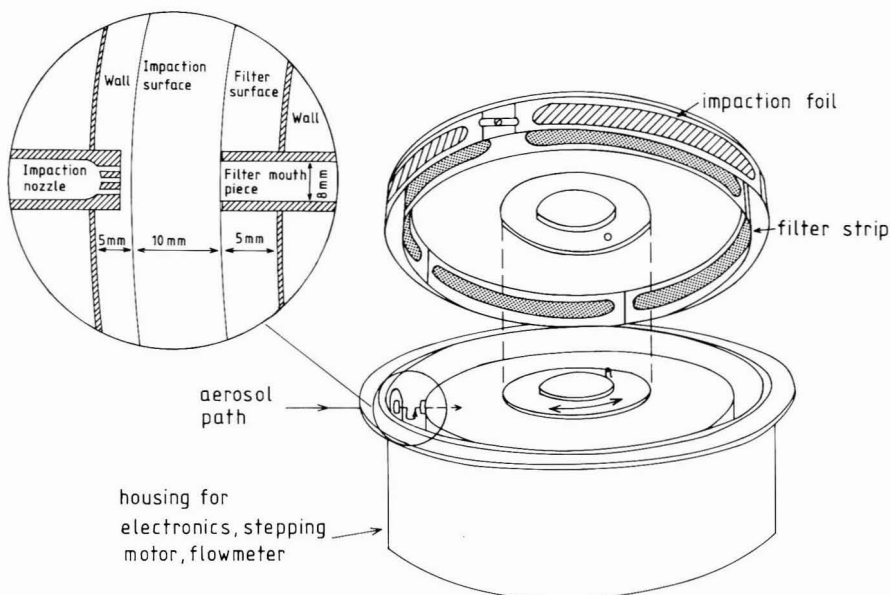


**Figure 1.** Schematic drawing of the sampler with the filter holder lifted. An enlargement of the impaction nozzle and the filter mouthpiece is shown in the upper left corner. The diameter of the sampler is about 35 cm.

number of sampling points is 70.

**Electronics.** To allow the most possible freedom of choice of sampling strategy, a dedicated microcomputer was developed. This processor allows full control of the sampler by setting, for example, start time, interval between samples, sampling lengths, etc. If something abnormal occurs, suitable action can be taken, e.g., forced rotation of the cylinder to a new sampling area due to deviation from the preset flow rate.

The computer also stores relevant data from optional external sensors, e.g., wind speed, wind direction, and relative humidity. For that purpose, it is equipped with an interface for voltage/frequency converters and a non-volatile memory for data collection.

The computer is constructed around a C-MOS microprocessor (to obtain high noise immunity and low power consumption), CDP 1805 (RCA), with a structure suitable for small controlling units with a limited need for arithmetic operations.

The program is written in assembly language to obtain a compact code in a 2-KB Erasable Programmable Read Only Memory (EPROM), and was developed by using an RCA Microboard Computer Development System. In order to be able to make program modifications quickly and easily, a combined editor assembler has also been developed.

The current program is an interrupt driven (50-Hz) real time system that has the following features: (1) setting time (month, day, hour, and minute); (2) setting start time for sampling; (3) setting sampling interval and length in minutes; (4) setting the separation between sample positions (1–99 motor steps); (5) manual control of stepping motor; (6) forced sample switching due to deviating flow rate; (7) storage of the absolute time and duration for each sample in a 16-KB EPROM together with the values of the variables in 1, 2, 3, 4, and data from the optional analog channels; (8) storage of the flow rate during sampling; (9) stopping the pump during rotating. The data stored in the EPROM can be read by the developed programming unit and can easily be transferred to the same data base as the

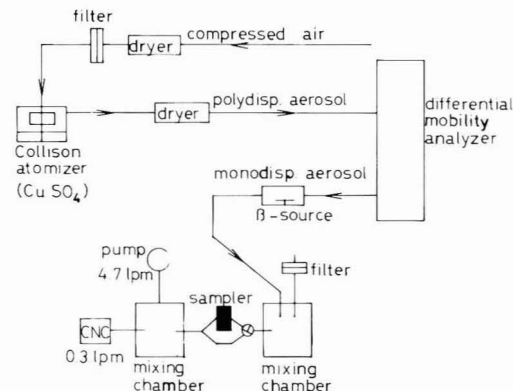


**Figure 2.** Experimental setup for penetration measurements at sub-micron particle sizes.

elemental concentrations from the PIXE analysis.

### Testing Procedures and Results

Different kinds of laboratory experiments have been performed to test the existing prototype with respect to the demands concerning its aerodynamical properties discussed above.

**Internal Losses.** The sampler was tested for submicron particles with an aerosol of  $\text{CuSO}_4$  produced with the equipment shown in Figure 2. The use of a dry aerosol was justified since bounce-off effects were not considered to cause any significant changes in the results for these particle sizes. A constant output atomizer (Thermo System Inc. TSI 3075) produced a polydisperse aerosol. An electrostatic classifier (TSI 3071) was used to select a well-defined particle size, and after passing a  $^{85}\text{Kr}$   $\beta$  source, the aerosol was drawn through the sampler without any filter and into a mixing chamber at a flow rate of 5 L/min. A sample of 0.3 L/min was drawn from the mixing chamber into a condensation nucleus counter (TSI 3020).



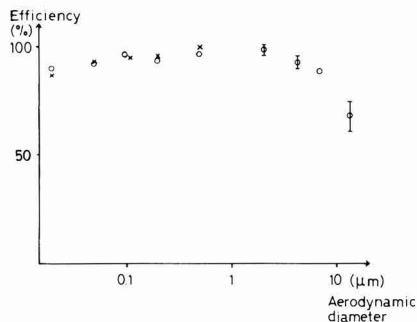


**Figure 3.** Efficiency for particle penetration through the sampler without filter for small particles ( $D < 0.5 \mu\text{m}$ ) and the sampling efficiency for particles larger than  $0.5 \mu\text{m}$ . Results obtained with the multijet impaction nozzle are shown by open circles (O) and the single jet by crosses (X). Error bars show one standard deviation on the measurements made (only given when  $> 1\%$ ).

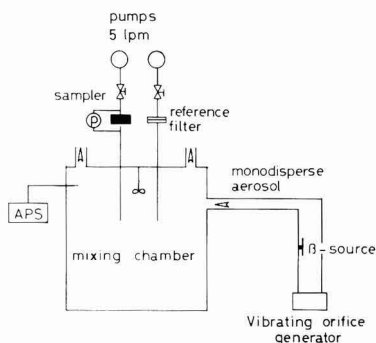


**Figure 4.** Experimental setup for studying internal losses of particle sizes between  $0.5\text{-}$  and  $15\text{-}\mu\text{m}$  aerodynamic diameter.

Penetration was determined by comparing the concentrations with and without the sampler, and the results are shown in Figure 3. During early experiments it was found that the penetration for the smaller particles varied from time to time and that the losses could exceed 25% with an electrically nonconducting interior. Thus, the experiments were performed with the interior in contact with the air stream covered with a conducting layer of silver colloidal paint. The penetration was found to be between 90 and 100% throughout the whole measured particle size interval  $0.02\text{--}0.5 \mu\text{m}$ . Since particle losses increase with decreasing particle size, the losses are most probably due to diffusion losses.

The tests were performed for both the multijet and a single jet impaction nozzle to find out if submicron particles were influenced by using quite different types of impaction nozzles. The two sets of results are in good agreement and differ at most by 2–3%.

The sampling efficiency, including the filter stage, for particles larger than  $0.5 \mu\text{m}$  was determined by using monodisperse methylene blue aerosols from a vibrating orifice generator (TSI 3050). The aerosol was homogenized in a mixing chamber and sampled with the sampler and a reference filter (Figure 4). To check whether the aerosol was quantitatively deposited within the area supposed to be analyzed with PIXE, that is, a circular area of 8-mm diameter, the impaction and filtration areas were punched out, and the methylene blue was dissolved in ethyl alcohol and analyzed with a spectrophotometer (Unicam SP1800, 660 nm). A summary of the results obtained for the absolute sampling efficiency of particles larger than  $0.5\text{-}\mu\text{m}$

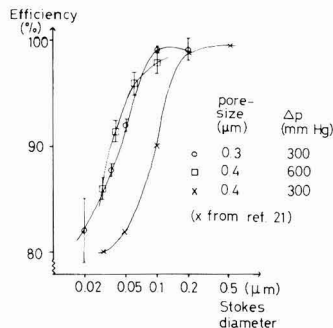


**Figure 5.** Collection efficiency for Nuclepore filter with pore sizes  $0.3$  and  $0.4 \mu\text{m}$  at differential pressures of  $300$  and  $600 \text{ mmHg}$ .

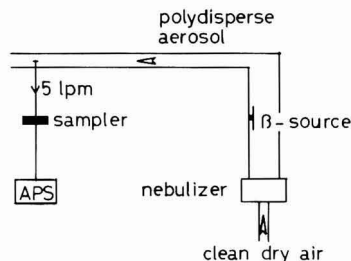


**Figure 6.** Experimental setup for the characterization of the impactor in the sampler.

aerodynamic diameter is shown in Figure 3.

**Filter Efficiency.** The Nuclepore filter was found to fit our sampling and analytical procedures best. The filter efficiency for two different pore diameters,  $0.4$  and  $0.3 \mu\text{m}$ , was tested according to a procedure described elsewhere (19). The  $0.4\text{-}\mu\text{m}$  pore diameter filter was tested at  $300$  and  $600 \text{ mmHg}$  pressure drop, while the  $0.3\text{-}\mu\text{m}$  filter was tested only at  $300 \text{ mmHg}$  (a pressure drop of  $600 \text{ mmHg}$  caused the filter to break). The flow rates obtained were  $2.8$  and  $5 \text{ L/min}$  for the  $0.4 \mu\text{m}$  filter at pressures of  $300$  and  $600 \text{ mmHg}$ , respectively, and  $5 \text{ L/min}$  for the finer filter. The results are presented in Figure 5. For the same flow rate the same efficiency is achieved for the two pore sizes, but when the flow rate is decreased, thereby decreasing the pressure drop, the efficiency changes by up to  $10\%$  for certain particle sizes (which can be of importance when sampling an aerosol with a significant amount of mass below  $0.1 \mu\text{m}$ ). The  $0.3\text{-}\mu\text{m}$  filter was found to break occasionally at the pressure drop tested. However, we see that, at the high pressure drop used in this study, there were no large losses for particles above  $0.05 \mu\text{m}$ . Similar, much more extensive measurements have been performed by Liu et al. (20) which provide data for other pore sizes and flow rates. Particles with diameters below  $0.05 \mu\text{m}$  do not represent significant mass in the atmospheric aerosol.

Leakage between the filter and the Teflon mouthpiece was measured by using a polydisperse submicron methylene blue aerosol. The collection efficiency was measured in an experimental setup similar to that for larger particles (see Figure 4). The leakage was found to be less than  $2\%$ .

**Particle Size Fractionation.** The impaction characteristics were determined by a penetration test without any filtration stage. By comparison of the penetration efficiencies with and without the impaction surface the impaction characteristics are obtained. The experimental setup can be seen in Figure 6 and consists of a polydisperse

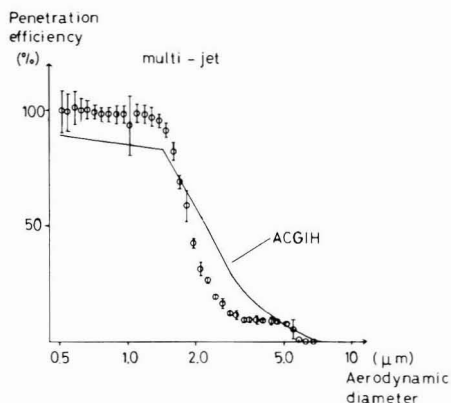


**Figure 7.** Multijet impactor characteristic obtained with the DOP aerosol. Alveolar convection for sick or infirm rather than healthy adults (17) is also shown. Error bars show one standard deviation on the measurements made (only given when  $>1\%$ ).

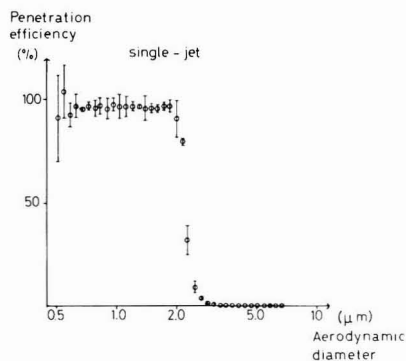


**Figure 8.** Single jet impactor characteristics obtained with the DOP aerosol. Error bars show one standard deviation on the measurements made (only given when  $>1\%$ ).

aerosol generator, a concentric nebulizer, to generate an aerosol with particles in the size range  $0.5\text{--}7\text{ }\mu\text{m}$ . Both dry and wet aerosols, NaCl and DOP (dioctyl phthalate) were used to investigate the losses. An aerodynamic particle sizer (TSI 3300) was used to detect and size classify the aerosol particles penetrating the sampler. Due to the rapidity with which impactor tests can be made in this arrangement, several different impactor configurations could be tested. Besides the described eight-hole nozzle, we also tested a single orifice nozzle with a cutoff diameter of  $2.0\text{ }\mu\text{m}$ . The eight-hole nozzle was chosen due to its lower air jet velocity and larger deposition area decreasing bounce off and giving a more evenly distributed deposition. The cutoff curves obtained with the DOP aerosol are presented in Figures 7 and 8. The internal losses given above have been disregarded. A comparison of the two experimental curves shows a less well-defined cutoff for the multijet impactor. Its unusual shape is probably due to the multiimpactor design, where the channels in the nozzle have different lengths. Thus, the pressure drop will be different for different holes, and thereby, different jet velocities will result. Figure 7 also shows the suggested ACGIH standard for comparison (discussed earlier).

Various impaction surfaces were also investigated. The time dependence of the bounce off was determined for Apiezon grease and low viscosity silicone oil on Nuclepore filters. A Kleenex paper tissue soaked with silicone oil

placed under the Nuclepore filter acted as a reservoir. The test aerosol was NaCl with a mass median aerodynamic diameter of about  $6\text{ }\mu\text{m}$  at a concentration of about  $2\text{ particles/cm}^3$ , similar to a maritime aerosol. After 4 h of exposure at a flow rate of  $5\text{ L/min}$  the bounce off was found to be 30% and 5% for Apiezon grease and silicone oil, respectively.

## Conclusions

An automatic two-stage aerosol sampler for stationary sampling in varying outdoor environments has been constructed and tested. The sampler is constructed to give an optimized sampling and analytical system together with PIXE for atmospheric aerosol measurements. The sampler can work with varying flow rate of up to  $5\text{ L/min}$ . The cutoff point between the two size fractions is defined by an impaction stage, which can have a cutoff between 2 and  $5\text{ }\mu\text{m}$ . The internal losses including wall losses, bounce off, and filtration leakage are below 15% in the particle size range  $0.05\text{--}10\text{ }\mu\text{m}$  for the maximum flow rate of  $5\text{ L/min}$ . The number of sample positions is 70 with a flow rate of  $5\text{ L/min}$ . A microprocessor controls the sampler and allows high flexibility in selecting the sampling program. A solid-state memory makes it possible to record sampling data both from the sampler (sampling time and flow rate) and from other meteorological instruments.

## Acknowledgments

During the experimental and analytical work the discussions with Mats Bohgard and Klas Malmqvist have been most valuable and are gratefully acknowledged. Bengt Martinsson and Erik Swietlicki have been very helpful in assisting in the laboratory experiments. Lars-Berne Nilsson has provided excellent work in manufacturing the sampler. Skillful help with the electronics was given by Erik Karlsson. The strong support during the whole project from Roland Akselsson has been most important. Important remarks on the manuscript were given by R. J. Charlson, University of Washington.

## Literature Cited

- Johansson, T. B.; van Grieken, R. E.; Winchester, J. W. *J. Geophys. Res.* **1976**, *81*, 1039.
- Dzubay, T. G.; Stevens, R. K.; Petersen, C. M. "X-Ray Fluorescence Analysis of Environmental Samples"; Dzubay, T. G., Ed.; Ann Arbor Science: Ann Arbor MI, 1977; p 95.
- Lannefors, H. O.; Hansson, H.-C.; Granat, L. *Atmos. Environ.* **1983**, *17*, 87.
- Lannefors, H. O.; Hansson, H.-C.; Winchester, J. W.; Akselsson, K. R.; Pallon, J. H.; Johansson, S. A. E.; Darzi, M.; Rheingrover, S. W. *Tellus* **1980**, *32*, 548.
- Martinsson, B. G.; Hansson, H.-C.; Lannefors, H. O. *Atmos. Environ.* **1984**, *18*, 2167–2182.
- Jaklevic, J. M.; Loo, B. W.; Goulding, F. S. "X-Ray Fluorescence Analysis of Environmental Samples"; Dzubay, T. G., Ed.; Ann Arbor Science: Ann Arbor, MI, 1977; p 3.
- Nelson, J. W. "X-Ray Fluorescence Analysis of Environmental Samples"; Dzubay, T. G., Ed.; Ann Arbor Science: Ann Arbor, MI, 1977; p 19.
- Whitby, K. T. *Atmos. Environ.* **1978**, *12*, 139.
- Lannefors, H. O.; Hansson, H.-C. *Stud. Environ. Sci.* **1980**, *8*.
- Lippmann, M. "Fine Particles"; Liu, B. Y. H., Ed.; Academic Press: New York, 1976; p 287.
- Stahlhofen, W.; Gebhart, J.; Heyder, J. *Am. Ind. Hyg. Assoc. J.* **1980**, *6*, 385.
- Report of Ad Hoc Working Group to Technical Committee 146—Air Quality, International Standards Organization *Am. Ind. Hyg. Assoc. J.* **1981**, *42*, A64.
- Ogden, T. L. "Aerosols in the Mining and Industrial Work Environments"; Marple, V. A.; Liu, B. Y. H. Eds.; Ann Arbor

- Science: Ann Arbor, MI, 1983; Vol. 1, p 185.
- (14) Lippmann, M.; Gurman, J.; Schlesinger, R. B. "Aerosols in the Mining and Industrial Work Environments"; Marple, V. A.; Liu, B. Y. H., Eds.; Ann Arbor Science: Ann Arbor, MI, 1983; Vol. 1, p 119.
- (15) Marple, V. A. Ph.D. Thesis, University of Minnesota, 1970.
- (16) Reischl, G. P.; John, W. *Staub-Reinhalt. Luft* 1978, 38, 55.
- (17) Dahneke, B. J. *Colloid Interface Sci.* 1973, 45, 584.
- (18) Fan, K. C.; Gentry, J. W. *Environ. Sci. Technol.* 1978, 12, 1289.
- (19) Bohgard, M.; Malmqvist, K. G.; Johansson, G. I.; Akesson, K. R. "Aerosols in the Mining and Industrial Work Environments"; Marple, V. A.; Liu, B. Y. H., Eds.; Ann Arbor Science: Ann Arbor, MI, 1983; Vol. 3, p 907.
- (20) Liu, B. Y. H.; Pui, D. Y. H.; Rubow, K. L. "Aerosols in the Mining and Industrial Works Environments"; Marple, V. A.; Liu, B. Y. H., Eds.; Ann Arbor Science: Ann Arbor, MI, 1983; Vol. 3, p 989.
- (21) Liu, B. Y. H.; Kuhlmei, G. "X-Ray Fluorescence Analysis of Environmental Samples"; Dzuby, T. G., Ed.; Ann Arbor Science: Ann Arbor, MI, 1977; p 107.

Received for review October 22, 1984. Accepted May 29, 1985.  
This project was partly supported by the National (Swedish) Environment Protection Board.

## Formation of Nitroarenes from the Reaction of Polycyclic Aromatic Hydrocarbons with Dinitrogen Pentaoxide

James N. Pitts, Jr.,\* Janet A. Sweetman, Barbara Zielinska, Roger Atkinson, Arthur M. Winer, and William P. Hargreaves

Statewide Air Pollution Research Center, University of California, Riverside, California 92521

■ Reactions of six polycyclic aromatic hydrocarbons (PAH) [fluoranthene (FL), pyrene (PY), benz[a]anthracene (BaA), chrysene (CHRY), benzo[a]pyrene (BaP), and perylene (PER)], deposited on glass-fiber filters, with gaseous  $N_2O_5$  in air were investigated in an all-Teflon chamber. Pyrene, FL, BaP, and BaA gave significant yields of nitro derivatives after only a 30-min exposure. In control exposures to  $NO_2$  plus  $HNO_3$  mixtures or to  $HNO_3$  alone, the yields of nitro derivatives of PY, FL, and BaA were very low relative to those in the  $N_2O_5$  exposures. The reactivity ranking of these PAH toward gaseous  $N_2O_5$  was  $PY > FL > BaP > BaA > PER > CHRY$ . This order is significantly different from that previously observed for nitration of PAH deposited on glass-fiber filters and exposed to a flow of gaseous  $NO_2 + HNO_3$  or for nitration of PAH in solution by  $NO_2/N_2O_4$  mixtures. It also differs from the reactivity ranking determined in this study for the reaction of these PAH with  $N_2O_5$  in  $CCl_4$  solution of  $PER > BaP > BaA \geq PY > FL \geq CHRY$ . Environmental implications are discussed.

### Introduction

Extracts of respirable ambient particulate organic matter (POM) are strongly mutagenic in the Ames assay without microsomal activation (1-10). Nitrated polycyclic aromatic hydrocarbons ( $NO_2$ -PAH), many of which are strong, direct mutagens (11), are present in ambient POM (12-19), diesel (20-28) and gasoline (16, 29, 30) exhaust particulates, soot from wood-burning fireplaces (16, 29), and coal fly ash (31, 32). These  $NO_2$ -PAH, in particular, 1-nitropyrene and the dinitropyrene isomers, make a significant contribution to the direct mutagenic activity of diesel POM (30, 33, 34). Assays of organic extracts of ambient POM, employing Ames strain TA98 and the nitroreductase-deficient strain TA98NR (35, 36), suggest that  $NO_2$ -PAH may also contribute significantly to the direct mutagenic activity of collected ambient POM (37, 38). Indeed, this is confirmed by the chemical identification of mutagenic  $NO_2$ -PAH in ambient POM (12-19), including highly mutagenic dinitropyrene isomers (15, 19).

Interest in these  $NO_2$ -PAH has been heightened by the recent observation of the induction of rat mammary gland tumors by 1-nitropyrene (39) and the induction of sarcomas in rats by subcutaneous injection of dinitropyrenes

(40). Considerable controversy exists, however, concerning the possible health effects of  $NO_2$ -PAH emitted in diesel exhaust (16, 41, 42).

In addition to being present in primary emissions, it has been proposed that some of the  $NO_2$ -PAH detected in ambient particulates may be the result of reactions of their parent PAH with gaseous copollutants in the atmosphere and/or during collection of the particulate organic matter (17-19, 43-50). Thus, laboratory experiments have shown that PAH deposited on filters can react with  $NO_2$  and traces of  $HNO_3$  in simulated atmospheres to form their nitro derivatives (43, 48). Additionally, 2-nitropyrene (17-19) and 2-nitrofluoranthene (18, 19) have recently been identified in ambient POM. Since these nitroarenes have not been reported to be direct emissions, their observation in ambient POM suggests they may be formed via atmospheric reactions (17-19).

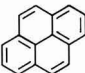
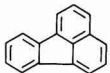
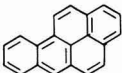
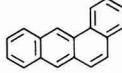
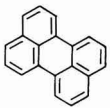
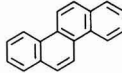
We have recently investigated the reactions of gaseous  $N_2O_5$  and  $NO_3$  radicals in simulated atmospheres with perylene and pyrene deposited on glass-fiber filters (51) and with naphthalene in the gas phase (52).  $N_2O_5$  and the  $NO_3$  radical are formed at night in polluted ambient air from the reaction sequence



Ambient atmospheric concentrations of the  $NO_3$  radical during nighttime hours, ranging from  $\leq 1$  up to 430 parts per trillion (ppt), have been measured by in situ long-path differential optical absorption spectroscopic techniques at a variety of locations in southern California and at other sites in the U.S. and Germany (19, 53-59). The corresponding  $N_2O_5$  concentrations can be calculated from these  $NO_3$  radical and  $NO_2$  concentrations and the equilibrium constant (60) and typically range from  $\sim 5$  ppt to  $\sim 15$  ppb during early evening hours (61).

As we have reported elsewhere (51, 52), pyrene deposited on glass-fiber filters and gaseous naphthalene react with  $N_2O_5$  to form  $NO_2$ -PAH and do not react to any observable extent with the  $NO_3$  radical under the conditions employed. These are the first reported reactions of gas-phase  $N_2O_5$  with organics in either the gaseous or adsorbed states. Interestingly, in these experiments pyrene exhibited a much higher reactivity than perylene toward  $N_2O_5$ . This

**Table I. Initial Conditions and NO<sub>2</sub>-PAH Yields from 30-min Exposures of PAH Deposited on Glass-Fiber Filters in a 360-L Teflon Chamber**

		maximum NO <sub>2</sub> -PAH yield, % (after 30 min)					
exposure no.	species present (estimated initial concn, ppm)	 pyrene	 fluoranthene	 benzo[a]pyrene	 benz[a]anthracene	 perylene	 chrysene
1	N <sub>2</sub> O <sub>5</sub> (~9) NO <sub>2</sub> (~1) HNO <sub>3</sub> (~1) NO <sub>3</sub> (~0.01)	23	11	9	2	traces <sup>a</sup>	ND <sup>b</sup>
2	N <sub>2</sub> O <sub>5</sub> (~9) NO <sub>2</sub> (~10) HNO <sub>3</sub> (~1) NO <sub>3</sub> (~0.001)	24	16	11	5	~3	ND
3	NO <sub>2</sub> (10) HNO <sub>3</sub> (~0.1)	~1	ND	4	traces	traces	ND
4	NO <sub>2</sub> (10) HNO <sub>3</sub> (1.5)	traces	ND	5	traces	~3	ND
5	HNO <sub>3</sub> (1.5)	ND	ND	ND	traces	traces	ND

<sup>a</sup>Traces, below 1%. <sup>b</sup>ND, not detected.

was in contrast to our previous results from exposure of adsorbed PAH to gaseous NO<sub>2</sub> + HNO<sub>3</sub> (43, 48), as well as those of other investigators involving reactions of these PAH in solution with the nitronium (NO<sub>2</sub><sup>+</sup>) ion (62, 63) or NO<sub>2</sub>/N<sub>2</sub>O<sub>4</sub> (64, 65).

This led us to investigate the relative reactivities toward gaseous N<sub>2</sub>O<sub>5</sub>, and the mutagenicity of the products formed, of six widely encountered combustion-generated PAH, fluoranthene (FL), pyrene (PY), benz[a]anthracene (BaA), chrysene (CHRY), benzo[a]pyrene (BaP), and perylene (PER), deposited on glass-fiber filters. In addition, we studied the relative reactivities of these six PAH toward N<sub>2</sub>O<sub>5</sub> and N<sub>2</sub>O<sub>4</sub> in CCl<sub>4</sub> solution. We report here the results of these experiments.

#### Experimental Procedures

**Exposures.** The glass fiber (GF) filters (Gelman type A-E) were precleaned by Soxhlet extraction with CH<sub>2</sub>Cl<sub>2</sub> and CH<sub>3</sub>CN for 24 h each. After this cleaning, the pH of a water extract of the filters was determined (66) to be ~10. The filters were then cut into 6.4 cm × 20 cm strips, and each strip was coated with 5 mL of PAH (Aldrich Chemical Co.; >99% purity) solution in toluene (at a concentration of ~0.05 mg mL<sup>-1</sup>) and the solvent allowed to evaporate.

The filters were clipped to a Teflon line and introduced into a ~360-L all-Teflon chamber, of square cross section (45 × 45 cm) and 190 cm length, filled with purified matrix air (67) of ≤5% relative humidity at ~295 K. This low relative humidity was employed to maximize the lifetime of N<sub>2</sub>O<sub>5</sub> in the chamber. After the filters were in place, the gaseous species, at known pressures (as measured by an MKS Baratron capacitance manometer) in 1 atm of ultrahigh purity N<sub>2</sub> in 0.53-L bulbs, were flushed into the chamber for ~2 min with a 2 L min<sup>-1</sup> flow of ultrahigh purity nitrogen. A fan rated at ~50 L s<sup>-1</sup> was run during this period to provide complete mixing.

N<sub>2</sub>O<sub>5</sub> was prepared by collection at 196 K of the products of the reaction of NO<sub>2</sub> with O<sub>3</sub> (68) and, on the basis of previous work in these laboratories (69, 70), contained minor amounts of NO<sub>2</sub> and nitric acid upon introduction into the environmental chamber. NO<sub>3</sub> radicals were always

present due to the thermal decomposition of N<sub>2</sub>O<sub>5</sub> via reaction 2, -2 (71). The NO<sub>2</sub> added in exposures 2-4 was prepared by the reaction of NO with O<sub>2</sub>. Measurements made with long path-length Fourier transform infrared (FT-IR) spectroscopy showed that NO<sub>2</sub> prepared in this manner contained typically ~1-2% of gaseous HNO<sub>3</sub> (E. C. Tuazon, unpublished data).

The experimental conditions for exposures 1-5 are summarized in Table I. During each exposure, all six PAH (see Table I for the structures of the PAH) were present in the chamber. A set of six PAH-coated filters (PY, CHRY, BaP, FL, BaA, and PER) was withdrawn from the chamber every 10 min during these 30-min exposures. After each filter set withdrawal, the fan was turned on for 2 min to ensure that the chamber contents were thoroughly mixed. The set of filters withdrawn after 30 min consisted of the six PAH-coated GF filters as well as an uncoated filter which was extracted and used as a control for the Ames mutagenicity assay.

An additional control exposure was carried out in which only blank filters (not coated with PAH) were introduced into the exposure chamber and exposed to N<sub>2</sub>O<sub>5</sub> and N<sub>2</sub>O<sub>5</sub> + NO<sub>2</sub> at levels approximately equal to those in exposures 1 and 2.

In exposure 1, in which ~9 ppm of N<sub>2</sub>O<sub>5</sub> was added to the chamber, the species initially present in this exposure were N<sub>2</sub>O<sub>5</sub>, NO<sub>2</sub>, HNO<sub>3</sub>, and the NO<sub>3</sub> radical, with the estimated initial concentrations given in Table I. In exposure 2, ~10 ppm of NO<sub>2</sub> was added to the chamber prior to the addition of N<sub>2</sub>O<sub>5</sub> to drive the equilibrium between NO<sub>3</sub> radicals, NO<sub>2</sub>, and N<sub>2</sub>O<sub>5</sub> toward N<sub>2</sub>O<sub>5</sub>.

In both exposures 1 and 2, ~1 ppm each of *n*-butane and 2,3-dimethylbutane were introduced into the chamber in order to estimate the NO<sub>3</sub> radical concentrations (and hence indirectly the N<sub>2</sub>O<sub>5</sub> lifetimes) (72). Prior to removing each set of filters a gas-phase sample was taken. From the differential decay rates of 2,3-dimethylbutane and *n*-butane (72), NO<sub>3</sub> radicals (and, hence, N<sub>2</sub>O<sub>5</sub>) were determined to be present in the gas phase throughout the duration of exposure 1, with a gas-phase NO<sub>3</sub> radical half-life of ~4 min and an average NO<sub>3</sub> radical concentration of 3.5 ppb. In exposure 2 the NO<sub>3</sub> radical concentration was a factor

of ~10 lower than that in exposure 1, as expected from the initial concentrations of  $\text{N}_2\text{O}_5$  and  $\text{NO}_2$ . In exposures 3–5,  $\text{NO}_2$  (10 ppm) + traces of  $\text{HNO}_3$ ,  $\text{NO}_2$  (10 ppm) +  $\text{HNO}_3$  (1.5 ppm), and  $\text{HNO}_3$  alone (1.5 ppm) were added to the chamber in concentrations approximating those present in exposures 1 and 2.

**Product Analyses.** The exposed filters were Soxhlet extracted with  $\text{CH}_2\text{Cl}_2$  for 20 h. Triphenylbenzene was added to the extracts as an internal standard, and the samples were filtered (0.5  $\mu\text{m}$  Millipore), concentrated under vacuum, and brought up to 5 mL volume with  $\text{CH}_2\text{Cl}_2$ . Aliquots (2 mL) of each solution were taken to dryness under a stream of pure  $\text{N}_2$  and were then redissolved in dimethyl sulfoxide for Ames mutagenicity assays. The remainder of each solution was used for chemical analyses.

Samples were analyzed by using a Beckman Model 334 high-performance liquid chromatograph (HPLC) equipped with a Beckman Model 164 UV detector. A 150 mm  $\times$  4.6 mm Vydac 201TP5415 column was employed for the separation of reactants and products with isocratic elution by  $\text{CH}_3\text{CN}/\text{H}_2\text{O}$  (in a suitable ratio predetermined for each PAH) at a flow rate of 1.5 mL  $\text{min}^{-1}$ . The PAH and their nitro derivatives were quantified on the basis of their ultraviolet absorption at 254 nm. Calibration curves relating the reactant or product concentrations to the (compound/internal standard) peak area ratios were constructed for each compound. Under the conditions employed the reversed-phase column did not separate the mononitro isomers of each PAH, and the most abundant isomer expected to be formed in the nitration reaction (i.e., 6- $\text{NO}_2$ -BaP, 1- $\text{NO}_2$ -PY, 3- $\text{NO}_2$ -PER, 7- $\text{NO}_2$ -BaA, and 3- $\text{NO}_2$ -FL) was used for construction of the calibration curves.

The extraction efficiency for each PAH was evaluated by analysis of three unexposed GF filters coated with each PAH. The recovery values were >95%, with a reproducibility of three replicate HPLC analyses agreeing to within  $\pm 5\%$ .

Identification of the products as nitro derivatives was based on their HPLC retention times matching those of authentic standards. The identities of all products formed in yields  $\geq 1\%$  were confirmed by gas chromatography-mass spectrometry (GC-MS) analyses using a Finnigan 3200 GC-MS/DS equipped with a 30 m  $\times$  0.26 mm fused silica DB-5 column and cool on-column injection. When nitro products were formed in low concentrations, multiple ion detection (MID) was employed.

**Mutagenicity Analyses.** The Ames assay was performed according to the recommended protocol (1, 73). Portions of the filter extracts were tested on *Salmonella typhimurium* strain TA98 and on the nitroreductase-deficient strains TA98NR (11) and TA98/1,8-DNP<sub>6</sub> (74, 75) without S9. Positive controls employed included 2-nitrofluorene, quercetin, and 1,8-dinitropyrene (see Table II for mutagenicity values). After preliminary spot tests to gauge the range of activity, each sample was tested in triplicate at eight doses, and the mean of the three responses was used to determine the dose-response curve. The slope of this dose-response curve was determined by a linear regression analysis. Since each dose was a known fraction of the total extract, the total activity of the filter extract was readily calculated.

**Reaction of  $\text{N}_2\text{O}_5$  with PAH in  $\text{CCl}_4$  Solution.** All experiments were carried out at room temperature and in the dark in a dry box under 1 atm of  $\text{N}_2$ . Freshly prepared  $\text{N}_2\text{O}_5$  (~1 g, >90% purity level as monitored in the gas phase) was dissolved in  $\text{CCl}_4$  (Spectra AR, Mallinckrodt,

stored over 5 Å molecular sieve). The resulting concentration of  $\text{N}_2\text{O}_5$  in  $\text{CCl}_4$  was ~1 mg  $\text{mL}^{-1}$  (0.01 mmol  $\text{mL}^{-1}$ ), and 0.5 mL of this solution was added with stirring to the PAH solutions in 10 mL of  $\text{CCl}_4$  (0.001 mmol  $\text{mL}^{-1}$  each). After 5 min, the reaction mixture was analyzed by using either HPLC or GC/MID (with the conditions as described above). The reactions of  $\text{N}_2\text{O}_5$  with the following PAH solutions were studied: a mixture of the six PAH, BaP + PY, BaP + BaA, BaP + CHRY, BaP + PER, PY + FL, PY + BaA, PY + CHRY, PY + PER, and FL + CHRY.

**Reaction of  $\text{N}_2\text{O}_4$  with PAH in  $\text{CCl}_4$  Solution.** One-milliliter aliquots of  $\text{N}_2\text{O}_4$  in  $\text{CCl}_4$  (0.2 mmol  $\text{mL}^{-1}$ ) were added with stirring to room temperature solutions of the six PAH in 30 mL of  $\text{CCl}_4$  and to four PAH (PY, FL, BaA, and CHRY) in 20 mL of  $\text{CCl}_4$  (~0.001 mmol  $\text{mL}^{-1}$  of each). After 10 min of reaction the mixtures were analyzed by GC/MID.

## Results

**$\text{NO}_2$ -PAH Formation in Chamber Exposures.** Five 30-min exposures of PAH-coated filters were carried out in the dark in a 360-L all-Teflon chamber. The species present in the chamber and their estimated initial concentration and the  $\text{NO}_2$ -PAH yields observed after a 30-min exposure are given in Table I. For BaP, PER, and BaA, the percent of PAH reacted was in agreement (to within  $\pm 5\%$ ) with the concentration of mono- $\text{NO}_2$ -PAH formed, indicating that the mononitro derivatives were the major products formed. In the case of PY and FL, the percent of these PAH reacting agreed with the amounts of mono- $\text{NO}_2$ -PAH formed to within  $\pm 10\%$  after 30 min of reaction (this higher degree of scatter may well have been due to their higher volatility). In addition, for these two PAH exposed to  $\text{N}_2\text{O}_5$ , traces of dinitro derivatives were detected by GC-MS with multiple ion detection (MID).

Comparison of the results of exposure 1 with exposure 2, where the  $\text{N}_2\text{O}_5 \rightleftharpoons \text{NO}_2 + \text{NO}_3$  equilibrium was shifted markedly toward  $\text{N}_2\text{O}_5$  by the addition of 10 ppm of  $\text{NO}_2$ , clearly indicates that the  $\text{NO}_3$  radical was not the prime nitrating species in these exposures. Thus, the yields of  $\text{NO}_2$ -PAH are reasonably similar in both exposures for all PAH tested. It should be noted that under the conditions of our experiments the  $\text{NO}_3$  radical was present in much lower concentrations than was  $\text{N}_2\text{O}_5$  (see Table I). Thus, a rate coefficient for reaction of these PAH with  $\text{NO}_3$  radicals comparable to that for reaction with  $\text{N}_2\text{O}_5$  would not have been observable under these conditions. However, since  $\text{N}_2\text{O}_5$  is present in urban atmospheres in a much higher concentration than is the  $\text{NO}_3$  radical,  $\text{N}_2\text{O}_5$  will also be the reactive specie under ambient conditions in polluted urban atmospheres.

The highest yield of nitration for 30-min exposures was observed in exposures 1 and 2 for PY (23 and 24%, respectively) followed by FL (11 and 16%, respectively) and BaP (9 and 11%, respectively). The maximum yields of  $\text{NO}_2$ -BaA (5%) and  $\text{NO}_2$ -PER (~3%) were observed in exposure 2, and no nitration of CHRY was detected in any of these exposures.

With the exception of FL, the nitro isomer distributions in exposures 1 and 2 for a given PAH are similar to those observed in nitration reactions in solution. Thus, the most abundant  $\text{NO}_2$ -PAH isomers formed were 1- $\text{NO}_2$ -PY, 3- $\text{NO}_2$ -PER, 6- $\text{NO}_2$ -BaP, and 7- $\text{NO}_2$ -BaA (with traces of other nitro isomers), respectively. In the case of BaP, in addition to 6- $\text{NO}_2$ -BaP, the main isomer observed, the 1- and 3- $\text{NO}_2$  isomers were formed in much lower yields. For FL, our MID data indicated that 3-, 8-, 7-, and 1- $\text{NO}_2$ -FL isomers were formed in approximately equal amounts in



Table II. Direct Mutagenic Activities of Extracts from PAH-Coated GF Filters (~250 µg per Filter) after 30-min Exposures

exposure <sup>a</sup> no.	strain <sup>b</sup>	10 <sup>5</sup> total revertants of filter extract						uncoated, exposed
		pyrene	fluoranthene	BaP	BaA	perylene	chrysene	
1	TA98	19.0	22.0	1.3	1.0	0.28	0.73	c
	TA98 NR	27.5	10.8	0.92	0.85	0.22	0.68	c
	TA98/1,8-DNP <sub>6</sub>	3.0	7.5	0.35	0.16	0.02	0.10	c
2	TA98	23.2	42.5	0.95	2.4	0.75	1.1	2.1
	TA98 NR	24.0	16.5	0.65	1.4	0.55	0.92	0.92
	TA98/1,8-DNP <sub>6</sub>	3.5	10.5	0.35	0.28	0.08	0.12	0.19
3	TA98	0.17	0.004	0.07	0.005	0.02	0.002	0.002
	TA98 NR	0.04	0.003	0.02	0.004	0.01	0.003	0.002
	TA98/1,8-DNP <sub>6</sub>	0.10	0.002	0.03	0.002	0.006	0.0006	0.0
4	TA98	0.06	0.001	0.11	0.008	0.04	0.02	0.0
	TA98 NR	0.03	0.001	0.04	0.16	0.04	0.01	0.0002
	TA98/1,8-DNP <sub>6</sub>	0.03	0.001	0.05	0.003	0.06	0.004	0.0
5	TA98	0.01	0.002	0.06	0.0008	0.02	0.0	0.001
	TA98 NR	0.001	0.002	0.06	0.0007	0.03	0.002	0.001
	TA98/1,8-DNP <sub>6</sub>	0.002	0.001	0.02	0.0	0.007	0.0006	0.0
control filters <sup>d</sup> (PAH-coated, unexposed)	TA98	0.005	0.002	0.01	0.002	0.03	0.004	
	TA98 NR	0.006	0.004	0.02	0.004	0.004	0.0007	
	TA98/1,8-DNP <sub>6</sub>	0.006	0.0002	0.002	0.0004	0.003	0.0007	

<sup>a</sup>Species present as in Table I. <sup>b</sup>Standard mutagen values (SMV) (rev µg<sup>-1</sup>) for strain TA98: 2-nitrofluorene, 490, 520, 600; quercetin, 12, 14; 1,8-dinitropyrene, 1.0 × 10<sup>6</sup>, 1.0 × 10<sup>6</sup>. SMV for strain TA98NR: 2-nitrofluorene, 42, 62; quercetin, 17, 18; 1,8-dinitropyrene, 1.1 × 10<sup>6</sup>, 1.2 × 10<sup>6</sup>. SMV for strain TA98/1,8-DNP<sub>6</sub>: 2-nitrofluorene, 54, 110; quercetin, 8.3, 18; 1,8-dinitropyrene, 1.6 × 10<sup>4</sup>. <sup>c</sup>No data; sample lost during workup procedure. <sup>d</sup>Average of three control filters.

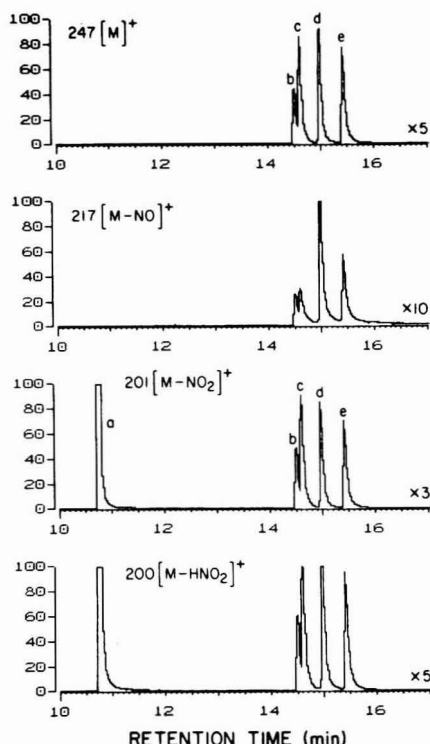


Figure 1. MID traces of extract of fluoranthene-coated GF filters exposed to N<sub>2</sub>O<sub>5</sub>/NO<sub>2</sub> for 30 min (exposure 2). For nitrofluoranthene the ions shown are 247 (M)<sup>+</sup>, 217 (M - NO)<sup>+</sup>, 201 (M - NO<sub>2</sub>)<sup>+</sup>, and 200 (M - HNO<sub>2</sub>)<sup>+</sup>. The peak identities are (a) fluoranthene and (b-e) nitrofluoranthenes. Retention time matching showed (d) to be 3-nitrofluoranthene. On the basis of reported relative retention times (20) the other isomers are identified as (b) 1-nitrofluoranthene, (c) 7-nitrofluoranthene, and (e) 8-nitrofluoranthene.

these exposures (see Figure 1). Interestingly, for nitration in solution involving NO<sub>2</sub>/N<sub>2</sub>O<sub>4</sub> in CH<sub>2</sub>Cl<sub>2</sub> or NO<sub>2</sub><sup>+</sup> ions,

the isomer distribution has been reported to be 3- > 8- >> 7- ≈ 1-NO<sub>2</sub>-FL (64, 76).

Since the N<sub>2</sub>O<sub>5</sub> used in these experiments contained minor amounts of NO<sub>2</sub> and HNO<sub>3</sub> upon introduction into the chamber, and a high concentration of NO<sub>2</sub> was used in exposure 2, control exposures were carried out to determine the degree of nitration caused by gaseous NO<sub>2</sub> + HNO<sub>3</sub> and by gaseous HNO<sub>3</sub>. The concentrations of these species in exposures 3-5 were in the range of those estimated for exposures 1 and 2, and the reaction times were the same.

Under these conditions, PY, FL, BaA, and, to a lesser extent, BaP showed much lower yields of nitration than occurred in exposures 1 and 2. The highest yield of nitration was observed for BaP, which formed ~5% of NO<sub>2</sub>-BaP upon exposure to either NO<sub>2</sub> (containing traces of HNO<sub>3</sub>) or to an NO<sub>2</sub> + HNO<sub>3</sub> mixture. In exposure 5 (HNO<sub>3</sub> alone), NO<sub>2</sub>-BaP was not detected, nor were any other PAH nitrated to an extent of ≥1%. In exposures 3 and 4, only small quantities (≤3%) of the nitro derivatives of PY, PER, and BaA were formed. Fluoranthene, which showed a high reactivity toward N<sub>2</sub>O<sub>5</sub> and N<sub>2</sub>O<sub>5</sub> + NO<sub>2</sub> mixtures, did not react with NO<sub>2</sub> + HNO<sub>3</sub> or HNO<sub>3</sub> under the conditions of these exposures. Therefore, the NO<sub>2</sub> and HNO<sub>3</sub> present in exposures 1 and 2 cannot be responsible for the high degrees of nitration observed in these exposures for PY and FL.

**Mutagenicity.** The direct mutagenic activities of the extracts of the 30-min filter exposures toward *Salmonella* strains TA98, TA98NR, and TA98/1,8-DNP<sub>6</sub> are shown in Table II. Strain TA98NR is an isolate of TA98 which is deficient in the "classical" bacterial nitroreductase, the enzyme that catalyzes the bioactivation of most mononitroarenes to mutagenic metabolites. Thus, a lower response on this strain relative to TA98 indicates the probable presence of mononitroarenes in the sample. However, TA98NR is still sensitive to the potent mutagens 1,8-dinitropyrene and 1,3-dinitropyrene, since these compounds are activated by a second "nonclassical" reductase. Strain TA98/1,8-DNP<sub>6</sub> is deficient in this enzyme and is consequently less sensitive to these dinitropyrenes. Thus, a lower response for TA98/1,8-DNP<sub>6</sub> relative to TA98NR

and TA98 may indicate the presence of dinitropyrenes in the sample (74, 75).

For exposures 1 and 2, the mutagenicities of extracts from FL- and PY-coated filters toward strain TA98 (Table II) are higher than would result from the mononitro-PAH yields alone (11). For example, in exposure 1 a 23% yield of nitropyrene would result in  $\sim 1 \times 10^5$  total revertants on the filter. The observed mutagenicity of  $2 \times 10^6$  revertants could be explained by  $\sim 1\%$  conversion of pyrene to dinitropyrenes. In accord with this, the lower response of extracts from filters coated with PY toward strain TA98/1,8-DNP<sub>6</sub>, relative to strains TA98 and TA98NR, indicates the presence of mutagenic dinitro-PAH (11).

As seen from Table II the response of 1,8-dinitropyrene on TA98NR is  $\sim 10\%$  greater than on TA98. If the dinitropyrenes present are contributing most of the mutagenicity found on the PY-coated filters in exposures 1 and 2, somewhat higher mutagenicity values on TA98NR than on TA98 would be expected. While this is consistent with the mutagenicity values observed for exposure 2, the value for TA98NR for the PY-coated filter in exposure 1 is somewhat higher than expected, for reasons that are not presently understood.

The mutagenicities of extracts from BaP-, BaA-, PER-, and CHRY-coated filters exposed to  $N_2O_5$  and  $N_2O_5 + NO_2$  (Table II, exposures 1 and 2) were also higher than expected from the measured  $NO_2$ -PAH yields. Furthermore, the mutagenicities of blank filters in exposure 2 were surprisingly high. One explanation for these high mutagenicity values involves migration of the volatile PAH PY and FL to these filters followed by nitration of the deposited PAH by gaseous  $N_2O_5$ . Another possibility is that the reactions of FL and PY with  $N_2O_5$  occurred in the gas phase followed by deposition of the less volatile  $NO_2$ -FL and  $NO_2$ -PY onto the filter surfaces. Indeed, traces of 1- $NO_2$ -PY and  $NO_2$ -FL isomers were detected by MID in extracts from the BaA- and CHRY-coated filters exposed to  $N_2O_5$ .

As expected, in additional exposures of uncoated filters (in the absence of PAH-coated filters) to  $N_2O_5$  and to  $N_2O_5 + NO_2$  at levels approximately equal to those in exposures 1 and 2, much lower direct mutagenicities toward TA98 were observed; they were comparable to those of the coated, but unexposed, filters.

The mutagenicity data for PAH-coated filters exposed to  $NO_2 + HNO_3$  and to  $HNO_3$  alone were generally low, consistent with the low or negligible  $NO_2$ -PAH yields observed. For FL, which did not react to any observable extent in these exposures, the mutagenic activities toward all tested strains were comparable to those of the unexposed controls.

**Reaction of PAH with  $N_2O_5$  in  $CCl_4$  Solution.** In polar solvents  $N_2O_5$  exists mainly in the ionic state ( $NO_2^+NO_3^-$ ), and therefore, in these solvents the same PAH reactivity order would be expected as that reported for electrophilic substitution reactions (63) involving the nitronium ion. However, it has been reported (77, 78) that  $N_2O_5$  exists in a covalent form in aprotic solvents, and thus  $CCl_4$  was selected as the solvent for testing the reactivity order of PAH toward  $N_2O_5$  in solution. Nine sets of reactions in which the PAH were combined in pairs and reacted with  $N_2O_5$  dissolved in  $CCl_4$  were carried out in the dark in a dry box under 1 atm of  $N_2$ . Additionally, a mixture of the six PAH was also reacted with  $N_2O_5$  in  $CCl_4$  solution. Since our preliminary experiments showed that under these conditions  $N_2O_5$  reacted very rapidly with PAH, forming polynitro derivatives when an excess of  $N_2O_5$  was added, we utilized a less than equimolar amount of

$N_2O_5$  (5  $\mu$ mol of  $N_2O_5$  for 20  $\mu$ mol of total PAH) in these experiments.

On the basis of HPLC and MID quantification, the following order of reactivity of these PAH with  $N_2O_5$  in  $CCl_4$  solution was established:



As control experiments, the reactions of  $N_2O_4$  with a mixture of these six PAH in  $CCl_4$  solution, and then with a mixture of the four less reactive PAH in  $CCl_4$  solution, were carried out. In contrast to the reaction of  $N_2O_4$  with PAH in  $CH_2Cl_2$  solution (64),  $N_2O_4$  in  $CCl_4$  solution was not very reactive toward the PAH tested, and a large excess of  $N_2O_4$  ( $\sim 10$ -fold) was necessary to form an observable yield of products after 10 min of reaction. The order of reactivity of PAH with  $N_2O_4$  in  $CCl_4$  solution was identical with that observed for reaction with  $N_2O_5$  in  $CCl_4$  solution.

### Discussion

The results presented in Tables I and II and discussed above confirm our earlier observation (51) that gas-phase  $N_2O_5$  is a potent nitrating agent for pyrene deposited on GF filters. Furthermore, the present data show that gas-phase  $N_2O_5$  also nitrates FL and, to a lesser extent, BaP and BaA. The small amount of nitration of perylene observed ( $\leq 3\%$ ) on exposure to  $N_2O_5$  or  $N_2O_5 + NO_2$  could be due to the presence of  $NO_2$  and  $HNO_3$ . Chrysene was not nitrated by  $N_2O_5$  or by  $NO_2$  and/or  $HNO_3$  mixtures. Thus, the order of reactivity toward gas-phase  $N_2O_5$  for the PAH tested was  $PY > FL > BaP > BaA > PER > CHRY$ .

This reactivity order for passive exposure to gaseous  $N_2O_5$  differs dramatically from that observed for  $N_2O_5$  in  $CCl_4$  solution of  $PER > BaP > BaA \geq PY > FL \geq CHRY$ . Moreover, the reactivity order for  $N_2O_5$  in  $CCl_4$  solution is similar to those established for electrophilic substitution reactions in solution, where the nitrating agent is either the  $NO_2^+$  ion (63) or  $NO_2/N_2O_4$  (64, 65). The reactivity order for  $N_2O_5$  in  $CCl_4$  is also similar to that established for adsorbed PAH exposed under "active flow conditions" to  $NO_2$  containing trace amounts of  $HNO_3$  (43, 48, 79).

The reasons for the unusual reactivity order for gaseous  $N_2O_5$  toward deposited PAH cannot be established at this time. However, fluoranthene and pyrene are significantly more volatile, by factors of  $\sim 40$  and  $\sim 20$ , respectively, than the other PAH studied (80). Indeed, in exposures 1 and 2 traces of  $NO_2$ -FL and  $NO_2$ -PY were observed on filters other than those originally coated with FL and PY. This suggests either that the reaction of these PAH with  $N_2O_5$  may occur in the gas phase near the filter surface, with the less volatile  $NO_2$ -PAH readsorbing on the filter, or that the migration of the volatile PAH, PY and FL, to other filters occurs followed by nitration of the adsorbed PY or FL on these filters by gaseous  $N_2O_5$ . If these reactions of the PAH with  $N_2O_5$  do occur in the gas phase, at least two factors would contribute to the observed reactivities, i.e., the rate constant for the gas-phase reaction of the individual PAH with  $N_2O_5$  and the PAH concentrations available for reaction, the latter being approximately determined by their volatilities. If these reactions occur with the PAH in the adsorbed state, the volatility of the PAH may effect their availability for reaction. Clearly, several interesting unresolved questions remain, and work is under way in this laboratory to address them.

Although exposures 3-5 were designed as control exposures for the  $NO_2$  and  $HNO_3$  present together with  $N_2O_5$  in exposures 1 and 2, some tentative conclusions can be drawn from the data in Table I. The  $\sim 5\%$  yields of  $NO_2$ -BaP in these passive  $NO_2 + HNO_3$  exposures (3 and

4) were consistent with our original results in an active exposure system (43, 48), in both cases with BaP deposited on GF filters. In contrast to a recent suggestion (81), gaseous  $\text{HNO}_3$  alone did not appreciably nitrate BaP in the present system.

The data in Table I show that perylene is also nitrated by  $\text{NO}_2/\text{HNO}_3$  mixtures, as observed previously (43, 48). However, the contribution of  $\text{HNO}_3$  to the overall yield of nitration is not presently known. Thus, although traces (<1%) of  $\text{NO}_2$ -PER were observed in the HPLC analysis of exposure 5 (to  $\text{HNO}_3$  alone), this was not confirmed by mass spectrometry.

However, as stated previously (43, 48), it is clear that traces of  $\text{HNO}_3$ , together with  $\text{NO}_2$ , seem necessary for nitration. This is further confirmed by an independent experiment in which PER was deposited on carbon black and exposed in a flow system to  $\text{NO}_2$  and  $\text{NO}_2 + \text{HNO}_3$  mixtures; traces of  $\text{HNO}_3$  were essential for the nitration reaction (82). Further work is clearly necessary to determine the order of reactivity of the six PAH examined toward  $\text{HNO}_3$  and to mixtures of  $\text{NO}_2 + \text{HNO}_3$ . Such studies involving longer exposures of these PAH under active and passive conditions over a range of relative humidities are currently being carried out in this laboratory.

**Environmental Significance.** In a recent study (83) of the reactions of wood smoke with  $\text{NO}_2$ ,  $\text{O}_3$ , and  $\text{NO}_2 + \text{O}_3$  mixtures, the greatest enhancement in mutagenicity was observed to result from the reaction of the wood smoke with mixtures of  $\text{NO}_2 + \text{O}_3$  in the dark. We have suggested (51, 84), consistent with our present data, that at least part of this increased mutagenicity was due to nitration of pyrene, fluoranthene, and certain other PAH present in their system by gaseous  $\text{N}_2\text{O}_5$  formed via reactions 1 and 2. Indeed, in recently published results from chemical analyses of extracts of wood smoke exposed to  $\text{NO}_2 + \text{O}_3$  mixtures, the formation of 1-nitropyrene was observed (85). Additionally, ~16–30% of the direct-acting mutagenicity of the reacted wood smoke occurred in the HPLC fraction containing  $\text{NO}_2$ -PAH (85).

As we have previously suggested (51, 84), under certain conditions  $\text{N}_2\text{O}_5$  may be a significant nitrating species affecting the mutagenicity of ambient POM. However, the extrapolation of data obtained under laboratory conditions to the ambient atmosphere involves several major assumptions. These include, for example, the assumptions that substrate effects, PAH concentrations, the physical state of the PAH, the presence of copollutants, relative humidity, etc. have no major impacts on PAH nitration reactivities. Despite these complicating factors, it is illustrative to carry out extrapolations of our laboratory data to ambient atmospheric conditions.

To make this extrapolation for  $\text{N}_2\text{O}_5$ , we have used the earlier data from our 6400-L environmental chamber experiments (51), in which the  $\text{N}_2\text{O}_5$  half-life was ~60 min, as compared to a half-life of ~4 min in the 360-L chamber used in the present work. The results from the 6400-L chamber showed that 0.6 ppm of  $\text{N}_2\text{O}_5$  led to an initial nitration rate for pyrene of ~3%  $\text{min}^{-1}$  (51). On the basis of a 1983 in situ DOAS study (58) conducted ~80 km downwind of central Los Angeles, an average concentration of ~0.6 ppb of  $\text{N}_2\text{O}_5$  for 4 h nightly can occur under conditions of moderate pollution. For such a scenario, an ~0.3% nitration of pyrene per night is estimated.

To date, the highest  $\text{N}_2\text{O}_5$  concentration in southern California, estimated from in situ DOAS measurements, was an ~4-h average of ~10 ppb of  $\text{N}_2\text{O}_5$  for the hours of 1800–2200 on Sept 18, 1979, in Riverside (53). Similar levels of  $\text{N}_2\text{O}_5$  have been calculated to occur at Deuelbach,

Germany (61), and are expected for other regions of the world with similar conditions of meteorology and atmospheric pollution.  $\text{N}_2\text{O}_5$  concentrations of this magnitude would lead to an estimated ~5% nitration of pyrene during a single night. It should be noted that pyrene is the most reactive of the PAH toward  $\text{N}_2\text{O}_5$  that we have examined and that it also forms dinitropyrenes which are very powerful direct mutagens (Table II) (11).

Finally, while our experiments were carried out at low relative humidities (<5%) in order to maximize the  $\text{N}_2\text{O}_5$  lifetimes in the chamber, the highest estimated ambient atmospheric  $\text{N}_2\text{O}_5$  concentrations of ~10–15 ppb occurred at relative humidities of ~50–60% (61). At this time, we do not know whether or not relative humidity has a major effect on these  $\text{N}_2\text{O}_5$  reactions with PAH; further work is being conducted to clarify this point.

#### Acknowledgments

We thank Sara M. Aschmann, Travis Dinoff, and Stacy Trouard for technical assistance. We appreciate the generous gift of dinitropyrene standards from R. Mermelstein (Xerox Corp.) and the *Salmonella* strains TA98 from Bruce Ames and TA98NR and TA98/1,8-DNP<sub>6</sub> from Herbert Rosenkranz.

**Registry No.** FL, 206-44-0; PY, 129-00-0; BaA, 56-55-3; CHRY, 218-01-9; BaP, 50-32-8; PER, 198-55-0; 3- $\text{NO}_2$ -FL, 892-21-7; 1- $\text{NO}_2$ -FL, 13177-28-1; 7- $\text{NO}_2$ -PL, 13177-31-6; 8- $\text{NO}_2$ -FL, 13177-32-7;  $\text{N}_2\text{O}_5$ , 10102-03-1;  $\text{NO}_2$ , 10102-44-0;  $\text{HNO}_3$ , 7697-37-2;  $\text{N}_2\text{O}_4$ , 10544-72-6.

#### Literature Cited

- Ames, B. N.; McCann, J.; Yamasaki, E. *Mutat. Res.* **1975**, *31*, 347–364.
- Pitts, J. N., Jr.; Grosjean, D.; Mischke, T. M.; Simmon, V. F.; Poole, D. *Toxicol. Lett.* **1977**, *1*, 65–70.
- Pitts, J. N., Jr.; Van Cauwenberghe, K. A.; Grosjean, D.; Schmid, J. P.; Fitz, D. R.; Belser, W. L., Jr.; Knudson, G. B.; Hynds, P. M. In "Application of Short-Term Bioassays in the Fractionation of Complex Environmental Mixtures"; Waters, M. D.; Nesnow, S.; Huisin, J. L.; Sandhu, S. S.; Claxton, L., Eds.; Plenum Press: New York, 1979; pp 355–379.
- Teranishi, K.; Hamada, K.; Watanabe, H. *Mutat. Res.* **1978**, *56*, 273–280.
- Alfheim, I.; Møller, M. *Sci. Total Environ.* **1979**, *13*, 275–278.
- Chrip, C. E.; Fischer, G. L. *Mutat. Res.* **1980**, *76*, 143–164.
- Talcott, R.; Wei, E. J. *Natl. Cancer Inst.* **1977**, *58*, 449–451.
- Tokiwa, H.; Morita, K.; Takeyoshi, H.; Takahashi, K.; Ohnishi, Y. *Mutat. Res.* **1977**, *48*, 237–248.
- Löfroth, G. *Chemosphere* **1978**, *7*, 791–798.
- Talcott, R.; Harger, W. *Mutat. Res.* **1980**, *79*, 177–180.
- Rosenkranz, H. S.; Mermelstein, R. *Mutat. Res.* **1983**, *114*, 217–267.
- Nielsen, T. *Anal. Chem.* **1983**, *55*, 286–290.
- Ramdahl, T.; Becher, G.; Bjørseth, A. *Environ. Sci. Technol.* **1982**, *16*, 861–865.
- Jäger, J. *J. Chromatogr.* **1978**, *152*, 575–578.
- Tokiwa, H.; Kitamori, S.; Nakagawa, R.; Horikawa, K.; Matamala, L. *Mutat. Res.* **1983**, *121*, 107–116.
- Gibson, T. L. *Mutat. Res.* **1983**, *122*, 115–121.
- Nielsen, T.; Seitz, B.; Ramdahl, T. *Atmos. Environ.* **1984**, *18*, 2159–2165.
- Pitts, J. N., Jr.; Sweetman, J. A.; Zielinska, B.; Winer, A. M.; Atkinson, R. *Atmos. Environ.*, in press.
- Pitts, J. N., Jr.; Winer, A. M. "Particulate and Gas Phase Mutagens in Ambient and Simulated Atmospheres". 1984, final report to California Air Resources Board, Contract A3-049-32.
- Paputa-Peck, M. C.; Marano, R. S.; Schuetzle, D.; Riley, T. L.; Hampton, C. V.; Prater, T. J.; Skewes, L. M.; Jensen, T. E.; Ruehle, P. H.; Bosch, L. C.; Duncan, W. P. *Anal. Chem.* **1983**, *55*, 1946–1954.

- (21) Petersen, B. A.; Chuang, C. C.; Margard, W. L.; Trayser, D. A., paper presented at the 74th Annual Meeting of the Air Pollution Control Association, Philadelphia, PA, June 1981.
- (22) Schuetzle, D.; Riley, T. L.; Prater, T. J.; Harvey, T. M.; Hunt, D. F. *Anal. Chem.* **1982**, *54*, 265-271.
- (23) Henderson, T. R.; Sun, J. D.; Royer, R. E.; Clark, C. R.; Li, A. P.; Harvey, T. M.; Hunt, D. H.; Fulford, J. E.; Lovette, A. M.; Davidson, W. R. *Environ. Sci. Technol.* **1983**, *17*, 443-449.
- (24) Pitts, J. N., Jr.; Lokensgard, D. M.; Harger, W.; Fisher, T. S.; Mejia, V.; Schuler, J. J.; Scorziell, G. M.; Katzenstein, Y. A. *Mutat. Res.* **1982**, *103*, 241-249.
- (25) Pederson, T. C.; Siak, J.-S. *J. Appl. Toxicol.* **1981**, *1*, 54-60.
- (26) Xu, X. B.; Nachtman, J. P.; Rappaport, S. M.; Wei, E. T.; Lewis, S.; Burlingame, A. L. *J. Appl. Toxicol.* **1981**, *1*, 196-198.
- (27) Schuetzle, D.; Lee, F. S.-C.; Prater, T. J.; Tejada, S. B. *Int. J. Environ. Anal. Chem.* **1981**, *9*, 93-144.
- (28) Xu, X. B.; Nachtman, J. P.; Jin, Z. L.; Wei, E. T.; Rappaport, S. M.; Burlingame, A. L. *Anal. Chim. Acta* **1982**, *136*, 163-174.
- (29) Gibson, T. L. *Atmos. Environ.* **1982**, *16*, 2037-2040.
- (30) Nishioka, M. G.; Petersen, B. A.; Lewtas, J. In "Polynuclear Aromatic Hydrocarbons: Physical and Biological Chemistry"; Cooke, M.; Dennis, A. J.; Fisher, G. L., Eds.; Battelle Press: Columbus, OH, 1982; pp 603-613.
- (31) Hanson, R. L.; Henderson, T. R.; Hobbs, C. H.; Clark, C. R.; Carpenter, R. L.; Dutcher, J. S.; Harvey, T. M.; Hunt, D. F. *J. Toxicol. Environ. Health* **1983**, *11*, 971-980.
- (32) Harris, W. R.; Chess, E. K.; Okamoto, D.; Remsen, J. F.; Later, D. W. *Environ. Mutagen.* **1984**, *6*, 131-144.
- (33) Schuetzle, D. *Environ. Health Perspect.* **1983**, *47*, 65-80.
- (34) Nakagawa, R.; Kitamori, S.; Horikawa, K.; Nakashima, K.; Tokiwa, H. *Mutat. Res.* **1983**, *124*, 201-211.
- (35) Rosenkranz, E. C.; McCoy, E. C.; Mermelstein, R.; Rosenkranz, H. S. *Carcinogenesis (London)* **1982**, *3*, 121-123.
- (36) Rosenkranz, H. S.; McCoy, E. C.; Mermelstein, R.; Speck, W. T. *Mutat. Res.* **1981**, *91*, 103-105.
- (37) Pitts, J. N., Jr.; Harger, W.; Lokensgard, D. M.; Fitz, D. R.; Scorziell, G. M.; Mejia, V. *Mutat. Res.* **1982**, *104*, 35-41.
- (38) Wang, C. Y.; Lee, M.-S.; King, C. M.; Warner, P. O. *Chemosphere* **1980**, *9*, 83-87.
- (39) Hirose, M.; Lee, M.-S.; Wang, C. Y.; King, C. M. *Cancer Res.* **1984**, *44*, 1158-1162.
- (40) Ohgaki, H.; Negishi, C.; Wakabayashi, K.; Kusama, K.; Sato, S.; Sugimura, T. *Carcinogenesis (London)* **1984**, *5*, 583-585.
- (41) Rosenkranz, H. S. *Mutat. Res.* **1982**, *101*, 1-10.
- (42) Rosenkranz, H. S. *Mutat. Res.* **1984**, *140*, 1-6.
- (43) Pitts, J. N., Jr.; Van Cauwenberghe, K. A.; Grosjean, D.; Schmid, J. P.; Fitz, D. R.; Belser, W. L., Jr.; Knudson, G. B.; Hynds, P. M. *Science (Washington, D.C.)* **1978**, *202*, 515-519.
- (44) Tokiwa, H.; Nakagawa, R.; Morita, K.; Onhishi, Y. *Mutat. Res.* **1981**, *85*, 195-205.
- (45) Hughes, M. M.; Natusch, D. F. S.; Taylor, D. R.; Zeller, M. V. In "Polynuclear Aromatic Hydrocarbons: Chemistry and Biological Effects"; Bjørseth, A.; Dennis, A. J., Eds.; Battelle Press: Columbus, OH, 1980; pp 1-8.
- (46) Jäger, J.; Hanus, V. *J. Hyg., Epidemiol. Microbiol. Immunol.* **1980**, *24*, 1-12.
- (47) Butler, J. D.; Crossley, P. *Atmos. Environ.* **1981**, *15*, 91-94.
- (48) Pitts, J. N., Jr. *Philos. Trans. R. Soc. London, Ser. A* **1979**, *A290*, 551-576.
- (49) Pitts, J. N., Jr. *Environ. Health Perspect.* **1983**, *47*, 115-140.
- (50) Brorström, E.; Grennfelt, P.; Lindskog, A. *Atmos. Environ.* **1983**, *17*, 601-605.
- (51) Pitts, J. N., Jr.; Zielinska, B.; Sweetman, J. A.; Atkinson, R.; Winer, A. M. *Atmos. Environ.* **1985**, *19*, 911-915.
- (52) Pitts, J. N., Jr.; Atkinson, R.; Sweetman, J. A.; Zielinska, B. *Atmos. Environ.* **1985**, *19*, 701-705.
- (53) Platt, U.; Perner, D.; Winer, A. M.; Harris, G. W.; Pitts, J. N., Jr. *Geophys. Res. Lett.* **1980**, *7*, 89-92.
- (54) Noxon, J. F.; Norton, R. B.; Marovich, E. *Geophys. Res. Lett.* **1980**, *7*, 125-128.
- (55) Platt, U.; Perner, D.; Schröder, J.; Kessler, C.; Toennissen, A. *J. Geophys. Res.* **1981**, *86*, 11965-11970.
- (56) Platt, U.; Perner, D.; Kessler, C. *Proc. Symp. Compos. Nonurban Troposphere*, **2nd** **1982**, 21-24.
- (57) Platt, U. F.; Winer, A. M.; Biermann, H. W.; Atkinson, R.; Pitts, J. N., Jr. *Environ. Sci. Technol.* **1984**, *18*, 365-369.
- (58) Pitts, J. N., Jr.; Biermann, H. W.; Atkinson, R.; Winer, A. M. *Geophys. Res. Lett.* **1984**, *11*, 557-560.
- (59) Noxon, J. F. *J. Geophys. Res.* **1983**, *88*, 11017-11021.
- (60) Tuazon, E. C.; Sanhueza, E.; Atkinson, R.; Carter, W. P. L.; Winer, A. M.; Pitts, J. N., Jr. *J. Phys. Chem.* **1984**, *88*, 3095-3098.
- (61) Atkinson, R.; Winer, A. M.; Pitts, J. N., Jr. *Atmos. Environ.*, in press.
- (62) Dewar, M. J. S.; Mole, T.; Warford, E. W. T. *J. Chem. Soc.* **1956**, 3581-3586.
- (63) Nielsen, T. *Environ. Sci. Technol.* **1984**, *18*, 157-163.
- (64) Radner, F. *Acta Chim. Scand., Ser. B* **1983**, *B37*, 65-67.
- (65) Pryor, W. A.; Gleicher, G. J.; Cosgrove, J. P.; Church, D. F. *J. Org. Chem.* **1984**, *49*, 5189-5194.
- (66) ASTM D202-77 *Annu. Book ASTM Stand.* **1981**, *39*, 74-77.
- (67) Doyle, G. J.; Bekowies, P. J.; Winer, A. M.; Pitts, J. N., Jr. *Environ. Sci. Technol.* **1977**, *11*, 45-51.
- (68) Schott, G.; Davidson, N. *J. Am. Chem. Soc.* **1958**, *80*, 1841-1853.
- (69) Tuazon, E. C.; Plum, C. N., Statewide Air Pollution Research Center, University of California, Riverside, CA, unpublished data, 1983.
- (70) Tuazon, E. C.; Atkinson, R.; Plum, C. N.; Winer, A. M.; Pitts, J. N., Jr. *Geophys. Res. Lett.* **1983**, *10*, 953-956.
- (71) Malko, M. W.; Troe, J. *Int. J. Chem. Kinet.* **1982**, *14*, 399-416.
- (72) Atkinson, R.; Plum, C. N.; Carter, W. P. L.; Winer, A. M.; Pitts, J. N., Jr. *J. Phys. Chem.* **1984**, *88*, 2361-2364.
- (73) Belser, W. L., Jr.; Shaffer, S. D.; Bliss, R. D.; Hynds, P. M.; Yamamoto, L.; Pitts, J. N., Jr.; Winer, J. A. *Environ. Mutagen.* **1981**, *3*, 123-139.
- (74) McCoy, E. C.; Rosenkranz, H. S.; Mermelstein, R. *Environ. Mutagen.* **1981**, *3*, 421-427.
- (75) McCoy, E. C.; McCoy, G. D.; Rosenkranz, H. S. *Biochem. Biophys. Res. Commun.* **1982**, *108*, 1362-1367.
- (76) Streitwieser, A., Jr.; Fahey, R. C. *J. Org. Chem.* **1962**, *27*, 2352-2355.
- (77) Gold, V.; Hughes, E. D.; Ingold, C. K.; Williams, G. H. *J. Chem. Soc.* **1950**, 2452-2466.
- (78) Schofield, K. "Aromatic Nitration"; Cambridge University Press: Cambridge, U.K., 1980.
- (79) Ramdahl, T.; Bjørseth, A.; Lokensgard, D. M.; Pitts, J. N., Jr. *Chemosphere* **1984**, *13*, 527-534.
- (80) Sonnefeld, W. J.; Zoller, W. H.; May, W. E. *Anal. Chem.* **1983**, *55*, 275-280.
- (81) Grosjean, D.; Fung, K.; Harrison, J. *Environ. Sci. Technol.* **1983**, *17*, 673-679.
- (82) Zielinska, B.; Pitts, J. N., Jr. Statewide Air Pollution Research Center, University of California, Riverside, CA, unpublished data, 1984.
- (83) Kamens, R. M.; Rives, G. D.; Perry, J. M.; Bell, D. A.; Paylor, R. F., Jr.; Goodman, R. G.; Claxton, L. D. *Environ. Sci. Technol.* **1984**, *18*, 523-530.
- (84) Pitts, J. N., Jr., presented at the Workshop on Genotoxic Air Pollutants, Quail Roost Conference Center, Rougemont, NC, April 24-27, 1984.
- (85) Kamens, R.; Bell, D.; Dietrich, A.; Perry, J.; Goodman, R.; Claxton, L.; Tejada, S. *Environ. Sci. Technol.* **1985**, *19*, 63-69.

Received for review March 7, 1985. Accepted June 24, 1985. This work was supported by the U.S. Department of Energy through Contract DE-AM03-76SF00034, David A. Ballantine and George Stapleton, Project Officers.



# NOTES

## Evaluation of Sorptive Partitioning of Nonionic Pollutants in Closed Systems by Headspace Analysis

Doug R. Garbarini<sup>†</sup> and Leonard W. Lion\*

Department of Environmental Engineering, Cornell University, Ithaca, New York 14853

■ An equilibrium headspace technique is shown to be applicable to the determination of sorption equilibria for the nonionic volatile organic compounds toluene and trichloroethylene (TCE). This procedure avoids the problems inherent in other experimental techniques that directly analyze aqueous phase concentration. Such problems include incomplete solid phase separation and subsequent measurements of solute bound to dissolved or colloidal sorbent as free solute. Sorptive partitioning coefficients may be determined by the headspace procedure in the absence of carrier solvents or knowledge of the aqueous concentration of the volatile compounds of concern. Experiments examining the sorption of toluene and TCE onto humic acids, alumina coated with humic acids, and two soil core samples demonstrated the applicability of the headspace technique to sorption studies.

### Introduction

The widespread contamination of ground waters in the United States by volatile organic compounds (VOC's) has resulted in an awareness of the need for definitive knowledge of the behavior and fate of such pollutants. The development of empirical relationships linking the structural and physicochemical properties of a specific organic pollutant with the organic content of a given sorbent, e.g., soil or sediment, in an attempt to predict sorptive binding, has been the topic of much recent research (1-4). Most of these studies have involved methods that rely on a direct sampling of the aqueous phase after centrifugation, settling, or filtration. Sampling of the aqueous phase may in some instances result in a measurement of "free contaminant", which apparently includes contaminant bound to residual colloidal sorbent or dissolved sorbent (5, 6). The observation of a "solids effect" (7, 8), i.e., measurement of an increased partition coefficient as the mass of sorbent used in experiments is decreased, may result from decreased concentrations of colloidal and dissolved sorbents and a concomitant decrease in solute bound to these sorbents (5, 6).

This paper describes the application of a headspace procedure to the measurement of sorptive partitioning, which avoids the difficulties associated with a direct sampling of the aqueous phase. Since solids effects are eliminated, "bound" solute in this study will include forms that may be mobile in soils, e.g., solute sorbed onto colloidal particles and dissolved humic materials. The analytical procedure is adapted from a method developed by Lincoff and Gossett (9) for measuring Henry's law constants for volatile compounds.

Lincoff and Gossett (9) have shown equilibrium partitioning in closed systems (EPICS) to be a simple and accurate technique for determining Henry's constants of volatile organic compounds in water when the dimensionless Henry's constant is less than 3. The method determines Henry's constants by comparing mass balances. Given two closed systems (bottles 1 and 2) containing the same total mass of organic compound, but different liquid and gas volumes, it was shown that (9)

$$H_c = \frac{(C_{g1}/C_{g2})V_{l1} - V_{l2}}{V_{g2} - (C_{g1}/C_{g2})V_{g1}} \quad (1)$$

where  $H_c$  = Henry's constant (dimensionless),  $C_{g1}$  and  $C_{g2}$  = volatile compound gas concentrations (example units  $\mu\text{g/L}$ ) of bottles 1 and 2,  $V_{l1}$  and  $V_{l2}$  = liquid volumes in bottles 1 and 2, and  $V_{g1}$  and  $V_{g2}$  = gas volumes in bottles 1 and 2.

Lincoff (10) has shown that an adaptation of the EPICS procedure may also be used to determine compound activity coefficients ( $\gamma$ ) in cases where the organic solute does not behave ideally in the aqueous phase.

By comparison of two identical bottles, no. 1 and 2, containing the same compound mass and the same liquid and gas volumes, where the volatile solute in bottle 1 behaves ideally (e.g., in distilled water) while the volatile solute in bottle 2 behaves nonideally (e.g., in an electrolyte), a relationship was developed to determine  $\gamma$  as follows (10):

bottle 1

$$M_T = C_{g1}V_g + C_{l1}V_l = C_{g1}V_g + (C_{g1}/H_c)V_l \quad (2)$$

bottle 2

$$M_T = C_{g2}V_g + C_{l2}V_l = C_{g2}V_g + [C_{g2}/(\gamma H_c)]V_l \quad (3)$$

where  $M_T$  = total mass of compound in the system,  $C_{l1}$  and  $C_{l2}$  = compound concentrations in the aqueous phase of bottles 1 and 2, and  $\gamma$  = the activity coefficient that relates the concentration of a compound in solution to its thermodynamic activity ( $A_1$ ), i.e.,  $\gamma = A_1/C_1$ . Combining eq 2 and 3 and solving for  $\gamma$  give

$$\gamma = (V_l/H_c)[(C_{g1}/C_{g2})(V_g + V_l/H_c) - V_{g1}]^{-1} \quad (4)$$

When  $\gamma$  and  $H_c$  are known, the equilibrium gas concentration of a VOC in a closed system serves as a direct measure of its liquid concentration [ $C_l = C_g/(H_c\gamma)$ ], and the EPICS method can logically be extended to the examination of sorption equilibria. Again, partitioning equilibria can be determined by comparing two similar systems containing the same liquid volume ( $V_l$ ), gas volume ( $V_g$ ), and total compound mass ( $M_T$ ), but in this case one system would contain a sorbent (bottle 2), the other none.

<sup>†</sup>Present address: Emergency and Remedial Response Division, U.S. Environmental Protection Agency, New York, NY 10278.



Under such circumstances relationships can be developed for examining sorption equilibria as follows:

bottle 1

$$M_T = C_{g1}V_g + \frac{C_{g1}}{\gamma H_c}V_l = C_{g1}\left(V_g + \frac{V_l}{\gamma H_c}\right) \quad (5)$$

bottle 2

$$M_T = C_{g2}V_g + \frac{C_{g2}}{\gamma H_c}V_l + X = C_{g2}\left(V_g + \frac{V_l}{\gamma H_c}\right) + X \quad (6)$$

where  $X$  = mass of contaminant sorbed. Setting eq 5 equal to eq 6 gives

$$X = (C_{g1} - C_{g2})[V_g + [V_l/(\gamma H_c)]] \quad (7)$$

and from combination of eq 5 and 7

$$\% \text{ sorbed} = \frac{X}{M_T} \times 100 = \frac{(C_{g1} - C_{g2}) \times 100}{C_{g1}} \quad (8)$$

$$X = \frac{\% \text{ sorbed} (M_T)}{100} \quad (9)$$

Equations 8 and 9 show that the percent of solute sorbed or the mass sorbed (parameters commonly evaluated in studies of sorption phenomena) may be determined through headspace analysis. However, when sorption is linearly related to the sorbate concentration, then the distribution coefficient for sorption may also be determined directly from headspace analysis as shown below.

Equations 5 and 6 may be written in terms of the aqueous phase concentrations:

$$M_T = C_{11}\gamma H_c V_g + C_{11}V_l = C_{11}(\gamma H_c V_g + V_l) \quad (10)$$

$$M_T = C_{12}\gamma H_c V_g + C_{12}V_l + X = C_{12}(\gamma H_c V_g + V_l) + X \quad (11)$$

When sorption of nonionic organic compounds to soils and sediments is described by a linear adsorption or constant partitioning isotherm, then

$$X/M = K_d C_{eq} \quad (12)$$

where  $K_d$  = the distribution coefficient for sorption,  $M$  = mass of sorbent employed, and  $C_{eq}$  = equilibrium concentration in the aqueous phase of the system where sorbent is present. Equating the total mass of compound in the bottles with and without sorbent (eq 10 and 11) gives

$$X = (V_l + H_c \gamma V_g)(C_T - C_{eq}) \quad (13)$$

where  $C_T = C_{11}$  = the equilibrium concentration in the aqueous phase of the system without sorbent and  $C_{eq} = C_{12}$  = the equilibrium concentration in the aqueous phase of the system with sorbent. By substitution of eq 12 into eq 13 and rearrangement, the following equation can be used to calculate  $K_d$ :

$$(C_{g1}/C_{g2}) = (C_T/C_{eq}) = K_d[M/(V_l + H_c \gamma V_g)] + 1 \quad (14)$$

where  $C_{g1}$  and  $C_{g2}$  are the gas concentrations in equilibrium with  $C_T$  and  $C_{eq}$ , respectively.

When gas chromatograph peak area or peak height response is linearly related to the gas concentrations being examined, the peak data may be directly substituted for gas concentrations in eq 1, 4, 8, and 14.

Figure 1 illustrates the dependence of the equilibrium ratio ( $C_T/C_{eq}$ ) on Henry's constant for conditions used in some of the sorption experiments. Figure 1A shows that the headspace technique is most sensitive for solutes with

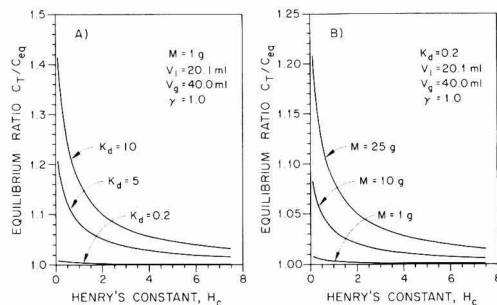


**Figure 1.** Calculated equilibrium gas concentration ratio in the headspace procedure as a function of Henry's constant, (A) sorptive partitioning coefficient ( $K_d$ ) and (B) mass of sorbent.

low Henry's constants and sorbents with high sorption capacity ( $K_d$ ). As illustrated in Figure 1B, sensitivity for measurement of compounds with low  $K_d$  values (approximately 0.5 and less) may be increased by increasing the mass of sorbent employed in analyses.

A major advantage of the EPICS technique is that knowledge of the total solute mass added to the system is not necessary for the determination of Henry's constants and activity coefficients for volatile compounds (see eq 1 and 4). This is also true for the measurement of  $K_d$  values (eq 14) using the headspace procedure as modified here; however,  $H_c$  and  $\gamma$  must first be independently determined. Freedom from the requirement that total solute mass be known provides an advantage over other procedures that rely upon carrier solvents, purge and trap techniques, or solvent extractions for determining aqueous phase equilibrium concentrations and subsequently use these data for calculating partition coefficients (2, 4, 11, 12).

An additional advantage is realized by the use of concentration ratios (eq 14) for the determination of linear sorptive partitioning coefficients. Commonly  $K_d$  is determined from the slope of the relationship between fraction or mass of solute sorbed (eq 8 or 9) and  $C_{eq}$ . This procedure can introduce large errors in situations where sorption is low, and the amount sorbed is, therefore, a small difference between two large values. The modified headspace procedure is, however, a "difference technique" in the sense that differences in the control and sample bottles are attributed to a particular reaction (in this case sorption). Partitioning equilibria for toluene and trichloroethylene (TCE) were evaluated in this study to demonstrate the applicability of the modified headspace technique to sorption studies. In the discussion which follows it is assumed that sorption is the only reaction that contributed measurably to observed differences between control and sample vial activities of the test compounds. Soil bacteria have been reported by some investigators to possess the ability to degrade toluene but not TCE (13, 14), although reductive dechlorination of TCE in anaerobic soils has been observed (15). On the basis of these results, reactions other than sorption are considered unlikely for TCE in the experiments described here, but possible biodegradation of toluene in test vials containing soil cannot be ruled out.

### Materials and Methods

Two soil core samples, a commercial humic acid and a hydrous aluminum oxide coated with humic acid, were used as sorbents. The soil samples were obtained from Offutt AFB, Omaha, NE, and Whiteman AFB, Knobnoster, MO, at core depths of 11–13 and 3–4.7 ft, respec-

tively. The soils were dried at 105 °C and ground, and material passing through a no. 20 sieve was used in the sorption experiments without further preparation. Humic acids were obtained from ICN Pharmaceuticals, Inc., and used without modification. Humic acid coated alumina oxide was prepared by dissolving 9 g of humic acid in 1 L of distilled water at pH 10 (pH raised with NaOH). Approximately 450 g of Al<sub>2</sub>O<sub>3</sub> (Fisher Scientific adsorption alumina 80–200 mesh) was added, and the pH of this stirred slurry was lowered to approximately 4 with concentrated HNO<sub>3</sub>. After being equilibrated for more than 48 h, the suspension was settled and the supernatant decanted. The coated solids were rinsed once with distilled water acidified to pH ≈ 4 and then dried at 105 °C. The organic carbon content of the sorbents was determined by dichromate oxidation using the Walkley–Black method for soils analysis (16).

The toluene and TCE used were analytical grade. Stock solutions of toluene were prepared by delivering 500 µL of toluene to a 2-L volume of water with an Eppendorf pipet. The mass delivered was determined by weight to be 0.422 ± 0.001 g (*n* = 4) giving a stock solution concentration of 211 mg/L (if no loss through volatilization is assumed). A methylene chloride extraction technique analogous to the procedure used by Henderson et al. (17) was used to verify the stock toluene solution concentration. The measured concentration was 214.1 ± 12.4 mg/L (*n* = 4); therefore, toluene losses during stock solution preparation were considered to be negligible. A stock-saturated solution was used for TCE experiments. TCE stock solution concentration was calculated to be 1290 mg/L by using the reported value for TCE vapor pressure (18) and the experimentally determined Henry's constant (*H*<sub>c</sub> = 0.397 at 25 °C using the EPICS procedure of Lincoff and Gossett). The stock solution concentrations are given here for reference purposes since, as noted above, knowledge of the mass of solute present is not required for the determination of *H*<sub>c</sub>, *γ*, or *K*<sub>d</sub> values.

Experiments were conducted in glass hypo-vials sealed with Teflon-lined rubber septa and aluminum crimp caps (Pierce Chemical Co.). Two bottle sizes were employed with nominal capacities of 150 and 50 mL; individual bottle volumes were determined by weight when filled to capacity with water. Experiments involving sorption equilibria of humic acid coated alumina and humic acids alone were performed in the 50-mL bottles while all other experiments were conducted in the 150-mL bottles.

Liquid volumes used in the determination of Henry's constants were 10 and 125 mL; those used in activity coefficient determination were 100 mL. Aliquots of TCE or toluene stock solution (300 µL of TCE and toluene for Henry's constants and 200 µL of TCE and 100–300 µL of toluene for activity coefficients) were transferred to the hypo-vials. Vials were then rapidly capped and equilibrated for at least 24 h in a circulating water bath at 25 °C. During this equilibration period, but at least 3 h prior to analysis, the bottles were removed 3 times and hand shaken for approximately 30 s.

In the sorption experiments 20 (for 50-mL bottles) or 50 mL (for 150-mL bottles) of 0.1 M NaCl was added to variable amounts of sorbent, while the amount of toluene and TCE stock solution was held constant. The NaCl electrolyte was chosen to swamp out any possible contribution of the sorbent to ionic strength (experiments that verify the swamping effect are discussed under Results and Discussion).

The bottles for sorption experiments were continuously rotated at room temperature for at least 12 h and then

placed in a 25 °C water bath overnight prior to gas-phase analysis. Gas concentration data for the experiments was obtained by removing 1 mL of bottle headspace with a gas-tight syringe (Precision Scientific, Inc.) and analysis with a Perkin-Elmer Model 900 gas chromatograph equipped with a flame ionization detector and a Carbo-Pack (60/80) with 1% SP-1000 column (Supelco, Inc.). Peak areas were obtained by interface of the GC signal with a Hewlett-Packard Model 3388A integrator. Peak heights were used when an integrator was not available. The gas chromatograph was operated isothermally at column temperatures of approximately 135 °C for TCE and 175 °C for toluene. Typically four or more replicate bottles were analyzed for each data point. The existence of a linear relationship between gas concentrations and gas chromatograph peak areas and peak heights over the range of gas concentrations studied was verified.

In sorption experiments in which the mass of sorbent was varied, the volume displaced by the sorbent was determined and used to obtain the actual volume of headspace in the bottle. With this information, observed gas concentrations were normalized to a uniform bottle size by using the following relationship:

$$C_{\text{normalized}} = C_{\text{obsd}} \frac{(V_1 + \gamma H_c V_g)_{\text{actual}}}{(V_1 + \gamma H_c V_g)_{\text{standard}}} \quad (15)$$

Gas concentrations for replicates were then averaged and used to evaluate partitioning equilibria.

Sorption experiments were also performed using <sup>14</sup>C-radiolabeled TCE to verify results obtained with the modified headspace technique and to examine the effect of using a swamping electrolyte vs. distilled water in sorption experiments. Methodology for the tracer experiment was adapted from that developed by LaPoe (19). Briefly, aliquots of radiolabeled TCE stock solution were added to 6-mL glass microreaction vessels (Supelco, Inc.) containing varying quantities (0–90 mg) of ICN humic acid in 5.50 mL of either 0.1 M NaCl electrolyte or distilled water. Aqueous-phase TCE concentrations (approximately 2.0–4.0 mg/L) and humic acid concentrations (0–15 mg/mL) employed were similar to those used in headspace sorption experiments. The vessels were rotated for 20 h at 25 °C and then centrifuged at 5000*g* for 30 min. <sup>14</sup>C activity in the centrifuged solution was assayed on a Beckman LS9800 liquid scintillation counter. It should be noted that the liquid-phase analyses performed are subject to particle effects should they occur. However, use of radiolabeled TCE avoids many of the other analytical difficulties previously discussed. Results of the confirmatory experiments are discussed below.

## Results and Discussion

Measured dimensionless Henry's law constants (25 °C) were 0.397 for TCE and 0.261 for toluene. Both values are within the range in which the EPICS technique is considered to be reliable (i.e., *H*<sub>c</sub> < 3). The measured value for TCE agreed quite closely with values cited in the literature of 0.411 [calculated for *T* = 25 °C from the regression equation for *H*<sub>c</sub> vs. temperature given by Lincoff and Gossett (9)] and 0.403 (20). The Henry's law constant for toluene also agreed closely with literature values of 0.270 (21) and 0.265 [calculated for *T* = 25 °C from the regression equation for *H*<sub>c</sub> vs. temperature given by Leighton and Calo (20)].

Activity coefficients measured for toluene and TCE in NaCl solutions of variable ionic strength are listed in Table I and show that both VOC's exhibited behavior typical of neutral molecules in electrolyte solutions, i.e., an increased

**Table I. Activity Coefficients for TCE and Toluene<sup>a</sup>**

compound	activity coefficient ( $\gamma$ ) for indicated ionic strength <sup>b</sup>			
	$I = 0.1$	$I = 0.3$	$I = 0.6$	$I = 1.0$
TCE	1.06	1.16	1.32	1.58
toluene	1.05	1.14	1.31	1.62

<sup>a</sup> Values obtained in NaCl electrolyte at 25 °C. <sup>b</sup> Electrolyte concentration as moles per liter.

**Table II. Effect of Electrolyte Composition on Toluene Activity<sup>a</sup>**

ionic strength	toluene activity coefficient (25 °C)		
	NaCl	CaCl <sub>2</sub>	AlCl <sub>3</sub>
0.10	1.05	1.02	1.04
0.30	1.14	1.08	1.06

<sup>a</sup> Ionic strength as moles per liter.

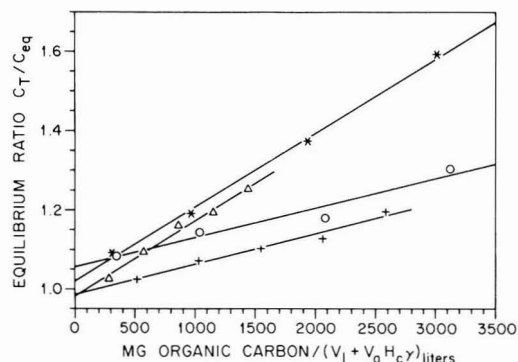


**Figure 2.** Sorption of toluene by humic acids (asterisk), Al<sub>2</sub>O<sub>3</sub> coated with humic acids (O), Offutt soil (Δ), and Whiteman soil (+).

salting out with increased ionic strengths. The activity coefficient,  $\gamma$ , may be related to ionic strength in solution through an empirical equation of the form (22)

$$\log \gamma = kI \quad (16)$$

where  $k$  is the "salting coefficient" and  $I$  is the ionic strength of the solution (mol/L).

The salting coefficients ( $k$ ) calculated for TCE and toluene in NaCl electrolyte were 0.194 and 0.208, respectively. Different electrolytes are reported to have varying effects on the activity of nonionic solutes (23). Activity coefficients for toluene in CaCl<sub>2</sub> and AlCl<sub>3</sub> solutions were determined and compared to those in NaCl (Table II) in order to examine such effects. It can be seen that electrolyte composition affected the activity of toluene, as the activity coefficients for AlCl<sub>3</sub> and CaCl<sub>2</sub> were significantly lower than those determined for NaCl at an ionic strength of 0.3 mol/L.

Results of the sorption studies for toluene and TCE are plotted by using the form of eq 14 in Figures 2 and 3, respectively. The masses of organic carbon used for the  $x$  axis were calculated by multiplying the masses of sorbent actually employed in the experiments by their respective fraction organic carbon. The linearity of relationships depicted in Figures 2 and 3 (all values of  $r^2 > 0.95$ ) suggests that a linear sorption isotherm was obeyed for the range of solute concentrations studied (approximately 2.6–3.5 and 0.4–0.7 mg/L for TCE and toluene, respectively).

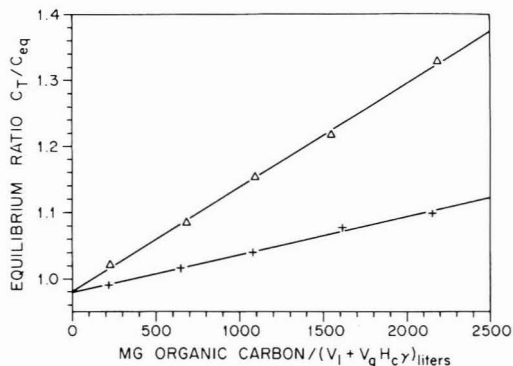


**Figure 3.** Sorption of TCE by humic acids (Δ) and Al<sub>2</sub>O<sub>3</sub> coated with humic acids (+).

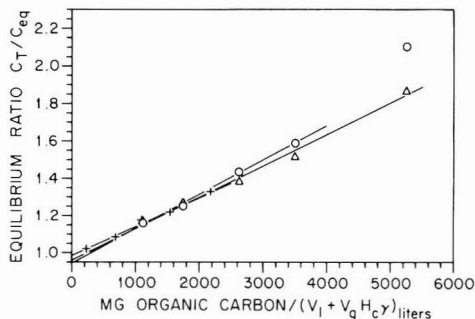


**Figure 4.** Sorption of TCE by humic acid. Comparison of results based on gas-phase analysis (+) and aqueous-phase analysis (Δ) in 0.1 M NaCl electrolyte and aqueous-phase analysis in distilled water (O).

Linearity also suggests that observed  $K_d$ 's were independent of the concentration of sorbent over the range of sorbent concentrations employed (0–15 mg of humic acid/mL; all other sorbents 0–1 g/mL), indicating that "particle effects" are avoided with the equilibrium headspace technique. Although some solute defined as sorbed by the headspace procedure may be in a "mobile" form (e.g., bound to colloidal solids or dissolved humic materials), the use of a 0.1 M NaCl electrolyte and the tendency of humic acids and colloidal particles to coagulate at high ionic strengths should act to minimize this difficulty. The ability to obtain  $K_d$  values which are not conditionally dependent on experimental solids concentration provides a distinct advantage to the headspace procedure over methods that utilize direct analysis of the aqueous phase.

Figure 4 compares plots of humic acid sorption data in 0.1 M NaCl using both the headspace (gas-phase analysis) and <sup>14</sup>C counting (liquid-phase analysis) procedures. Also shown are sorption data for the humic acid in distilled water using the counting procedure. As can be seen the slopes or  $K_{oc}$ 's ( $K_d$ 's normalized to fraction organic carbon) of the plotted data are quite similar.  $K_{oc}$ 's determined in 0.1 M NaCl by using the two different procedures are not significantly different ( $K_{oc} = 157.6 \pm 4.0$  for the headspace procedure and  $K_{oc} = 168.6 \pm 8.3$  for the results based on <sup>14</sup>C analysis of the aqueous phase). Similarly,  $K_{oc}$  determined for humic acid in electrolyte by using the counting procedure was not significantly different from that determined in distilled water by the counting procedure when the data point for 15 mg/mL organic carbon is excluded ( $K_{oc} = 183.4 \pm 7.4$ ). This data point appears to be anomalous.

Table III. Toluene and TCE Distribution Coefficients (25 °C)

contaminant	sorbent	% OC	$K_d$	$K_{oc}$	predicted <sup>a</sup> $K_{oc}$ using solubility (3)	predicted <sup>b</sup> $K_{oc}$ using $K_{ow}$ (4)	predicted <sup>b</sup> $K_{oc}$ using $K_{ow}$ (2)
toluene	ICN humic acid coated $Al_2O_3$	0.54	0.40	74	86	267	309
toluene	ICN humic acid	33.5	62.5	187	86	267	309
toluene	Offutt AFB soil	0.23	0.44	191	86	267	309
toluene	Whiteman AFB soil	0.41	0.32	77	86	267	309
TCE	ICN humic acid coated $Al_2O_3$	0.40	0.23	58	46	138	123
TCE	ICN humic acid	33.5	52.7	158	46	138	123

<sup>a</sup> Solubility for TCE = 1290 mg/L calculated as described under Materials and Methods. Solubility for toluene = 515 mg/L (25). <sup>b</sup>  $K_{ow}$  = 195 for TCE (26) and 490 for toluene (4).

alously high, perhaps because of salting out of TCE from distilled water at the highest solids concentration. Ionic strength effects on the EPICS procedure are discussed in more detail below.

The correspondence of results based on gas-phase and aqueous-phase analyses verify the applicability of head-space analyses to sorption studies. In addition, the similarity of results determined in distilled water and 0.1 M NaCl indicates the use of NaCl electrolyte did not have a significant effect on the magnitude of observed  $K_{oc}$  values.

Previous investigators have shown sorption of nonionic organic compounds onto soils and sediments to be dependent upon the organic content of the sorbent (1–4, 24). The partitioning observed in experiments described here does not indicate that organic carbon content is the sole determinant in sorption capacity. Calculated  $K_d$ 's and  $K_{oc}$ 's determined by linear regression of the data are given in Table III as are predicted  $K_{oc}$  values calculated from empirical equations given by other investigators (2–4). Observed values for  $K_{oc}$  are of the same order of magnitude as those predicted on the basis of either compound solubility (3) or octanol–water partitioning coefficient,  $K_{ow}$  (2, 4). Although normalization of  $K_d$ 's per unit mass organic carbon does converge the results,  $K_{oc}$ 's for toluene sorption onto the sorbents still vary by a factor of 2.5 with the sorbents of highest and lowest organic carbon content having the largest and almost identical  $K_{oc}$ 's. These findings are qualitatively in accordance with those of others (27, 28). Mingelgrin and Gerstl (28) have compiled a list of  $K_{om}$  values ( $K_d$ 's normalized to fraction organic matter) for a variety of nonionic compounds on a variety of soils that show differences ranging from a factor of 3 to over an order of magnitude in  $K_{om}$  values for a given compound from soil-to-soil.

The  $K_{oc}$ 's determined for TCE and toluene sorption onto humic acids were more than 2.5 times greater than those determined for the same humic acids when coated onto  $Al_2O_3$ . These data suggest that the sorptive capacity of the humic acid may be reduced by the presence of the  $Al_2O_3$  matrix. Possible reasons for the observed reduction in sorptive capacity may include differences in the physical and chemical nature of the free vs. coated humics, selective adsorption of a certain fraction of the humic acid to the  $Al_2O_3$  surface, and pH differences in the aqueous phases containing the respective sorbents.

Davis (29) has indicated that the complexation of natural dissolved organic matter to hydrous aluminum oxides may involve specific adsorption governed by the interaction of weakly acidic functional groups of the organic matter with relatively basic surface hydroxyls of the aluminum oxide. Such adsorption may alter the adsorbed organic materials physically (structural changes) or chemically (by bond formation). Therefore, the coating procedure em-

ployed here may have resulted in an adsorbed humic material which was not as accessible to the binding of VOC's as the free dissolved and colloidal humic acids.

Davis et al. (30) also observed that organic matter with a molecular weight of >1000 formed stronger complexes with alumina surfaces than lower molecular weight organic matter and that most of the organics adsorbed to the alumina were within the molecular weight range of 1000–3000. Selective removal of organic materials based upon molecular functional group arrangement was suggested. Such a selective removal may have occurred in the coating procedure. This may have resulted in  $Al_2O_3$ -bound humic acid which was less active than the composite humic acids in sorbing nonionic organic pollutants.

Carter et al. (31) in their study of DDT binding to humic acids found that solution pH had an effect on the amount of DDT sorbed. Since the solution pHs were not controlled in the experiments reported here, pH effects may have contributed to the observed disparate binding of the free vs.  $Al_2O_3$ -coated humic acids.

Although Chiou et al. (32) have shown that mineral surfaces are unlikely to play a significant role in the sorption of nonionic pollutants from aqueous solutions, the results observed here with free vs. coated humic acids do suggest that the interaction of a mineral surface with a humic coating may influence the binding capacity of the coating material.

Various mineral surfaces adsorb humic materials by different mechanisms (e.g., adsorption by nonspecific Coulombic attraction is dependent upon mineral surface charge) (33). If such mechanisms effectively result in dissimilar humic coatings, they may help explain the observed disparities in measured  $K_{oc}$  values such as those shown in Table III. The validity of this speculation awaits further research.

The application of the EPICS technique to sorption equilibria studies requires that there be no significant ionic strength contribution to the aqueous phase by the sorbent. Such contributions would result in increased activity of the solute and a complementary increase in measured gas concentration. In an effort to "swamp out" any such effects, 0.1 M NaCl electrolyte was used in all sorption experiments. Three experiments were performed to determine if the 0.1 M NaCl electrolyte was indeed swamping.

The first experiment involved measuring the specific conductance of distilled water contacted with humic acid and humic acid coated  $Al_2O_3$  in mass to volume ratios equivalent to those in experiments containing the largest masses of these sorbents. Measured conductivities were compared with the conductance of a 0.1 M NaCl solution. Results showed that possible contributions to the activity coefficient of a 0.1 M NaCl solution as determined by this type of a comparison would be less than 0.8% for the humic acids and less than 0.5% for  $Al_2O_3$  coated with



humic acids. However, it is possible that the presence of a charged interface may influence the activity of a nonionic solute (for example, by altering the structure of water near the interface) while not markedly increasing conductivity since solid particles are relatively nonmobile in comparison to dissolved ions.

In the second experiment, 20 mL of 0.1 M NaCl was added to a series of bottles containing 0, 5, and 15 g of  $\text{Al}_2\text{O}_3$ , a material that had previously been shown to have no detectable sorption capacity for TCE or toluene. Aliquots of TCE stock solution were added and equilibrated as described previously for sorption experiments. If the  $\text{Al}_2\text{O}_3$  was significantly contributing to the ionic strength of the solution, the gas concentrations in the bottles containing 15 g of sorbent would have been noticeably higher than those in bottles with 5 g of sorbent and these noticeably higher than those without sorbent. This was not the case as the averaged normalized GC peak heights of TCE in the 0-, 5-, and 15-g bottles were equal within the  $\pm 2\%$  precision of the GC analytical technique.

In the third experiment, 18 g of humic acid coated  $\text{Al}_2\text{O}_3$  was added to two sets of bottles, one containing 20 mL of 0.1 M NaCl and 100  $\mu\text{L}$  of saturated TCE stock solution and the other 20 mL of 0.3 M NaCl and 95.1  $\mu\text{L}$  of saturated TCE stock solution. On the basis of the activity coefficients determined for these ionic strengths (see above discussion) the two sets of bottles should have given the same gas chromatographic response unless there was a significant contribution to ionic strength by the humic coated material, in which case the 0.1 M NaCl bottle would have given a larger response. Average GC peak heights determined for the two sets of bottles were again equivalent within the limits of analytical precision, supporting the premise that the electrolyte was indeed swamping.

## Conclusions

The results of this study indicate that an equilibrium headspace technique is reliable for the study of sorption equilibria of volatile nonionic organic compounds. Since the gas phase is analyzed, the technique evades problems such as losses through volatilization, difficult extractions, the use of carrier solvents, and incomplete solids separation (and therefore possible solids effects) which often burden other techniques. The procedure is relatively simple and allows the determination of distribution coefficients from raw gas chromatography (GC) data when the GC response is linearly related to the activity being examined.  $K_d$  values may be determined independent of knowledge of the mass of solute used in partitioning experiments.

The distribution coefficients determined above indicate that partitioning of a nonionic organic contaminant is affected by the specific physicochemical nature of the organic phase. These findings are qualitatively in agreement with those of Shin et al. (27) and Mingelgrin et al. (28). In the future, precise (better than an order of magnitude) prediction of sorption of nonionic organic pollutants by groundwater matrices might be achieved through detailed characterization of sorbent phases beyond their organic content. To facilitate this end, additional research is needed to identify relevant (to sorption) physicochemical parameters of soils, sediments, and the solid phases encountered in groundwater aquifers.

## Acknowledgments

We thank Thomas Stauffer of the Environics Laboratory at Tyndall AFB for his assistance in the conduct of this

research and Capt. Robert (Blum) La Poe for his critique of the manuscript and assistance with the radiotracer sorption experiments.

**Registry No.** TCE, 79-01-6;  $\text{H}_2\text{O}$ , 7732-18-5; toluene, 108-88-3.

## Literature Cited

- (1) Chiou, C. T.; Peters, L. J.; Freed, J. H. *Science (Washington, D.C.)* **1979**, *206*, 831-832.
- (2) Karickhoff, S. W.; Brown, D. C.; Scott, T. A. *Water Res.* **1979**, *13*, 241-248.
- (3) Means, J. C.; Wood, G. S.; Hassett, J. J.; Banwart, W. L. *Environ. Sci. Technol.* **1980**, *14*, 1524-1528.
- (4) Schwarzenbach, R. P.; Westall, J. *Environ. Sci. Technol.* **1981**, *15*, 1360-1367.
- (5) Gschwend, P. M.; Wu, S. *Environ. Sci. Technol.* **1985**, *19*, 90-96.
- (6) Voice, T. C.; Rice, C. P.; Weber, W. J., Jr. *Environ. Sci. Technol.* **1983**, *17*, 513-517.
- (7) Grover, R.; Hance, R. J. *Soil Sci.* **1970**, *109*, 136-138.
- (8) O'Connor, D. J.; Connally, J. P. *Water Res.* **1980**, *14*, 1517-1523.
- (9) Lincoff, A. H.; Gossett, J. M. In "Gas Transfer at Water Surfaces"; Brutsaert, W.; Jirka, G. H., Eds.; D. Reidel Publishing Co.: Dordrecht, Holland, 1984; pp 17-25.
- (10) Lincoff, A. H. M.S. Thesis, Cornell University, 1983.
- (11) Diachenko, G. W. Ph.D. Thesis, University of Maryland, 1981.
- (12) Weber, W. J., Jr.; Voice, T. C.; Pirbazari, M.; Hunt, G. E.; Ulanoff, D. E. *Water Res.* **1983**, *17*, 1443-1453.
- (13) Wilson, J. T.; McNabb, J. F.; Balkwill, D. L.; Ghiorse, W. C. *Ground Water* **1983**, *21*, 134-142.
- (14) Wilson, J. T.; Enfield, C. G.; Dunlap, W. J.; Cosby, R. L.; Foster, D. A.; Baskin, L. B. *J. Environ. Qual.* **1981**, *10*, 501-506.
- (15) Kleopfer, R. D.; Easley, D. M.; Hass, B. B., Jr.; Deihl, T. G.; Jackson, D. E.; Wurrey, C. J. *Environ. Sci. Technol.* **1985**, *19*, 277-280.
- (16) Allison, L. E. In "Methods of Soil Analysis: Part 2. Chemical and Microbiological Properties"; Black, C. A., Ed.; American Society of Agronomy: Madison, WI, 1965; pp 1367-1378.
- (17) Henderson, J. E.; Peyton, G. R.; Glaze, W. H. In "Identification and Analysis of Organic Pollutants in Water"; Keith, L. H., Ed.; Ann Arbor Science Publishers: Ann Arbor, MI, 1976; pp 105-111.
- (18) Schlessinger, G. G. In "Handbook of Chemistry and Physics", 52nd ed.; Weast, R. C., Ed.; CRC Press: Cleveland, OH, 1971; pp D151-D175.
- (19) La Poe (Blum), R. Ph.D. Thesis, Cornell University, 1985.
- (20) Leighton, D. T.; Calo, J. M. *J. Chem. Eng. Data* **1981**, *26*, 382-385.
- (21) MacKay, D.; Shiu, W. Y.; Sutherland, R. P. *Environ. Sci. Technol.* **1979**, *13*, 333-337.
- (22) Garrels, R. M.; Christ, C. L. "Solutions, Minerals, and Equilibria"; Harper and Row: San Francisco, CA, 1965; pp 67-70.
- (23) Randall, M.; Failey, C. F. *Chem. Rev.* **1927**, *4*, 271-284.
- (24) Lambert, S. M.; Porter, P. E.; Schieferstein, P. H. *Weeds* **1965**, *13*, 185-190.
- (25) U.S. Environmental Protection Agency "Innovative and Alternative Technology Assessment Manual"; Office of Water Program Operations: Washington, DC, 1980.
- (26) Rodgers, R. D.; McFarland, J. C. *Environ. Monit. Assess.* **1981**, *1*, 155-162.
- (27) Shin, Y.; Chodan, J. J.; Walcott, A. R. *J. Agric. Food Chem.* **1970**, *18*, 1129-1133.
- (28) Mingelgrin, U.; Gerstl, Z. *J. Environ. Qual.* **1983**, *12*, 1-11.
- (29) Davis, J. A. *Geochim. Cosmochim. Acta* **1982**, *46*, 2381-2393.
- (30) Davis, J. A.; Gloor, R. *Environ. Sci. Technol.* **1981**, *15*, 1223-1228.
- (31) Carter, C. W.; Suffet, I. H. *Environ. Sci. Technol.* **1982**, *16*, 735-740.
- (32) Chiou, C. T.; Shoup, T. D.; Porter, P. E. *Org. Geochem.* **1985**, *8*, 9-14.



(33) Greenland, D. J. *Soil Sci.* 1971, 111, 34-41.

Received for review September 11, 1984. Revised manuscript received February 1, 1985. Accepted June 7, 1985. This research was sponsored by the U.S. Air Force Office of Scientific Research

through its Summer Faculty Graduate Student Research Program under Contract F-49620-82-C-0035 and through Subcontract SCEE 83RIP/02. The research was undertaken at the Air Force Engineering and Services Laboratory, Tyndall, AFB, FL, and the Environmental Engineering Laboratories at Cornell University.

## Concentrations of Krypton-85 near the Nevada Test Site

R. Frank Grossman\* and Robert W. Holloway

Environmental Monitoring Systems Laboratory, U.S. Environmental Protection Agency, Las Vegas, Nevada 89114

■ Since 1972, the Environmental Monitoring Systems Laboratory has operated a network of noble gas samplers around the Nevada Test Site (NTS). For 10 of those years, the network also included several samplers on the NTS. The network was established to measure the concentrations of noble gases released to the atmosphere by underground nuclear detonations, by posttest operations, and by seepage from the ground from previous underground tests. During this 12-year period, the concentrations of krypton-85 measured in samples collected around the NTS gradually increased with time from 16 pCi/m<sup>3</sup> in 1972 to 25 pCi/m<sup>3</sup> in 1983. This increase was not found to be due to nuclear testing activities at the NTS but to the worldwide use of nuclear technology, a trend that has been predicted by previous investigators. The observed trend of increasing concentration was considerably less than had been projected by other authors, being only one-eighth to one-fifth of that projected. It is suggested that the difference from predictions is due to a decrease in the rate of growth in the number of nuclear power plants and, more significantly, the slow growth of nuclear fuel reprocessing activities.

### Introduction

Since April 1972, a network of air samplers has been operated on and around the Nevada Test Site to monitor the concentrations of noble gases released to the atmosphere by underground nuclear detonations, postshot operations, and seepage through the ground. The first year of continuous operation of this network was reported earlier by this laboratory (1). Also, a series of environmental monitoring reports since 1972 (2-13) have summarized the data from the noble gas sampling network for each calendar year to assess any radiation exposures to off-site residents. For the first time, this report reviews the results of the noble gas network collected over a 12-year period to identify long-term trends and to present descriptive statistics of the data.

### Network Operations

The initial network that was established around the Nevada Test Site included samplers at four on-site and six off-site locations. Over the years, additional stations were added, both on site and off site, to improve coverage. In 1982, the operation and analysis of the onsite samplers were turned over to the Reynolds Electrical and Engineering Co., a contractor at the Nevada Test Site for the U.S. Department of Energy. Also, the off-site network was expanded to 16 stations, 15 of which were part of the Community Radiation Monitoring Program, which is described in ref 11. Figure 1 shows the location of all the off-site stations relative to the Nevada Test Site.

This laboratory was also involved in the environmental monitoring conducted around the Three-Mile Island Nu-

clear Power Station shortly following the accident in March 1979. Noble gases were monitored by collecting compressed air samples from one station 0.4 mile from the reactor and several stations in nearby towns. The samples were analyzed at the EMSL-LV Laboratory through Oct 1983 and subsequently by personnel of the Office of Radiation Programs, EPA.

### Analytical Procedures

During the period 1972-1982, air-compressing units designed to collect 1 m<sup>3</sup> of air, as described by Andrews (14), were used throughout the network to collect weekly air samples in dual pressure tanks. Continued operation of the compressors resulted in a deterioration of the design pressure of 400 psi; however, the analytical laboratory was able to adapt to a smaller sample size of 0.6-0.7 m<sup>3</sup> instead of the desired 1 m<sup>3</sup>.

In 1982, an air sampler that liquified air by cryogenic techniques was fielded; however, some compressor-type samplers continued to be used as replacements for the cryogenic units during breakdowns. The cryogenic samplers were adjusted to collect the same size air sample each week as the compressor units.

All samples were returned to the Las Vegas Laboratory for analysis. The analytical procedure was described by Johns et al. (17). The procedure involves the separation and purification of krypton and xenon by adsorption on chromatographic columns and the subsequent analysis of the radioactivity in the krypton and xenon fractions by liquid scintillation counting.

### Data Analysis

The accuracy of the krypton-85 measurements is evaluated periodically with samples of known radioactivity. The bias of the measurements has been within 8% of the standard samples. As an estimate of the precision of the krypton-85 analyses, at least 30 samples per year are split and analyzed separately. The precision of the measurements, expressed as percent coefficient of variation, as determined during the years 1978 and 1981-1983 has been 8-14%.

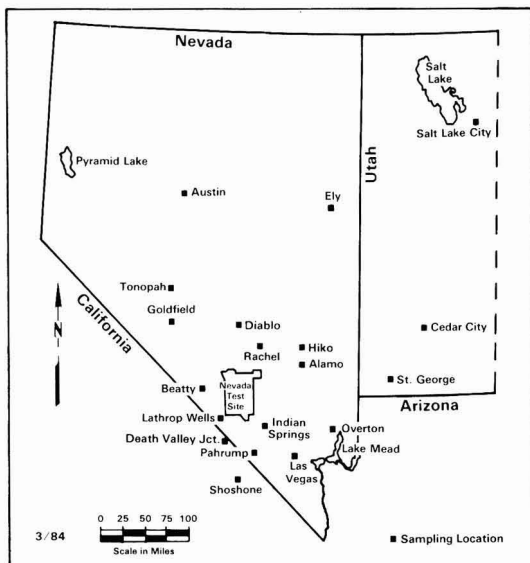
A correlation goodness of fit test was applied to the krypton-85 data grouped by year. The results of the test indicated that the data could generally be separated into either normal, log-normal, or mixed distributions with each year showing a unique pattern. As the distribution of the data varied between normal and log normal, normal statistics was used for convenience to summarize the data for this report.

Table I summarizes the data by listing the annual mean concentrations of krypton-85 for each station for the years 1972-1983. As shown by the annual means, the concentration of krypton-85 has been gradually increasing. From the data in Table I, the relationship of off-site krypton-85 concentration with time is  $pCi/m^3 = 14.88 + 0.83t$  and the

**Table I. Mean Annual Krypton-85 Concentration (pCi/m<sup>3</sup>) by Station and Network, 1972–1983**

	1972	1973	1974	1975	1976	1977	1978	1979	1980	1981	1982	1983
off site												
Alamo										26.1	24.4	24.6
Austin											24.2	25.2
Beatty	16.0	16.3	17.2	18.7	20.2	20.0	20.3	18.7	20.8	24.0	24.6	24.4
Cedar City											24.6	24.3
Death Vally Jct	15.7	15.3	17.5	16.9	19.6	19.7	19.8	18.8				
Diablo/Rachel <sup>a</sup>	16.3	16.2	17.1	18.3	19.4	19.1	19.9	20.6			24.1	24.9
Goldfield											24.7	24.5
Hiko	15.7	15.6	17.4	17.3	17.0	19.0	19.9	19.3	21.3	23.9	26.4	
Indian Springs				20.0	19.6	19.9	20.2	18.9	20.9	24.4	24.2	24.8
Las Vegas	15.8	15.6	17.3	17.7	18.2	19.5	20.1	19.2	18.7	24.0	24.1	24.0
Lathrop Wells								18.6	21.6	23.5	24.2	25.7
Overton										26.2	24.1	24.8
Pahrump										23.2	24.1	23.7
Salt Lake City											24.6	25.4
Shoshone											24.8	25.3
St. George											23.5	24.8
Tonopah	16.1	16.0	17.5	16.9	19.2	19.2	20.0	18.4	21.3	24.6	23.7	25.5
network average	15.9	15.8	17.3	17.9	19.0	19.5	20.0	18.8	21.0	24.0	24.4	24.8
on site												
area 12	15.6	15.8	17.6	18.0	19.5	19.2	20.0	19.0	21.0	24.1	24.5 <sup>b</sup>	24.8 <sup>b</sup>
area 15								19.2	21.4	24.6	25.0 <sup>b</sup>	24.9 <sup>b</sup>
area 51			18.4	18.1	19.8	19.3	20.0	19.0	20.6	24.2	23.8 <sup>b</sup>	
area 400								18.4	21.0	22.9	24.4 <sup>b</sup>	25.3 <sup>b</sup>
BJY	16.8	18.3	19.3	18.7	20.5	21.3	22.0	21.0	23.2	26.0	25.4 <sup>b</sup>	26.5 <sup>b</sup>
Desert Rock	15.9	16.0	18.0	13.6								
gate 700	15.8	16.1	17.4	13.4								25.6 <sup>b</sup>
Mercury			18.7	17.6	18.8	19.5	19.9	18.9	21.4	23.0	24.2 <sup>b</sup>	
area 5												25.3 <sup>b</sup>
area 20												25.5 <sup>b</sup>
network average	16.0	16.6	18.2	17.9	19.6	19.8	20.4	19.3	21.5	24.2	24.6	25.0
TMI network <sup>c</sup>								22.7	25.1	25.0	25.9	25.7

<sup>a</sup> Station at Diablo was moved to Rachel in March 1979. <sup>b</sup> Measurements made by Reynolds Electrical Engineering Co., Inc., and reported by Scoggins (14, 15). <sup>c</sup> Average concentrations were derived from data distribution less than 60 pCi/m<sup>3</sup>.



**Figure 1.** Sampling locations used around the Nevada Test Site to monitor for noble gases.

relationship of on-site concentrations with time is  $\text{pCi/m}^3 = 15.42 + 0.81t$ , where  $t$  is the number of years after Jan 1, 1972. The correlation coefficient for both linear regressions is 0.96.

From Table I, one can also observe that the on-site mean krypton-85 concentrations were consistently higher than

those off site, except for 1975, when the means, both on site and off site, were the same. When the on-site and off-site means were tested to determine if they were statistically different for each year, the hypothesis that the means were statistically the same was rejected at the 0.01 significance level for the years 1973 and 1974 and at the 0.05 significance level for the years 1976 and 1978–1980.

The on-site station at BGY was consistently higher than all other on-site stations. This station was located in an area that received drainage winds from all the test areas.

As a check on seasonal variations of the krypton-85 concentrations, the monthly mean concentrations for the off-site network were plotted with time. No identifiable variation was observed other than the gradual increase in concentration with time.

## Discussion

Since the beginning of the nuclear industry in the 1950s, krypton-85 has been released to the atmosphere by nuclear weapons tests, operating nuclear power reactors, and nuclear fuel reprocessing plants, the latter one being the greatest contributor to the present atmospheric burden of krypton-85 (18). As the half-life of krypton-85 is relatively long (10.76 years) and there is no removal process from the atmosphere, the releases of krypton-85 by the nuclear industry results in a cumulative buildup in the troposphere. This buildup is supported by the data in this report; however, the linear regression followed by the trend in concentrations does not agree with the second degree polynomial expressions found by Rozanski (19) to fit the krypton-85 measurements he obtained for the Northern and Southern Hemispheres from a data review for the period 1950–1977. However, the linear regression is similar

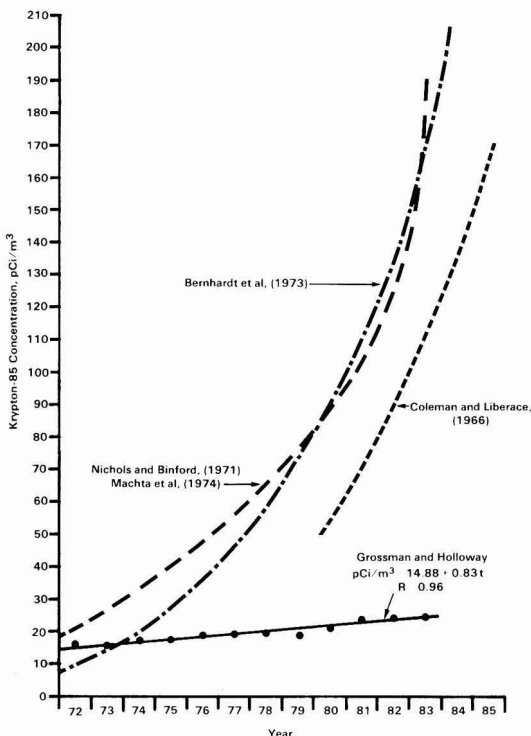


**Figure 2.** Comparison of predicted krypton-85 concentrations by other individuals with concentrations measured around the Nevada Test Site.

to the projection of historical krypton-85 concentrations reported for the period 1954–1969 by the United Nations Scientific Committee on the Effects of Atomic Radiation (20). The slope of the UNSCEAR data is about 0.95 as compared to 0.83 for the EPA data; however, these data are for adjacent time periods. The EPA data do show that the krypton-85 concentration is less than the projections by Bernhardt et al. (21), Liberace and Coleman (22), Nichols and Benford (23), and Machta et al. (24), who projected concentrations of 180, 100, and 200 pCi/m<sup>3</sup>, respectively, for the year 1983. A comparison of their projections with the trend observed in off-site concentrations by this Laboratory is shown in Figure 2. This can be explained by the fact that there has been a reduced installation of nuclear reactors and a suspension of commercial nuclear fuel reprocessing in the United States. Only limited processing of nuclear fuel is being continued by facilities of the U.S. Department of Energy.

There is little concern about the possible health effects to inhabitants of the earth exposed only to the projected ambient krypton-85 concentrations. Other authors (18, 25) have estimated that their projections of about 1000 pCi/m<sup>3</sup> by the year 2000 would only result in a radiation dose to the skin of about 1–2 mrem/year, which is insignificant compared to the 170 mrem/year allowed for the general population.

However, Boeck (26) concluded that the global electrical conductivity of the atmosphere could be measurably altered by a concentration of 1000 pCi/m<sup>3</sup> krypton-85, which by its radioactive decay produces ion pairs in the atmosphere. According to Boeck, our present knowledge of atmospheric processes is insufficient to determine the extent of consequent weather changes and whether they would be harmful or beneficial.

**Table II. Krypton-85 Releases from Nuclear Facilities within the United States**

year	curies	year	curies
1972	1 060 000	1978	545 000
1973	754 000	1979	495 000
1974	774 000	1980	682 000
1975	567 000	1981	905 000
1976	779 000	1982	531 000
1977	560 000	1983	598 000

There is generally fair agreement between the EPA network averages and the krypton-85 concentrations measured in the Northern Hemisphere and reported by other individuals. Wardaszko (27) reported a value of 18 pCi/m<sup>3</sup> at Warsaw, Poland, for 1973. The EPA off-site network average was 15.8 pCi/m<sup>3</sup> for the same year. Janssens et al. (28) reported background concentrations of 0.7–0.8 Bq/m<sup>3</sup> (18.9–21.6 pCi/m<sup>3</sup>) for the years 1979 and 1980, while the EPA network averages were 18.8 and 21.0 pCi/m<sup>3</sup> for the same years. Csongor (25) also reported that the krypton-85 concentration in Hungary was 17 pCi/m<sup>3</sup> in 1975 and was increasing at a rate of 1 pCi/m<sup>3</sup> annually; the EPA network average for 1975 was 17.9 pCi/m<sup>3</sup> with an annual increase of 0.83 pCi/m<sup>3</sup>.

A comparison of the NTS off-site network averages with those for the Three-Mile Island (TMI) network shows the Three-Mile Island network to have a higher background for each of the years 1979–1983, by as much as 0.9–3.9 pCi/m<sup>3</sup>.

The lack of a seasonal variation in krypton-85 concentrations is in contrast to the annual springtime increase in concentration of particulate airborne radioactivity normally resulting from downward-mixing radioactive debris that was injected into the stratosphere by past atmospheric nuclear tests. This suggests that the concentrations of krypton-85 that we observe are directly from sources on the earth's surface. Table II lists the total quantities of krypton-85 released to the atmosphere during the years 1972–1983 by nuclear facilities under the management of the U.S. Department of Energy (29). As these facilities include all the locations of nuclear fuel processing by the Federal Government within the United States, all major sources of krypton-85 should be included. From the total annual releases, which ranged from 500 000 to 1 000 000 Ci for this 12-year period, the krypton-85 concentration within the Northern Hemisphere resulting from the releases was estimated to be about 3 pCi/m<sup>3</sup>, assuming a correction for radioactive decay, homogeneous mixing throughout the Northern Hemisphere, and a volume of  $4.3 \times 10^{18}$  m<sup>3</sup> for the earth's troposphere estimated by Poldervaart (30). As the average annual network concentration of krypton-85 for 1983 (Table I) was 25 pCi/m<sup>3</sup>, the contributions of krypton-85 to the Northern Hemisphere by other countries appears to be more significant than that of the United States.

### Conclusions

The concentrations of krypton-85 measured in air samples collected on and around the Nevada Test Site over the last 12 years have shown that the on-site seepage of krypton-85 is only rarely detectable on site, although the on-site station averages were consistently higher than the off-site averages by 0.1–0.9 pCi/m<sup>3</sup>. The trend of the concentrations year to year has been increasing in accordance with the linear regression: annual off-site average concentration in pCi/m<sup>3</sup> =  $14.88 + 0.83t$  and annual on-site average concentration =  $15.42 + 0.81t$ , where  $t$  is the number of years after 1972. The correlation coefficient

for both equations is 0.96. The observed trend in concentrations has resulted in levels that have been one-eighth of levels predicted by others.

No seasonal variation in krypton-85 concentrations was observed during this 12-year period. This is in sharp contrast to the well-known spring peak of fission product radioactivity from atmospheric weapons testing. Since the spring peak is known to be caused by the intrusion of debris from the stratosphere, it seems clear that the stratosphere is not a significant source of krypton-85. This suggests that the annual increases in krypton-85 observed in this work are the result of sources on the earth's surface which we suspect to be nuclear fuel reprocessing facilities.

The contribution by the federally operated nuclear fuel processing facilities in the United States to the 1983 ambient krypton-85 concentration of 25 pCi/m<sup>3</sup> was estimated to be only 12%, leaving nuclear fuel processing in foreign countries as the major source of the worldwide inventory of krypton-85.

**Registry No.** <sup>85</sup>Kr, 13983-27-2.

### Literature Cited

- (1) Andrews, V. E.; Wruble, D. T. In "Noble Gases"; Stanley, R. E.; Moghissi, A. A., Eds.; National Technical Information Service, U.S. Department of Commerce: Springfield, VA, 1973; CONF-730915, pp 281-289.
- (2) U.S. EPA "Environmental Monitoring Report for the Nevada Test Site and Other Test Areas for Underground Nuclear Detonations, January-December 1972"; National Technical Information Services, U.S. Department of Commerce: Springfield, VA, 1973; NERC-LV-539-23.
- (3) U.S. EPA "Environmental Monitoring Report for the Nevada Test Site and Other Test Areas for Underground Nuclear Detonations, January-December 1973"; National Technical Information Services, U.S. Department of Commerce: Springfield, VA, 1974; NERC-LV-539-31.
- (4) U.S. EPA "Environmental Monitoring Report for the Nevada Test Site and Other Test Areas for Underground Nuclear Detonations, January-December 1974"; National Technical Information Services, U.S. Department of Commerce: Springfield, VA, 1975; NERC-LV-539-39.
- (5) U.S. EPA "Environmental Monitoring Report for the Nevada Test Site and Other Test Areas for Underground Nuclear Detonations, January-December 1975"; National Technical Information Services, U.S. Department of Commerce: Springfield, VA, 1976; EMSL-LV-539-4.
- (6) U.S. EPA "Environmental Monitoring Report for the Nevada Test Site and Other Test Areas for Underground Nuclear Detonations, January-December 1976"; National Technical Information Services, U.S. Department of Commerce: Springfield, VA, 1977; EMSL-LV-539-12.
- (7) U.S. EPA "Environmental Monitoring Report for the Nevada Test Site and Other Test Areas for Underground Nuclear Detonations, January-December 1977"; National Technical Information Services, U.S. Department of Commerce: Springfield, VA, 1978; EMSL-LV-0539-18.
- (8) U.S. EPA "Environmental Monitoring Report for the Nevada Test Site and Other Test Areas for Underground Nuclear Detonations, January-December 1978"; National Technical Information Services, U.S. Department of Commerce: Springfield, VA, 1979; EMSL-LV-0539-31.
- (9) U.S. EPA "Environmental Monitoring Report for the Nevada Test Site and Other Test Areas for Underground Nuclear Detonations, January-December 1979"; National Technical Information Services, U.S. Department of Commerce: Springfield, VA, 1980; EMSL-LV-0539-36.
- (10) U.S. EPA "Environmental Monitoring Report for the Nevada Test Site and Other Test Areas for Underground Nuclear Detonations, January-December 1980"; National Technical Information Services, U.S. Department of Commerce: Springfield, VA, 1981; EPA-600/4-81-047.
- (11) U.S. EPA "Environmental Monitoring Report for the Nevada Test Site and Other Test Areas for Underground Nuclear Detonations, January-December 1981"; National Technical Information Services, U.S. Department of Commerce: Springfield, VA, 1982; EPA-600/4-82-061.
- (12) U.S. EPA "Environmental Monitoring Report for the Nevada Test Site and Other Test Areas for Underground Nuclear Detonations, January-December 1982"; National Technical Information Services, U.S. Department of Commerce: Springfield, VA, 1983; EPA-600/4-83-032.
- (13) U.S. EPA "Environmental Monitoring Report for the Nevada Test Site and Other Test Areas for Underground Nuclear Detonations, January-December 1983"; National Technical Information Services, U.S. Department of Commerce: Springfield, VA, 1984; EPA-600/4-84-040.
- (14) Andrews, V. E. "Noble Gas Sampling System"; National Technical Information Service: Springfield, VA, 1977; EMSL-LV-539-7.
- (15) Scoggins, W. A. "Environmental Surveillance Report for the Nevada Test Site (January through December 1982)"; DOE/NV/00410-76, National Technical Information Service, U.S. Department of Commerce: Springfield, VA, 1983; p 33.
- (16) Scoggins, W. A. "Environmental Surveillance Report for the Nevada Test Site (January through December 1983)"; National Technical Information Service, U.S. Department of Commerce: Springfield, VA, 1984; DOE/NV/10327-4, p 29.
- (17) Johns, F. B.; Hahn, P. B.; Thome, D. J.; Bretthauer, E. W. "Radiochemical Analytical Procedures for Analysis of Environmental Samples"; National Technical Information Service, U.S. Department of Commerce: Springfield, VA, 1979; EMSL-LV-0539-17.
- (18) NCRP "Krypton-85 In The Atmosphere - Accumulation, Biological Significance, and Control Technology". Washington, DC, National Council on Radiation Protection and Measurements Report 44.
- (19) Rozanski, K. *Environ. Int.* **1979**, *2*, 139-143.
- (20) United Nations Scientific Committee on the Effects of Atomic Radiation "Ionizing Radiation: Levels and Effects"; United Nations: New York, 1972; Vol. 1, p 72.
- (21) Bernhardt, D. E.; Moghissi, A. A.; Cochran, J. A. In "Noble Gases"; Stanley, R. E.; Moghissi, A. A., Eds.; National Technical Information Service, U.S. Department of Commerce: Springfield, VA, 1973; CONF-730915, pp 4-19.
- (22) Coleman, J. R.; Liberace, R. *Radiol. Health Data Rep.* **1966**, *7*, 615.
- (23) Nichols, J. P.; Binford, F. T. "Status of Noble Gas Removal and Disposal"; Oak Ridge National Laboratory: Oak Ridge, TN, 1971; ORNL-TM-3515 (as presented in NCRP, 1975, p 34).
- (24) Machta, L.; Ferber, G. J.; Heffter, J. L. "Regional and Global Scale Dispersion of Krypton-85 for Population-Dose Calculations"; Physical Behavior of Radioactive Contaminants in the Atmosphere, International Atomic Energy Agency: Vienna, 1974; p 411 (as presented in NCRP, 1975, p 34).
- (25) Csongor, E. *Low Radioact. Meas. Appl. Proc. Int. Symp.* **1977**, 471-474.
- (26) Boeck, W. L. *Science (Washington, D.C.)* **1976**, *193*, 195-198.
- (27) Wardaszko, T. In "Noble Gases"; Stanley, R. E.; Moghissi, A. A., Eds.; National Technical Information Service, U.S. Department of Commerce: Springfield, VA, 1973; CONF-730915, pp 20-23.
- (28) Janssens, A.; Raes, F.; Cottens, E.; Eggermont, G.; Beuyse, J. (1981), "Measurement of Low-Level Activity of Krypton-85 in Air"; International Atomic Energy Agency: Berlin, West Germany, 1981, CONF-810409, pp 447-458.
- (29) Effluent Information System, managed by EG&G, Idaho, Inc., for the U.S. Department of Energy, Idaho Falls, ID 83415.
- (30) Poldervaart, A., Ed. "Crust of the Earth"; Geological Society of America: New York, 1955; p 121-123.

Received for review September 27, 1984. Revised manuscript received April 15, 1985. Accepted May 24, 1985.

## Decontamination of Soil through Enhanced Formation of Bound Residues

Duane F. Berry and Stephen A. Boyd\*

Department of Crop and Soil Sciences, Michigan State University, East Lansing, Michigan 48824-1114

■ Soil contaminated with the potent carcinogen 3,3'-dichlorobenzidine (DCB) was treated with various reagents in an attempt to enhance the formation of bound (non-extractable) DCB residues. When ferulic acid and  $H_2O_2$  were added to the contaminated soil, a significant decrease in the level of free DCB was observed. Additions of peroxidase to soil did not affect the binding of DCB. Vanillic acid and glucose were also tested in the same fashion as ferulic acid but produced no effect. Additions of ferulic acid and  $H_2O_2$  are believed to accelerate the natural process of humus formation which is mediated by indigenous peroxidase enzymes and which leads to the formation of bound residues in soil. These results may provide the basis for development of a rapid and inexpensive method for the containment of certain hazardous contaminants in soil.

### Introduction

Surface soils contaminated by recalcitrant organic pollutants have proven extremely difficult to manage. Two basic approaches have been used in the majority of cases: containment with clay barriers or excavation of the contaminated soil. Unfortunately, the effectiveness of these approaches is limited by the lengthy periods of time required for their execution and by the enormous expense involved. In this report, we provide evidence that in some cases of soil contamination it may be possible to detoxify soil, *in situ*, by enhancing the covalent attachment of certain hazardous organic chemicals to soil humic constituents. It is suggested that this process essentially obliterates the chemical identity of the pollutant and effectively diminishes its bioavailability.

Oxidative coupling of polyphenols in soils is an important synthetic process leading to the formation of humic substances (1-3). Peroxidase enzymes are important biocatalysts in these oxidative coupling reactions that ultimately yield high molecular weight polymers of remarkable stability (mean residence time > 500 years) (1-3). Xenobiotic compounds present in soil may also become covalently bound to soil humic materials during oxidative coupling (4-6). Incorporated xenobiotics, or bound residues, cannot be removed from soil by conventional extraction techniques. It is generally accepted that incorporated residues are less toxic, less bioavailable, and less mobile than the free species, and as such the formation of bound residues serves to decontaminate soil (4, 6, 7).

The overall objective of the research reported here was to develop an *in situ* method for detoxifying contaminated soil. Our approach was to enhance the formation of bound residues between the potent carcinogen 3,3'-dichlorobenzidine (DCB) and soil humic constituents by increasing the oxidative coupling activity of soil. DCB was selected as a model compound because aromatic amines, as a class of compounds, are important soil pollutants that are known to form bound residues with soil humus (8-11).

When added to soil, DCB becomes covalently bound to soil humic constituents which results in a binding curve typical of most aromatic amines (12). This binding curve is characterized by an initial decrease in solvent-extractable DCB followed by a period where the extractable levels remain essentially constant (12). DCB is not mineralized or volatilized in soil at a significant rate, and therefore, the

progressive loss of solvent-extractable DCB, coupled with increasing extractability (of the bound residue) by alkali, can be attributed to the formation of humus-bound DCB residues (12). Studies with model compounds have provided strong evidence that aromatic amines such as DCB form covalent linkages to quinoidal sites of soil humus via nucleophilic addition of the amine group (10, 13). By subsequent addition and oxidation reactions the aromatic amine residues may become even more strongly bound to soil humic constituents (10).

### Experimental Section

3,3'-Dichlorobenzidine (3,3'-dichloro-4,4'-diaminobiphenyl) (ring uniformly  $^{14}C$  labeled), purchased from ICN Pharmaceuticals, Inc., had a radiochemical purity of >99% and specific activity of 35 mCi mmol<sup>-1</sup>. The [ $^{14}C$ ]DCB was dissolved in absolute ethanol and stored in the dark at 0 °C until used.

A Rubicon sand (93.5% sand, 2.5% organic matter, pH 7.7, and cation-exchange capacity of 66 mmol kg<sup>-1</sup>) was moistened to 37% field capacity with deionized  $H_2O$  containing unlabeled DCB and  $^{14}C$ -labeled DCB. Final DCB concentrations were 5 µg of DCB and 21.3 nCi of [ $^{14}C$ ]DCB (g of air-dried soil)<sup>-1</sup>. The amended soil was incubated at room temperature in closed amber glass jars. Samples (10 g) were taken in triplicate at 0, 1, 2, 3, 7, 10, and 14 days and stored frozen. After sampling on day 14, the soil was divided into 200-g (air-dried basis) portions for the following treatments: no reagent addition; ferulic acid;  $H_2O_2$ ; peroxidase and  $H_2O_2$ ; peroxidase,  $H_2O_2$ , and ferulic acid; deactivated (boiled for 1 h) peroxidase,  $H_2O_2$ , and ferulic acid; vanillic acid; vanillic acid and  $H_2O_2$ ; peroxidase,  $H_2O_2$ , and vanillic acid; glucose; glucose and  $H_2O_2$ . Peroxidase [from horseradish, Sigma type III, 155 purpurogallin units (mg of solid)<sup>-1</sup>] and  $H_2O_2$  were added as aqueous solutions at levels of 100 units of peroxidase and 77.5 µmol of  $H_2O_2$  (g of air-dried soil)<sup>-1</sup>. A total of 10 mL of  $H_2O$  was added to each 200-g portion of soil. Ferulic acid (or vanillic acid or glucose; data not shown) was added as a solid at the level of 15 µmol (g of air-dried soil)<sup>-1</sup>. An additional treatment was included in which peroxidase,  $H_2O_2$ , and ferulic acid were added at concentrations 10-fold less than those given above (data not shown). Order of addition was always ferulic acid, then peroxidase, and then  $H_2O_2$ . Soil samples (10 g) were withdrawn in triplicate on days 15-17 and 21 and stored frozen. The entire experiment was duplicated. Soil samples were placed in 125-mL Erlenmeyer flasks and extracted with 40 mL of 3:2 (v/v) ethyl acetate-methanol for 12 h on a swirl shaker. The solid and liquid phases were separated by centrifugation, and the liquid phase was assayed for  $^{14}C$  by liquid scintillation counting.

### Results and Discussion

In order to demonstrate our ability to manipulate DCB binding, we first allowed DCB to establish its normal unaltered binding curve during a 14-day time period (Figure 1). After a 14-day incubation of [ $^{14}C$ ]DCB in soil, peroxidase [from horseradish (HRP)], hydrogen peroxide ( $H_2O_2$ ), ferulic acid, vanillic acid, and glucose were added alone and in various combinations in an attempt to en-



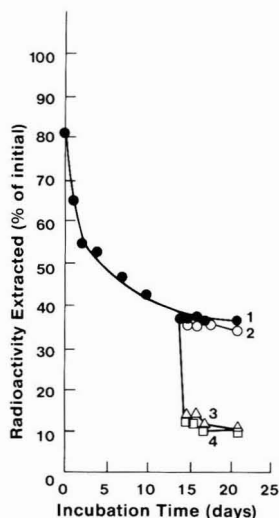


**Figure 1.** Solvent-extractable radioactivity from [ $^{14}\text{C}$ ]DCB-amended soil. After a 14-day incubation, soil was divided for the following treatments: control, no reagent addition (curve 1); peroxidase and  $\text{H}_2\text{O}_2$  (curve 2); peroxidase,  $\text{H}_2\text{O}_2$ , and ferulic acid (curve 3); deactivated peroxidase,  $\text{H}_2\text{O}_2$ , and ferulic acid (curve 4).

hance DCB binding. Binding of DCB was monitored by measuring solvent-extractable radioactivity. Previous results have shown that, in soil, the levels of solvent-extractable DCB mirrored solvent-extractable radioactivity (12). Similar results were obtained by Voorman and Penner for 4,4'-methylenebis(2-chloroaniline), a compound that is structurally similar to DCB (14).

The addition of HRP and  $\text{H}_2\text{O}_2$  to DCB-amended soil (curve 2) resulted in no significant alteration in the amount of solvent-extractable radioactivity. In contrast, relative to the control (i.e., no reagent addition, curve 1) a dramatic 65% decrease in the amount of solvent-extractable radioactivity was observed which resulted from the addition of ferulic acid,  $\text{H}_2\text{O}_2$ , and either active HRP (curve 3) or inactive HRP (curve 4). These data demonstrated that peroxidase enzyme additions were not required to enhance DCB binding. Addition of these reagents at 10-fold lower levels resulted in a 38% decrease. When we added either ferulic acid or  $\text{H}_2\text{O}_2$  alone, we observed no enhancement effect. However, a single addition of ferulic and  $\text{H}_2\text{O}_2$  to DCB-contaminated soil significantly decreased extractable radioactivity and thus dramatically decreased the level of free DCB in soil.

Although the mechanism by which the enhancement process occurs is still not well-defined, we can present a plausible explanation based on our previous studies (15) concerning the peroxidase-mediated cross-coupling of anilines to model humic acids. In that study it was demonstrated that phenolic compounds containing the three-C acrylic group (e.g., ferulic acid) were highly reactive with HRP, in contrast to other naturally occurring polyphenols that did not contain the acrylic group (e.g., vanillic acid). Furthermore, the rate at which chloroaniline became coupled to the model humic acids during oxidative coupling was directly dependent on the reactivity of the polyphenol toward HRP. Thus, ferulic acid greatly enhanced the incorporation of chloroaniline into model humic acids whereas vanillic acid produced a much smaller effect. By

analogy, we propose that the addition of ferulic acid and  $\text{H}_2\text{O}_2$  to soil provides indigenous peroxidase enzymes with highly reactive substrates. The net effect is to raise the overall level of oxidative coupling in soil which leads to the enhanced incorporation of DCB. To test this hypothesis, vanillic acid and  $\text{H}_2\text{O}_2$  were added to DCB-amended soil in the same fashion as ferulic acid. The observation that vanillic acid did not elicit the increased binding observed for ferulic acid substantiated our interpretation. Glucose was also added as a control, and no effect was observed. The specificity of the reaction for ferulic acid argues strongly for the involvement of indigenous peroxidase enzymes.

Previous investigators have alluded to the use of enzyme additions to enhance the binding of recalcitrant pollutants in soil (4). In fact, this technology has recently been developed for the treatment of aqueous wastes from coal-conversion processes (16). Our results are significant because they demonstrate that, in soil, indigenous enzyme activity can be raised through the addition of highly reactive substrates, i.e., ferulic acid and  $\text{H}_2\text{O}_2$ . Whereas enzyme addition to soils or aqueous wastes may be economically prohibitive, addition of these inexpensive, naturally occurring reagents is feasible from an economical standpoint. Thus, this method of soil detoxification, accomplished by the stimulation of indigenous oxidative coupling enzymes, offers great promise as an effective and economical means for the containment of certain hazardous contaminants in soils.

**Registry No.** DCB, 91-94-1;  $\text{H}_2\text{O}_2$ , 7722-84-1; ferulic acid, 1135-24-6; vanillic acid, 121-34-6; glucose, 50-99-7.

#### Literature Cited

- (1) Stevenson, F. J. "Humus Chemistry"; Wiley: New York, 1982.
- (2) Sjöblad, R. D.; Bollag, J.-M. In "Soil Biochemistry"; Paul, E. A.; Ladd, J. M., Eds.; Dekker: New York, 1979; Vol. 5, pp 1130-1152.
- (3) Haider, K.; Martin, J. P.; Fillip, Z. In "Soil Biochemistry"; Paul, E. A.; McClaren, A. D., Eds.; Dekker: New York, 1975; Vol. 4, pp 196-244.
- (4) Bollag, J.-M.; Loll, M. *J. Experimentia* 1983, 39, 1221-1231.
- (5) Bollag, J.-M.; Minard, R. O.; Liu, S. Y. *Environ. Sci. Technol.* 1983, 17, 72-80.
- (6) Bollag, J.-M. In "Aquatic and Terrestrial Humic Material"; Christman, R. F.; Gjessing, E. T., Eds.; Ann Arbor Science Publishers: Ann Arbor, MI, 1983; pp 121-141.
- (7) Freitag, D.; Scheunert, I.; Klein, W.; Korte, F. *J. Agric. Food Chem.* 1984, 32, 203-207.
- (8) Bartha, R. *J. Agric. Food Chem.* 1971, 19, 385-387.
- (9) Hsu, T.-S.; Bartha, R. *Soil Sci.* 1974, 116, 444-452.
- (10) Parris, G. E. *Environ. Sci. Technol.* 1980, 14, 1099-1106.
- (11) Parris, G. E. *Residue Rev.* 1980, 76, 1-30.
- (12) Boyd, S. A.; Kao, C.-W.; Sulfita, J. M. *Environ. Toxicol. Chem.* 1984, 3, 201-208.
- (13) Saxena, A.; Bartha, R. *Bull. Environ. Contam. Toxicol.* 1983, 30, 485-491.
- (14) Voorman, R.; Penner, D., submitted for publication in *Environ. Toxicol. Chem.*
- (15) Berry, D. F.; Boyd, S. A. *Soil Biol. Biochem.*, in press.
- (16) Klibanov, M. A.; Tu, T.-M.; Scott, K. P. *Science (Washington, D.C.)* 1983, 221, 259-261.

Received for review January 30, 1985. Accepted June 17, 1985. This work was supported by a Toxicology Research Grant from the Michigan Agricultural Experiment Station and the Michigan State University Center for Environmental Toxicology. Contribution No. 11661 of the Michigan Agricultural Experiment Station.

# A Theory for Critical Flow through Hypodermic Needles

Thomas J. Overcamp

Department of Environmental Systems Engineering, Clemson University, Clemson, South Carolina 29634-0919

■ The classical theory of isothermal, compressible flow through a long tube is applied to predict the critical flow through hypodermic needles which are frequently used in air sampling for flow regulation. Agreement between the predictions and published data is generally good. The model predicts the variations of the critical flow rate with the needle length and with the upstream pressure that are shown by the data.

## Introduction

Critical flow devices are frequently used in air sampling since they provide a constant flow rate if the pressure downstream of the device is less than a critical fraction of the upstream pressure. This fraction is approximately 0.5 for plate orifices and 0.4 for hypodermic needles. Commercial hypodermic needles are used extensively due to their low cost and wide availability.

Corn and Bell (1), Lodge et al. (2), and Urone and Ross (3) reported data on critical flow rates through hypodermic tubing or hypodermic needles. Lodge et al. (2) gave practical information on the use of hypodermic needles in air sampling including the protection of the needle to prevent plugging and the effects of storage and reuse on the flow rate. DiNardi and Sacco (4) described a simple holder for a hypodermic needle that can be assembled from commercially available fittings.

Past investigators have compared the measured critical flow rate for hypodermic needles to Fliegner's formula (5, 6) which is a semiempirical equation for the critical mass flow rate:

$$w_{\max} = 0.0404 \frac{C_D A p_0}{\sqrt{T_0}} \quad (1)$$

in which  $w_{\max}$  is the critical mass flow rate (kg/s),  $C_D$  is the empirical discharge coefficient,  $A$  is the cross-sectional area of the needle ( $m^2$ ),  $p_0$  is the upstream total pressure (Pa), and  $T_0$  is the upstream temperature (K). Corn and Bell (1) found that the discharge coefficient varied from 0.30 to 0.66 for the needles that they tested. On the basis of Fliegner's formula, they predicted that the critical mass flow rate should vary directly with the upstream pressure. This implies that the actual volumetric flow rate is independent of upstream pressure. Urone and Ross (3) showed that the volumetric flow rate actually decreased with decreasing upstream pressure. They proposed an empirical correction factor, based on incompressible flow of gases through an orifice, to account for this decrease.

In this paper, the classical theory of isothermal, compressible flow of gases through a long duct (6) is used to predict the critical flow of air through hypodermic needles. These predictions are compared to available data.

## Theory

A hypodermic needle has a smooth, converging inlet that leads into the smooth needle of constant cross section. Conventional needles have a sharp, beveled tip. For simplicity, the needles are assumed to be tubes whose length  $L$  is the nominal length of the needle and whose tip is square cut. Subscript 0 refers to upstream reservoir conditions, subscript 1 refers to the conditions at the entrance

to the constant cross-sectional area needle, and subscript 2 refers to the conditions at the exit of the needle. The theory is based on the classical theory of one-dimensional, compressible flow with friction (6).

The Mach number  $M$ , which is the ratio of the gas velocity  $v$  to the local speed of sound, is defined as

$$M = \frac{v}{\sqrt{\gamma RT}} \quad (2)$$

in which  $\gamma$  is the ratio of the heat capacity of the gas at constant pressure to the heat capacity at constant volume,  $R$  is the specific gas constant, and  $T$  is the gas temperature. The Reynolds number of the flow is

$$Re = \frac{\rho v D}{\mu} \quad (3)$$

in which  $\rho$  is the mass density,  $D$  is the diameter, and  $\mu$  is absolute viscosity. The ideal gas law is

$$p = \rho RT \quad (4)$$

where  $p$  is the absolute pressure.

If the flow in the short converging section is assumed to be frictionless and adiabatic, the temperature and pressure at the entrance to constant area needle are given by

$$T_1 = T_0 [1 + (\gamma - 1)M_1^2/2]^{-1} \quad (5)$$

and

$$p_1 = p_0 [1 + (\gamma - 1)M_1^2/2]^{(\gamma-1)/\gamma} \quad (6)$$

In the constant area portion of the needle, frictional effects cannot be ignored. On the basis of the results of incompressible flow, the Fanning friction factor for laminar flow is

$$f = 16/Re \quad (7)$$

For turbulent flow in smooth tubes, the Fanning friction factor is given by the Blasius formula (7):

$$f = 0.0791/Re^{1/4} \quad (8)$$

For the Reynolds numbers less than 2000, the flow will be laminar. For the Reynolds numbers greater than around 3000, the flow is generally turbulent. In the intermediate region, there is a transition between laminar and turbulent flow, and the friction factor falls between the values computed with eq 7 and 8. Since little information is available on flow transition in hypodermic needles, it is assumed that eq 7 is valid if the Reynolds number is less than 2000 and that eq 8 is valid if the Reynolds number exceeds 2000. This assumption results in a discontinuity in the friction factor at a Reynolds number of 2000.

Due to the small flow rates, the high thermal conductivity of the needles, and the viscous dissipation of the high speed flow, it is assumed that the flow in the constant area section of the needle is isothermal. This implies that the Reynolds number is constant in this section of the needle.

If the flow is isothermal, the relationship between the friction factor, the length-to-diameter ratio, and  $M_1$  at critical flow is given by

$$\frac{4fL}{D} = \frac{1 - \gamma M_1^2}{\gamma M_1^2} + \ln(\gamma M_1^2) \quad (9)$$

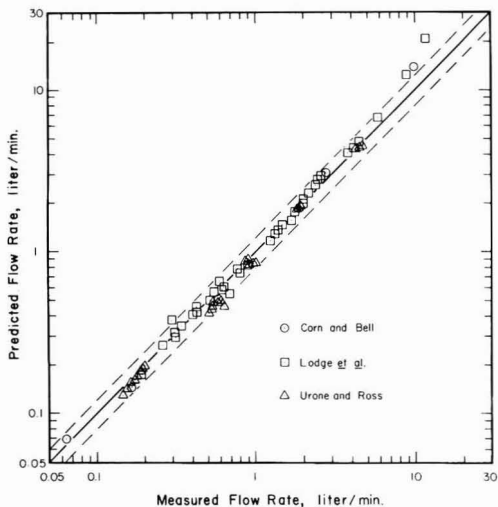


**Figure 1.** Predicted critical flow rate vs. measured critical flow rate. The solid line is the line of perfect agreement, and the dashed lines indicate  $\pm 20\%$  error bands.

The actual volumetric flow rate based on upstream conditions is

$$Q_0 = v_1 \left( \frac{\pi D_1^2}{4} \right) \left( \frac{p_1}{p_0} \right) \left( \frac{T_0}{T_1} \right) \quad (10)$$

### Data

Corn and Bell (1) constructed critical flow elements from hypodermic tubing without the converging section. The pieces of tubing were approximately 25 mm long and were embedded in wooden dowel holders. They gave mean flow rates for three to nine needles each of five different gauge tubes ranging from Stubs gauge number 30 to 15.

Lodge et al. (2) tested 42 combinations of needle gauge and needle length. The gauges ranged from Stubs gauge number 25 to 13. The nominal needle lengths ranged from 12.7 ( $1/2$  in.) to 89 mm ( $3 1/2$  in.). Their data are the means of the critical flow rates through 12 different needles of each size for an upstream pressure of 630 mmHg. The relative standard deviations for their measurements ranged from 1% to 15% with a mean relative standard deviation of about 4%.

Urone and Ross (3) gave data on the critical flow rates for five different needles for various upstream pressures. The needle gauges ranged from Stubs gauge number 27 to 18. The nominal length of the needle ranged from 12.7 mm ( $1/2$  in.) for the 27-gauge needle to 38 mm ( $1 1/2$  in.) for the 18-gauge needle.

### Results and Discussion

Equations 2–10 were solved by iterative techniques for the needle dimensions and upstream conditions for each case in the three data sets. For 6 of the 81 cases, the successive iterations alternated between a laminar flow solution with a Reynolds number slightly less than 2000 and a turbulent flow solution with a Reynolds number slightly greater than 2000. This failure to converge is a result of the discontinuity in the friction factor curve given by eq 7 and 8. Although the flow rates for the laminar and turbulent solutions differed by less than 10%, and were in fair agreement with the data, predictions for these cases are not given.

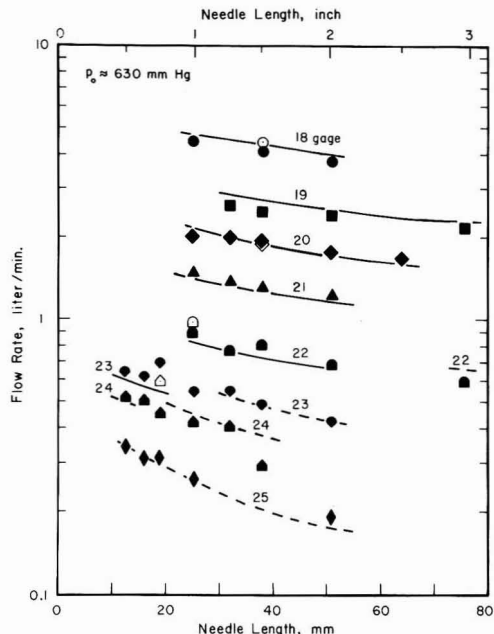


**Figure 2.** Critical flow rate vs. length. The open symbols are the data of Urone and Ross, and the darkened symbols are the data of Lodge et al. The solid lines are the turbulent flow predictions, and the dashed lines are the laminar flow predictions.

The computed values of  $M_1$  ranged from 0.19 to 0.55. The computed values of  $Re_1$  ranged from 400 to 15000.

Figure 1 shows predicted flow rates vs. measured flow rates for the 75 cases in the three data sets for which a unique solution was obtained. The solid line is the line of perfect agreement. The two dashed lines give  $\pm 20\%$  error bands. Except for three points having measured flows greater than 8 L/min, most data points fall within the dashed lines. One of these three points is a case from the data of Corn and Bell with a length-to-diameter ratio of 18 for which the theory based on flow in a long tube may not be appropriate. The other two points, which are from Lodge et al., had length-to-diameter ratios of 49 and 65 which are more typical of the rest of the data. The common factors among these three cases are the larger diameter of the needles (Stubs gauge numbers 17 to 13) and computed Reynolds numbers on the order of  $10^4$ . Since the model overpredicts the measured flow for these cases, this suggests that the friction factor predicted by using the Blasius formula, eq 7, is too low. It is plausible that a slight surface roughness affects the friction factor at these higher Reynolds numbers.

Figure 2 shows measured values of flow rate vs. needle length. The data of Lodge et al. (2) are indicated by the darkened symbols. The four data points indicated by open symbols are observations taken from Urone and Ross (3) that had upstream pressures ranging from 626 to 637 mmHg. The solid lines are the predictions using the turbulent flow model, and the dashed lines are the predictions using the laminar flow model. For needle gauges 21 through 18, the computed Reynolds numbers are 2700 or above which should be in the turbulent range. There is good agreement between the predicted and measured values. For the needle gauge 25 data, the computed Reynolds numbers are 1700 or less which is in the laminar range. This case also has good agreement between the

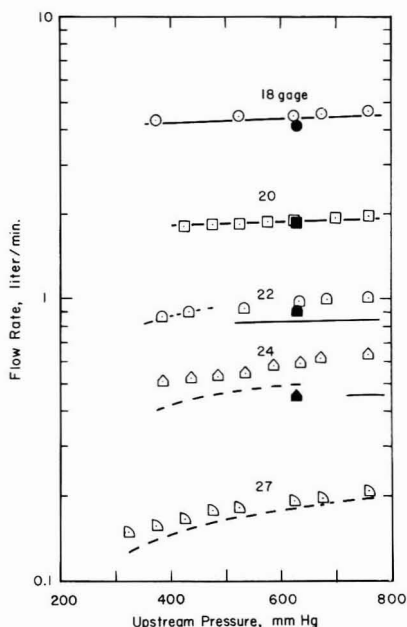


**Figure 3.** Critical flow rate vs. upstream pressure. The open symbols are the data of Urone and Ross, and the darkened symbols are the data of Lodge et al. The solid lines are the turbulent flow predictions, and the dashed lines are the laminar flow predictions.

predicted and measured values. For the 22, 23, and 24 needle gauge data, the computed Reynolds numbers indicate a transition from turbulent to laminar flow as the length increases. The laminar and turbulent predictions of the model are shown for their appropriate ranges of validity. The gap in the predictions for the 22-, 23-, and 24-gauge needles is a result of the discontinuity in the friction factor. The agreement between predicted and measured values is not quite as satisfactory as for the cases in which flow transition was not a factor.

Figure 3 shows measured values of flow rate vs. upstream pressure. The data indicated by the open symbols are those of Urone and Ross (3). The four data points indicated by darkened symbols are cases taken from Lodge et

al. (2) that had the same needle gauge and length as the Urone and Ross data. The turbulent flow predictions for the 20 and 18 gauge needles are in very good agreement with the data. The laminar flow predictions for the 27-gauge needle are in good agreement with measured values at higher pressures and slightly overpredict flow rates at lower pressures. The predictions for the 24- and 22-gauge needles indicate that a transition from laminar to turbulent flow occurs as upstream pressure increases. Again the agreement between predicted and measured values is not quite as satisfactory as for the cases in which flow transition was not a factor.

The modeling results and the data indicate that Fliegner's formula, which was developed for critical flow through nozzles and orifices, should not be used to predict critical flow rates through hypodermic needles.

The good agreement between the model and the data of Urone and Ross (3) indicates that the model can be used to correct flow rates for variations in the upstream pressure as long as the model does not predict that the flow undergoes a transition from laminar to turbulent flow or vice versa.

#### Acknowledgments

I thank John Nerney of Becton-Dickinson for data on B-D hypodermic needles and Paul Urone for information on his experiments.

#### Literature Cited

- (1) Corn, M.; Bell, W. *Ind. Hyg. Assoc. J.* **1963**, *24*, 502-504.
- (2) Lodge, J. P., Jr.; Pate, J. B.; Ammons, B. E.; Swanson, G. A. *J. Air Pollut. Control Assoc.* **1966**, *16*, 197-200.
- (3) Urone, P.; Ross, R. C. *Environ. Sci. Technol.* **1979**, *13*, 351-353.
- (4) DiNardi, S. R.; Sacco, C. L. *J. Air Pollut. Control Assoc.* **1978**, *28*, 603-604.
- (5) Fliegner, A. *Proc.—Inst. Civ. Eng.* **1874**, *39*, 370-375.
- (6) Shapiro, A. H. "The Dynamics and Thermodynamics of Compressible Fluid Flow"; Ronald Press: New York, 1953; Vol. 1, pp 159-189.
- (7) Perry, R. H.; Green D. W., Maloney, J. O., Eds. "Perry's Chemical Engineers' Handbook", 6th ed.; McGraw-Hill: New York, 1984; p 5-24.

Received for review February 28, 1985. Accepted May 13, 1985. This work was partially supported under National Science Foundation Grant ISP-8011451.

# INCREASE YOUR LIBRARY SHELF SPACE BY 90%

## *... without adding a single shelf!*



When you manage a library these days, you're well aware that space is precious. And, additional shelves for backfiles volumes are expensive.

Well, the American Chemical Society knows your concerns. That's why all the Society's 21 primary publications in the field of chemistry are available in microfilm editions—including complete volumes back to 1879.

If you are setting up a microfilm system, expanding or changing one, or just want to discuss the possibilities—an ACS Sales Representative is ready to work with you. Just give us a call at

800-424-6747, or write to the Sales Office, American Chemical Society,  
1155 Sixteenth Street, N.W., Washington, D.C. 20036.



Start Saving Space in Your Chemical Reference Files NOW!

**AMERICAN CHEMICAL SOCIETY PUBLICATIONS**  
*Chemical Publishers since 1879.*

Accounts of Chemical Research  
Chemical & Engineering News  
Environmental Science & Technology  
Inorganic Chemistry  
Journal of Medicinal Chemistry  
The Journal of Organic Chemistry  
The Journal of Physical Chemistry

Analytical Chemistry  
Biochemistry  
CHEMTECH  
Chemical Reviews  
Langmuir  
Macromolecules  
Organometallics

I&EC Fundamentals  
I&EC Process Design & Development  
I&EC Product Research & Development  
Journal of Agricultural & Food Chemistry  
Journal of the American Chemical Society  
Journal of Chemical Information & Computer Sciences  
Journal of Chemical & Engineering Data



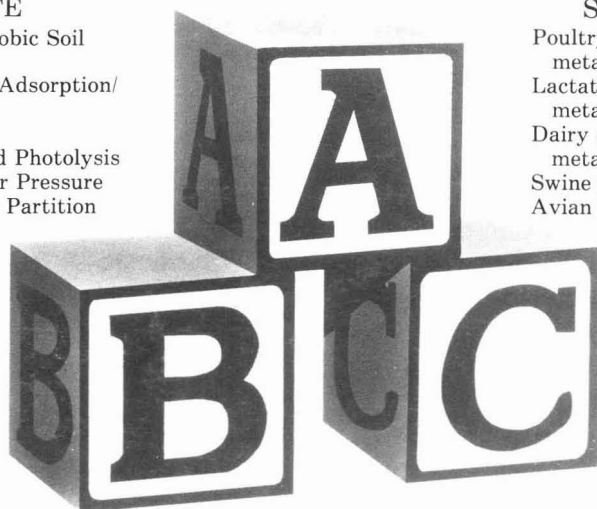
# Building Blocks Of Success

## ENVIRONMENTAL FATE

Aerobic/Anaerobic Soil  
Metabolism  
Soil/Sediment Adsorption/  
Desorption  
Soil Leaching  
Hydrolysis and Photolysis  
Ambient Vapor Pressure  
Octanol/Water Partition  
Coefficients

## LARGE ANIMAL STUDIES

Poultry residue and  
metabolism  
Lactating goat  
metabolism  
Dairy cow residue and  
metabolism  
Swine residue  
Avian Toxicology



## AQUATIC TOXICOLOGY

Freshwater Static Acute  
Bioassays  
Saltwater Static Acute  
Bioassays  
Algal Bioassays  
Earthworm Toxicity Tests  
Effluent Toxicity Studies  
Dynamic Acute Toxicity  
Tests  
Bioconcentration Studies  
Early Life Stage & Chronic  
Investigations  
Pond Studies

## PHARMACEUTICAL

Complete Drug Stability  
Testing  
Complete ANDA Bio-  
equivalence Clinical  
Facility — In house  
analytical capability  
Full Internal QA Audits

## RESIDUE

Trace Metals  
Chlorinated hydrocarbons  
Organophosphates  
Triazines  
PCB's  
Permethrin  
Glyphosate

## TERRESTRIAL DISSIPATION STUDIES

Field and Forest

## INSTRUMENTS

*Model 1002A GPC*  
Automatic Gel Permeation  
Preparative Chromatograph

*Model 600 AUTOVAP™*  
automatically  
evaporates/concentrates,  
solvent exchanges and  
transfers samples to  
autoloader vials



Phone: 314/474-8579  
Telex: 821 814

Write or Call for  
More Information  
PO Box 1097

® ANALYTICAL BIO-CHEMISTRY LABORATORIES, INC. Columbia, Missouri 65205